

Molecular investigation of mitophagy in neuronal cell models

By

Lois Lee Dekkers

MSc Biomedical Sciences



A thesis presented for the degree of Doctor of Philosophy

School of Biochemistry and Immunology

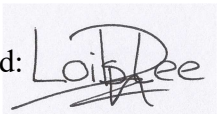
Trinity College Dublin

February 2018

Declaration

I declare that this thesis has not been submitted as an exercise for a degree at this or any other university and it is entirely my own work.

I agree to deposit this thesis in the University's open access institutional repository or allow the Library to do so on my behalf, subject to Irish Copyright Legislation and Trinity College Library conditions of use and acknowledgement.

Signed: 

Date: 13 February 2018

Acknowledgements

I would like to express my thanks and appreciation to my supervisor Dr. James Murray for his continued support and advice. Thank you for always being there for me. I wish you every success for your future career.

I would also like to thank FP7 MSCA and the TINTIN (Training in neurodegeneration, therapeutics intervention and neurorepair, Project ID: 608381) network for funding and giving me the opportunity to be part of a great team of fellow scientist. Thank you TINTIN fellows for the fun times and support whenever we had to write another report. A special thank you goes out to Prof. Patrick Schloss and Yasmina Martí. Patrick, thank you for welcoming me in your lab in Mannheim, Germany. Yasmina, thank you for teaching me how to culture and differentiate the hiPSC and for being my guide in Mannheim. I really enjoyed my time in Mannheim and I wish I could have stayed longer. The same goes for Björn Windshügel in ESP in Hamburg. Thank you for having me coming over and for showing me around. Last, but not least, a big thank you goes out to Catherine McPartlin for managing TINTIN and making sure we were all on track. I know we did not make it easy on you.

My thanks go out to the previous and current members of the JTM lab too. Ryan, Ana, Salma, and Sadia, thank you for the fun times we have had! Salma and Sadia, it is a pity that you started your PhD when I was finishing up because I am sure we would have had great times in the lab. I hope you will all become amazing scientists and good luck with all the Western blots (I hope you are not tired of them yet).

A big thank you goes out to my three best friends Nicoleta, Gerard, and Cécile. I am so lucky to have met you! I want to thank you for the great and fun times we had both inside and outside the lab, the amusing, but also honest, conversations, and for the support you gave me. I wish you all the best in your career and private life and I hope that we can see each other often (I miss hanging out with you already)!

My biggest thanks go out to my parents and sister. Thank you for your support and for always being there for me. You showed me that the sky is the limit and I know I would have not been able to get this far in life without you.

Abstract

Autophagy functions as a cellular recycling and quality control pathway and is likely responsible for maintenance of viable mitochondria by mitophagy, even though exact mechanisms remain unclear. Mitophagy is characterised by accumulation of the protein kinase PINK1 on damaged mitochondria from where it recruits the E3-ligase Parkin, leading to ubiquitination of damaged mitochondrial proteins, marking them for autophagic engulfment. *PINK1* and *PARK2* (Parkin) mutations are linked to early-onset Parkinson's disease (PD), suggesting defects in mitophagy could contribute to PD pathogenesis. Considering most research regarding mitophagy and PD are carried out in non-neuronal cell models, this study sought to identify the mechanisms of mitochondrial degradation and whether this involved the autophagy pathway in cell models of neuronal origin (SH-SY5Y cells), and in mouse embryonic stem cells (mESC), and human induced pluripotent stem cells (hiPSC) that have the potential to become differentiated towards the neuronal lineage.

In SH-SY5Y cells, treatment with the mitochondrial uncoupler FCCP led to activation of autophagy and degradation of mitochondrial markers TOM20, TIM23, and VDAC1. Inhibition of ULK1 or PIK3C3 did not affect degradation of damaged mitochondria, suggesting canonical autophagy is not involved. Proteasomal degradation was important instead. FCCP did not lead to mitochondrial degradation in mESC and likely inhibited autophagy. In presumptive neuronal precursor hiPSC, FCCP induced autophagy, but not classical mitophagy. hiPSC differentiated into presumptive dopamine (DA) neurons showed FCCP-mediated loss of mitochondrial markers in control cells, which was not affected by autophagic or proteasomal inhibition. PD hiPSC had fragmented mitochondria and increased susceptibility to

FCCP cytotoxicity, suggesting mitochondria could be intrinsically damaged. Combined, the findings show mitophagy and involvement of autophagy are differentially regulated in different cell types of neuronal origin, underscoring the importance of appropriate selection of cell models for PD related research. The data also supports the notion that mitophagy/autophagy are differentially regulated in presumptive DA neurons obtained from hiPSC of normal and PD patients, suggesting that hiPSC cells may provide a good model system for further investigation of mitophagy in PD.

Table of Contents

Declaration.....	ii
Acknowledgements.....	iii
Abstract.....	v
Table of Contents.....	vii
Abbreviations.....	xi
Introduction.....	1
1.0 Parkinson’s disease and its effect on dopamine neurons.....	2
1.0.1 Characteristics of Parkinson’s disease.....	2
1.0.2 Events that could contribute to the development of Parkinson’s disease.....	3
1.0.3 Development of the dopamine neuron.....	4
1.0.4 Characteristics of the dopamine neuron.....	6
1.0.5 Dopamine neurons are more susceptible to oxidative stress.....	6
1.0.6 Mitochondria and neurons.....	8
1.0.7 Mitophagy in neurons.....	11
1.1 Mitochondria.....	14
1.1.1 Mitochondrial bioenergetics.....	16
1.1.2 Mitochondrial dynamics.....	17
1.1.3 Mitochondrial dynamics and mitophagy.....	19
1.2 Autophagy and its involvement in mitophagy.....	20
1.2.1 Classical control of autophagy.....	20
1.2.2 Link between ULK1 and mitophagy.....	26
1.2.3 Link between LC3B and mitophagy.....	27
1.2.4 Link between p62 and mitophagy.....	28
1.3 Mitophagy.....	29
1.3.1 Importance of mitophagy for cell viability and survival.....	29
1.3.2 Molecular sub-types of mitophagy.....	30
1.3.3 Hypoxia induced mitophagy.....	32
1.3.4 Mitophagy induced by autophagy receptors.....	34
1.3.5 PINK1/Parkin-mediated mitophagy.....	36
1.3.6 PINK1 interacts with Parkin.....	38
1.3.7 Parkin ubiquitinates proteins on the mitochondrial outer membrane.....	39
1.3.8 Involvement of the ubiquitin-proteasome system during mitophagy.....	40
1.3.9 Effects of defective Parkin on mitochondrial health.....	40
1.3.10 Effects of defective PINK1 on mitochondrial health.....	41

1.3.11 Effects of PD linked mutations on mitochondrial health in patient samples	43
1.4 Aim of thesis	45
Material and Methods	46
2.0 Materials	47
2.0.1 Equipment	47
2.0.2 Chemicals	48
2.0.3 Tissue culture reagents and media.....	51
2.0.4 Buffers and solutions.....	53
2.0.5 Antibodies	55
2.1 Cell culture	57
2.1.1 Maintenance of cultured cell lines.....	58
2.1.2 Maintenance of undifferentiated mouse embryonic stem cells	58
2.1.3 Maintenance of undifferentiated human induced pluripotent stem cell colonies	59
2.1.4 Picking of undifferentiated human induced pluripotent stem cell colonies	61
2.1.5 Freezing of undifferentiated human induced pluripotent stem cell colonies	61
2.1.6 Generation of neuronal precursor cells	62
2.1.7 Differentiation of neuronal precursor cells into dopaminergic neurons.....	63
2.2 Cell viability assays.....	63
2.2.1 Crystal Violet assay.....	63
2.3 Microscopy.....	64
2.3.1 Immunocytochemistry.....	64
2.4 Molecular biology	65
2.4.1 Calcium phosphate transfection	65
2.4.2 RNA isolation.....	65
2.4.3 cDNA synthesis.....	66
2.4.4 Real-time quantitative polymerase chain reaction (RT-qPCR).....	66
2.5 Protein analysis.....	67
2.5.1 Preparation of cell extracts	67
2.5.2 SDS-poly-acrylamide gel electrophoresis (SDS-PAGE)	68
2.5.3 Western immunoblotting.....	69
2.6 Protein-protein interactions	70
2.6.1 Immunoprecipitation	70
2.7 Statistical analysis.....	70

Characterisation of mitophagy in SH-SY5Y cells.....	72
3.0 Introduction.....	73
3.1 FCCP inhibits mTORC1 signalling and activates the Ras pathway.....	76
3.2 FCCP induces autophagy in SH-SY5Y cells.....	83
3.3 FCCP induces mitophagy in SH-SY5Y cells	94
3.4 Proteasomal inhibition prevents FCCP-induced Parkin degradation and mitophagy.....	100
3.5 Discussion.....	104
Effects of autophagic inhibition on mitophagy in SH-SY5Y cells	107
4.0 Introduction.....	108
4.1 SH-SY5Y cells do not respond to different modulators of autophagy	112
4.2 ULK1 inhibition induces PINK1 expression and Parkin degradation.....	115
4.3 PIK3C3 inhibition does not affect removal of FCCP damaged mitochondria	127
4.4 PIK3C3 inhibition partially prevents FCCP cytotoxicity	136
4.5 ULK1 inhibition promotes Beclin1 phosphorylation	139
4.6 Discussion.....	144
Effects of FCCP on mitophagy and autophagy in stem cell models.....	149
5.0 Introduction.....	150
5.1 Undifferentiated mESC respond to autophagic activators and inhibitors.....	155
5.2 FCCP induces PINK1 expression in undifferentiated mESC.....	158
5.3 ULK1 inhibition induces PINK1 expression in undifferentiated mESC.....	160
5.4 ULK1 inhibition affects basal turnover of the mitochondrial marker VDAC1 in undifferentiated mESC.....	162
5.5 Differentiation of hiPSC into presumptive dopaminergic neurons	164
5.6. FCCP induces autophagy, but not mitophagy, in presumptive NPC.....	168
5.7 Inhibition of lysosomal degradation affects basal turnover of TOM20 and VDAC1 in presumptive NPC.....	178
5.8 Proteasomal or autophagic inhibition does not affect expression of mitochondrial markers upon FCCP treatment.....	183
5.9 Preliminary analysis of FCCP-mediated degradation of mitochondrial markers in presumptive dopaminergic neurons	191
5.10 Preliminary analysis of proteasomal and autophagic inhibition shows partial rescue of FCCP-induced TOM20 and TIM23 degradation in PD presumptive dopaminergic neurons	196
5.11 Discussion.....	204
General discussion	211
6.0 General discussion	212

6.0.1 FCCP activates autophagy and induces clearance of mitochondrial markers in SH-SY5Y cells.....	212
6.0.2 Removal of FCCP-damaged mitochondrial markers might not depend on canonical autophagy in SH-SY5Y cells.....	214
6.0.3 The proteasome is involved in FCCP-induced degradation of mitochondrial markers in SH-SY5Y cells.....	216
6.0.4 Control and PD hiPSC respond differently to FCCP treatment	217
6.0.5 Caveats of the study	219
6.0.6 Updated model of PINK1/Parkin-mediated mitophagy	221
6.1 Conclusions	225
Perspectives	226
7.0 Perspectives	227
Appendix	231
References	236

Abbreviations

$\Delta\Psi$	Membrane potential
46C	46C mouse embryonic stem cells
AA	Ascorbic acid
Acetyl-CoA	Acetyl coenzyme A
ADP	Adenosine diphosphate
AMBRA1	Autophagy/Beclin1 regulator 1
AMPK	AMP-activated protein kinase
ANT	Adenine nucleotide translocase
APS	Ammonium persulfate
AR-JP	Autosomal recessive, juvenile Parkinsonism
ATG	Autophagy-related protein
ATP	Adenosine triphosphate
Baf A1	Bafilomycin A1
Bcl2-L-13	Bcl-2-like protein 13
BDNF	Brain-derived neurotrophic factor
BNIP3	Bcl-2/adenovirus E1B 19-kDa interacting protein 3
BSA	Bovine serum albumin
CI-IV	Complex I-IV
CALCOCO2	Calcium binding and coiled-coil domain 2
CCCP	Carbonyl cyanide m-chlorophenylhydrazone
CHX	Cycloheximide
CQ	Chloroquine
CRISPR-Cas9	Clustered regularly interspaced short palindromic repeats associated nuclease Cas9

DA	Dopamine
DAT	Dopamine transporter
dbcAMP	Dibutyryl adenosine 3', 5'-cyclic monophosphate sodium salt
DMEM	Dulbecco's modified Eagle's medium
DMSO	Dimethylsulfoxide
DOPAC	3, 4-Dihydroxy-phenylacetic acid
Drp1	Dynamin-related protein 1
DTT	Dithiothreitol
EBSS	Earle's balanced salt solution
ECL	Enhanced chemiluminescent
EGF	Epidermal growth factor
En	Engrailed homeobox
ER	Endoplasmic reticulum
ERK	Extracellular signal-regulated kinases
ESC	Embryonic stem cells
ESCRT	Endosomal sorting complexes required for transport
ETC	Electron transport chain
FAD(H ₂)	Flavin adenine dinucleotide (reduced)
FBS	Foetal bovine serum
FCCP	Carbonyl cyanide-4-(trifluoromethoxy)phenylhydrazine
FGF8b	Fibroblast growth factor 8b
FGFb	Human basic fibroblast growth factor
FIS1	Mitochondrial fission 1 protein
FKBP8	FK506 binding protein 8
FUNDC1	FUN14 domain containing 1

GABA	Gamma-aminobutyric acid
GABARAP	Gamma-aminobutyric acid receptor-associated protein
GDNF	Glial cell line-derived neurotrophic factor
Gfer	Growth factor erv1-like
GFP	Green fluorescent protein
GSK3	Glycogen synthase kinase 3
HBS	HEPES buffered saline
HDAC	Histone deacetylase
HEK293T	Human embryonic kidney 293T cells
hiPSC	Human induced pluripotent stem cells
hLIF	Human leukaemia inhibitory factor
HPLC	High-performance liquid chromatography
HRP	Horseradish peroxidase
Hsp	Heat shock protein
HVA	Homovanillic acid
IF	Immunofluorescence
IL- β	Interleukin- β
IMS	Intermembrane space
IP	Immunoprecipitation
IP3R	Inositol triphosphate receptor
IRS-1	Insulin receptor substrate 1
iULK1	Small molecule inhibitor of ULK1
Klf4	Kruppel-like factor 4
KO-DMEM	KnockOut Dulbecco's modified Eagle's medium
LAMP1	Lysosomal associated membrane protein 1

LB	Lewy body
LC3B	Microtubule-associated protein 1 light chain 3B (MAP1LC3B)
L-DOPA	L-dihydroxyphenylalanine
LIR	LC3 interacting region
Lmx1	LIM homeobox transcription factor 1
LRRK2	Leucine rich repeat kinase 2
LSB	Low salt buffer
MAM	Mitochondria-associated membrane
MAPK	Mitogen-activated protein kinase
MCU	Mitochondrial calcium uniporter
MDV	Mitochondria-derived vesicles
MEF	Mouse embryonic fibroblasts
MEK	Mitogen-activated protein kinase kinase
MEM	Minimal essential medium
mESC	Mouse embryonic stem cells
MFN	Mitofusin
MIM	Mitochondrial inner membrane
MIRO	Mitochondrial Rho GTPase
MOM	Mitochondrial outer membrane
MPP	Mitochondrial processing peptidase
MPP+	1-Methyl-4-phenylpyridinium
mPTP	Mitochondrial permeability transition pore
MPTP	1-Methyl-4-phenyl-1, 2, 3, 6-tetrahydropyridine
mtDNA	Mitochondrial DNA
mTORC1	Mechanistic target of rapamycin complex 1

MTS	Mitochondrial targeting signal
NaCAE	Na ⁺ Ca ²⁺ exchanger
NAD(H)	Nicotinamide adenine dinucleotide (reduced)
NE	Norepinephrine
NEAA	Non-essential amino acids
NIX	NIP3-like protein X
NO	Nitric oxide
NOS	Nitric oxide synthase
NPC	Neuronal precursor cell
NURR1	Nuclear receptor related 1
Oct3/4	Octamer-binding transcription factor 3/4
OPA1	Optic atrophy 1
Opti-MEM	Opti-minimal essential medium
OPTN	Optineurin
OXPHOS	Oxidative phosphorylation
PARK2	Parkin
PARL	Presenilin associated rhomboid-like protease
Pax	Paired box
PBS	Phosphate-buffered saline
PD	Parkinson's disease
PE	Phosphatidylethanolamine
PEI	Polyethylenimine
PGC-1 α	Peroxisome proliferator-activated receptor-gamma coactivator-1 α
PGK1	Phosphoglycerate kinase 1

PHB2	Prohibitin 2
P _i	Inorganic phosphate
PI3K	Phosphatidylinositol 3-kinase
PIK3C3	Phosphatidylinositol 3-kinase catalytic subunit type 3 (Vps34)
PIK3R4	Phosphoinositide-3-kinase, regulatory subunit 4 (Vps15)
PINK1	PTEN-induced putative kinase protein 1
Pitx3	Paired like homeodomain 3
PKA	Protein kinase A
PMF	Proton motive force
PPP	Pentose phosphate pathway
PtdIns	Phosphatidylinositol
PtdIns(3)P	Phosphatidylinositol 3-phosphate
PTEN	Phosphatase and tensin homolog
PVDF	Polyvinylidene difluoride
Rap	Rapamycin
RING	Really interesting new gene
ROCK	Rho-associated, coiled-coil containing protein kinase
ROS	Reactive oxygen species
RT	Room temperature
RT-qPCR	Real-time quantitative polymerase chain reaction
S6K1	p70 ribosomal S6 kinase 1
SD	Standard deviation
SDS	Sodium dodecyl sulfate
SDS-PAGE	SDS-poly-acrylamide gel electrophoresis
SEM	Standard error of the mean

SERCA	Sarco/endoplasmic reticulum calcium ATPase
SHH	Sonic Hedgehog
SN	Substantia nigra
SNc	Substantia nigra pars compacta
SNCA	α -Synuclein gene
Sox2	SRY-box 2
SQSTM1	Sequestosome 1
SRY	Sex determining region Y
TALEN	Transcription activator-like effector nucleases
TAX1BP1	Tax1-binding protein 1
TBS	Tris-buffered saline
TBS-T	Tris-buffered saline-Tween 20
TCA	Tricarboxylic acid
TEA	Tris-acetate-EDTA
TGF- β	Transforming growth factor β
TH	Tyrosine hydroxylase
TIM	Translocase of the inner mitochondrial membrane
TLR	Toll-like receptor
TOM	Translocase of the outer mitochondrial membrane
TSC	Tuberous sclerosis complex
Tuj-1	Neuron specific class III β -tubulin
Ub	Ubiquitin
Ubl	Ubiquitin-like
UBR	Ubiquitin protein ligase E3 component n-recognin
ULK	Unc-51-like kinase

UPS	Ubiquitin-proteasome system
UVRAG	UV radiation resistance-associated gene
VDAC	Voltage-dependent anion channel
VM	Ventral midbrain
VMAT2	Vesicular monoamine transporter 2
Vps	Vacuolar protein sorting
WB	Western blotting
WIPI	WD repeat domain phosphoinositide-interacting protein
WT	Wildtype
ZFN	Zinc finger nucleases

Chapter 1

Introduction

1.0 Parkinson's disease and its effect on dopamine neurons

1.0.1 Characteristics of Parkinson's disease

Parkinson's disease (PD) is a progressive neurodegenerative disorder affecting 1 % of the older adult population over the age of 60 and is a major social health problem due to its prevalence and lack of effective treatment (Haelterman et al., 2014, Reeve et al., 2014). There is no cure yet for PD and available treatment, which targets dopamine neurons, can only help control patient symptoms. Clinical characteristics of PD encompass tremor, increased muscle tone, slow movements, and impaired gait and balance, but depression and sleep disturbance are often observed as well. Pathological hallmarks include the Lewy bodies (LBs), protein aggregates that contain mainly α -synuclein, that can be found in neurons and neurites, glia, and presynaptic terminals, and progressive loss of dopamine (DA) neurons in the substantia nigra (SN), resulting in depletion of DA and derangements of neuronal circuits in the target regions of these neurons (Jellinger, 2009, Exner et al., 2012). However, not all Parkinson affected people have LBs and sometimes LBs are found in individuals that did not have any reported PD symptoms.

The majority of PD cases are sporadic with only approximately 5-10 % of the PD cases being familial (Celardo et al., 2014). Risk factors for development of sporadic PD are barely known, but age is considered to be important. Autosomal dominant PD is often caused by mutations in genes encoding α -synuclein (*SNCA*), leucine rich repeat kinase 2 (*LRRK2*), or vacuolar protein sorting 35 (*VPS35*), which all affect complex I of the electron transport chain (ETC). Complex I is one of the four complexes that make up the mitochondrial ETC that is responsible for generation of energy in the form of adenosine triphosphate (ATP) (see section 1.1.1). Mutated

SNCA, *LRRK2*, and *VPS35* negatively affect complex I activity, resulting in altered mitochondrial function and reduced ATP production. Autosomal recessive, juvenile Parkinsonism (AR-JP) has been linked to mutations in either *PARK2* (Parkin), phosphatase and tensin homolog (PTEN)-induced putative kinase protein 1 (*PINK1*), or *DJ-1* (Valente et al., 2004, Celardo et al., 2014). Defects in *PARK2* are responsible for most children and young adults PD cases, whereas mutations in *PINK1* are the second most frequent cause (Valente et al., 2004). Both Parkin and PINK1 are involved in the selective removal of mitochondria by the autophagy system, named mitophagy, which will be discussed in section 1.3.5.

1.0.2 Events that could contribute to the development of Parkinson's disease

It is unknown whether observed mitochondrial pathology is the primary cause of pathogenesis in PD or whether mitochondrial damage is a consequence of damaged neurons. However, the fact that many of the genes responsible for familial forms of PD are related to mitochondria or mitochondrial function and the observation that exposure to the mitochondrial neurotoxin 1-methyl-4-phenyl-1, 2, 3, 6-tetrahydropyridine (MPTP) mimicked PD pathology in animal models, strengthens the hypothesis that mitochondrial dysfunction may lie at the basis of PD (Martinez and Greenamyre, 2012, Haelterman et al., 2014). MPTP inhibits complex 1 activity and exposure to its toxic metabolite 1-methyl-4-phenylpyridinium (MPP⁺) caused mitochondrial fragmentation in primary neurons and neuronally-derived SH-SY5Y cells, which led to increased mitophagy (Zhu et al., 2007, Wang et al., 2011b).

Neuroinflammatory mechanisms could also be a possible contributor to the death of DA neurons as observed by both post-mortem and *in vivo* studies in PD patients

(Hirsch and Hunot, 2009). Mitochondrial defects or defective mitophagy can lead to exposure of mitochondrial DNA (mtDNA), which is able to activate a Toll-like receptor (TLR) 9-mediated inflammatory response since it contains hypomethylated CpG motifs resembling bacterial DNA (Zhang et al., 2010, Oka et al., 2012). Furthermore, mtDNA can activate caspase-1 and can increase pro-inflammatory cytokine levels including interleukin-1 β (IL- β) (Miura et al., 2010, Nakahira et al., 2011). IL- β can directly bind to surface receptors on DA neurons or it can activate glial cells, the non-neuronal cells supporting and protecting neurons, thereby activating cell death pathways in DA neurons.

1.0.3 Development of the dopamine neuron

DA neurons are generated in the floor plate region of the mesencephalon during embryonic development (Ono et al., 2007). First, the ventral midbrain (VM) region is formed, which relies on signals arising from the floor plate of the midbrain and the isthmus organiser (Hegarty et al., 2013). Both the floor plate and the isthmus organiser are responsible for the regional identity of the VM, the specification and proliferation of VM DA neuronal precursors (NPC), DA NPC neurogenesis, and differentiation and survival of DA neurons (Arenas et al., 2015).

The floor plate controls ventral identities and is responsible for the secretion of Sonic Hedgehog (SHH) (Echelard et al., 1993) and the expression of the transcription factors *Hes1* (also expressed by the isthmus organiser) (Baek et al., 2006) and *Nato3* (Ono et al., 2010). The isthmus organiser, which is a signalling centre separating the midbrain from the hindbrain, secretes fibroblast growth factor 8 (FGF8) (Rhinn and Brand, 2001) and expresses the transcription factors *Engrailed* *homeobox 1* and *2*

(*En1* and *En2*) (Davis and Joyner, 1988), *LIM homeobox transcription factor 1 beta* (*Lmx1b*) (Adams et al., 2000, Smidt et al., 2000), *Paired box 2* and *5* (*Pax2* and *Pax5*) (Urbánek et al., 1997), and *Wnt1* (Wilkinson et al., 1987, Davis and Joyner, 1988, Crossley and Martin, 1995, Adams et al., 2000). Combined, these factors ensure the appropriate patterning of the VM region.

Next, the identity of VM DA NPC that ultimately generate VM DA neurons is formed. This depends on FGF8 (Saarimäki-Vire et al., 2007, Lahti et al., 2012), SHH, which subsequently induces *Lmx1a* expression (Andersson et al., 2006) and regulates *FoxA2* expression (Chung et al., 2009), Wnt family proteins (Wilkinson et al., 1987, Davis and Joyner, 1988, Parr et al., 1993, Rawal et al., 2006, Andersson et al., 2008) and expression of *Lmx1b* (Lin et al., 2009, Deng et al., 2011, Yan et al., 2011).

Upon acquiring a DA phenotype, the DA NPC become gradually post-mitotic. Shortly after the final mitosis when DA NPC are actively migrating to their final positions, expression of tyrosine hydroxylase (TH), the rate-limiting enzyme for DA synthesis (see section 1.0.4), is induced (Specht et al., 1981a, Specht et al., 1981b, Puelles and Verney, 1998). Next, the differentiation and subsequent long-term survival of VM DA neurons is promoted by *Lmx1b* (Dai et al., 2008), *Nuclear receptor related 1* (*Nurr1*) (Zetterström et al., 1996, Bäckman et al., 1999), *Paired like homeodomain 3* (*Pitx3*) (Smidt et al., 2004), *En1* and *En2* (Albéri et al., 2004). This is followed by axonal pathfinding (Nakamura et al., 2000, Gates et al., 2004, Van den Heuvel and Pasterkamp, 2008) and the development of synapses (Hegarty et al., 2013), which mark the final step in the generation of post-mitotic VM DA neurons.

1.0.4 Characteristics of the dopamine neuron

Mammalian brains contain different populations of DA neurons, namely midbrain DA neurons, located in the ventral mesodiencephalon, and DA neurons in the substantia nigra pars compacta (SNc). Midbrain DA neurons are responsible for amongst others regulation of emotion, maintenance of memory, and creation of associations with rewarding stimuli, whereas DA neurons in the SNc are involved in control of voluntary movement (Exner et al., 2012, Bissonette and Roesch, 2015). Loss of DA neurons in the SNc results in deletion of DA and derangements of neuronal circuits in basal ganglia target regions of these neurons, leading to impaired motor function as observed in PD (Exner et al, 2012).

DA neurons belong to the family of catecholaminergic neurons that are involved in movement, mood, and attention (Bear et al., 2007). Catecholaminergic neurons synthesise neurotransmitters that contain a chemical structure known as a catechol that have the amino acid tyrosine as precursor. Tyrosine is converted by TH into L-dihydroxyphenylalanine (L-DOPA), which is subsequently converted into DA by dopa decarboxylase (Molinoff and Axelrod, 1971). (Nor)adrenergic neurons are able to further convert DA into either norepinephrine (NE) or epinephrine, also known as adrenaline. DA is stored in synaptic vesicles and will be released into the synaptic cleft upon an action potential, where it can interact with dopaminergic receptors on the postsynaptic neuron.

1.0.5 Dopamine neurons are more susceptible to oxidative stress

DA neurons are more susceptible to oxidative stress, and are thus more vulnerable, than other neurons, but it is not known why. One hypothesis is that cytotoxic free

radicals are generated by oxidation of cytosolic DA and its metabolites. Oxidised DA can form covalent bonds with several (mitochondrial) proteins and it can make α -synuclein, a protein found in pathological lesions in PD, more prone to aggregation (Van Laar et al., 2009). However, this is contradictory to results obtained with the drug Levodopa, which is among the most effective and safest treatments for PD. Levodopa, the chemical name for L-DOPA, is able to cross the blood-brain barrier and can boost synthesis of DA in DA neurons that are still viable, thus alleviating some of the symptoms associated with DA loss. Large clinical trials did not show enhanced disease progression, even though neuroimaging data suggest that loss of nigrostriatal dopamine nerve terminals might be accelerated or that the dopamine transporter (DAT) might be affected (Fahn, 2004). It was shown that dysfunction of vesicular monoamine transporter 2 (VMAT2), which is responsible for uptake of DA into presynaptic vesicles, can induce nigrostriatal degeneration (Caudle et al., 2007).

Another hypothesis why DA neurons could be more vulnerable to oxidative stress is that they have higher levels of activity compared to other neurons. DA neurons in the SN, the main area of the brain that is affected in PD patients, have pacemaker properties, meaning that these neurons can generate bursts of electrical activity that lead to DA release in postsynaptic brain regions (Zweifel et al., 2009, Guzman et al., 2010). Therefore, DA neurons require high amounts of ATP and produce more reactive oxygen species (ROS) as a result, making them more susceptible to damage. Furthermore, these DA neurons utilise L-type calcium channels for their pacemaking activity, which have a long activation span (Exner et al., 2012). Reliance on L-type calcium channels is increased by age and leads to continued elevated levels of calcium

in the cytoplasm, which might stimulate mitochondrial respiration and ROS production.

Lastly, another source of oxidative stress could be excitotoxicity (Exner et al., 2012). DA neurons receive high glutamatergic input and overstimulation of their glutamate receptors can evoke a cascade of damaging events, including high influx of calcium that can affect calcium storage capacity of both mitochondria and endoplasmic reticulum (ER), which could be further intensified by decreased ATP production. Glutamate receptors are regulated by ATP and a decrease in ATP, which has been observed in PD, might favour their overstimulation.

On their own, hypotheses described in this section cannot explain increased susceptibility of SN DA neurons to oxidative stress, suggesting that their increased vulnerability is likely a combination of events.

1.0.6 Mitochondria and neurons

As mentioned earlier, mitochondrial pathology is observed in brains of deceased PD patients, making mitochondria a popular topic for PD related research. Neurons consist of three structural domains that have their own function: the cell body (soma), an axon, and dendrites with many branches, and due to their unique metabolic requirements, mitochondria are not evenly distributed in these different domains (Hollenbeck and Saxton, 2005) (Figure 1.0.6). Mitochondria can be found in the soma, but they also travel up and down to axons and dendrites, making regulation of mitochondrial homeostasis more complex. Defects in transport or either fission or fusion of mitochondria greatly alters formation and function of the synapse, showing

that a delicate balance in mitochondrial dynamics is important for proper function of neurons (Li et al., 2004, Verstreken et al., 2005, Li et al., 2008).

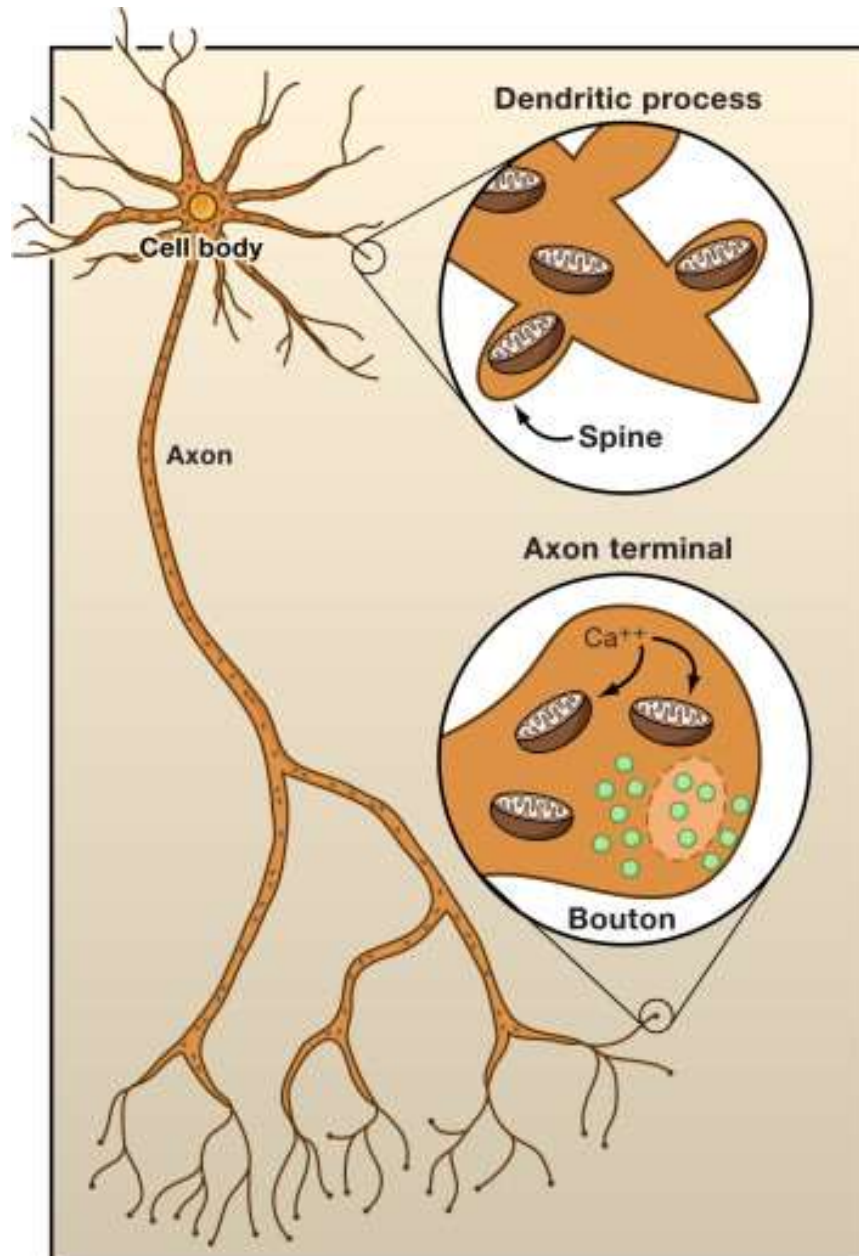


Figure 1.0.6. Mitochondria in a neuron. Neurons contain several hundred mitochondria that are not evenly distributed in different neuronal domains. Mitochondria are particularly found in presynaptic and postsynaptic terminals that have a high demand for ATP. In the dendritic processes (top), mitochondrial recruitment to the spines is associated with neuronal activation. In the boutons at the nerve terminal (bottom), mitochondria are important for the cycling of the reserve pool of synaptic vesicles (green vesicles highlighted by dashed oval) and Ca^{2+} buffering, as well as organisation and proper structure of the bouton. Figure adapted from (Chan, 2006).

Neurons are heavily reliant on ATP production, which is associated with high amounts of mitochondrial stress, and mitochondria are particularly located in areas with high demand for ATP, such as presynaptic and postsynaptic terminals, to sustain neuronal activity (Palay, 1956). This includes axonal transport, maintenance of ion gradients through ATP-dependent pumps, and synaptic neurotransmission (Celardo et al., 2014). Due to high levels of mitochondria in neurons, it is not surprising that about 20 % of oxygen is consumed by the brain in a resting human, even though it only represents about 2 % of the body weight (Clarke and Sokoloff, 1999).

ATP production in neurons depends on oxidative phosphorylation (OXPHOS) rather than glycolysis, generating as much as 95 % of ATP found in neurons (Erecinska et al., 1994). Neurons do not switch to glycolysis when OXPHOS becomes limited, a phenomenon observed in other cell types, since inhibition of mitochondrial respiration resulted in a collapse in mitochondrial membrane potential, rapid decline in ATP concentration, and spontaneous apoptotic cell death (Almeida et al., 2001). It was shown that induction of glycolysis in neurons led to decreased utilisation of glucose through the pentose phosphate pathway (PPP), which ultimately resulted in decreased regeneration levels of reduced glutathione, an important antioxidant (Herrero-Mendez et al., 2009). Taken into account the long life-span of neurons, subjection to high levels of oxidative stress, very low glutathione concentrations as well as low activity of γ -glutamyl cysteine synthetase, the rate-limiting step in glutathione synthesis, diversion of glucose towards PPP might serve as a defence mechanism against oxidative stress and could be of more importance to neuronal health than utilisation of glycolysis (Bolaños et al., 2010).

1.0.7 Mitophagy in neurons

Neurons are post-mitotic non-proliferating cells that need to survive for the lifetime of the organism. Besides being more vulnerable to oxidative stress, neurons produce high levels of ROS, have high levels of iron that can trigger ROS formation, and have relatively low levels of antioxidants (Cui et al., 2004, Chinta and Andersen, 2008). Mitochondria are susceptible to damage and have a long half-life in polarised neurons, indicating the importance of refurbishment of the mitochondrial pool to prevent accumulation of oxidative damage and to maintain cell health (Menziez and Gold, 1971, O'Toole et al., 2008). The mitochondrial quality control system and mitophagy are responsible for maintaining a healthy mitochondrial pool by taking care of amongst others proper distribution of mitochondria to synaptic terminals, function of synapses and dendritic spines, maintenance of ETC activity and electrical connectivity, protection of mtDNA integrity, and apoptosis (Amadoro et al., 2014).

Mitophagy is characterised by PINK1 accumulation on damaged mitochondria from where it selectively recruits Parkin that subsequently ubiquitinates proteins on the mitochondrial outer membrane (MOM) (Figure 1.0.7). Defects in mitophagy have been implicated in PD. To date, mechanisms of mitophagy have been mainly studied in non-neuronal cell lines and it is unclear how this process is regulated in neurons. Research has shown that neuronal mitochondria can undergo transport, biogenesis, fission and fusion, and selective degradation similar to non-neuronal mitochondria (Vives-Bauza et al., 2010, Fischer et al., 2012, Sheng and Cai, 2012, Youle and van der Bliek, 2012). It was found that mitophagy carried out by the PINK1/Parkin pathway is present in primary neurons as well as replicating cell types (Seibler et al., 2011, Van Humbeeck et al., 2011, Yu et al., 2011, Cai et al., 2012, Joselin et al., 2012,

Koyano et al., 2013, McCoy et al., 2014), however, Parkin translocation remains controversial since other *in vitro* (Van Laar et al., 2011, Rakovic et al., 2013) and even *in vivo* (Sterky et al., 2011, Yu et al., 2011, Lee et al., 2012, Vincow et al., 2013) studies could not detect Parkin recruitment to damaged mitochondria or actual mitophagy in neurons, indicating that this process still needs to be investigated extensively.

Discrepancies in Parkin recruitment and existence of mitophagy might be explained by the possibility that mitophagy in neurons could be a slow and regulated process or that Parkin-independent mitophagy could play a role in this specific cell type. Rat primary cortical neurons did not show Parkin translocation to mitochondria upon a 6 hour exposure to the mitochondrial uncoupler carbonyl cyanide m-chlorophenylhydrazone (CCCP), however, Parkin did translocate to damaged mitochondria in neurons and mitophagy was observed after a prolonged CCCP exposure of 24 hours (Van Laar et al., 2011, Cai et al., 2012). It has also been suggested that mitophagy could be a more tightly controlled process in neurons than in other cell types (Mouton-Liger et al., 2017). Neurons are less prone to lose mitochondria because of their reliance on OXPHOS for their energy requirements and do not switch to glycolysis easily, suggesting that Parkin-mediated mitophagy could be a difficult process to monitor (Bolaños, 2016).

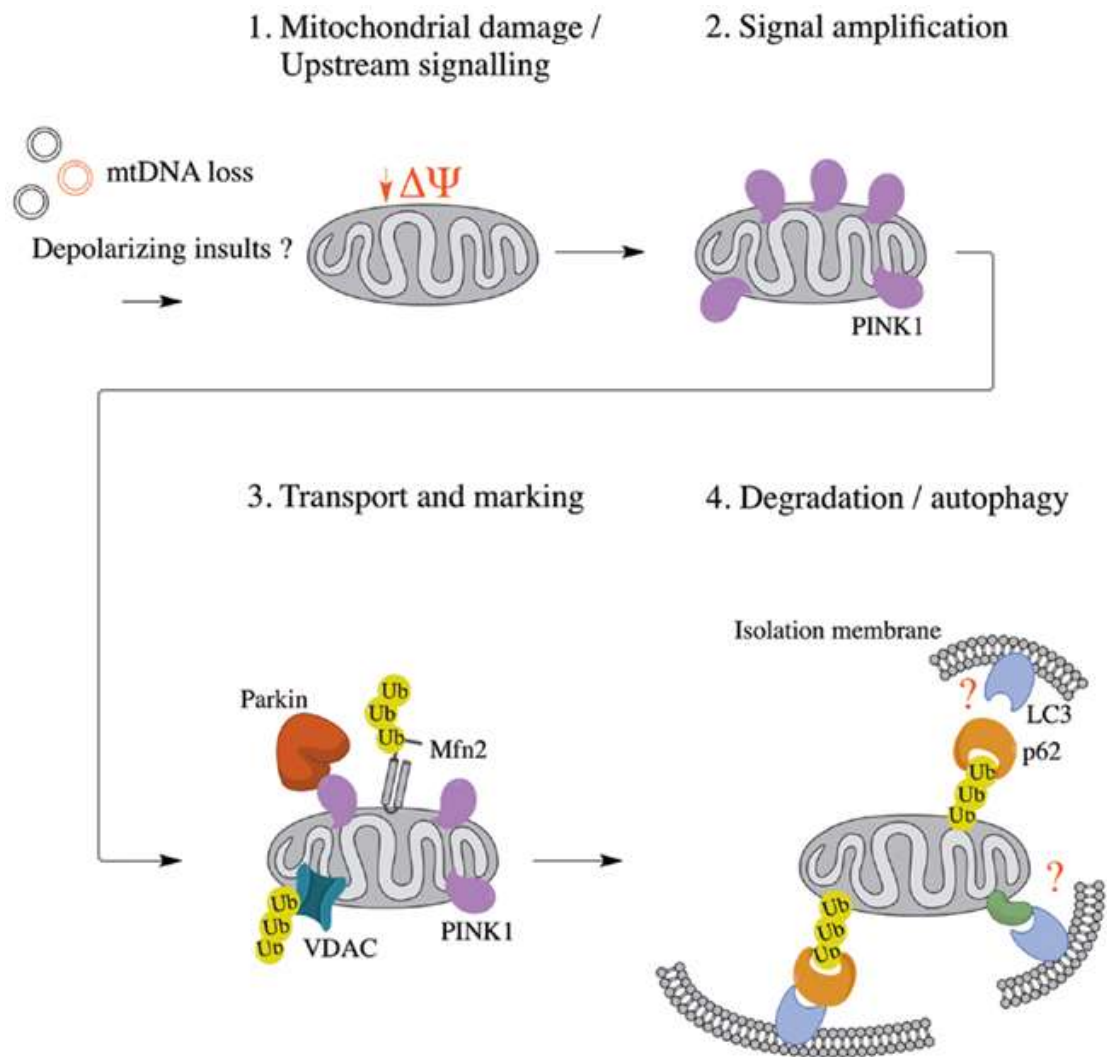


Figure 1.0.7. PINK1/Parkin-mediated mitophagy. PINK1/Parkin-mediated mitophagy can be defined in four major steps. (1) Mitophagy is activated by either mitochondrial damage or upstream signalling. (2) Damaged mitochondria accumulate PINK1 on their MOM, leading to signal amplification. (3) PINK1 selectively recruits Parkin to damaged mitochondria, which subsequently ubiquitinates mitochondrial proteins, including voltage-dependent anion channel (VDAC) and mitofusin 2 (MFN2). Note that Parkin translocation to damaged mitochondria in neurons is controversial and that more research on this topic is needed. (4) Ubiquitinated proteins are recognised by ubiquitin binding proteins (e.g. p62), resulting in envelopment of damaged mitochondria by isolation membranes, which is mediated by microtubule-associated protein 1 light chain 3B (LC3B), and delivery to autophagosomes, leading to their degradation. Other unidentified receptors could also be involved in recruitment of the isolation membrane. Figure adapted from (Grenier et al., 2013).

1.1 Mitochondria

Mitochondria are double membraned organelles responsible for generation of energy in the form of ATP by carrying out a series of oxidative reactions (Figure 1.1.0). Mitochondria have different functions in a cell, ranging from ATP production and generation of intermediate metabolites to controlling intercellular calcium levels and programmed cell death. Energy demands of the cell are met by structural changes of mitochondria, but cell bioenergetics can directly influence mitochondrial structure as well. Use of toxins that inhibit mitochondrial respiration cause cell death, thereby illustrating the importance of mitochondrial ATP (Berg et al., 2002).

Mitochondria have their own genome and are thought to be derived from ancient bacteria forming a symbiotic relationship with early prokaryotic cells some 1.45 billion years ago (Margulis, 1970, Margulis, 1981, Emelyanov, 2001). Indeed, mitochondria bear resemblance to their bacteria-like ancestors and display similar characteristics such as a double membrane, circular plasmid DNA and the ability to synthesise ATP across its membranes (Ernster and Schatz, 1981). This does, however, give rise to an extra challenge for dividing cells since mitochondria need to be segregated effectively. Efficient segregation is achieved through mitochondrial remodelling where mitochondria can divide and fuse with each other within the cell, which is known as mitochondrial dynamics. There is a constant cycle of fission, in which a singular mitochondrion divides into two mitochondria, and fusion, where a singular mitochondrion is formed by joining two mitochondria. Mitochondrial dynamics are of high importance for cells and defects in this mechanism are implicated in decreased cell health.

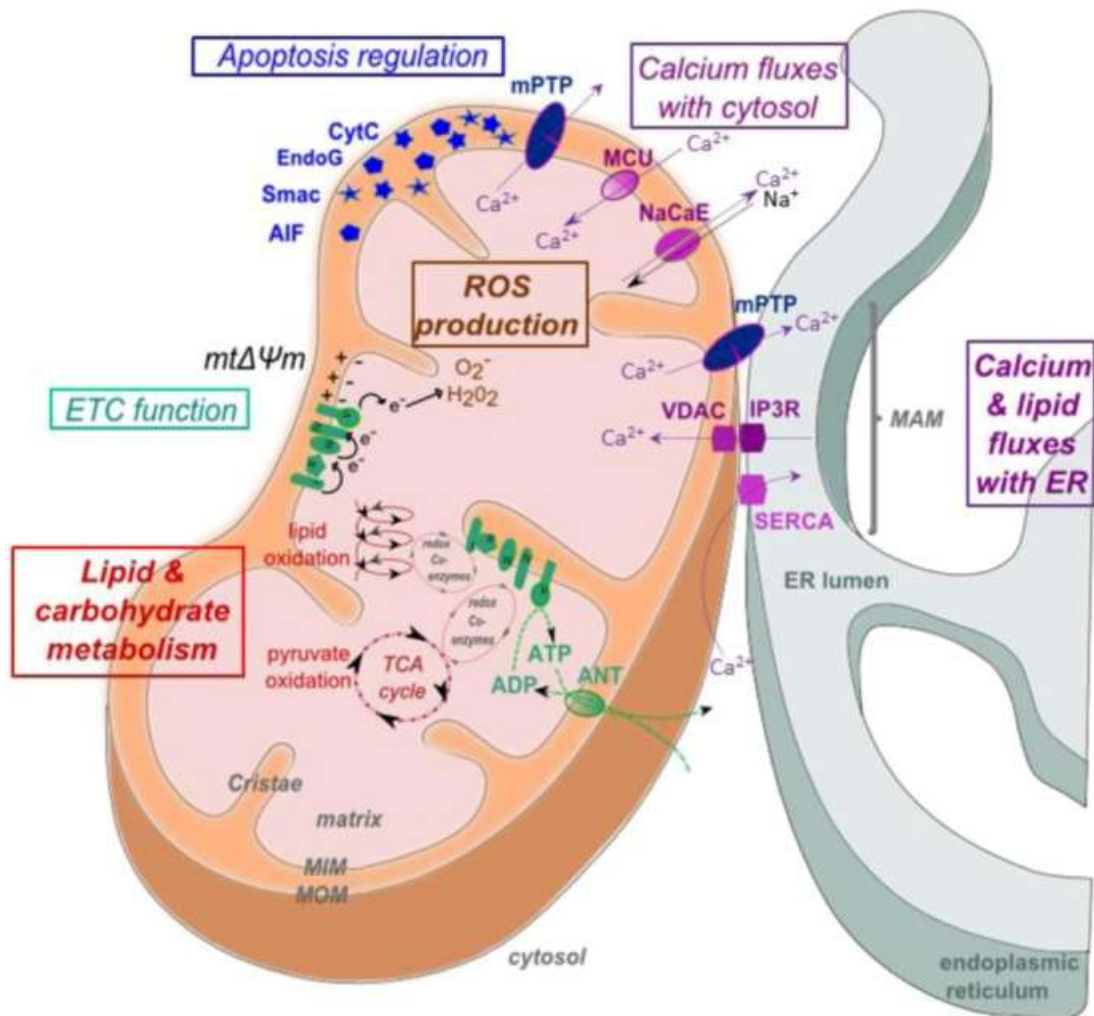


Figure 1.1.0. Mitochondrial structure and function. Mitochondria consist of a mitochondrial outer membrane (MOM), a mitochondrial inner membrane (MIM), the mitochondrial matrix, and cristae. The main functions of mitochondria are β -oxidation of fatty acids and oxidation of acetyl coenzyme A (acetyl-CoA) by the tricarboxylic acid (TCA) cycle (in red) and generation of ATP through the electron transport chain (ETC), which uses coenzymes generated by β -oxidation and TCA cycle as substrates (in green). Electrons that leak from the ETC cause the formation of reactive oxygen species (ROS) by reacting with O_2 (in brown). Other main functions of mitochondria include the regulation of apoptosis by release of caspase activators stored in the intermitochondrial membrane space upon pro-apoptotic signalling, leading to opening of the mitochondrial permeability transition pore (mPTP) (in blue), and exchange of Ca^{2+} with the cytosol via the mitochondrial calcium uniporter (MCU) and Na^+Ca^{2+} exchanger (NaCAE), and with the endoplasmic reticulum (ER) via the mPTP (in violet). ANT = adenine nucleotide translocase, IP3R = inositol triphosphate receptor, MAM = mitochondria-associated membrane, $mt\Delta\Psi_m$ = proton gradient, SERCA = sarco/endoplasmic reticulum calcium ATPase, VDAC = voltage-dependent anion channel. Figure adapted from (Brault et al., 2013).

1.1.1 Mitochondrial bioenergetics

Energy in cells is usually utilised in the form of ATP, providing free energy required for most cellular processes when hydrolysed. ATP is generated by either glycolysis or OXPHOS in mammalian cells, yielding a net amount of two or thirty-six molecules of ATP respectively, with OXPHOS being responsible for production of 80-90 % of ATP in healthy non-proliferative tissue (Lodish et al., 2000). Reduced electron carriers such as nicotinamide adenine dinucleotide (NADH) and reduced flavin adenine dinucleotide (FADH₂) feed electrons into ETC complexes, which is necessary for production of ATP, and several pathways have been implicated in their generation; fatty acid β -oxidation, amino acid oxidation, tricarboxylic acid cycle (TCA cycle, also known as Krebs cycle) and ETC complexes (Lodish et al., 2000, Nelson et al., 2008).

In short, four complexes (CI-IV) located on the mitochondrial inner membrane (MIM) make up the ETC (Figure 1.1.1). A proton (H⁺) gradient is created between the MIM and the intermembrane space (IMS) by free energy provided by electrons from NADH and FADH₂. H⁺ is pumped from the mitochondrial matrix into the IMS by the membrane spanning complexes of the ETC, namely CI, CIII, and CIV. A gradient across the membrane is created by pumping H⁺ against the concentration gradient, thereby effectively storing energy in the form of a transmembrane electrochemical gradient known as proton motive force (PMF). This results in a high concentration of protons forced into the IMS that travel back into the matrix containing a low proton gradient by another transmembrane complex known as ATP synthase (also referred to as CV), which is coupled to, but not part of, the ETC (Scheffler, 2007). Rotation of ATP synthase happens by energy generated by PMF and is used to form ATP by combining adenosine diphosphate (ADP) with inorganic phosphate (P_i). The adenine

nucleotide translocase (ANT) exchanges ATP for ADP and translocates the newly formed ATP to the cytosol.

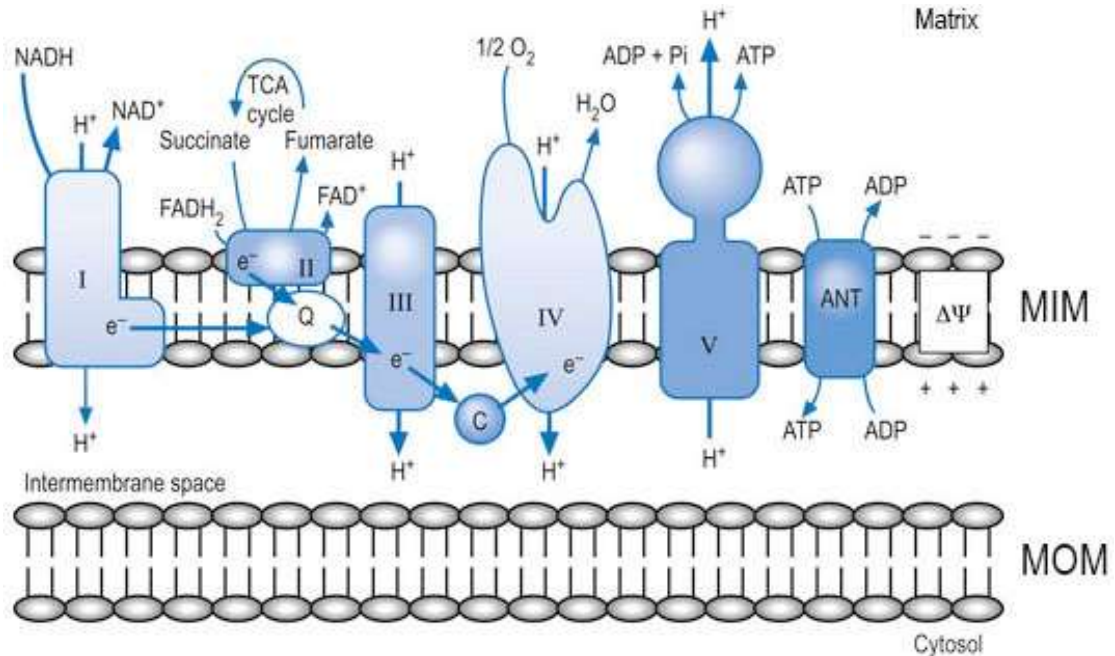


Figure 1.1.1. *Oxidative phosphorylation.* NADH and FADH₂ are used to create an electrochemical gradient by pumping H⁺ across the MIM via ETC complexes. Protons can travel back into the matrix through ATP synthase, thereby utilising the potential energy to generate ATP, which is translocated to the cytosol by ANT. Figure adapted from (Beck, 2008).

1.1.2 Mitochondrial dynamics

First thought to be static singular and isolated organelles in the cytoplasm, recent technological advances showed that mitochondria are actually arranged as a highly dynamic and interconnected tubular network within eukaryotic cells (Chen and Chan, 2009). Size, shape, structural organisation, and movement of mitochondria along the cytoskeleton is regulated by frequent fission and fusion events, which is a highly regulated process of critical importance to mitochondrial function. Maintenance of mitochondrial morphology, sharing and stability of mtDNA, respiratory capacity control, response to cellular stresses, and apoptosis are all processes regulated by

mitochondrial dynamics (Lee et al., 2004, Frezza et al., 2006, Detmer and Chan, 2007b).

Mitochondrial fission is necessary for cell division, since *de novo* mitochondria cannot be generated, as well as transport of mitochondria from the neuronal cell body to the synapse, and is facilitated by dynamin-related protein 1 (Drp1) (Scott and Logan, 2011). The exact mechanism by which Drp1 acts is currently unknown, but Drp1 is recruited from the cytosol to mitochondria and binds to an unidentified MOM receptor that likely results in constriction following oligomerisation, leading to scission of mitochondrial tubules (Chan, 2012) (Figure 1.1.2).

Mitochondrial fusion is important for promotion of exchange of mtDNA and other vital components and is carried out by mitofusin (MFN) 1 and 2 on separate adjacent mitochondria that fuse the MOM by forming homo-oligomeric and hetero-oligomeric complexes with themselves, bringing the outer membranes together. This tethers mitochondria, leading to fusion of the inner membrane regulated by optic atrophy 1 (OPA1) (Koshiba et al., 2004, Detmer and Chan, 2007a). Mutations in *OPA1* can lead to the development of optic atrophy that is caused by loss of retinal ganglion cells located in the inner retina and which project their axons via the optic nerve to the brain (Alavi and Fuhrmann, 2013). This leads to a slow progressive loss of bilateral visual function with an onset typically within the first two decades of life.

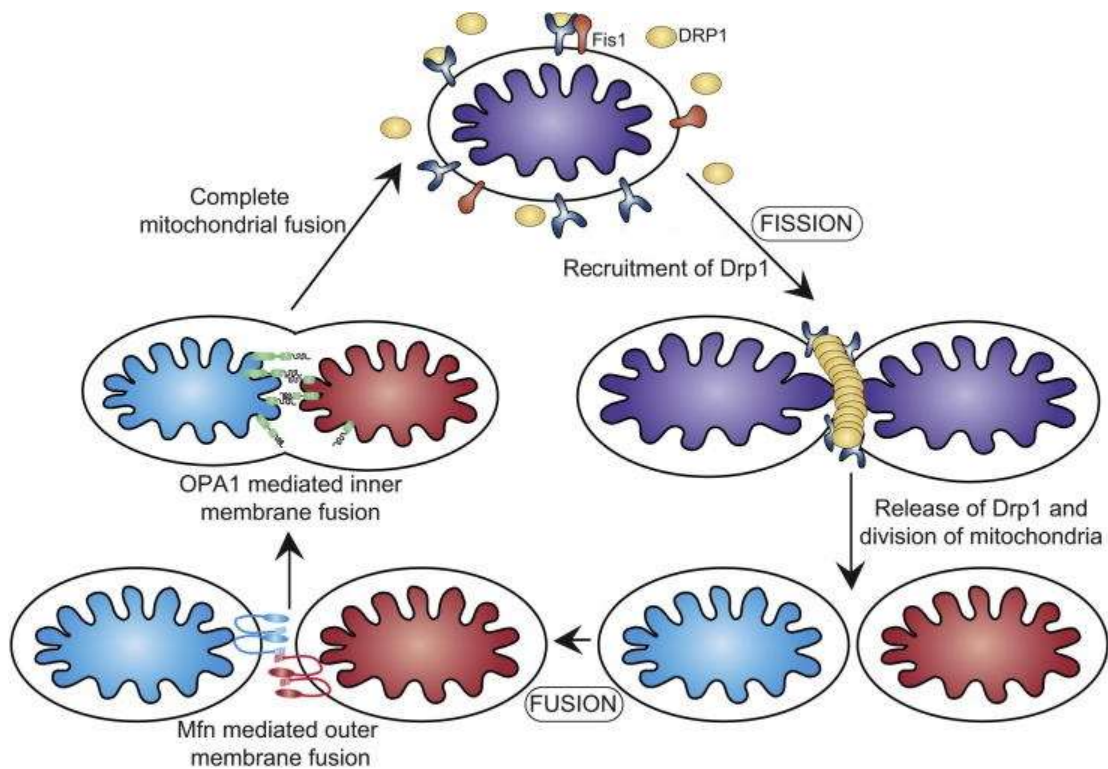


Figure 1.1.2. Mitochondrial dynamics. Mitochondrial fission is induced by recruitment of Drp1 to mitochondria, leading to scission of mitochondrial tubules. Mitochondrial fusion is a two-step process that requires outer membrane fusion facilitated by MFN, followed by inner membrane fusion promoted by OPA1. Figure adapted from (Osellame et al., 2012).

1.1.3 Mitochondrial dynamics and mitophagy

To carry out mitophagy, cells rely on mitochondrial dynamics to remodel their mitochondrial network. In order to maintain overall health of the mitochondrial network, mitochondrial parts suffering from unrecoverable damage are segregated from healthy mitochondria by fission, resulting in generation of two daughter mitochondria (Ikeda et al., 2015). The daughter mitochondrion with a normal membrane potential can fuse with other mitochondria, whereas the daughter mitochondrion with decreased membrane potential cannot, and this ultimately leads to its selective removal by mitophagy (Twig et al., 2008).

Research has shown that PINK1 and Parkin play a role in mitochondrial dynamics as well. The involvement of both PINK1 and Parkin in fission and fusion could serve as a mechanism to ensure successful fission of damaged mitochondria and prevention of fusion of damaged mitochondria with healthy mitochondria. Knockdown of PINK1 in neurons led to elongated mitochondria, suggesting it is involved in fission (Yu et al., 2011). PINK1 was found to displace protein kinase A (PKA), which normally phospho-inhibits Drp1, from the MOM, thereby ensuring fission of damaged mitochondria (Pryde et al., 2016). On the contrary, studies carried out in cell lines such as SH-SY5Y (Dagda et al., 2009, Lutz et al., 2009) and HeLa (Exner et al., 2007a) showed that mitochondria fragment upon PINK1 knockdown. However, it was proposed that this could be the result of excessive fission since an increase in fission proteins and decrease in fusion proteins was reported (Cui et al., 2010). Parkin, on the other hand, is responsible for inhibition of fusion by ubiquitination and subsequent proteasomal degradation of MFN1 and MFN2 (Gegg et al., 2010, Tanaka et al., 2010, Chen and Dorn, 2013, Sarraf et al., 2013).

1.2 Autophagy and its involvement in mitophagy

1.2.1 Classical control of autophagy

Autophagy, carried out by autophagy-related (ATG) proteins, mediates degradation of cytoplasmic components to recycle metabolites and can be activated by cellular stressors such as nutrient and energy starvation, damaged organelles, protein aggregates, and invading pathogens. Macroautophagy is the most prevalent form of autophagy and during this process, which is either selective or nonselective, a part of the cytoplasm is sequestered by the phagophore (isolation membrane), resulting in formation of a double-membraned vesicle called autophagosome in which

dysfunctional organelles and cytoplasm are sequestered (Figure 1.2.1.1). The autophagosome eventually fuses with a lysosome, becoming an autophagolysosome. The cargo of the autophagolysosome is degraded and released into the cytoplasm for reuse. Damaged or superfluous organelles, as well as other protein aggregates that could otherwise be toxic, are removed via selective autophagy.

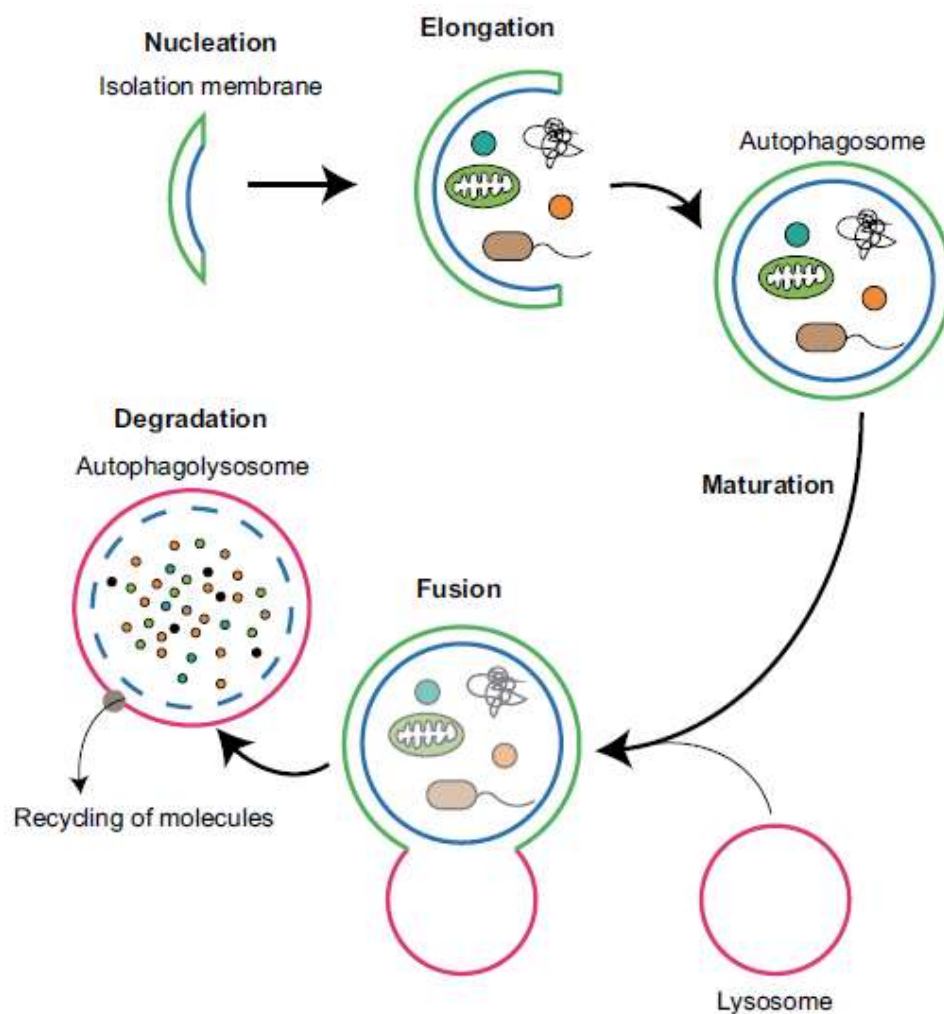


Figure 1.2.1.1. Overview of autophagy. Cellular stresses induce autophagy, which can be divided into several steps; formation of an isolation membrane (phagophore) around cytoplasmic material that needs to be sequestered (nucleation), elongation of the isolation membrane to form a double-membraned autophagosome (elongation), completion and transport of an autophagosome to a lysosome (maturation), docking and fusion between an autophagosome and a lysosome to form an autophagolysosome (fusion), and degradation of the cargo of an autophagolysosome (degradation). Figure adapted from (Nakamura and Yoshimori, 2017).

Contents needing to be degraded are ubiquitinated and recognised by sequestosome 1 (SQSTM1/p62, will be called p62 in remainder of thesis), which is an ubiquitin binding protein triggering degradation of proteins through either the proteasome or lysosome (Vadlamudi et al., 1996). p62 mediates clumping of ubiquitinated proteins and can bring aggregates to the autophagosome by direct binding to microtubule-associated protein 1 light chain 3B (LC3B) that is incorporated in the autophagosomal membrane, thereby being degraded itself as well (Pankiv et al., 2007).

The main nutrient-sensitive proteins involved in the autophagy pathway in mammals are glucose/energy sensing AMP-activated protein kinase (AMPK) and nutrient/growth factor sensing mechanistic target of rapamycin complex 1 (mTORC1) (Kim et al., 2011). Autophagy is promoted by activation of UNC-51-like kinase 1 (ULK1) that is inhibited by mTORC1 by means of phosphorylation under nutrient-rich conditions (Figure 1.2.1.2). In response to starvation, mTORC1 dissociates from the ULK1 complex (consisting of ULK1, ULK2, FIP200, ATG13, and ATG101), leading to dephosphorylation of ULK1 and trans-phosphorylation of ATG13 and FIP200, resulting in activation of the ULK1 complex (Hara et al., 2008, Ganley et al., 2009, Hosokawa et al., 2009a, Hosokawa et al., 2009b, Jung et al., 2009, Mercer et al., 2009). In addition, ULK1 can be activated by AMPK as well, either by direct phosphorylation of ULK1 (Bach et al., 2011, Kim et al., 2011) or by relieving mTORC1-mediated autophagy repression (AMPK is a negative regulator of mTORC1) (Inoki et al., 2003, Gwinn et al., 2008).

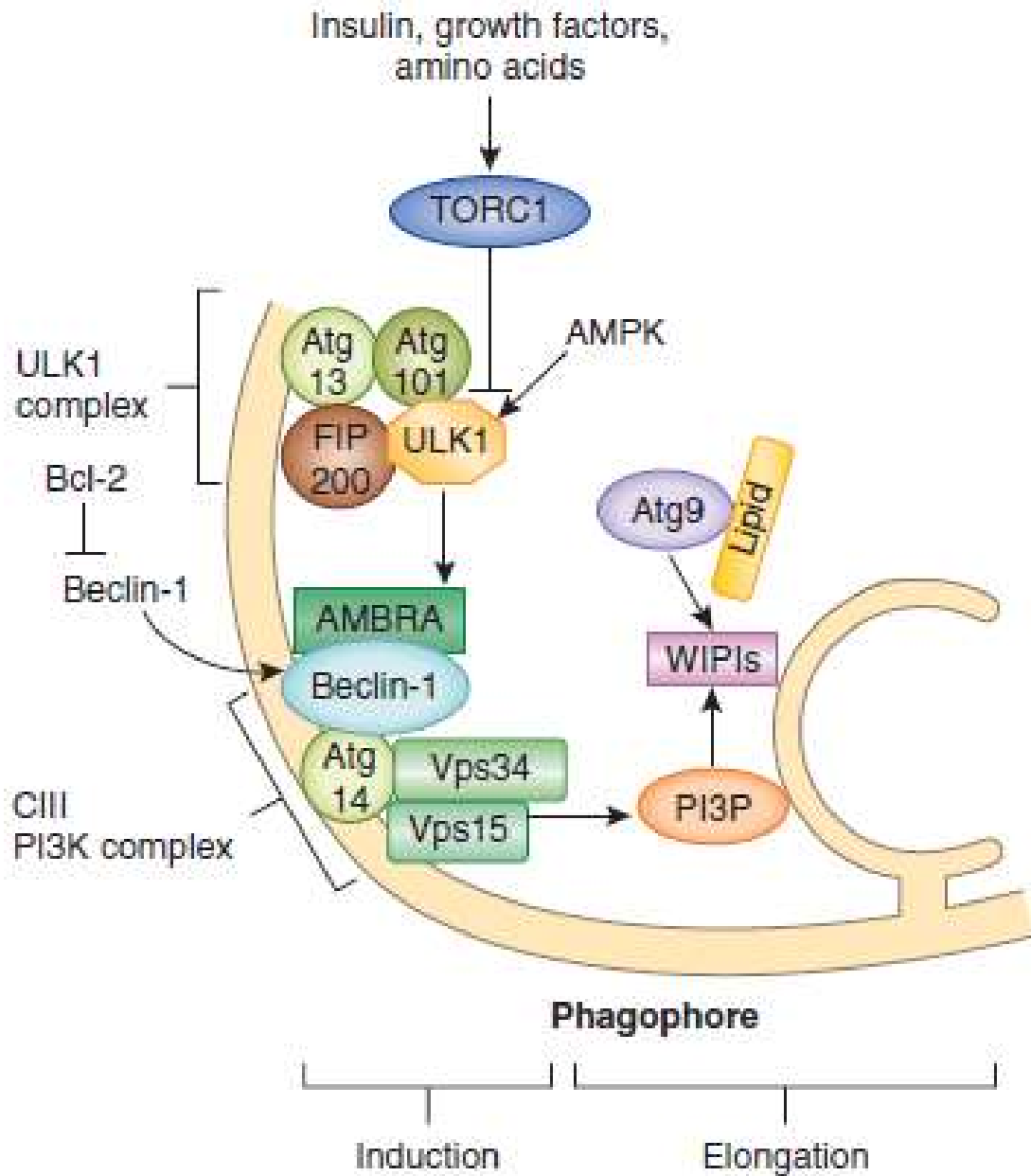


Figure 1.2.1.2. Autophagy induction. Autophagy is induced by either mTORC1 inhibition or AMPK activation, which results in ULK1 phosphorylation and subsequent activation of the ULK1 complex, consisting of ULK1, FIP200, ATG13, and ATG101. ULK1 phosphorylates Beclin1, which is a component of the phosphatidylinositol 3-kinase catalytic subunit type 3 (PIK3C3, described as CIII PI3K in Figure) complex together with hVps15, UVRAG, and ATG14L. This complex is normally tethered to the cytoskeleton, but localises to the phagophore upon ULK1-mediated phosphorylation of AMBRA1. Phosphatidylinositol 3-phosphate (PtdIns(3)P) is generated by the PIK3C3 complex and it specifically binds the PtdIns(3)P effectors WD repeat domain phosphoinositide-interacting protein 1 (WIP1) and WIP2 to catalyse the ubiquitination-like reactions that regulate elongation of the isolation membrane. Figure adapted from (Nixon, 2013).

Following ULK1 activation, ULK1 phosphorylates in turn Beclin1, which together with phosphoinositide-3-kinase, regulatory subunit 4 (PIK3R4, also known as hVps15), UV radiation resistance-associated gene (UVRAG), and ATG14L, is part of the phosphatidylinositol 3-kinase catalytic subunit type 3 (PIK3C3, also known as Vps34) complex (Kim et al., 2013, Russell et al., 2013, Russell et al., 2014). This complex is normally tethered to the cytoskeleton, but localises to the phagophore upon phosphorylation of autophagy/Beclin1 regulator 1 (AMBRA1) through ULK1 (Di Bartolomeo et al., 2010, Itakura and Mizushima, 2010, Matsunaga et al., 2010, Fan et al., 2011). Activation (Kim et al., 2013, Russell et al., 2013), regulation (Pattingre et al., 2005, Wei et al., 2008, Zalckvar et al., 2009), and correct localisation (Di Bartolomeo et al., 2010, Itakura and Mizushima, 2010, Fan et al., 2011) of the PIK3C3 complex is necessary for expansion of the membrane by generating phosphatidylinositol 3-phosphate (PtdIns(3)P) by phosphorylation of phosphatidylinositol (PtdIns) at the phagophore.

Another complex that is recruited to the phagophore is the ubiquitin-like (Ubl) conjugation system ATG5-ATG12-ATG16L, formed by ATG7 and ATG10, which is required for both elongation and targeting of LC3B to the isolation membrane (Mizushima, 1998, Mizushima et al., 2001, Tanida et al., 2001, Mizushima et al., 2002, Mizushima, 2003, Fujita et al., 2008b) (Figure 1.2.1.3). LC3B is processed by ATG4 into LC3B-I that is further transformed by ATG7 and ATG3 before finally being conjugated to phosphatidylethanolamine (PE) to form membrane-bound LC3B-II, which is considered to be important for biogenesis and closure of the isolation membrane (Kabeya et al., 2000, Tanida et al., 2001, Tanida et al., 2002, Kabeya et al., 2004, Tanida et al., 2006, Fujita et al., 2008a). LC3B-II localised to the outer

membrane of the complete autophagosome can be recycled via re-cleavage by ATG4B.

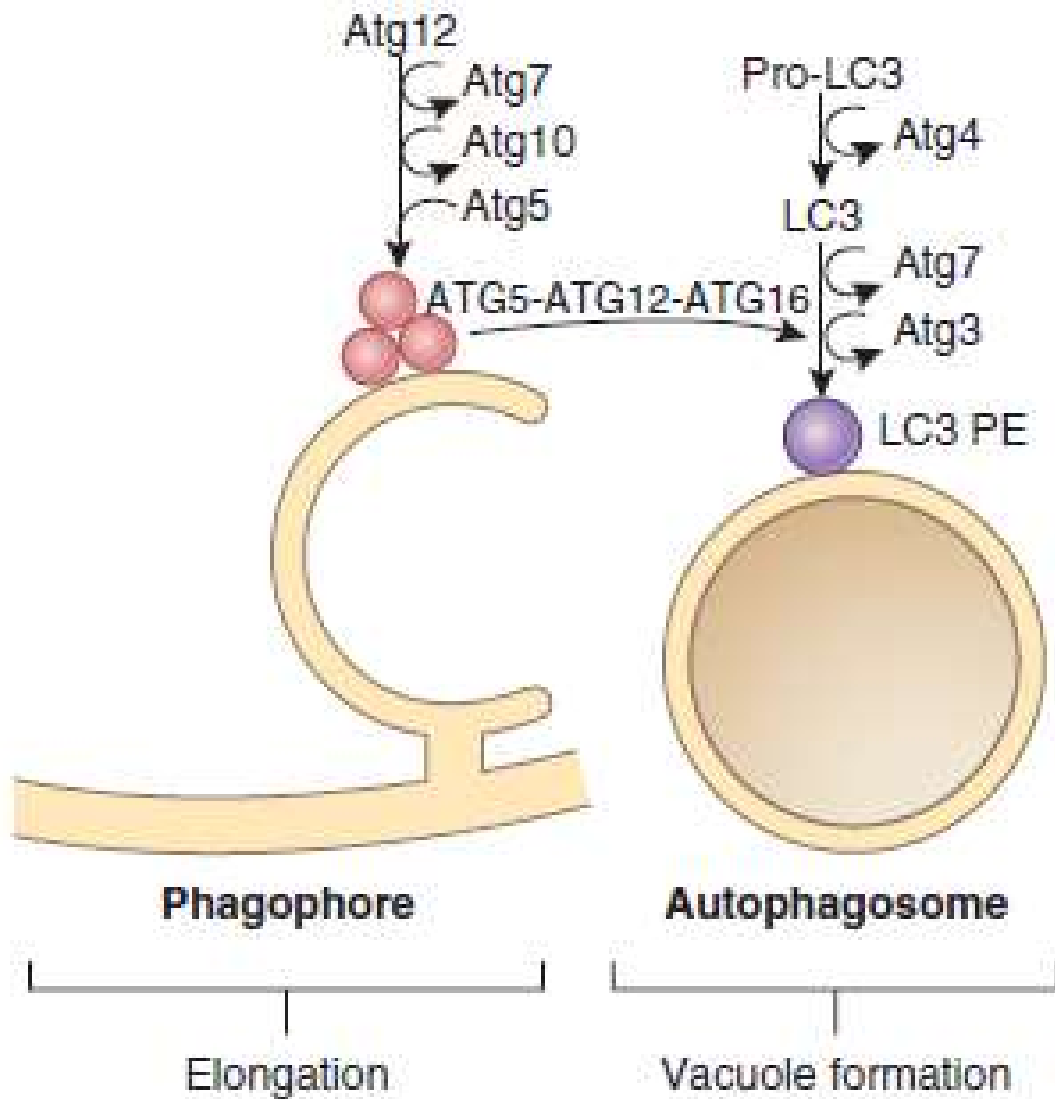


Figure 1.2.1.3. Autophagosome formation. Targeting of LC3B to the isolation membrane is mediated by the ATG5-ATG12-ATG16L3 ubiquitin-like conjugation system, which is formed in the presence of ATG7 and ATG10. Pro-LC3B is processed by ATG4 into LC3B-I that is subsequently processed by ATG3 and ATG7. The ATG5-ATG12-ATG16L3 complex induces the covalent conjugation of phosphatidylethanolamine (PE) to LC3B, forming LC3B-II, which facilitates closure of the isolation membrane. LC3B-II localised to the outer surface of an autophagosome can be removed by ATG4B, whereas LC3B on the inner surface is eventually degraded upon fusion between an autophagosome and a lysosome. Figure adapted from (Nixon, 2013).

1.2.2 Link between ULK1 and mitophagy

Mitophagy is thought to be a specialised type of autophagy and proteins involved in autophagy were found to play a role in mitophagy as well. Mitochondria are selectively cleared during reticulocyte maturation and defects were seen in this mitochondrial clearance in ULK1-knockout mice (Kundu et al., 2008). Moreover, ULK1-deficient mouse embryonic fibroblasts (MEF) had disruptions in mitochondrial clearance too, showing that involvement of ULK1, which is an important initiator of autophagy, in mitochondrial clearance is not restricted to reticulocytes. Treatment of MEF with the mitochondrial uncoupler carbonyl cyanide-4-(trifluoromethoxy)phenylhydrazone (FCCP) caused translocation of ULK1 to depolarised mitochondria, giving rise to ULK1 puncta that only emerged at mitochondria for a short period of time, suggesting ULK1 might merely function at the early stage of mitophagy (Itakura et al., 2012).

Not only ULK1, but also proteins of the ULK1 complex or ULK1 stabilisers are required for mitophagy. Inhibition or knockdown of a complex stabilising and activating ULK1, consisting of heat shock protein (Hsp) 90 that is likely involved in mitochondrial homeostasis and co-chaperone Cdc37, resulted in defective clearance of damaged mitochondria upon CCCP treatment (Joo et al., 2011). Loss of another protein important for stabilising ULK1, namely p32, a critical regulator of mitochondrial bioenergetics, led to impaired clearance of depolarised mitochondria (Fogal et al., 2010, Jiao et al., 2015). Lastly, either loss of AMPK, an upstream activator of ULK1, or inability of AMPK to phosphorylate ULK1, gave rise to abnormal p62 accumulation and defective mitophagy during nutrient deprivation (Egan et al., 2011).

1.2.3 Link between LC3B and mitophagy

Binding of ubiquitinated substrates on damaged mitochondria to LC3B incorporated in autophagosomal membranes could facilitate selective removal of these damaged mitochondria. During nutrient deprivation, it was demonstrated that an isolation membrane containing LC3B arised near mitochondria that grew to envelop and sequester parts of mitochondria or even whole mitochondria into autophagosomes, leading to degradation of mitochondrial contents (Kim and Lemasters, 2011a). In addition, endogenous LC3B was shown to be recruited to mitochondria during mitophagy, leading to LC3B decoration of mitochondria and their delivery to lysosomes (Stolz et al., 2017). Cells without ATG3, which is involved in conjugation of cytosolic LC3B-I to PE to form membrane bound LC3B-II associated with isolation membranes, still generated autophagosome-like structures close to mitochondria, but failed to enclose these neighbouring mitochondria, suggesting LC3B plays an essential role in incorporation of damaged mitochondria into autophagosomes (Itakura et al., 2012).

Moreover, different autophagy receptors involved in mitophagy have all been found to bind to LC3B directly. FUN14 domain containing 1 (FUNDC1) (Wu et al., 2014), Bcl-2/adenovirus E1B 19-kDa interacting protein 3 (BNIP3) (Hanna et al., 2012), its homologue NIP3-like protein X (NIX; also known as BNIP3L) (Novak et al., 2010), AMBRA1 (Novak et al., 2010, Hanna et al., 2012, Strappazon et al., 2014), prohibitin 2 (PHB2) (Wei et al., 2017), and FK506 binding protein 8 (FKBP8) (Bhujabal et al., 2017) all contain a LC3B interacting region (LIR) motif and enhanced LC3B recruitment and binding to damaged mitochondria during mitophagy.

A LIR motif is a short linear motif with the core consensus sequence W/F/Y-x-x-L/I/V that is surrounded by at least one acidic residue and that is found in all characterised LIR motifs to date (Johansen and Lamark, 2011). The conserved hydrophobic residues of the core LIR motif dock into hydrophobic pockets in the Ubl domain, while electrostatic interactions with the N-terminal arm of LC3B are formed by adjacent acidic residues. This leads to the formation of an extended β -conformation of the core LIR motif that forms an intermolecular parallel β -sheet with the β 2 strand of LC3B, allowing the LIR motif to interact with LC3B (Noda et al., 2010).

1.2.4 Link between p62 and mitophagy

The autophagy adaptor protein p62 mediates clumping of ubiquitinated proteins and recruitment of autophagosomes to ubiquitinated aggregates by binding to LC3B (Pankiv et al., 2007). Involvement of LC3B in mitophagy suggests p62 could play a part in it too. This hypothesis is supported by the finding that polyubiquitin chains on MOM proteins induced by Parkin are K63-linked (see section 1.3.8), which triggers autophagy by recruitment of p62 (Ding et al., 2010, Geisler et al., 2010, Lee et al., 2010). Nevertheless, requirement of p62 for successful mitophagy remains controversial and more research on this topic is needed.

Mitophagy was not affected or altered in p62-knockout cells, suggesting p62 is dispensable for mitophagy (Narendra et al., 2010b, Okatsu et al., 2010), whereas another study showed that loss of p62 led to disruptions in mitochondrial aggregation, sensitising cells to apoptosis upon mitochondrial depolarisation (Xiao et al., 2017). p62 was found to mediate mitochondrial aggregation and its recruitment to CCCP damaged mitochondria was promoted by Parkin (Ding et al., 2010, Geisler et al.,

2010, Lee et al., 2010, Narendra et al., 2010b, Okatsu et al., 2010). It was also shown that phosphorylation of p62 at Ser403 is vital for efficient autophagosomal engulfment of polyubiquitinated mitochondria since lack of Ser403 phosphorylation led to mitochondria not being enclosed by autophagosomes despite p62's ability to still interact with mitochondria (Matsumoto et al., 2015).

Taking the above into consideration, more studies have been published describing a role for p62 in mitophagy than studies that did not, suggesting p62 could indeed be necessary for effective mitophagy.

1.3 Mitophagy

1.3.1 Importance of mitophagy for cell viability and survival

Maintaining a healthy population of mitochondria is of key importance for a cell and defective mitophagy could have disastrous effects. Aged, damaged, and depolarised mitochondria release pro-apoptotic proteins, generate ROS, and their ATP hydrolysis can become ineffective, thereby opposing a threat to cellular well-being. Mitochondria are both a major source, as well as target, of ROS that are able to induce nuclear and mtDNA damage, to promote apoptosis, to induce immune responses, to damage membranes, and to deactivate enzymes by oxidation of cofactors (Turrens, 2003). Interestingly, ROS can have a negative impact on mitophagy too since they can affect Parkin solubility, leading to Parkin inactivation and aggregation (Wong et al., 2007). Cells can tackle harmful effects caused by ROS via ROS neutralisation through antioxidant systems under normal conditions, however, damaged mitochondria produce more ROS that exceed the capacity of the antioxidant system, which ultimately results in cell death.

1.3.2 Molecular sub-types of mitophagy

Three types of mitophagy have been described that have different modes of action (Lemasters, 2014). Type 1 mitophagy is likely carried out by receptors such as BNIP3 and NIX and is induced by nutrient deprivation. Individual mitochondria are sequestered by isolation membranes that grow into phagophores and eventually mature into autophagosomes, resulting in degradation by lysosomes (Kim and Lemasters, 2011a) (Figure 1.3.2). This type of mitophagy is often preceded by mitochondrial fission and mitochondrial depolarisation does not take place until sequestration is complete (Kim and Lemasters, 2011a, Lemasters, 2014).

Mitophagy type 2 is characterised by depolarisation of mitochondria, which leads to accumulation of PINK1 on the MOM and PINK1-dependent recruitment of Parkin (Narendra et al., 2010b). Parkin is responsible for ubiquitination of MOM proteins, marking them for autophagic engulfment (Narendra et al., 2008). LC3B binds to depolarised mitochondria, discontinuously at first, with a continuous ring formed over time (Kim and Lemasters, 2011b). Labelling by LC3B only occurs when mitochondria are depolarised for a substantial amount of time since mitochondria that subsequently repolarise did not display LC3B-labelling. Mitochondrial fission likely takes place, even though conflicting results have been published (Twig et al., 2008, Kim and Lemasters, 2011b). Lastly, it has been suggested that this type of mitophagy is likely carried out by autophagy adaptors, such as p62, which bind to ubiquitinated proteins instead of initiation by autophagy receptors.

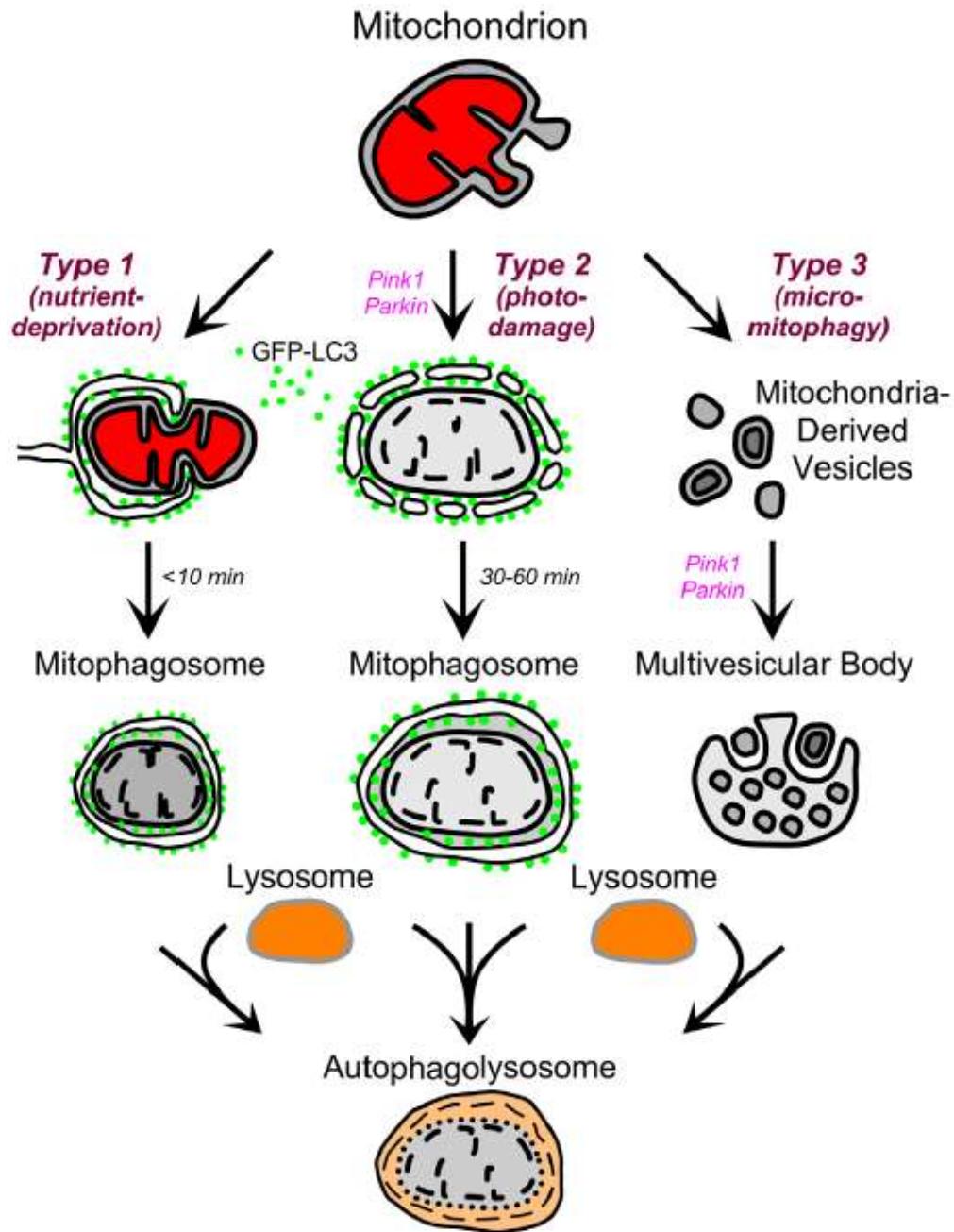


Figure 1.3.2. Molecular sub-types of mitophagy. Three types of mitophagy with different modes of action have been identified. Nutrient-deprivation activates type 1 mitophagy that is characterised by the formation of an isolation membrane close to an individual mitochondrion. These isolation membranes grow into phagophores and eventually mature into auto(mito)phagosomes that fuse with lysosomes. Mitochondrial depolarisation takes place in type 2 mitophagy, which leads to PINK1 accumulation on the MOM and PINK1-dependent recruitment of Parkin. LC3B binds to depolarised mitochondria, discontinuously at first, with a continuous ring formed over time. In type 3 mitophagy, which is driven by oxidative stress and that depends on PINK1 and Parkin, mitochondria-derived vesicles (MDV) bud off from mitochondria and fuse with multivesicular bodies, resulting in lysosomal degradation. Red denotes mitochondrial polarisation. Figure adapted from (Lemasters, 2014).

Damaged mitochondrial components can also be removed and degraded by formation of mitochondria-derived vesicles (MDV) that bud off and fuse with multivesicular bodies (a specialised subset of endosomes), which ultimately leads to lysosomal degradation (Soubannier et al., 2012a, Soubannier et al., 2012b). This type of micromitophagy is described as type 3 mitophagy and does not require mitochondrial depolarisation. MDV formation is driven by oxidative stress and occurs independently of ATG5 and LC3B, but does depend upon PINK1 and Parkin as well.

1.3.3 Hypoxia induced mitophagy

Upon hypoxia, mitochondria can be selectively removed by an ubiquitin (Ub)-independent mechanism mediated by mitochondrial receptors, namely BNIP3 and its homologue NIX, and FUNDC1 (Novak et al., 2010, Hanna et al., 2012). Both BNIP3 and NIX bind to LC3B, which is involved in phagophore membrane elongation, and gamma-aminobutyric acid receptor-associated protein (GABARAP) that is involved in later stages of autophagosome maturation (Weidberg et al., 2010), through their conserved LIR motifs (Novak et al., 2010, Hanna et al., 2012) (Figure 1.3.3.1). Loss of both BNIP3 and NIX inhibited hypoxia-induced mitophagy, whereas disruptions in interactions between BNIP3 and LC3B or NIX and LC3B did not completely block it, indicating that BNIP3 and NIX complement each other (Bellot et al., 2009, Novak et al., 2010, Hanna et al., 2012).

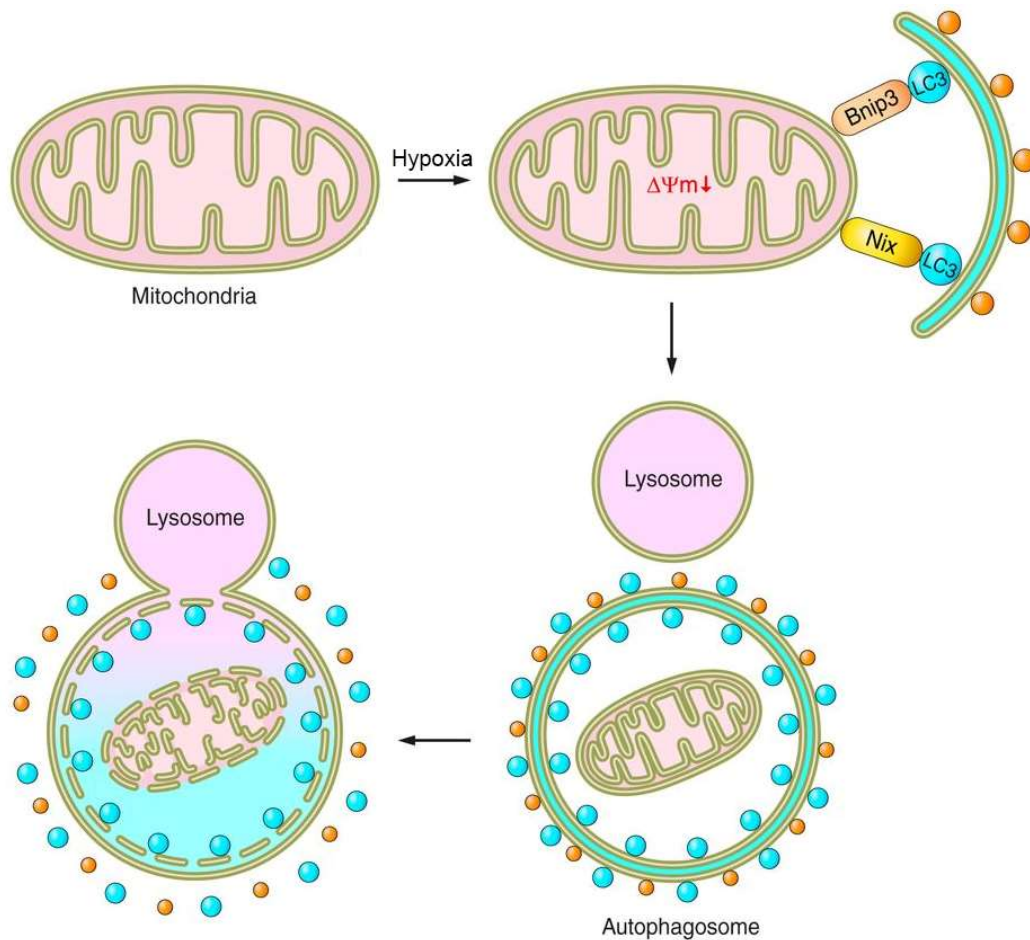


Figure 1.3.3.1. *BNIP3/NIX-mediated mitophagy upon hypoxia.* Upon hypoxia, BNIP3 and NIX on the MOM of damaged mitochondria can bind LC3B through their conserved LIR motifs, leading to phagophore formation and ultimately resulting in mitochondrial degradation through fusion between the formed autophagosome and a lysosome. Figure adapted from (Maejima et al., 2015).

The other identified mitochondrial receptor FUNDC1 is dephosphorylated upon hypoxia, allowing recruitment of ULK1 and ULK1-mediated phosphorylation of FUNDC1, which enhances FUNDC1's binding to LC3B (Liu et al., 2012, Wu et al., 2014) (Figure 1.3.3.2). FUNDC1 was also found to interact with both Drp1 and OPA1 to coordinate mitochondrial fission and fusion during mitophagy (Chen et al., 2016).

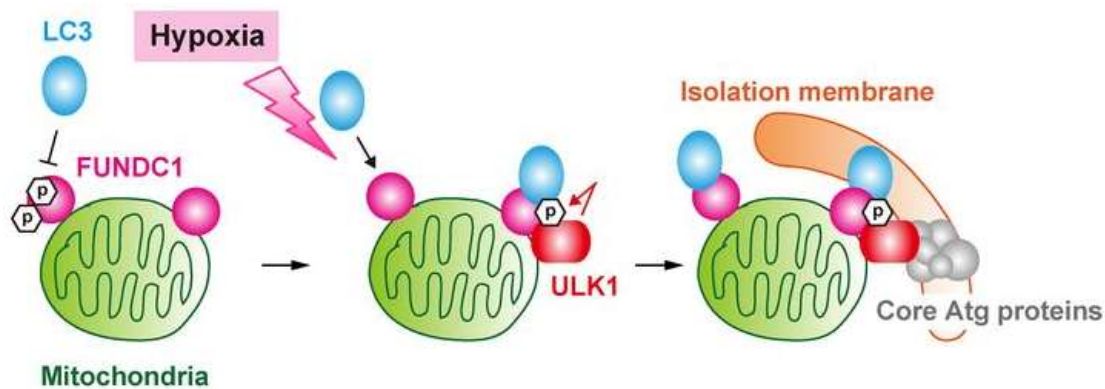


Figure 1.3.3.2. *FUNDC1-mediated mitophagy upon hypoxia.* The mitochondrial receptor FUNDC1 is normally phosphorylated, but dephosphorylates upon hypoxia, allowing ULK1 recruitment and ULK1-mediated phosphorylation of FUNDC1, which enhances the binding between FUNDC1 and LC3B. This leads to phagophore formation and ultimately results in mitochondrial degradation through fusion between the formed autophagosome and a lysosome. Figure adapted from (Okamoto, 2014).

1.3.4 Mitophagy induced by autophagy receptors

Not surprisingly, receptors important for efficient autophagy have been implicated in mitophagy too. AMBRA1, which is involved in targeting of the PIK3C3 complex to the phagophore, is activated upon mitophagy induction, leading to its binding to Beclin1 to initiate phagophore formation at a mitochondrion (Strappazzon et al., 2014) (Figure 1.3.4). AMBRA1 can bind LC3B through a LIR motif and does not require p62, suggesting AMBRA1 might act as an adapter by guiding damaged mitochondria to autophagosomes to facilitate mitochondrial clearance. AMBRA1 was also shown to interact with Parkin to promote mitochondrial clearance, suggesting two different mechanisms could exist that complement each other to allow efficient mitophagy (Van Humbeeck et al., 2011). Parkin, on one hand, ubiquitinates MOM proteins that can be recognised by p62, meaning that only pre-existing phagophores can be recruited to mitochondria since LC3B only associates with phagophores after they have started to form (Tooze and Yoshimori, 2010). AMBRA1, on the other hand, can

bind LC3B directly and does not require p62, therefore being able to induce phagophores at mitochondria directly by locally stimulating the activity of the PIK3C3 complex, which is essential for formation of new phagophores (Tooze and Yoshimori, 2010, Strappazon et al., 2014).

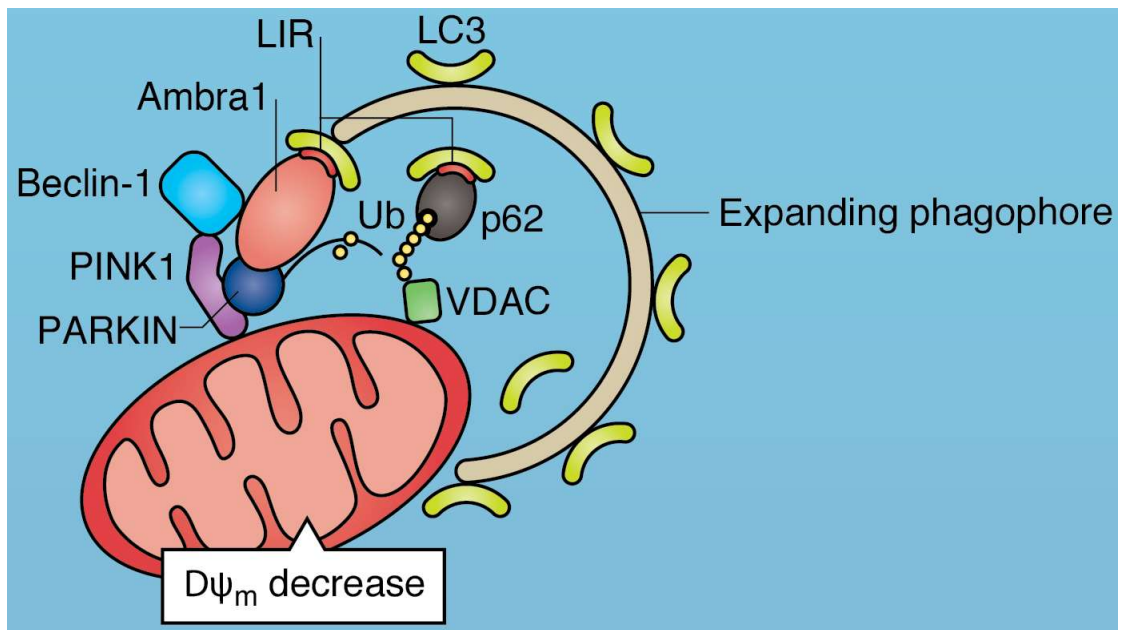


Figure 1.3.4. *AMBRA1* in *PINK/Parkin*-mediated mitophagy. Mitochondrial depolarisation leads to PINK1 accumulation, which selectively recruits Parkin, leading to ubiquitination of MOM proteins and p62 recruitment to allow binding to pre-existing phagophores. *AMBRA1* facilitates *PINK1/Parkin*-mediated mitophagy by interaction with Parkin to promote mitochondrial clearance. Activated *AMBRA1* binds to Beclin1 and it can directly bind LC3B too through its LIR motif to stimulate phagophore formation by locally stimulating PIK3C3 complex activity. Note that *AMBRA1* can also facilitate mitochondrial clearance independent of Parkin (not shown in figure). Figure adapted from (Cianfanelli et al., 2015).

The function of other autophagy receptors concerning mitophagy have not been extensively studied yet. Bcl-2-like protein 13 (Bcl2-L-13), the mammalian homologue of ATG32, the first described mitophagy receptor in yeast (Murakawa et al., 2015), PHB2 (Wei et al., 2017), and FKBP8 (Bhujabal et al., 2017) were all found to bind LC3B, whereas optineurin (OPTN) (Wong and Holzbaur, 2014, Wong and Holzbaur,

2015) and tax1-binding protein 1 (TAX1BP1) (Lazarou et al., 2015) merely recruited LC3B upon mitochondrial damage. OPTN and NPD52 (also known as calcium binding and coiled-coil domain 2 (CALCOCO2)) were identified as primary receptors for PINK1/Parkin-mediated mitophagy and were shown to be recruited to mitochondria by phosphorylated Ub that was mediated by PINK1 and enhanced by Parkin (Wong and Holzbaur, 2014, Lazarou et al., 2015, Wong and Holzbaur, 2015).

1.3.5 PINK1/Parkin-mediated mitophagy

PINK1/Parkin-mediated mitophagy is the most well-known type of mitophagy since *PINK1* and *PARK2* mutations are linked to PD. Damaged mitochondria are sensed by the serine/threonine kinase PINK1 that is imported into all mitochondria and then rapidly degraded and maintained at very low levels, while Parkin marks damaged mitochondria for autophagic engulfment by ubiquitination of specific mitochondrial proteins (Figure 1.3.5, left panel). The N-terminus of PINK1 contains a mitochondrial targeting signal (MTS), leading to its import through translocase of the outer mitochondrial membrane (TOM) complex on the MOM, consisting of TOM20, TOM22, TOM40, TOM70, as well as several other small Tom proteins (Valente et al., 2004, Neupert and Herrmann, 2007, Schmidt et al., 2010, Becker et al., 2012). Cleavage of the MTS by mitochondrial processing peptidase (MPP) takes place after full-length PINK1 (63 kDa) has been imported through the translocase of the inner mitochondrial membrane (TIM) complex, generating a PINK1 protein of ~60 kDa that is further cleaved in its conserved membrane anchor by presenilin associated rhomboid-like protease (PARL), generating a 52-kDa form of PINK1 that can exit mitochondria (Jin et al., 2010, Meissner et al., 2011). This 52-kDa form of PINK1 binds to cytosolic Parkin, thereby repressing its translocation to mitochondria (thus

inhibiting mitophagy) before it is recognized by ubiquitin protein ligase E3 component n-recognin (UBR) 1, UBR2, and UBR4, leading to its degradation by the proteasome (Yamano and Youle, 2013, Fedorowicz et al., 2014). However, a small subset of cleaved PINK1 was reported to be degraded by autophagy as well, which was likely mediated by UBR4 since UBR4 is involved in autophagy too (Tasaki et al., 2013, Kawajiri et al., 2010).

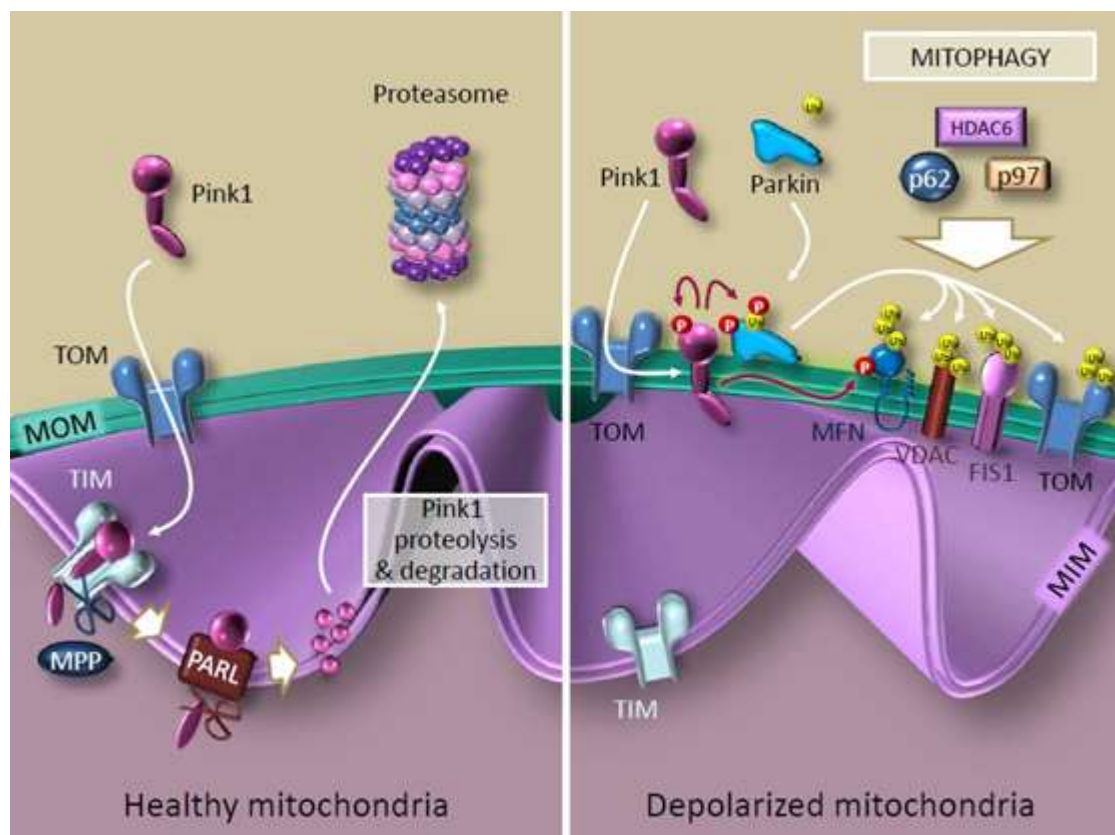


Figure 1.3.5. *Involvement of PINK1 and Parkin during mitochondrial depolarisation.* PINK1 is imported into the MIM in healthy mitochondria through the TOM and TIM complexes, where its MTS is cleaved by PARL, resulting in rapid degradation of PINK1 by the proteasome (left panel). Upon depolarisation, TIM-mediated import of PINK1 is impaired and PINK1 accumulates on the MOM, leading to selective recruitment of Parkin and ubiquitination of Parkin-targets on the MOM. Ubiquitinated proteins can recruit autophagy adaptors such as p62, HDAC6, or p97, which will recruit and tether the phagophore membrane, leading to induction of mitophagy. Figure adapted from (Von Stockum et al., 2015).

Degradation of PINK1 is inhibited upon loss of membrane potential. Mimicking mitochondrial damage with uncouplers, such as CCCP or FCCP that mainly affect membrane potential and transmembrane pH gradient, leads to PINK1 accumulation on the MOM (Jin et al., 2010, Narendra et al., 2010b) (Figure 1.3.5, right panel). PINK1 is still imported through the TOM complex, but cannot be processed by either MPP or PARL anymore, resulting in PINK1 accumulation on the MOM with its kinase domain facing the cytosol (Jin et al., 2010, Narendra et al., 2010b, Meissner et al., 2011). The PINK1 complex formed following a decrease in membrane potential consists of two PINK1 molecules and is correlated with intermolecular phosphorylation of PINK1 on Thr257 (Kondapalli et al., 2012, Okatsu et al., 2013). Other mitochondrial poisons that do not affect the MIM, such as ATP synthase and ETC inhibitors, do not lead to activation of PINK1 and concomitant phosphorylation of Parkin at Ser65 by PINK1, which is an important step in the activation of mitophagy (Kondapalli et al., 2012).

1.3.6 PINK1 interacts with Parkin

Following PINK1 accumulation on the MOM upon mitochondrial depolarisation, PINK1 selectively recruits Parkin to mitochondria. Processing, proper localisation, and autophosphorylation of PINK1 are required for activation of Parkin, which can take place via different mechanisms (Shi et al., 2011, Greene et al., 2012, Okatsu et al., 2012). Firstly, PINK1 can directly phosphorylate Parkin in its really interesting new gene (RING) finger domain at either Ser65 (Kim et al., 2008, Kondapalli et al., 2012, Shiba-Fukushima et al., 2012, Iguchi et al., 2013) or Thr175 and Thr217 (Kim et al., 2008), although some studies could not confirm these findings (Narendra et al., 2010b, Vives-Bauza et al., 2010, Lazarou et al., 2012). Secondly, PINK1 was reported

to locally induce self-association of Parkin, which is likely essential for its activation (Lazarou et al., 2012, Lazarou et al., 2013). Thirdly, PINK1 can directly phosphorylate Ub at Ser65, which in turn activates Parkin (Kazlauskaite et al., 2014). Parkin activation was only completely abrogated when both Parkin and Ub were mutated at Ser65, indicating that optimal activation of Parkin depends on phosphorylation of both proteins.

1.3.7 Parkin ubiquitinates proteins on the mitochondrial outer membrane

Upon translocation to mitochondria and activation by PINK1, Parkin mainly ubiquitinates MOM proteins to cause their degradation (Sarraf et al., 2013). Proteins that have been found to be ubiquitinated by Parkin include MFN1 and MFN2 (Gegg et al., 2010, Tanaka et al., 2010, Chen and Dorn, 2013, Sarraf et al., 2013), voltage-dependent anion channel (VDAC) 1, 2, and 3 (Geisler et al., 2010, Sun et al., 2012), mitochondrial Rho GTPases (MIRO) 1 and 2 (Birsa et al., 2014), mitochondrial fission 1 protein (FIS1) (Chan et al., 2011, Yamano et al., 2014), hexokinase 1 and 2, TOMM20, TOMM70, and p62 (Sarraf et al., 2013). Induced ubiquitination and degradation of MFN1 and 2 by Parkin is necessary for mitophagy to occur since it prevents activation of an inhibitory pathway in which depolarized and fragmented mitochondria become large spheroids that are not recognized by autophagosomes (Ding et al., 2012). However, not all MOM proteins are degraded during mitophagy. The anti-apoptotic protein Bcl-2 that is anchored to the MOM escapes degradation by translocation to the ER, which is essential for suppression of unwanted apoptosis during mitophagy (Shirane and Nakayama, 2003, Saita et al., 2013). This translocation depends on E3 activity of Parkin, indicating that Parkin also functions in prevention of apoptosis during mitophagy.

1.3.8 Involvement of the ubiquitin-proteasome system during mitophagy

Parkin requires two other classes of enzymes before it can ubiquitinate proteins. An E1 Ub-activating enzyme binds Ub and transfers it to the active site of an E2 Ub-conjugating enzyme, from where Ub is transferred onto lysine (K) residues of the substrate by a substrate-binding E3 ligase, in this case Parkin, resulting in protein ubiquitination (Pickart and Eddins, 2004). Ub itself contains seven lysines, positioned at amino residues 6, 11, 27, 29, 33, 48, and 63, and poly-Ub chains can be generated by addition of Ub to any of these lysines, resulting in different types of poly-Ub chains that have different cellular outcomes (Peng et al., 2003). Upon CCCP treatment, Parkin is able to induce both K48-linked and K63-linked polyubiquitination on mitochondria (Chan et al., 2011, Narendra et al., 2014). Parkin can amplify the signal by direct binding to and usage of K63-linked Ub-chains as a secondary docking site from where it can generate additional K63-linked Ub-chains (Zheng and Hunter, 2013). K48-linked polyubiquitination was found to activate the ubiquitin-proteasome system (UPS) (Ciechanover and Brundin, 2003), whereas K63-linked polyubiquitination triggers autophagy by recruitment of the Ub binding factors histone deacetylase 6 (HDAC6) and p62 (Ding et al., 2010, Geisler et al., 2010, Lee et al., 2010). Parkin itself can become ubiquitinated too by attachment of K6-linked Ub-chains, which likely plays a role in its own degradation (Durcan et al., 2014, Ordureau et al., 2014).

1.3.9 Effects of defective Parkin on mitochondrial health

Mutations in or loss of Parkin can have detrimental effects on cells. It has been shown that mutations in Parkin can lead to disruptions in its folding, generating an insoluble protein (Geisler et al., 2010, Narendra et al., 2010a), that Parkin translocation to

mitochondria upon mitochondrial depolarisation is halted, thereby inhibiting mitophagy (Geisler et al., 2010, Lee et al., 2010, Narendra et al., 2010a, Okatsu et al., 2010), that Parkin still translocates to mitochondria upon depolarisation, but that it is unable to clear them (Geisler et al., 2010, Lee et al., 2010, Narendra et al., 2010a, Okatsu et al., 2010), and that Parkin can still interact with PINK1, but that it does not lead to its stabilisation (Shiba et al., 2009).

In *Drosophila*, it was found that loss of Parkin led to defects in mitochondrial morphology and increased sensitivity to oxidative stress, which is a phenotype similar to loss of PINK1 function phenotypes (Clark et al., 2006). In *Drosophila* neurons, mitochondria also showed decreased CI and CIV activity and increased production of ROS upon loss of Parkin (Whitworth et al., 2005). Moreover, low mitochondrial membrane function and membrane potential, high amounts of mtDNA deletions, loss of DA neurons and DA levels in the SN, and severe neurobehavioral deficits were observed in Parkin knockout mice crossed with mice in which mtDNA deletions are specifically increased in the SN, suggesting that increase in mtDNA deletions with age contributes to DA neurodegeneration in mice/human with non-functional Parkin (Song et al., 2017).

1.3.10 Effects of defective PINK1 on mitochondrial health

Similarly to Parkin, loss of PINK1 is implicated in different mitochondrial defects in cells too. Stable knockdown of PINK1 induced mitochondrial fragmentation, increased oxidative stress levels, impaired mitochondrial handling of calcium, and reduced ATP synthesis, which coincided with decreased autophagy flux (Gautier et al., 2008, Dagda et al., 2009, Gegg et al., 2009). In addition to these defects,

deficiency in or deletion of the PINK1 homologue in *Drosophila* resulted in decreased CI activity and reduced levels of mtDNA and mitochondrial proteins, whereas mitochondria in PINK1 knockout mice had decreased membrane potential, increased ROS production, and were more sensitive to apoptotic stimuli that act through the mitochondrial pathway (Clark et al., 2006, Park et al., 2006, Morais et al., 2009, Wang et al., 2011a).

Based on studies performed in neurons, it became clear that mitochondrial defects caused by defective or mutated PINK1 can have broad effects on cellular mechanisms. PINK1-deficient rats, for instance, exhibited decreased CI and increased CII activity in their striatal synaptic mitochondria and proteomics illustrated that PINK1 deficiency led to defects in fatty acid metabolism, oxidation reduction, and generation of precursor metabolites and energy (Stauch et al., 2016, Villeneuve et al., 2016). Neuronal stem cells generated from *PINK1*^{-/-} mice also presented with mitochondrial defects, as well as elevated levels of glycolysis and increased apoptosis (Agnihotri et al., 2017). In *Drosophila* neurons, reduced ATP levels caused by PINK1 deficiency were responsible for altered synaptic function (Morais et al., 2009). Young PINK1 mutant flies did not show any loss of DA neurons, however, DA neuron numbers were significantly decreased in 30 days old flies (Park et al., 2006). These flies also had reduced TH, necessary for DA synthesis, and DA levels. The finding that PD-linked mutant PINK1 upregulated TH and DA levels in DA neurons, leading to increased vulnerability to oxidative stress, further strengthened the link between PINK1, TH, and DA, and suggests that PINK1 might have widespread functions extending beyond mitophagy (Zhou et al., 2014).

1.3.11 Effects of PD linked mutations on mitochondrial health in patient samples

Most experiments concerning the effects of defective or loss of PINK1 or Parkin are carried out in cell lines or animal models and often require overexpression of the mutants, which could lead to artefacts. Use of human induced pluripotent stem cells (hiPSC) derived from PD patients would be a more suitable method for studying PINK1 and Parkin in relation to PD. hiPSC can be differentiated into DA neurons, demonstrating the power of this model for PD-related research.

Parkin mutated hiPSC-derived neurons were unable to execute mitophagy and had abnormal mitochondrial morphology, impaired mitochondrial homeostasis, and increased oxidative stress (Imaizumi et al., 2012). More studies confirmed abnormal mitochondrial morphology, in which reduced mitochondrial volume, increased susceptibility to mitochondrial toxins, and reduced amount of differentiated DA neurons were also found (Shaltouki et al., 2015, Chung et al., 2016). Other cellular processes, such as DA uptake and release (Jiang et al., 2012), microtubule dynamics (Ren et al., 2015), proteasomal degradation and anti-oxidative pathway (Chang et al., 2016), and apoptosis (Konovalova et al., 2015), were affected, suggesting that Parkin is likely involved in different processes in DA neurons.

PINK1 mutant hiPSC-derived DA neuronal cells, on the other hand, were more sensitive to cell death and production of ROS and showed increased rate of basal oxygen consumption and proton leakage, suggesting mitochondria were intrinsically damaged (Cooper et al., 2012). These cells also had decreased mitochondrial membrane potential and CI activity (Morais et al., 2014). Furthermore, no reduction in mtDNA upon mitochondrial depolarisation was detected, which was observed in

wildtype (WT) hiPSC, suggesting mitophagy did not take place (Seibler et al., 2011). Interestingly, the authors found that peroxisome proliferator-activated receptor-gamma coactivator-1 α (PGC-1 α) levels were significantly increased in PINK1 mutant cells. PGC-1 α is an important inducer of mitochondrial biogenesis, which might suggest that upregulation of this protein could be a compensatory response to restore mitochondrial function.

1.4 Aim of thesis

Over the past ten years, mitophagy has received a lot of attention from the scientific community, however, uncertainties concerning its regulation and involvement of autophagy still exist. Defective mitophagy is implicated in PD, though it has been mainly studied in non-neuronal cells, which might not reflect the mitophagic process in neurons. Therefore, it is important to study mitophagy in a more appropriate setting, namely neuronal cells.

The aims of this thesis were:

- 1) Characterisation of mitophagy and involvement of proteins regulating autophagy and/or proteasomal degradation during mitophagy in a neuroblastoma (SH-SY5Y) cell line.
- 2) Assessment whether mitophagy can be induced in undifferentiated mouse embryonic stem cells (mESC) and which autophagy-related proteins are involved in this process.
- 3) Examination on whether mitophagy can be successfully induced in a control and PD hiPSC line containing a *SNCA* triplication and which autophagy and/or proteasomal degradation related proteins are involved.
- 4) Evaluation of differences between control and PD hiPSC in terms of mitophagy.

Chapter 2

Material and Methods

2.0 Materials

2.0.1 Equipment

Balances (Satorius, TE64 and TE412)

Cell culture hood (NuAire laminar flow hood)

ChemiDoc MP Imaging System (BioRad)

Countess® Automated Cell Counter (Invitrogen)

Electroblot transfer tanks (BioRad, Trans-blot Cell; Invitrogen, XCell II Blot Module)

Electrophoresis power supply (BioRad)

Eppendorf 5424 microcentrifuge (Thermo Electron Corporation)

Eppendorf 5810R refrigerated microcentrifuge (Thermo Electron Corporation)

Eppendorf Personal cycler with heated lid

Gilson Pipettes; P2, P10, P20, P200 & P1000

Heat block (Stuart, SBH 200D)

LightCycler Nano (Roche)

LUNA-II automated cell counter (Logos Biosystems)

Mammalian cell culture incubator (Sanyo CO2 incubator)

Microscope (Nikon Eclipse TS100; Olympus BX51 upright microscope)

Mr. Frosty (Thermo Fisher Scientific)

NanoDrop spectrophotometer ND-1000

pH meter (Hanna instruments)

PipetteAid (Drummond Scientific)

Rocker (See-saw rocker SSL4, Stuart)

Scanner (EPSON 4990 Perfection)

SDS-PAGE systems (Invitrogen, Mini-Cell; BioRad, Criterion Cell)

Spectrophotometer (Eppendorf, BioPhotometer)

Vibra Cell Sonicator; Stepped Microtip, 630-0422 (Sonics)

Vibrax shaker (IKA Vibrax, VXR Basic)

Vortex (Scientific Industries, Genie 2)

Water bath (Grant JB Series)

2.0.2 Chemicals

All chemicals and reagents were obtained from Sigma Aldrich (Wicklow, Ireland) or Melford (England), unless indicated otherwise.

Acrylamide (40 %; Santa Cruz Biotechnology)

Ammonium persulfate (APS; BioRad)

Bafilomycin A1 (Enzo Scientific)

β -glycerol phosphate (Calbiochem)

Bicine

Bis-Tris

β -mercaptoethanol

Bovine serum albumin (BSA)

Butan-1-ol

Calcium chloride

CHAPS

Chlorobutanol

Chloroform

Chloroquine (Roche)

Complete Protease Inhibitor Cocktail, EDTA free (Roche)

Coomassie plus assay reagent (Thermo Fisher Scientific)

Crystal Violet

Cycloheximide (CHX)

DAPI

Dimethylsulfoxide (DMSO)

Dithiothreitol (DTT)

EDTA

EGTA

Enhanced chemiluminescent (ECL) HRP substrate detection kit (Millipore)

Ethanol

FCCP

Formaldehyde (37 %)

HEPES

High-performance liquid chromatography (HPLC) grade water

Hydromount (Thermo Fisher Scientific)

Immobilon-P polyvinylidene difluoride transfer (PVDF) membrane (Millipore)

Isopropanol

LDS sample buffer 4x (Invitrogen)

MES

Methanol

MG132 (Calbiochem)

MOPS

Non-fat dried milk powder (Marvel)

PD184352 (Rudy Marquez, University of Glasgow)

PerfeCTa SYBR Green FastMix 2x (VWR)

Ponceau S

Potassium chloride

Potassium phosphate monobasic

Precision plus protein all blue standards (BioRad)

Protein G Sepharose beads (GE Biosciences)

qScript cDNA SuperMix 5x (VWR)

Rapamycin (Calbiochem)

SAR405 (University of Dundee)

Sodium chloride

Sodium dodecyl sulfate

Sodium fluoride

Sodium orthovanadate

Sodium phosphate

Sodium phosphate dibasic heptahydrate

Sodium pyrophosphate

Sucrose

TEMED

Tris Base

Triton X100

TRIzol (Invitrogen)

Tween 20

V34-IN1 (University of Dundee)

Whatman 3MM blotting and chromatography paper (Thermo Fisher Scientific)

2.0.3 Tissue culture reagents and media

All media and reagents were obtained from Sigma Aldrich (Wicklow, Ireland) or Invitrogen/Gibco (Paisley, Scotland), unless indicated otherwise.

0.25% Trypsin-EDTA dissociation media

2.5% Trypsin (10x)

Accutase

Ascorbic acid

B-27 supplement (50x)

Brain-derived neurotrophic factor (BDNF; Miltenyi Biotech)

CHIR99021

Collagenase IV

dbcAMP

Dulbecco's modified Eagle's medium (DMEM)

Dulbecco's modified Eagle's medium (DMEM) + GlutaMAX

Dulbecco's modified Eagle's medium (DMEM)/Nutrient mixture F-12 Ham 1:1

Dulbecco's modified Eagle's medium (DMEM)/Nutrient mixture F-12 Ham 1:1 +

GlutaMAX

Dulbecco's phosphate-buffered saline (D-PBS)

Eagle's minimum essential medium (MEM) non-essential amino acid solution (100x)

Earle's Balanced Salt Solution (EBSS)

EmbryoMax ES cell qualified fetal bovine serum (Millipore)

Epidermal growth factor (EGF; Miltenyi Biotech)

Fibroblast growth factor 8b (FGF8b; Miltenyi Biotech)

Foetal bovine serum (FBS; Labtech)

Gelatin from cold water fish skin

Glial cell line-derived neurotrophic factor (GDNF; Miltenyi Biotech)

Human basic fibroblast growth factor (FGFb; Miltenyi Biotech)

Human leukaemia inhibitory factor (hLIF)

KnockOut Dulbecco's modified Eagle's medium (KO-DMEM)

KnockOut Dulbecco's modified Eagle's medium (KO-DMEM)/Nutrient mixture F-12

Ham 1:1

KnockOut serum replacement

L-glutamine (200 mM)

Matrigel (BD biosciences)

mFreSR (STEMCELL Technologies)

N-2 supplement (100x)

Neurobasal medium

Normocin (Invivogen)

Penicillin/Streptomycin

Rho-associated, coiled-coil containing protein kinase (ROCK) inhibitor (BD Biosciences)

SB 431542

Sonic Hedgehog (SHH; Miltenyi Biotech)

StemMACS iPS-Brew XF basal medium (Miltenyi Biotech)

StemMACS iPS-Brew XF supplement 50x (Miltenyi Biotech)

StemMACS passaging solution XF (Miltenyi Biotech)

Trypan blue

2.0.4 Buffers and solutions

CTK solution:

5 mL 2.5% Trypsin 10x, 5 mL 1 mg/mL Collagenase IV, 0.5 mL 0.1 M calcium chloride, 10 mL KnockOut serum replacement, 30 mL ddH₂O.

HEPES buffered saline (HBS):

140 mM sodium chloride, 0.75 mM sodium phosphate dibasic heptahydrate, 25 mM HEPES, pH 7.05.

LDS protein electrophoresis sample buffer (4x):

900 µL 4 x LDS sample buffer, 100 µL 500 mM dithiothreitol.

Low salt buffer:

50 mM Tris Base, pH 7.5, 1 mM EGTA, 1 mM EDTA, 1 mM activated sodium orthovanadate, 10 mM β-glycerol phosphate, 50 mM sodium fluoride, 5 mM sodium pyrophosphate, 0.27 M sucrose, 0.3 % (w/v) CHAPS, 0.1 % (v/v) β-mercaptoethanol.

Lysis buffer:

50 mM Tris Base, pH 7.5, 1 mM EGTA, 1 mM EDTA, 1 mM activated sodium orthovanadate, 10 mM β-glycerol phosphate, 50 mM sodium fluoride, 5 mM sodium pyrophosphate, 0.27 M sucrose, 0.3 % (w/v) CHAPS. 0.1 % (v/v) β-mercaptoethanol and Complete Protease Inhibitor Cocktail (1 tablet per 50 mL of buffer) were added just before use.

MES SDS NuPAGE protein electrophoresis buffer:

50 mM MES, pH 7.7, 50 mM Tris Base, 3.5 mM sodium dodecyl sulfate, 1 mM EDTA.

MOPS SDS NuPAGE protein electrophoresis buffer:

50 mM MOPS, pH 7.7, 50 mM Tris Base, 3.5 mM sodium dodecyl sulfate, 1 mM EDTA.

Phosphate-buffered saline solution (PBS):

137 mM sodium chloride, 2.7 mM potassium chloride, 10 mM sodium phosphate, 1.8 mM potassium phosphate monobasic, pH 7.4.

Stripping buffer:

Tris buffered saline solution, pH 7.5, 2% (w/v) sodium dodecyl sulfate with 0.1 % (v/v) β -mercaptoethanol added just before use.

Tris-buffered saline solution (TBS):

2 mM Tris Base, pH 7.5, 15 mM sodium chloride.

Tris-buffered saline solution-Tween 20 (TBS-T):

2 mM Tris Base, pH 7.5, 15 mM sodium chloride, 0.1 % (v/v) Tween 20.

Western blotting blocking buffer:

5% (w/v) non-fat dried milk solution in tris-buffered saline solution-Tween.

Western blotting transfer buffer:

25 mM Bicine, pH 7.2, 25 mM Bis-Tris, 1 mM EDTA, 50 μ M chlorobutanol.

2.0.5 Antibodies

Antibodies used for immunofluorescence (IF), immunoprecipitation (IP), or Western blot (WB) analysis, are listed in Table 2.0.5 (commercial primary antibodies), Table 2.0.6 (lab made primary antibodies), and Table 2.0.7 (horseradish peroxidase (HRP)-conjugated or fluorescent-labelled secondary antibodies).

Name	Species	Dilution	Manufacturer
β -actin	Mouse	1:10,000	Sigma
p44/42 MAPK (ERK1/2)	Rabbit	1:2,000	Cell Signaling
p-p44/42 MAPK (pERK1/2; T202/Y204)	Mouse	1:2,000	Cell Signaling
LAMP1	Mouse	1:2,000	Antibodies-online
mTORC1	Rabbit	1:1,000	Cell Signaling
p-mTORC1 (S2448)	Rabbit	1:1,000	Cell Signaling
p62/SQSTM1	Rabbit	1:1,000	MBL
Parkin	Mouse	1:200	Santa Cruz Biotechnology
PINK1	Rabbit	1:500	Novus Biologicals
		1:200	Santa Cruz Biotechnology
S6K1	Rabbit	1:1,000	Santa Cruz Biotechnology
p-S6K1 (Thr389)	Rabbit	1:1,000	Santa Cruz Biotechnology
TIM23	Mouse	1:1,000	BD Transduction Laboratories
TOM20	Mouse	1:1,000 IF	BD Transduction
		1:1,000 WB	Laboratories
ULK1	Rabbit	1:200	Santa Cruz Biotechnology
UVRAG	Rabbit	1:500	Imgenex
VDAC1	Rabbit	1:1,000	Abcam

Table 2.0.5. Commercial primary antibodies.

Name	Species	Concentration	Source
Beclin1 (S633C)	Sheep	2.0 µg IP	Murray lab
		0.1 µg/mL WB	
p-Beclin1 (Ser30)	Rabbit	0.5 µg/mL	Murray lab
hVps15 (S634B)	Sheep	0.5 µg/mL	Murray lab
LC3B (S623C)	Sheep	1 µg/ mL IF	Murray lab
		0.5 µg/mL WB	
PIK3C3 (S284C)	Sheep	2.0 µg IP	Murray lab
		0.5 µg/mL WB	

Table 2.0.6. *Lab made primary antibodies.*

Antibody generated	Host species	Dilution	Manufacturer
Alexa Fluor 488 α -Rabbit	Donkey	1:1,000	Thermo Fisher Scientific
Alexa Fluor 488 α -Sheep	Donkey	1:1,000	Thermo Fisher Scientific
Alexa Fluor 594 α -Mouse	Donkey	1:1,000	Thermo Fisher Scientific
Rabbit-HRP	Goat	1:10,000	Thermo Fisher Scientific
Sheep-HRP	Rabbit	1:10,000	Thermo Fisher Scientific
Mouse-HRP	Rabbit	1:10,000	Thermo Fisher Scientific
Protein G-HRP		1:2,000	BioRad

Table 2.0.7. *Horseradish peroxidase-conjugated (HRP) and fluorescent-labelled secondary antibodies.*

2.1 Cell culture

All cell culture work was done under sterile conditions in a NuAire laminar flow hood. Cells were maintained at 37 °C and 5 % CO₂ (7.5 % CO₂ for HEK293T cells) in a humidified incubator and cell growth and viability were monitored daily using a Nikon Eclipse TS100 light microscope. Cell numbers and cell viability were assessed by exclusion of trypan blue dye and determined with the use of Countess or LUNA-II automated cell counters.

2.1.1 Maintenance of cultured cell lines

SH-SY5Y cells were kindly provided by Dr. Daniela Zisterer (Trinity College Dublin, Dublin) and were maintained in a 1:1 mixture of Dulbecco's modified Eagle's medium (DMEM) and Nutrient mixture F-12 Ham (F-12) supplemented with 10 % foetal bovine serum (FBS), 100 units/mL penicillin, and 100 µg/mL streptomycin. Human Embryonic Kidney 293T (HEK293T) cells were obtained from Cancer Research, UK cell repository and were grown in DMEM supplemented with 10 % FBS, 100 units/mL penicillin, and 100 µg/mL streptomycin. Cells were cultured in T75 or T175 flasks until they reached 80-90 % confluency and were then subcultured, usually every 6-7 days for SH-SY5Y cells and every 2-3 days for HEK293T cells.

2.1.2 Maintenance of undifferentiated mouse embryonic stem cells

46C mouse embryonic stem cells (Sox-1-GFP knock-in ESCs) were a kind gift from Dr. Gavin Davey (Trinity College Dublin, Dublin) and were cultured in KnockOut DMEM supplemented with 15 % knockout serum replacement, 100 units/mL penicillin, 100 µg/mL streptomycin, 2 mM L-glutamine, 1x non-essential amino acids (NEAA), 0.1 mM β-mercaptoethanol, and 10 µg/mL human leukaemia inhibitory factor (hLIF). 46C cells were maintained in gelatin coated T25 flasks (0.1 % gelatin from cold water fish skin) that were prepared freshly before use. Gelatin (3 mL for T25 flask and 2 mL for 6-well plates) was incubated at room temperature (RT) for 30 minutes after which it was aspirated. Flasks or plates were dried for 1 hour at 37 °C and were washed once in phosphate-buffered saline (PBS) before use. 46C cells were passaged every other day and medium was changed in between passages if it turned yellow. Fresh 46C medium was made every two weeks.

2.1.3 Maintenance of undifferentiated human induced pluripotent stem cell colonies

Undifferentiated PD AST23 (EDi001-A, female, 50-54 years old) human induced pluripotent stem cells (hiPSC) were obtained from Dr. Gavin Davey (Trinity College Dublin, Dublin) through the TINTIN network. Undifferentiated PD hiPSC colonies were maintained in 6-well plates and first cultured on a feeder layer consisting of mouse embryonic fibroblasts (MEF) in order to grow and expand them (see Table 2.1.3 for cell culture media recipes). Plates were coated with 1 mL 0.1 % gelatin solution (cold water fish skin) for 10 minutes at 37 °C prior to the addition of MEF. MEF were seeded (60,000-70,000 cells/well) one day before introducing undifferentiated PD hiPSC colonies, whereas medium was changed from MEF medium to hiPSC medium 1 hour before the addition of undifferentiated PD hiPSC colonies. An inhibitor of Rho-associated, coiled-coil containing protein kinase (ROCK; 10 μ M final concentration) was added when undifferentiated PD hiPSC colonies were introduced for the first time. Cells were allowed to adjust for 2 days after which the medium (without ROCK inhibitor) was changed daily until colonies were ready to be picked.

Undifferentiated PD hiPSC colonies were maintained feeder free in Matrigel coated plates in StemMACS iPS-Brew XF medium (see Table 2.1.3 for recipe) in order to be able to differentiate them. Matrigel was thawed on ice approximately 1 hour before use and was used at a 1:100 dilution in KnockOut DMEM. One millilitre of Matrigel was added to a 6-well plate and was incubated at RT for at least 1 hour. Matrigel was aspirated before undifferentiated PD hiPSC colonies were transferred to the plate. Medium was changed daily.

Cell line	Medium	Supplements
MEF	DMEM + GlutaMAX	10 % FBS, 100 units/mL penicillin, 100 µg/mL streptomycin, 1x NEAA, 0.001 % β-mercaptoethanol
NPC (BDNF medium)	1:1 mixture of ND medium (with supplements) and Neurobasal medium	0.5 % penicillin/streptomycin, 0.5 % NEAA (1x final concentration), 0.5 % L-Glutamine (2 mM final concentration), 0.5 % N-2 supplement (1x final concentration), 1 % B-27 supplement (1x final concentration), 10 ng/mL BDNF, 10 ng/mL GDNF, 10 µM dbcAMP, 100 µM ascorbic acid*
NPC (DopaNPC medium)	1:1 mixture of ND medium (with supplements) and Neurobasal medium	0.5 % penicillin/streptomycin, 0.5 % NEAA (1x final concentration), 0.5 % L-Glutamine (2 mM final concentration), 0.5 % N-2 supplement (1x final concentration), 1 % B-27 supplement (1x final concentration), 3 µM CHIR99021, 2 µM SB 431542, 10 ng/mL hLIF
NPC (ND medium)	1:1 mixture of DMEM/F-12 + GlutaMAX	100 units/mL penicillin, 100 µg/mL streptomycin, 1x NEAA, 2mM L-Glutamine, 1x N-2 supplement, 1x B-27 supplement
NPC (SHH medium)	1:1 mixture of ND medium (with supplements) and Neurobasal medium	0.5 % penicillin/streptomycin, 0.5 % NEAA (1x final concentration), 0.5 % L-Glutamine (2 mM final concentration), 0.5 % N-2 supplement (1x final concentration), 1 % B-27 supplement (1x final concentration), 20 ng/mL EGF, 20 ng/mL FGF8b, 25 ng/mL SHH, 100 µM ascorbic acid*
Undifferentiated colonies on Matrigel	StemMACS iPS-Brew XF basal medium	2 % StemMACS iPS-Brew XF 50x supplement, 100 µg/mL Normocin
Undifferentiated colonies on MEF (hiPSC medium)	1:1 mixture of KnockOut DMEM/F-12	20 % KnockOut serum replacement, 100 units/mL penicillin and 100 µg/mL streptomycin, 1x NEAA, 2 mM L-glutamine, 0.001 % β-mercaptoethanol, 20 ng/mL FGFb

Table 2.1.3. Specific media supplementation as required for hiPSC. * Ascorbic acid was added freshly before use to the required volume of medium.

2.1.4 Picking of undifferentiated human induced pluripotent stem cell colonies

The process of picking undifferentiated PD hiPSC colonies is the same for both colonies grown on MEF or colonies grown feeder free. Colonies that were ready to be picked were big and often appeared to be dense in the centre of the colony. Colonies of which its centre was turning dark were starting to differentiate and were ignored. A p20 Gilson pipette was used to scrape colonies into roughly six parts. Colonies were gently scraped off the bottom of the plate and 20 μ L of cells was taken up. A total of 60 μ L of cells (approximately 1.5 colony) was added to 1 mL of appropriate medium in a new plate that either contained MEF (in hiPSC medium) or was coated with Matrigel (in StemMACS iPS-Brew XF medium). Cells were allowed to attach overnight in the incubator at 37 °C. An extra 1 mL of medium was added the following morning and the medium was changed daily until colonies were ready to be picked.

2.1.5 Freezing of undifferentiated human induced pluripotent stem cell colonies

ROCK inhibitor (10 μ M final concentration) was added to the undifferentiated PD hiPSC colonies maintained on MEF 1 hour prior to freezing. Colonies were washed once in PBS and were incubated with 1 mL of CTK solution for 4-5 minutes at 37 °C. After washing the colonies twice in PBS, 1 mL of hiPSC medium was added and colonies were carefully scraped with a cell scraper (Corning). Intact colonies were transferred to a 15 mL Falcon tube (Corning) and were centrifuged at 300 rcf for 5 minutes. Medium was removed and colonies were resuspended in 1 mL freezing medium (500 μ L hiPSC medium, 400 μ L ES cell qualified FBS, 100 μ L dimethylsulfoxide (DMSO)). Vials were transferred to a Mr. Frosty freezing container

(Thermo Fisher Scientific) and were left at -80 °C overnight before being relocated to liquid N₂ for long-term storage.

Undifferentiated PD hiPSC colonies cultured in Matrigel coated plates were first washed in PBS before adding 800 µL StemMACS passaging solution XF to each well. The passaging solution was carefully removed after a 4 minute incubation period at RT and 2 mL of KnockOut DMEM/F-12 (without supplements) was used to wash the colonies. Another 2 mL of KnockOut DMEM/F-12 (without supplements) was added and colonies were scraped with a cell scraper. Intact colonies were transferred to a 15 mL Falcon tube and were centrifuged for 5 minutes at 300 rcf. Medium was removed and colonies were resuspended in 1 mL mFreSR. Vials were transferred to a Mr. Frosty freezing container and were left at -80 °C overnight before being relocated to liquid N₂ for long-term storage.

2.1.6 Generation of neuronal precursor cells

Neuronal precursor cells (NPC) were generated from undifferentiated PD hiPSC colonies cultured on Matrigel. About 7-10 manually picked undifferentiated PD hiPSC colonies in a single well were cultured for 3 days in StemMACS iPS-Brew XF medium before changing the medium to DopaNPC medium (see Table 2.1.3 for recipes of the media). Undifferentiated PD hiPSC colonies were maintained in DopaNPC medium for 7 days and medium was changed every 2 days. Colonies were not picked during this period. Medium was removed after these 7 days and PD hiPSC were washed once in PBS. PD hiPSC were detached by the addition of 1 mL Accutase that was incubated for 7 minutes at 37 °C. PD hiPSC were centrifuged for 5 minutes at 600 rcf and split 1:3. Medium was changed every 2 days and PD hiPSC were

subcultured 1:3 once a week for 6 weeks after which the stable NPC line was generated that was split 1:10 regularly.

2.1.7 Differentiation of neuronal precursor cells into dopaminergic neurons

NPC generated from hiPSC of a healthy donor (male, 23 years old) were a generous gift from Prof. Patrick Schloss (CIMH, Mannheim). NPC were seeded at a density of 30,000 cells/well in Matrigel coated 6-well plates and were allowed to settle overnight. The medium was changed to SHH medium (see Table 2.1.3 for recipe) the following day and NPC were cultured in this medium for 14 days to induce a midbrain phenotype. NPC were not subcultured and medium was changed every 2 days. Terminal differentiation of NPC into dopaminergic neurons was induced by culturing the cells in BDNF medium for 4 weeks. Medium was changed every 2 days.

2.2 Cell viability assays

2.2.1 Crystal Violet assay

SH-SY5Y cells were stained with Crystal Violet to measure cell proliferation. SH-SY5Y cells were seeded at a concentration of 4×10^5 cells per well in a 6-well plate and were incubated overnight. Cells were treated with different inhibitors for 24 hours after which they were washed once in PBS and fixed with 100 % methanol on the see-saw rocker for 10 minutes. Cells were stained with 0.5 % Crystal Violet solution for 10 minutes on the see-saw rocker, followed by several washes in a large beaker of water until excess stain had been removed. Plates were allowed to air-dry overnight after which they were destained by the addition of 1 % sodium dodecyl sulfate (SDS) to each well. Plates were placed on the see-saw rocker for several minutes until the Crystal Violet dye had been released. Five hundred microliter of this solution was

transferred to a cuvette and the absorbance was read at 563 nm on a spectrophotometer. Dilutions of the destained samples were made using 1 % SDS in case the concentrations were beyond the detection limits of the instrument and the samples were re-read.

2.3 Microscopy

2.3.1 Immunocytochemistry

SH-SY5Y cells or NPC were cultured on uncoated or Matrigel coated 13 mm glass coverslips (VWR) respectively, to a confluency of approximately 50-60 %. Cells were washed once in PBS after treatments of interest and were fixed in 3.7 % formaldehyde in PBS for 20 minutes, which was followed by permeabilisation of cells with 0.1 % Triton X100 in PBS for 10 minutes. To reduce nonspecific binding of antibodies, cells were blocked in 3 % bovine serum albumin (BSA) in PBS for 20 minutes. Both primary (see Table 2.0.5 & 2.0.6) and fluorescent-labelled secondary (see Table 2.0.7) antibodies were diluted in 3 % BSA in PBS and were incubated for 1 hour each. DAPI was used as a counterstain at a concentration of 0.5 µg/mL in PBS and was incubated for 5 minutes prior to mounting coverslips on glass slides with the use of Hydromount. Cells were washed three times in PBS between different steps and both secondary antibody and DAPI incubations were carried out in the dark. Slides were stored in the dark at 4 °C until imaged. Imaging was done using an Olympus BX51 upright microscope and a 60x oil immersion objective.

2.4 Molecular biology

2.4.1 Calcium phosphate transfection

SH-SY5Y cells were split to 50 % confluency on uncoated coverslips in 6-well plates 1-2 hours prior to transfection. A calcium chloride/DNA precipitate was prepared by the addition of 12.2 μL 2 M calcium chloride and 4 μg DNA to sterile ddH₂O (final volume 0.1 mL). The calcium chloride/DNA precipitate was slowly added to 0.1 mL 2x HEPES buffered saline (HBS) solution and this mixture was added to cells dropwise. Cells were incubated for 16-24 hours at 37 °C after which they were washed and maintained in fresh medium. Cells were treated with different chemical reagents for different time points before fixation (see section 2.3.1).

2.4.2 RNA isolation

SH-SY5Y cells or NPC cultured in 6-well plates were treated with 5 μM carbonyl cyanide-4-(trifluoromethoxy)phenylhydrazone (FCCP) for different time points after which they were washed once in PBS. Cells were trypsinised for 5 minutes at 37 °C (7 minutes with accutase for NPC) and trypsinisation was neutralised with fresh medium. Cells were pelleted at 250 x g (600 ref for NPC) for 5 minutes at RT and 1 mL of TRIzol was added directly to unwashed cells after removal of the supernatant. Samples were homogenised by pipetting and incubated for 5 minutes at RT after which they were snap frozen in liquid N₂ and stored at -20 °C.

RNA was separated by the addition of 0.2 mL chloroform. Samples were shaken vigorously for 15 seconds and incubated for 3 minutes at RT before centrifugation at 12,000 x g for 15 minutes at 4 °C. The upper aqueous phase containing the RNA was removed and transferred to a new microcentrifuge tube. RNA was precipitated by the

addition of 0.5 mL isopropanol and was incubated for 10 minutes at RT before centrifugation at 12,000 x g for 10 minutes at 4 °C to obtain RNA pellets. The supernatant was removed and the RNA pellets were washed twice in 0.5 mL 75 % ethanol, were vortexed briefly, and were centrifuged at 7,500 x g for 5 minutes at 4 °C. The ethanol was removed and pellets were allowed to air dry. RNA pellets were resuspended in 30 µL high-performance liquid chromatography (HPLC) grade water and were heated for 10 minutes at 60 °C. Concentration and purity of RNA was determined with the use of a NanoDrop spectrophotometer ND-1000. RNA was stored at -80 °C.

2.4.3 cDNA synthesis

RNA was diluted to a concentration of 100 ng/µL for cDNA synthesis. cDNA reactions were set up on ice and to a final volume of 10 µL in RNase-free microcentrifuge tubes, containing 5 µL 100 ng/µL prepared RNA, 2 µL qScript cDNA SuperMix 5x, and 3 µL HPLC grade water. Samples were mixed by vortexing and were briefly centrifuged. Reactions were cycled for 5 minutes at 25 °C, 30 minutes at 42 °C, and 5 minutes at 85 °C, after which they were kept at either 4 °C for short term storage or at -20 °C for long term storage. cDNA synthesis was carried out with an Eppendorf Personal cycler with heated lid.

2.4.4 Real-time quantitative polymerase chain reaction (RT-qPCR)

cDNA was diluted 1:10 in HPLC grade water following cDNA synthesis. Biological replicates were run in triplicate and RNA samples were run to check for genomic DNA contamination. Reactions of 10 µL were set up on ice in LightCycler Nano 8-tube strips (Roche) and consisted of 5 µL PerfeCTa SYBR Green FastMix 2x, 2.5 µL

HPLC grade water, 0.5 μ L primers, and 2 μ L 1:10 diluted cDNA. Strips were briefly centrifuged before placing in a LightCycler Nano (Roche). The LightCycler was set to run for a 2 minute initial denaturation at 95 °C, followed by a 45 cycle amplification of 95 °C for 10 seconds and 60 °C for 45 seconds. Prevalidated RealTime ready Parkin, PINK1, and 18s primers were purchased from Roche with 18s being the housekeeping gene used for normalisation.

2.5 Protein analysis

2.5.1 Preparation of cell extracts

Plates or dishes were placed on ice and medium was aspirated. Cells were washed in ice-cold PBS once and excess PBS was removed by aspiration. Cells were lysed in 100-200 μ L lysis buffer, depending on size of culture dish to generate protein lysates between 1-2 mg/mL. Cells were scraped and transferred to microcentrifuge tubes. Whole cell lysates were either used immediately or snap frozen in liquid N₂ and stored at -20 °C for later analysis.

Protein concentrations were determined by Bradford Assay. In duplicate, 2 μ L of whole cell lysate was added to 500 μ L of Coomassie plus assay reagent, which was vortexed briefly and was incubated for 10 minutes in the dark at RT. Absorbance was read at 595 nm on a spectrophotometer. Protein concentrations were calculated against a pre-determined BSA standard curve (0.025-1.5 mg/mL) that was prepared for each bottle of Coomassie plus protein assay reagent separately.

2.5.2 SDS-poly-acrylamide gel electrophoresis (SDS-PAGE)

To prepare samples for SDS-poly-acrylamide gel electrophoresis (SDS-PAGE) analysis, 4x NuPAGE LDS sample buffer containing dithiothreitol (DTT; 1:10) was added to whole cell lysates to obtain a final concentration of 1x LDS. Samples were sonicated using a MicroTip sonicator (20 % output, two times for 5 seconds) and heated for 10 minutes at 70 °C. Whole cell lysates were separated by gel electrophoresis on 8 % and 10 % Bis-Tris gels, depending on protein size to be analysed. Gels were prepared according to the recipes in Table 2.5.2.

	Stack	Resolve	
	4%	8%	10%
Acrylamide:Bis (30 % : 2 %) [mL]	0.500	2.000	2.500
1.25 M Bis Tris, pH 6.7 [mL]	1.071	2.143	2.143
Water [mL]	2.144	3.287	2.787
10 % APS [μ L]	25	50	50
TEMED [μ L]	10	20	20

Table 2.5.2. Recipes for SDS-PAGE gels.

The resolving gel was overlaid with a small layer of butan-1-ol saturated against 1.25 M Bis-Tris solution to ensure a boundary level between stacking and resolving gel. The butanol overlay was rinsed off with distilled water once resolving gel had set and stacking gel was poured on top. Gels were run in either MOPS or MES buffer, depending on the mass of proteins that required separation. Depending on the cell line, 20-30 μ g of protein was loaded and samples were run alongside precision plus protein all blue standards to determine progress of protein migration. Gels were run at 150 V until protein markers were sufficiently separated.

2.5.3 Western immunoblotting

Proteins resolved by SDS-PAGE were transferred onto Immobilon-P polyvinylidene difluoride transfer (PVDF) membrane by wet electroblotting. In short, PVDF membrane was activated in methanol and pre-soaked in transfer buffer. A sandwich was made with a pre-soaked sponge pad and a sheet of Whatman 3MM filter paper at the cathode (-), followed by gel, PVDF membrane, and another pre-soaked sheet of Whatman 3MM paper and sponge pad at the anode (+). Proteins were electroblotted in transfer buffer for either 2 hours at 40 V or 8 hours at 10 V at 4 °C.

In case it was deemed necessary, the efficiency and quality of SDS-PAGE and electroblotting were confirmed by brief staining of the membranes with Ponceau S that was washed away with tap water. Next, membranes were incubated in 5 % (w/v) non-fat dried milk solution in tris-buffered saline with Tween 20 (TBS-T) for either 1 hour at RT or overnight at 4 °C to reduce non-specific antibody binding. Membranes were incubated with primary antibodies diluted in blocking buffer according to Table 2.0.5 & 2.0.6 for 2 hours at RT. After washing in TBS-T three times for 10 minutes, membranes were incubated for 1 hour at RT with horseradish peroxidase (HRP)-conjugated secondary antibodies generated specifically against the primary antibody species (Table 2.0.7). Membranes were washed three times for 10 minutes in TBS-T and protein detection was carried out using enhanced chemiluminescent (ECL) HRP substrate detection kit. Signal generated by the HRP substrate was promptly detected using a ChemiDoc MP Imaging System. Intensity of protein bands was quantified densitometrically using ImageJ software, if required.

2.6 Protein-protein interactions

2.6.1 Immunoprecipitation

Whole cell extracts for immunoprecipitation (IP) were obtained as described in section 2.5.1. To remove insoluble material, protein lysates were clarified by centrifugation at 16,000 x g for 15 minutes at 4 °C. Supernatant was transferred to a new microcentrifuge tube and protein concentration was measured by Bradford Assay (see section 2.5.1). A volume of around 1 mg of protein was transferred into a new microcentrifuge tube and volumes were normalised with lysis buffer. Desired proteins were immunoprecipitated by overnight incubation with appropriated antibodies (see Table 2.0.6) on a vibrax shaker at 4 °C. Immunocomplexes were captured by adding 20 µL of a 50 % Protein G Sepharose beads slurry (pre-washed in distilled water followed by low salt buffer (LSB)) and incubated for 1 hour at 4 °C on the vibrax shaker. Beads were collected by centrifugation at 2,500 x g for 1 minute and supernatants were saved for future analysis. Beads were washed in ice-cold lysis buffer (without protease inhibitors) three times for 10 minutes on a vibrax shaker at 4 °C followed by one wash in ice-cold TBS to remove detergents and salts. Samples were resuspended in 30 µL of 2x NuPAGE LDS sample buffer + DTT (1:10) and heated at 70 °C for 10 minutes after which they were analysed by Western immunoblotting (section 2.5.2 & 2.5.3).

2.7 Statistical analysis

Statistical analysis was carried out using GraphPad Prism (Version 7). Statistical significance was indicated when $p < 0.05$. Unpaired t-test was used to compare two conditions. One-way ANOVA with Dunnett's test was used to compare a control

mean with the other means of more than two groups of individual treatments. One-way ANOVA with Šidák test was used to compare selected pairs of means.

Chapter 3

Characterisation of mitophagy in SH-SY5Y cells

3.0 Introduction

Mitophagy is a tightly regulated process responsible for removal of damaged or superfluous mitochondria. It is characterised by mitochondrial depolarisation that leads to accumulation of PINK1 on the MOM and PINK1-dependent recruitment of Parkin, which is responsible for ubiquitination of mitochondrial proteins. This leads to LC3B labelling of depolarised mitochondria, marking them for autophagic engulfment (Narendra et al., 2008, Narendra et al., 2010b, Kim and Lemasters, 2011b).

Autophagy is prevented under nutrient-rich conditions by mTORC1-mediated inhibition of the ULK1 complex (Russell et al., 2014). Release of mTORC1 in response to starvation leads to activation of the ULK1 complex and subsequent activation of the PIK3C3 complex that localises to the phagophore to generate PtdIns(3)P that are necessary for expansion of the membrane. Cytosolic LC3B is targeted to the isolation membrane by the ATG5-ATG12-ATG16L system where it is processed into LC3B-I and conjugated to PE to form the membrane bound LC3B-II (Kabeya et al., 2000, Mizushima et al., 2001, Fujita et al., 2008b). The ubiquitin binding protein p62 binds to ubiquitinated proteins destined for degradation and delivers them to the autophagosome by direct binding to LC3B, thereby being degraded itself as well (Pankiv et al., 2007).

To date, it is unclear whether observed mitochondrial defects and damage in PD are the primary cause of pathogenesis or consequence of damaged neurons. However, the hypothesis that mitochondrial dysfunction may lie at the basis of PD is strengthened by the fact that many of the genes involved in familial forms of PD are related to mitochondria or their function. Mutations in either *PARK2* or *PINK1* have been linked

to autosomal recessive, juvenile parkinsonism (AR-JP) and both account for the majority of these cases, suggesting defects in mitophagy are implicated in the development of PD (Valente et al., 2004, Celardo et al., 2014). Therefore, it is important to utilise neuronal cell models in order to study mitophagy and consequences of defects in mitophagy. Neurons are a specialised cell type that are non-proliferating and need to survive for the lifetime of the organism. They produce high levels of ROS and are more vulnerable to oxidative stress compared to other cell types, indicating that it is important to prevent accumulation of oxidative damage by renewing their mitochondrial pool by means of mitophagy (Cui et al., 2004, Chinta and Andersen, 2008, Kageyama et al., 2012). Surprisingly, mitophagy is mostly studied in non-neuronal cell lines and obtained results might not reflect execution and regulation of mitophagy in neurons. HeLa cells, for example, are often used to study mitophagy, but do not express Parkin (Denison et al., 2003).

A cell line often used to study PD mechanisms is SH-SY5Y, which represents a neuronal tumour cell line from a patient with neuroblastoma that expresses neurofilament proteins, shows specific uptake of norepinephrine (NE), and exhibits neuronal marker enzyme activity, including tyrosine and dopamine- β -hydroxylases (Xie et al., 2010). Furthermore, SH-SY5Y cells express dopamine transporter (DAT) that is only expressed in dopamine (DA) neurons in the central nervous system and they are able to synthesise DA and NE. Thus, SH-SY5Y cells are a more suitable cell model for investigation of mitophagy in relation to PD since they provide an unlimited supply of cells of human origin with similar characteristics to human DAergic neurons and will therefore be utilised in this study.

SH-SY5Y cells have been used to study mitophagy, but not much is known about how mitophagy is regulated in these cells. Both PINK and Parkin are expressed in SH-SY5Y cells with a relatively high endogenous Parkin expression in contrast to other cells, hence there is no need to overexpress Parkin (Zhou et al., 2008). Induction of mitochondrial damage in SH-SY5Y cells by the mitochondrial uncoupler FCCP was shown to induce PINK1 accumulation, to increase ubiquitination of the mitochondrial marker TOM20 with TOM20 degradation upon prolonged mitochondrial damage, and to induce autophagosome formation as seen by LC3B-II accumulation (Gao et al., 2015, Berezhnov et al., 2016, Ivankovic et al., 2016). Endogenous Parkin was recruited to mitochondria and mitochondria were found to be sequestered and cleared upon CCCP, a FCCP analogue, treatment (Geisler et al., 2010). The same group also showed interaction between PINK1 and Parkin upon CCCP treatment and VDAC1 ubiquitination after mitochondrial depolarisation. p62 protein expression was significantly increased following induction of mitophagy and CCCP caused co-localisation of p62 with TOM20 (Ivankovic et al., 2016).

PINK1/Parkin-mediated mitophagy can be induced in SH-SY5Y cells and autophagy is involved in this process (Geisler et al., 2010, Gao et al., 2015, Berezhnov et al., 2016, Ivankovic et al., 2016). The main aims of this chapter were to confirm that FCCP induces PINK1/Parkin-mediated mitophagy in SH-SY5Y cells and to investigate if autophagy was also activated. The effects of FCCP on the expression of different proteins involved in autophagy, as well as mitochondrial marker proteins, were investigated. Lastly, the effects of proteasomal inhibition on the expression of mitochondrial marker proteins was examined upon FCCP treatment since the ubiquitin-proteasome system (UPS) is known to be involved in mitophagy.

3.1 FCCP inhibits mTORC1 signalling and activates the Ras pathway

SH-SY5Y cells were challenged with 5 μ M of the chemical uncoupler FCCP for different time points to examine if FCCP induces autophagy in SH-SY5Y cells. Microscopic analysis revealed that cells were elongated and had lost their cytoplasmic inclusions at 4 hours of FCCP treatment, which did not change at 8 hours (Figure 3.1.1). However, 16 hours of FCCP treatment resulted in cells that were rounded up and detached, while possible signs of apoptosis, namely presence of blebbing and small cells, were observed at 24 hours.

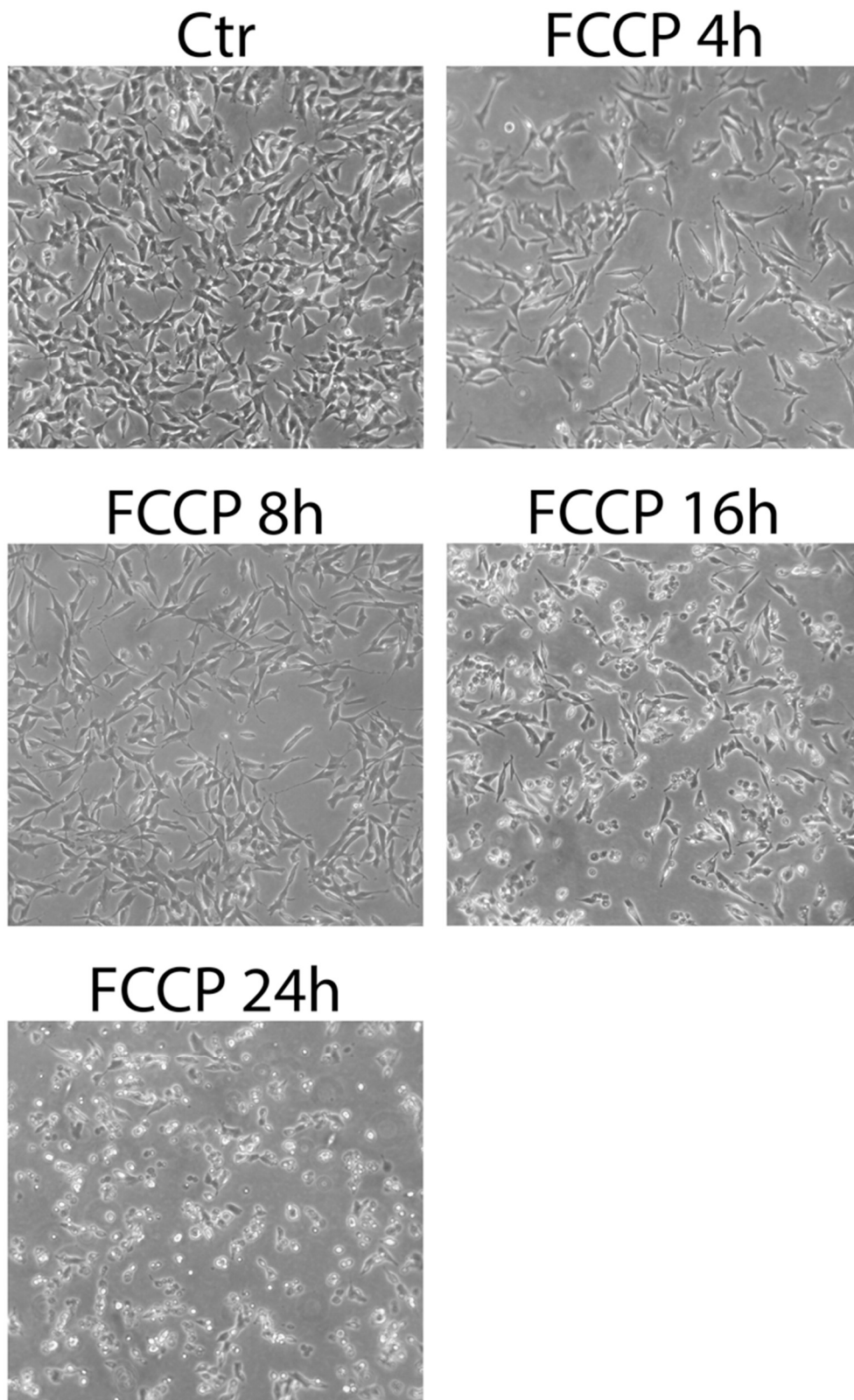


Figure 3.1.1. *Prolonged FCCCP incubation leads to detachment of SH-SY5Y cells.* Prolonged incubation of SH-SY5Y cells with FCCCP leads to cellular detachment and possibly apoptosis. SH-SY5Y cells were treated with 5 μ M FCCCP. Phase contrast images were taken at indicated time points using a Nikon TMS microscope, magnification = 10x. Data represents one out of a total of three experiments.

To confirm activation of the autophagy pathway upon FCCP treatment, activity of the mTORC1 pathway, which is the first step in autophagy activation, was determined (Russell et al., 2014). Autophagy is initiated by inhibition of mTORC1, which subsequently leads to activation of ULK1. Expression levels of p70 ribosomal S6 kinase 1 (S6K1), a downstream target of mTORC1 responsible for protein synthesis, were analysed upon FCCP treatment to investigate if FCCP leads to mTORC1 inhibition and therefore activation of autophagy (Laplante and Sabatini, 2009).

A 5 μ M FCCP time course showed that mTOR expression did not change over time, whereas both total and phosphorylated S6K1 expression decreased, indicating mTORC1 suppression on autophagy was lost (Figure 3.1.2 A).

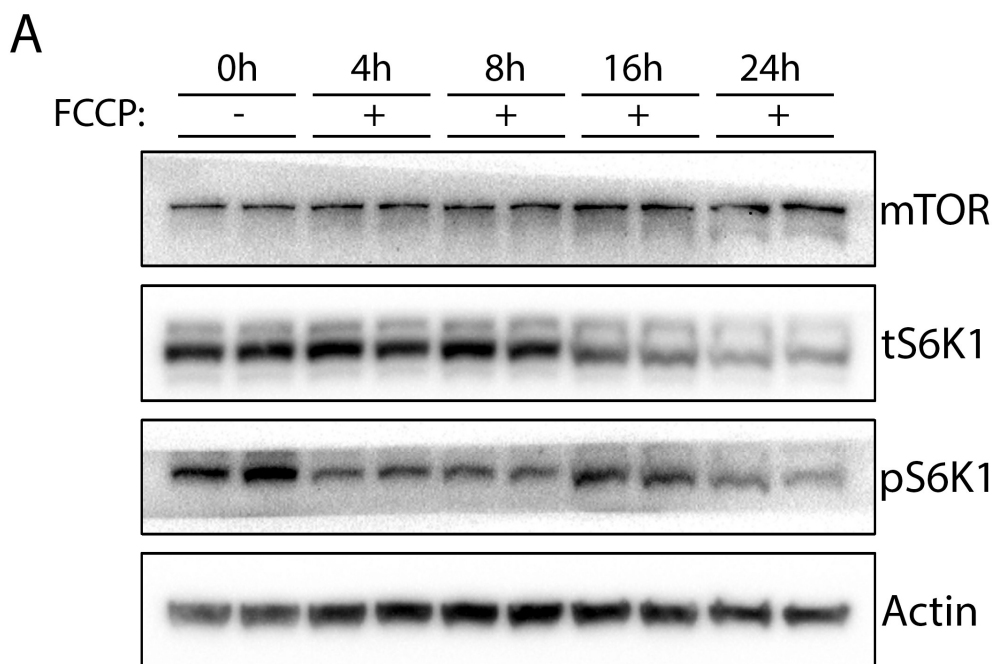


Figure 3.1.2 (A). *FCCP induces autophagy by mTORC1 inhibition.* The mTORC1 pathway is inhibited in SH-SY5Y cells upon FCCP treatment, thereby activating autophagy. (A) SH-SY5Y cells were treated with 5 μ M FCCP for indicated time points. Protein lysates (20 μ g) were probed for the mTORC1 signalling pathway related proteins mTOR, tS6K1, and pS6K1. β -actin was used as loading control. Data represents one out of a total of three independent experiments.

Densitometric analysis confirmed tS6K1 degradation by showing a significant decrease at 16 hours ($p < 0.001$) and 24 hours ($p < 0.0001$) of FCCP treatment (Figure 3.1.2 B). Normalisation of pS6K1 to tS6K1 showed that pS6K1 was significantly increased at 16 hours ($p < 0.05$), after which expression returned to basal levels at 24 hours of FCCP treatment.

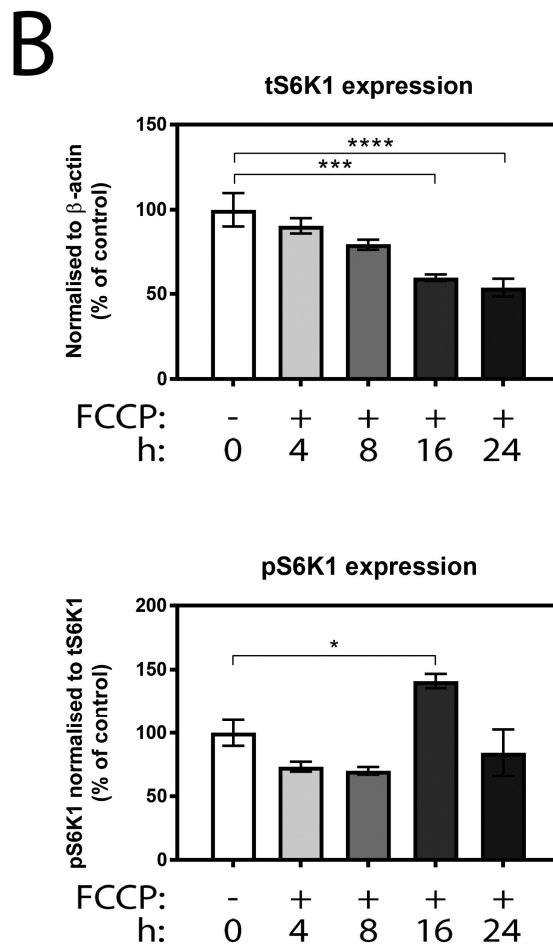


Figure 3.1.2 (B). *FCCP induces autophagy by mTORC1 inhibition.* mTOR and tS6K1 densitometry normalised to corresponding β -actin levels and pS6K1 densitometry normalised to corresponding tS6K1 levels. Densitometric analysis was pooled from three independent experiments in panel A and data is shown as percentage of control. Error bars = SEM, one-way ANOVA, * $p < 0.05$, *** $p < 0.001$, **** $p < 0.0001$.

Literature showed that decreased S6K1 activity upon mTORC1 inhibition led to disinhibition of insulin receptor substrate 1 (IRS-1), resulting in enhanced activity of

the extracellular signal-regulated kinases (ERK) pathway (Melemedjian et al., 2013). To investigate whether the ERK pathway was activated upon FCCP treatment, SH-SY5Y cells were co-treated with 5 μ M FCCP and 2 μ M PD184352, an inhibitor of mitogen-activated protein kinase kinase (MEK), which is an upstream effector of ERK1/2. While FCCP and PD184352 treatment on their own did not result in morphologic changes of the cells, combined treatment led to condensed and detached cells showing early signs of apoptosis, suggesting SH-SY5Y cells rely on ERK1/2 activity to be able to survive FCCP treatment (Figure 3.1.3).

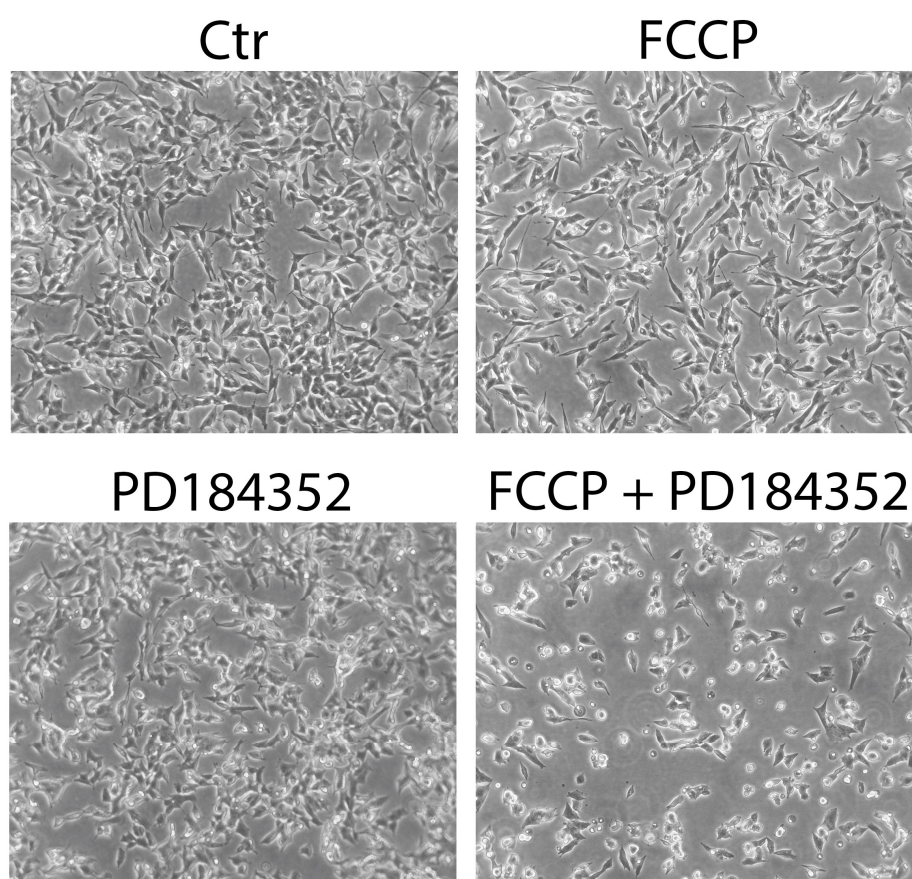


Figure 3.1.3. *Inhibition of the MAPK/ERK pathway exacerbates FCCP-induced detachment of SH-SY5Y cells.* Incubation with the mitogen-activated protein kinase (MAPK)/ERK pathway inhibitor PD184352 does not change SH-SY5Y cell morphology, but does induce a condensed cellular appearance and does increase cell detachment when co-treated with FCCP. SH-SY5Y cells were treated with either 5 μ M FCCP, 2 μ M PD184352, or both, for 16 hours. Phase contrast images were taken using a Nikon TMS microscope, magnification = 10x. Data represents one out of a total of three independent experiments.

Treatment of SH-SY5Y cells with FCCP led to decreased S6K1 phosphorylation, as seen previously (see Figure 3.1.2 A & B), indicating inhibition of mTORC1 signalling (Figure 3.1.4 A). It also led to increased ERK1/2 phosphorylation, showing that the ERK pathway was activated. This was confirmed by MEK inhibition by PD184352, which successfully suppressed ERK1/2 and S6K1 phosphorylation when co-treated with FCCP.

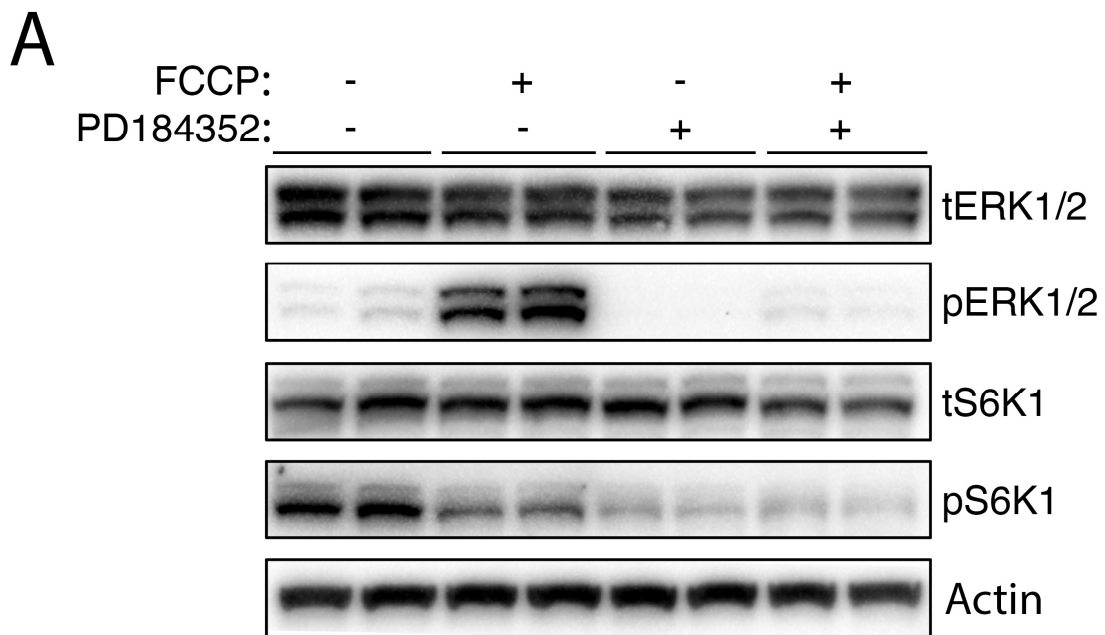


Figure 3.1.4 (A). *FCCP activates the ERK pathway.* FCCP inhibits mTORC1 signalling, shown by decreased pS6K1 phosphorylation, and thereby induces autophagy by activation of ERK1/2. The MAPK/ERK pathway inhibitor PD184352 abolishes S6K1 phosphorylation, as well as ERK1/2 phosphorylation, when co-treated with FCCP. SH-SY5Y cells were treated with either 5 μ M FCCP, 2 μ M PD184352, or both, for 16 hours. Protein lysates (20 μ g) were probed for total and phosphorylated mTORC1 signalling pathway related proteins ERK1/2 and S6K1. β -actin was used as loading control. Data represents one out of a total of three independent experiments.

All treatments led to decreased tERK1/2 expression, but only PD184352 treatment was statistically significant ($p < 0.05$) (Figure 3.1.4 B). FCCP treatment increased pERK1/2 expression ($p < 0.001$), while co-treatment of FCCP and PD184352 led to a

significant decrease in pERK1/2 ($p < 0.0001$), as well as pS6K1 ($p < 0.05$), when compared to FCCP treatment on its own. pS6K1 expression was decreased upon the different treatments (FCCP $p < 0.001$, PD184352 $p < 0.0001$, FCCP + PD184352 $p < 0.0001$), whereas tS6K1 expression was unaffected.

B

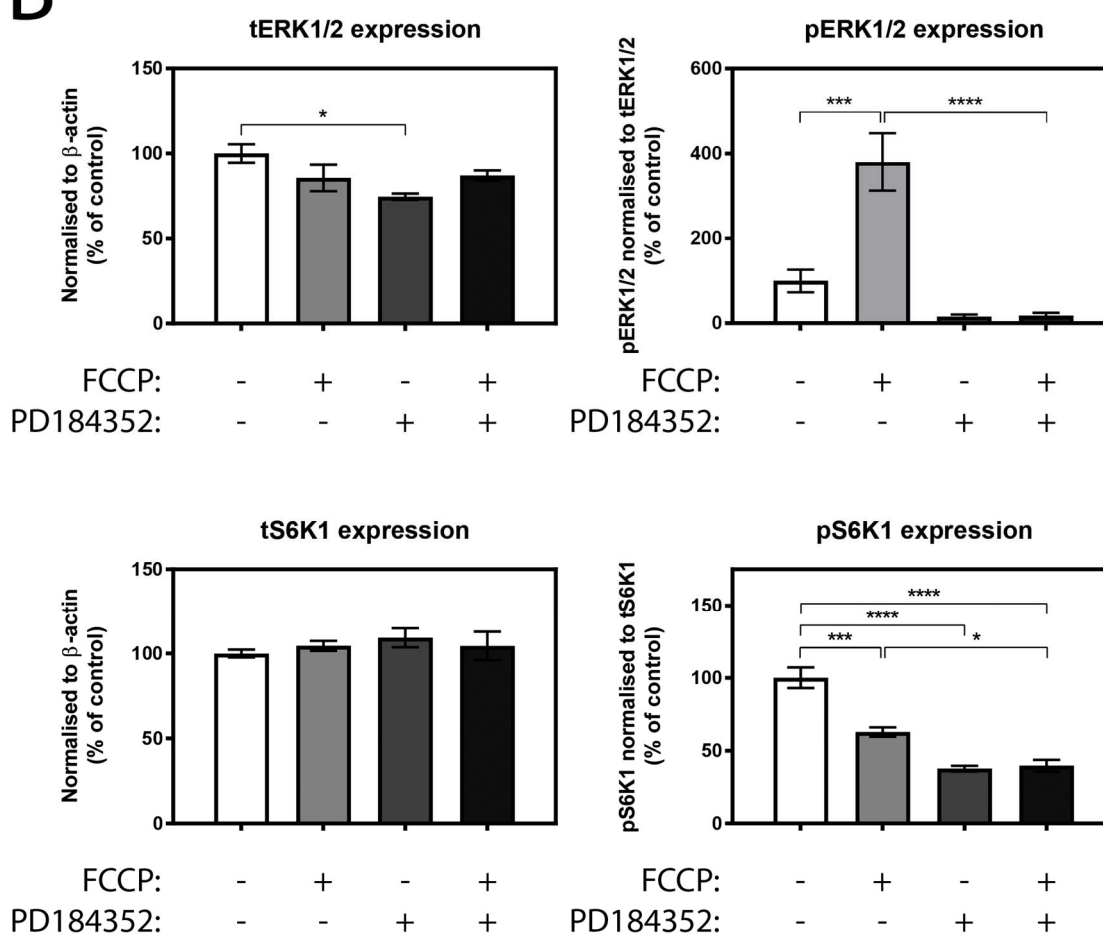


Figure 3.1.4 (B). FCCP activates the ERK pathway. tERK1/2 and tS6K1 densitometry normalised to corresponding β -actin levels and pERK1/2 and pS6K1 densitometry normalised to corresponding tERK1/2 and tS6K1 levels. Densitometric analysis was pooled from three independent experiments in panel A and data is shown as percentage of control. Error bars = SEM, one-way ANOVA, * $p < 0.05$, *** $p < 0.001$, **** $p < 0.0001$.

3.2 FCCP induces autophagy in SH-SY5Y cells

After establishing FCCP inhibits mTORC1 signalling, the autophagic flux upon 5 μ M FCCP treatment in SH-SY5Y cells was determined by monitoring the turnover of autophagy marker proteins. The mitophagy marker Parkin was degraded over time, whereas PINK1 expression did not increase substantially (Figure 3.2.1). The time course made evident that signs of induction of mitophagy on protein level, which are decreased Parkin and increased PINK1 expression, were most clear at 24 hours of FCCP treatment.

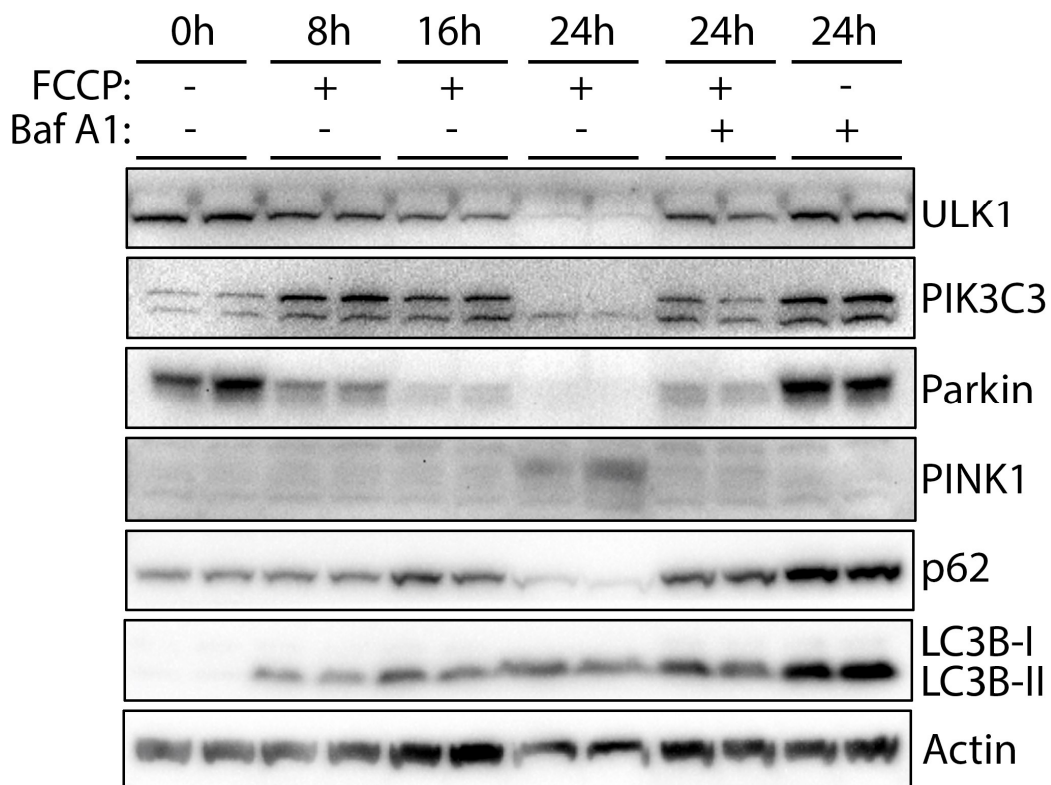


Figure 3.2.1. *FCCP activates autophagy in SH-SY5Y cells.* Autophagy is activated in SH-SY5Y cells by FCCP. Co-treatment of SH-SY5Y cells with FCCP and the lysosomal inhibitor Baf A1 does not result in accumulation of mitophagy and autophagy related proteins. SH-SY5Y cells were treated with either 5 μ M FCCP, 100 nM Baf A1, or both, for indicated time points (Baf A1 24 hours only). Protein lysates (20 μ g) were probed for mitophagy marker proteins Parkin and PINK1, and autophagy marker proteins ULK1, PIK3C3, p62, and LC3B. β -actin was used as loading control. Data represents one out of a total of three independent experiments.

Activation of autophagy by FCCP was further confirmed by decreased ULK1 expression and increased LC3B-I to LC3B-II turnover. The upper band of PIK3C3 was increased as well. Normally, p62 binds ubiquitinated cargo and delivers it to the autophagosome, thereby being degraded itself. Autophagic activity is therefore marked by decreased p62 levels. Unexpectedly, p62 expression increased after 16 hours of FCCP treatment. Incubation with 100 nM of the lysosomal inhibitor Bafilomycin A1 (Baf A1), which is a potent inhibitor of the late phase of autophagy where it inhibits fusion between autophagosomes and lysosomes, thereby preventing the formation of the autolysosome, resulting in increased LC3B-II levels since its degradation is prevented (Yamamoto et al., 1998), further accumulated p62, as well as LC3B-II, ULK1, and PIK3C3, indicating autophagy was active. Combined treatment of FCCP and Baf A1 led to decreased expression of the immunoblotted proteins when compared to Baf A1 treatment.

It has been reported that p62 can be synthesised de novo, therefore to address this, protein synthesis was inhibited in SH-SY5Y cells by the addition of cycloheximide (CHX) to see if p62 protein was synthesised following FCCP treatment. Cells treated with 10 μ M CHX for 24 hours had somas that were shortened, whereas FCCP (5 μ M) treated cells were rounded up, condensed, and detached, which are characteristics of apoptotic cell death (Figure 3.2.2). The observed FCCP phenotype was worsened by co-treatment with CHX.

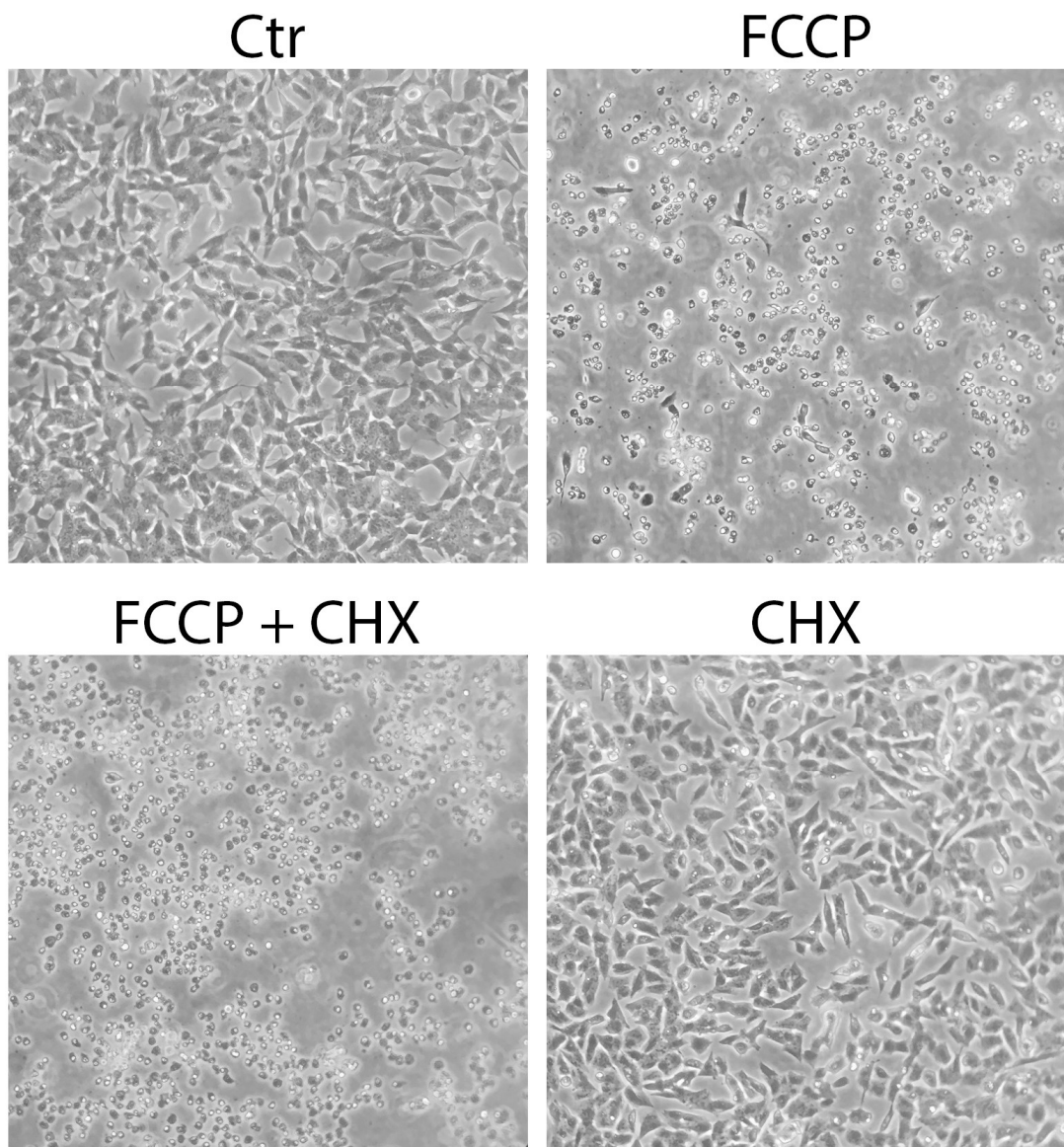


Figure 3.2.2. *Inhibition of protein synthesis changes morphology of SH-SY5Y cells.* Prolonged incubation with the protein synthesis inhibitor CHX results in shortened SH-SY5Y cells, whereas FCCP treatment leads to rounded up, condensed, and detached cells. FCCP-induced effects on cell morphology are exacerbated by CHX. SH-SY5Y cells were treated with either 5 μ M FCCP, 10 μ M CHX, or both, for 24 hours. Phase contrast images were taken using a Nikon TMS microscope, magnification = 10x. Data represents one out of a total of three independent experiments.

Immunoblotting showed increased p62 expression upon FCCP treatment, which was inhibited by CHX, indicating FCCP induces *de novo* protein synthesis of p62 (Figure 3.2.3 A). LC3B-II and VDAC1 were immunoblotted too and their FCCP-induced accumulation was not affected by protein synthesis inhibition.

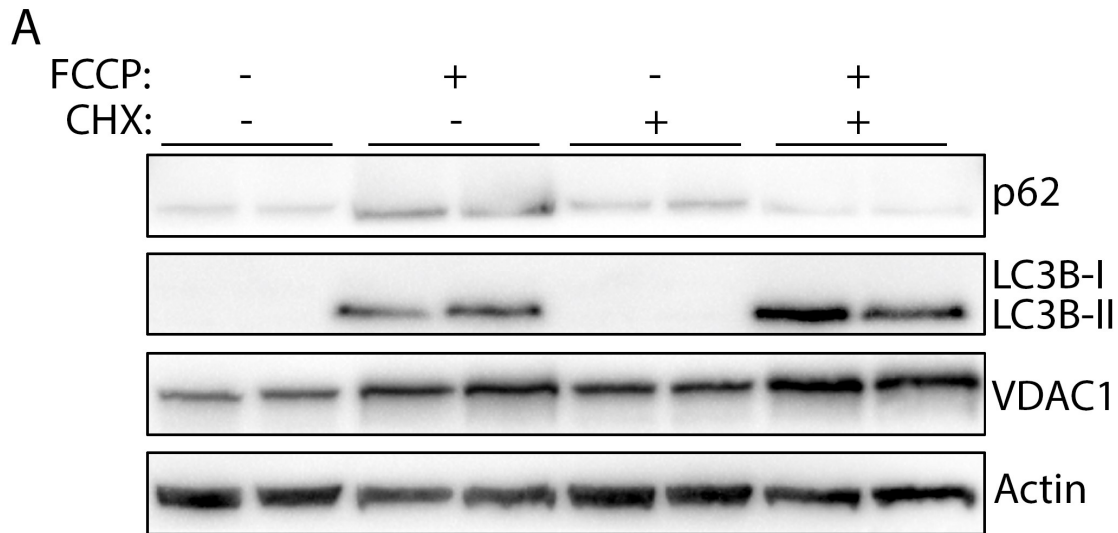


Figure 3.2.3 (A). *FCCP induces de novo protein synthesis of p62.* Treatment of SH-SY5Y cells with FCCP induces *de novo* protein synthesis of p62. FCCP-mediated LC3B-II and VDAC1 accumulation is not affected by CHX treatment. SH-SY5Y cells were treated with either 5 μ M FCCP, 10 μ M CHX, or both, for 24 hours. Protein lysates (20 μ g) were probed for autophagy marker proteins p62 and LC3B, and the mitochondrial marker protein VDAC1. β -actin was used as loading control. p62 and LC3B data represents one out of a total of three independent experiments, whereas VDAC1 data represents one out of a total of two independent experiments.

Densitometry confirmed FCCP treatment increased p62 expression ($p < 0.0001$), which was significantly decreased when cells were co-treated with CHX ($p < 0.0001$) (Figure 3.2.3 B). It also showed that FCCP treatment caused a significant ($p < 0.0001$) increase in LC3B-II accumulation, which was not significantly affected by co-treatment of FCCP and CHX when results were normalised to corresponding β -actin expression. A significant increase in LC3B-II accumulation was also observed upon combined treatment of FCCP and CHX when compared to control ($p < 0.001$) or CHX treatment ($p < 0.0001$). The FCCP-induced increase in VDAC1 expression was not affected by co-treatment with CHX, suggesting VDAC1 could be recycled.

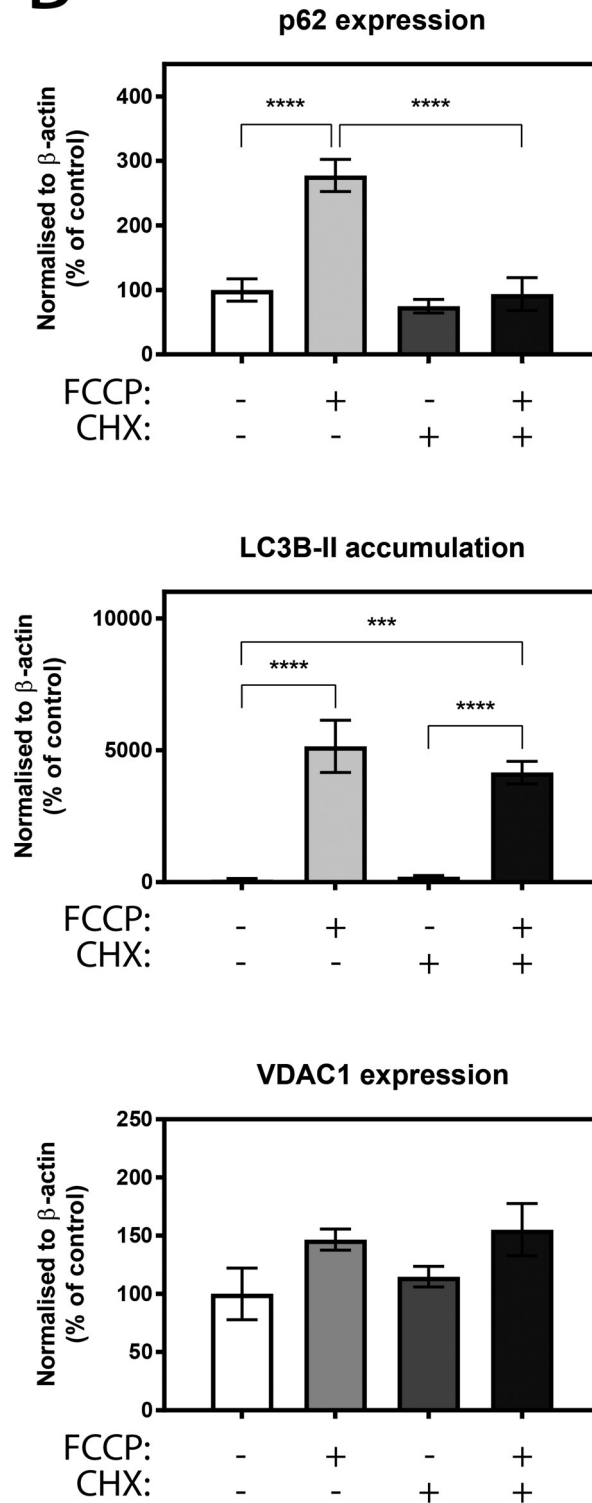
B

Figure 3.2.3 (B). FCCP induces *de novo* protein synthesis of p62. p62, LC3B-II, and VDAC1 densitometry normalised to corresponding β -actin levels. Densitometric analysis was pooled from the independent experiments in panel A (three independent experiments for p62 and LC3B data and two independent experiments for VDAC1 data) and data is shown as percentage of control. Error bars = SEM, one-way ANOVA, *** $p < 0.001$, **** $p < 0.0001$.

The effects of FCCP on autophagy and mitochondria were also visualised by epifluorescence microscopy. SH-SY5Y cells were transfected with 4 μg GFP-LC3B and mitochondria were stained with TOM20. Cytosolic localisation of GFP-LC3B was indicated by green staining, whereas LC3B-positive autophagosomes were indicated by bright green puncta. Non-treated cells had few, if any, LC3B puncta while cells deprived of amino acids (EBSS treatment) over a 24 hour period showed an increase in LC3B puncta (Figure 3.2.4 A). Amino acid deprivation did not have a visual effect on TOM20 staining and no overlap of TOM20 staining and LC3B puncta was observed.

Prevention of autophagic cargo degradation, which also prevents LC3B-II degradation, by Baf A1 (100 nM) resulted in increased LC3B-II-positive puncta formation that accumulated over time (Figure 3.2.4 B). Cytosolic staining of LC3B was less intense when more LC3B puncta were present, indicating cytosolic LC3B-I was converted to membrane-bound LC3B-II. Similar to amino acid deprivation, no visual effects on TOM20 staining and no overlap of TOM20 staining and LC3B puncta was seen.

FCCP treatment (5 μM) led to an increased amount of LC3B puncta at each time point, with decreased cytosolic LC3B from 8 hours onwards (Figure 3.2.4 C). TOM20 staining was disintegrated upon FCCP treatment, which was most clear at 24 hours, indicating that FCCP caused fragmentation of the mitochondrial network. LC3B puncta and mitochondrial TOM20 staining did not overlap. Inhibition of autophagic cargo degradation by Baf A1 did not affect FCCP-induced disintegration of TOM20 staining or the amount of LC3B puncta (Figure 3.2.4 D).

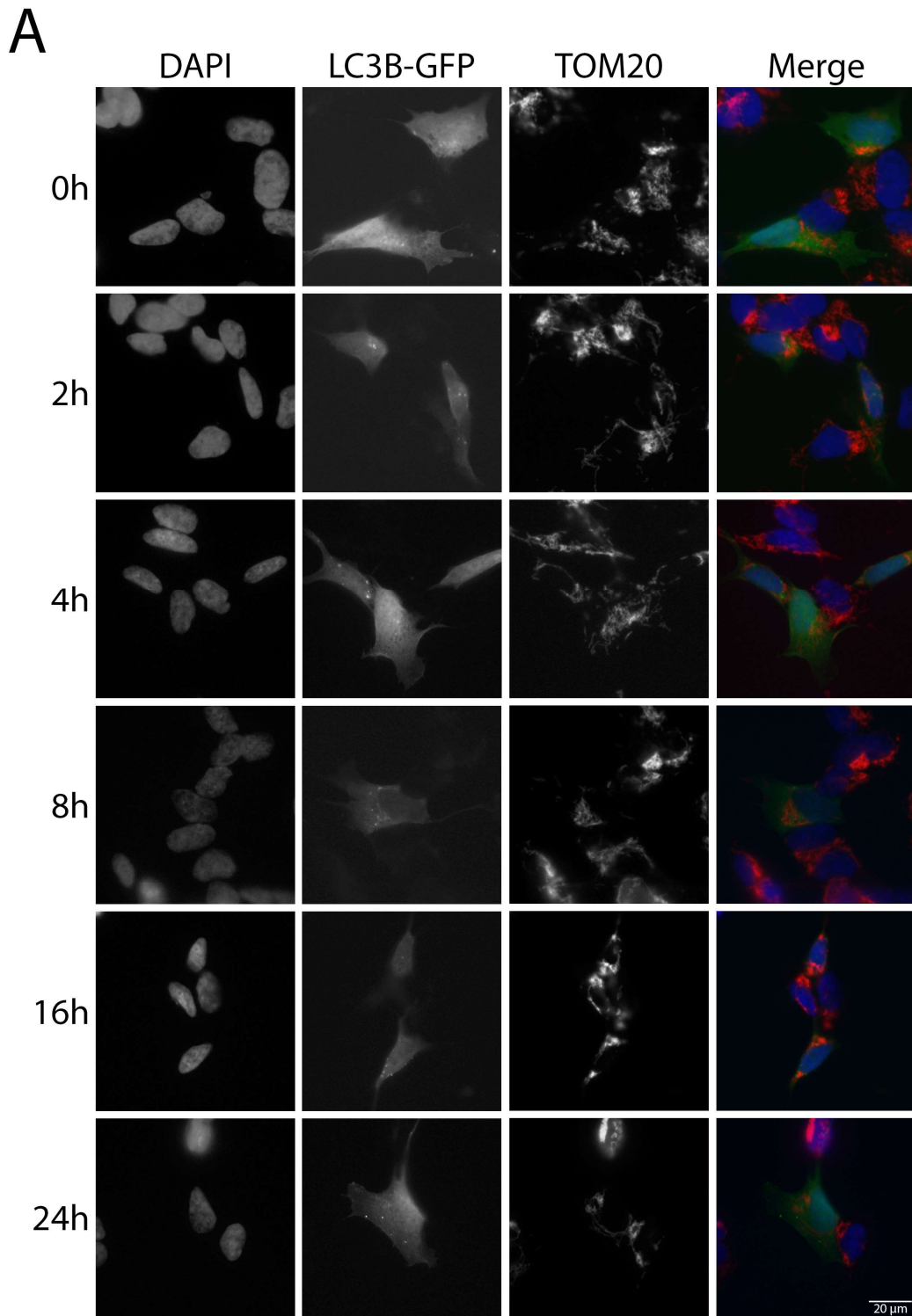


Figure 3.2.4 (A). FCCP treatment fragments mitochondria and increases the amount of LC3B puncta. Amino acid deprivation of SH-SY5Y cells results in increased amount of LC3B puncta over time and does not have a visual effect on TOM20 staining. SH-SY5Y cells were transfected with 4 μg GFP-LC3B (green) and were starved in EBSS medium for indicated time points before fixation of the cells. Mitochondria were visualised by TOM20 staining (red) and nuclei are labelled with DAPI (blue). Data represents one experiment. Magnification = 60x, scale bar = 20 μm .

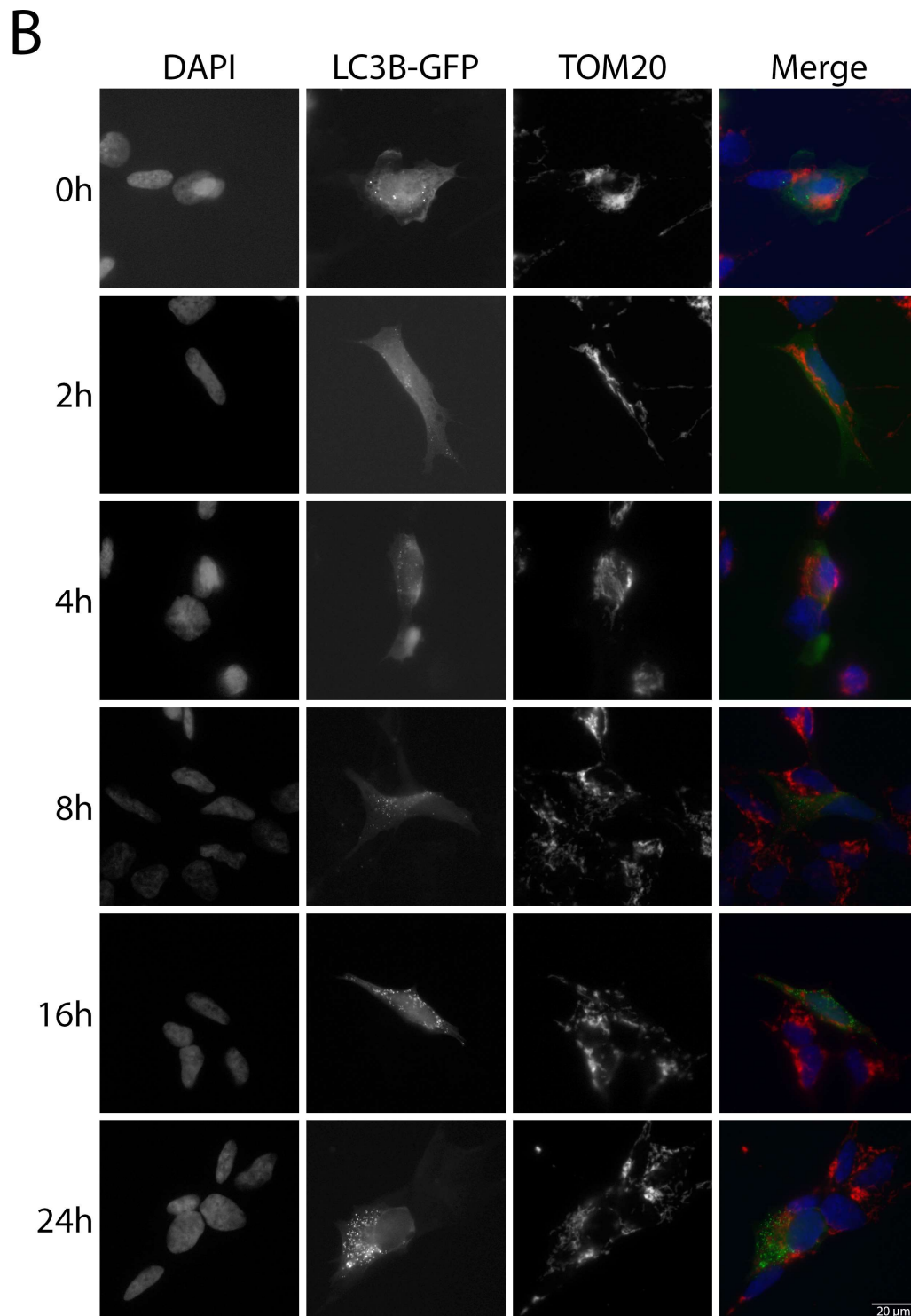


Figure 3.2.4 (B). *FCCP treatment fragments mitochondria and increases the amount of LC3B puncta.* Prevention of autophagic cargo degradation, which also prevents LC3B-II degradation, results in increased amount of LC3B puncta over time and does not have a visual effect on TOM20 staining. SH-SY5Y cells were transfected with 4 μg GFP-LC3B (green) and were treated with 100 nM Baf A1 for indicated time points before fixation of the cells. Mitochondria were visualised by TOM20 staining (red) and nuclei are labelled with DAPI (blue). Data represents one experiment. Magnification = 60x, scale bar = 20 μm .

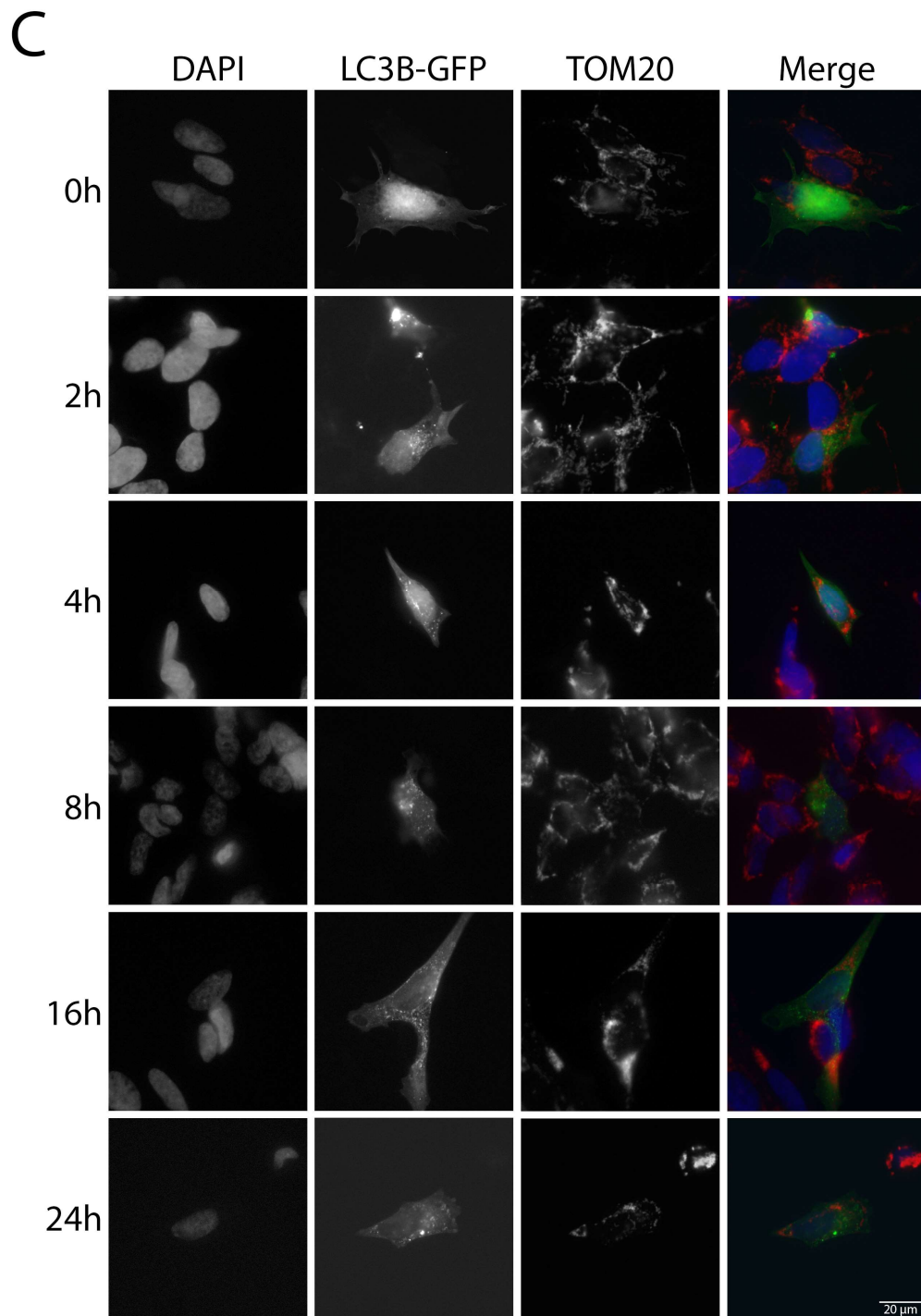


Figure 3.2.4 (C). FCCP treatment fragments mitochondria and increases the amount of LC3B puncta. FCCP-induced mitochondrial damage results in disintegration of TOM20 staining, suggesting mitochondrial fragmentation, and in increased amount of LC3B puncta over time, however, TOM20 staining and LC3B puncta do not overlap. SH-SY5Y cells were transfected with 4 μg GFP-LC3B (green) and were treated with 5 μM FCCP for indicated time points before fixation of the cells. Mitochondria were visualised by TOM20 staining (red) and nuclei are labelled with DAPI (blue). Data represents one experiment. Magnification = 60x, scale bar = 20 μm .

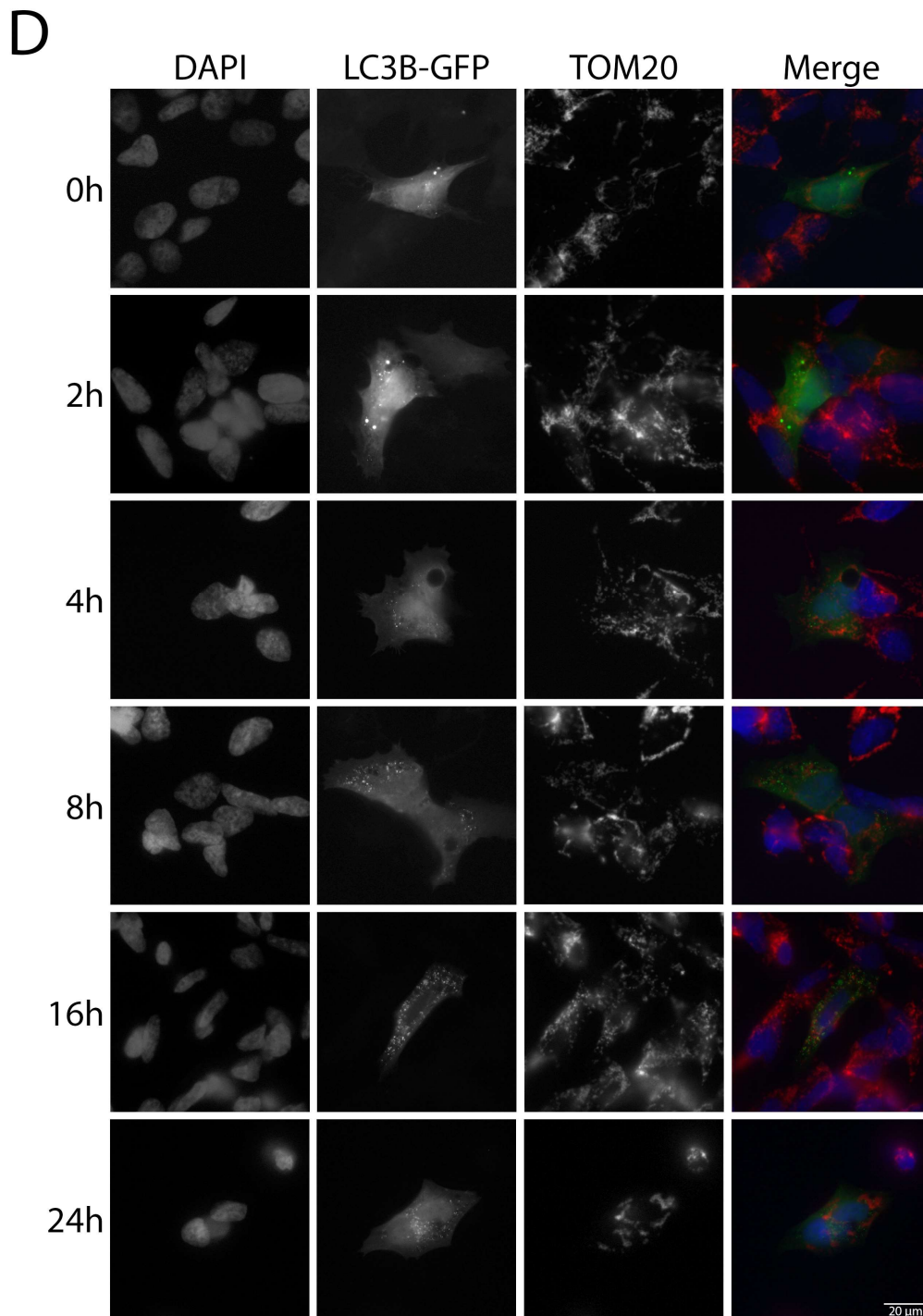


Figure 3.2.4 (D). FCCP treatment fragments mitochondria and increases the amount of LC3B puncta. Prevention of autophagic cargo degradation by Baf A1 does not have an additive effect on FCCP-induced disintegration of TOM20 staining or increased amount of LC3B puncta. TOM20 staining and LC3B puncta do not overlap. SH-SY5Y cells were transfected with 4 μ g GFP-LC3B (green) and were treated with 5 μ M FCCP + 100 nM Baf A1 for indicated time points before fixation of the cells. Mitochondria were visualised by TOM20 staining (red) and nuclei are labelled with DAPI (blue). Data represents one experiment. Magnification = 60x, scale bar = 20 μ m.

To clarify that the ultimate fate of SH-SY5Y cells upon FCCP treatment was not condensed, small, and detached cells, SH-SY5Y cells were allowed to recover from FCCP treatment. SH-SY5Y cells were treated with 5 μ M FCCP for either 4 or 16 hours and were given a 30 or 90 minutes recovery period after removal of the FCCP. Cells that were treated for 4 hours were elongated, whereas a 16 hour treatment led to increased amounts of small, condensed, and detached cells that was observed after both recovery periods (data not shown).

When SH-SY5Y cells were treated with FCCP for 4 hours, reduced Parkin expression and increased PINK1 expression were observed after both recovery periods of 30 and 90 minutes, showing mitophagy was still induced (Figure 3.2.5). Four hour treated cells did not have increased p62 expression (upper band, see arrow), which was seen at 16 hours of FCCP treatment. LC3B-I was converted in LC3B-II upon FCCP treatment, but LC3B turnover was decreased after 30 minutes of recovery and returned to control conditions after a 90 minute recovery period, indicating that while mitophagy was still active after depletion of FCCP, autophagic activity restored to basal conditions. Parkin expression was completely absent when cells were treated for 16 hours, which did not change after both recovery periods, whereas PINK1 expression decreased after recovery. p62 expression was increased and LC3B-II accumulated, but LC3B-II levels did not decrease to basal levels, suggesting autophagy cannot be halted after a 16 hour period of FCCP treatment.

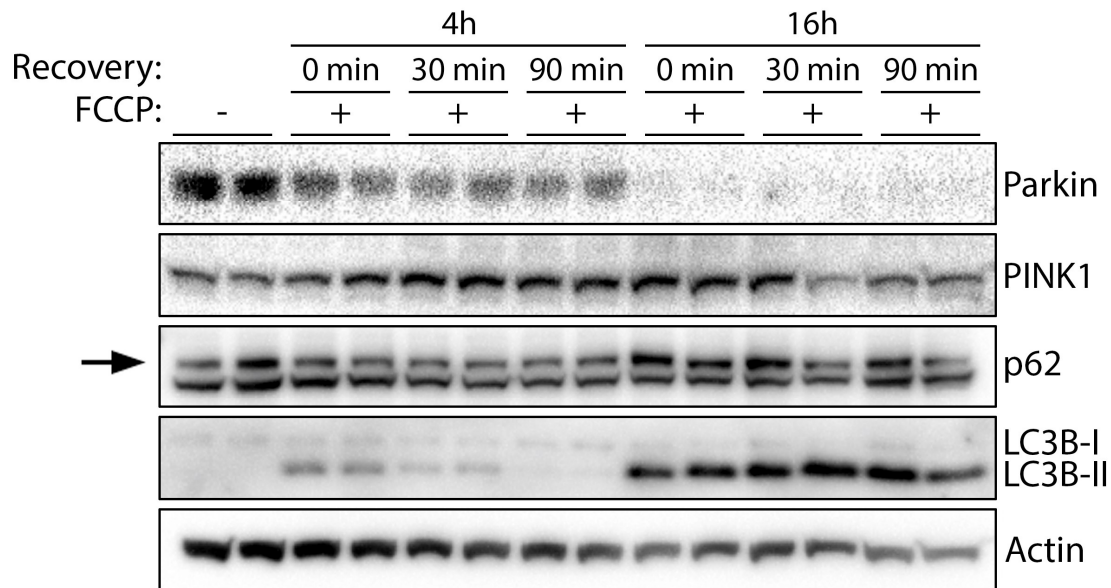


Figure 3.2.5. Autophagic activity is restored when SH-SY5Y cells are allowed to recover after a 4 hour, but not after a 16 hour, FCCCP incubation period. SH-SY5Y cells showed signs of restored autophagic, but not mitophagic, activity after being allowed to recover following a 4 hour FCCCP treatment, but not after a 16 hour FCCCP treatment. SH-SY5Y cells were treated with 5 μ M FCCCP for either 4 or 16 hours after which cells were washed and were allowed to recover for either 30 or 90 minutes before lysis. Protein lysates (20 μ g) were probed for mitophagy marker proteins Parkin and PINK1, and autophagy marker proteins p62 and LC3B. β -actin was used as loading control. Data represents one out of a total of four independent experiments.

3.3 FCCCP induces mitophagy in SH-SY5Y cells

As shown in the previous section, decreased Parkin and increased PINK1 expression were observed in SH-SY5Y cells after 24 hours of 5 μ M FCCCP treatment (Figure 3.3.1 A). LC3B-I to LC3B-II conversion, which indicated induction of autophagosome formation, was also observed. Inhibition of fusion between autophagosomes and lysosomes by 100 nM Baf A1 led to LC3B-II accumulation as expected, but did not affect Parkin or PINK1 expression in SH-SY5Y cells.

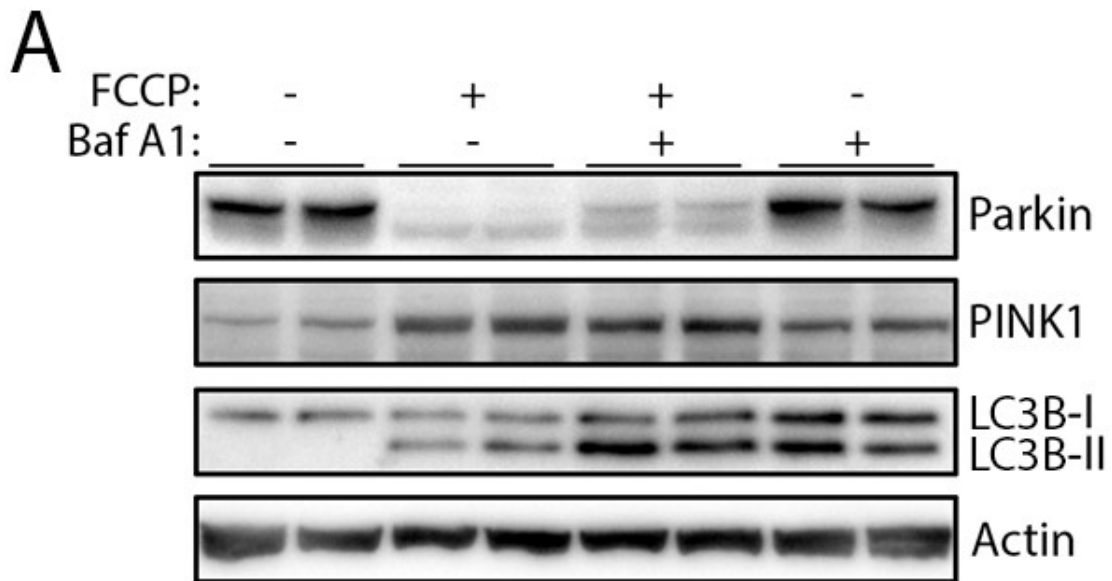


Figure 3.3.1 (A). *FCCP induces mitophagy in SH-SY5Y cells.* FCCP induces mitophagy in SH-SY5Y cells, seen by decreased Parkin and increased PINK1 expression, which is not affected by inhibition of autophagosome degradation. SH-SY5Y cells were treated with either 5 μ M FCCP, 100 nM Baf A1, or both, for 24 hours. Protein lysates (20 μ g) were probed for mitophagy marker proteins Parkin and PINK1 and the autophagy marker protein LC3B. β -actin was used as loading control. Data represents one out of a total of three independent experiments.

FCCP led to a significant decrease in Parkin expression ($p < 0.0001$) and this was not affected by combined treatment with Baf A1 ($p < 0.0001$) (Figure 3.3.1 B). Parkin expression was significantly degraded upon co-treatment of FCCP and Baf A1 ($p < 0.001$) when compared to Baf A1 treatment. Baf A1 treatment led to PINK1 degradation when compared to control ($p < 0.05$) or combined treatment of FCCP and Baf A1 ($p < 0.01$). LC3B-II accumulation was observed upon all treatments (FCCP $p < 0.001$, Baf A1 $p < 0.0001$, FCCP + Baf A1 $p < 0.001$).

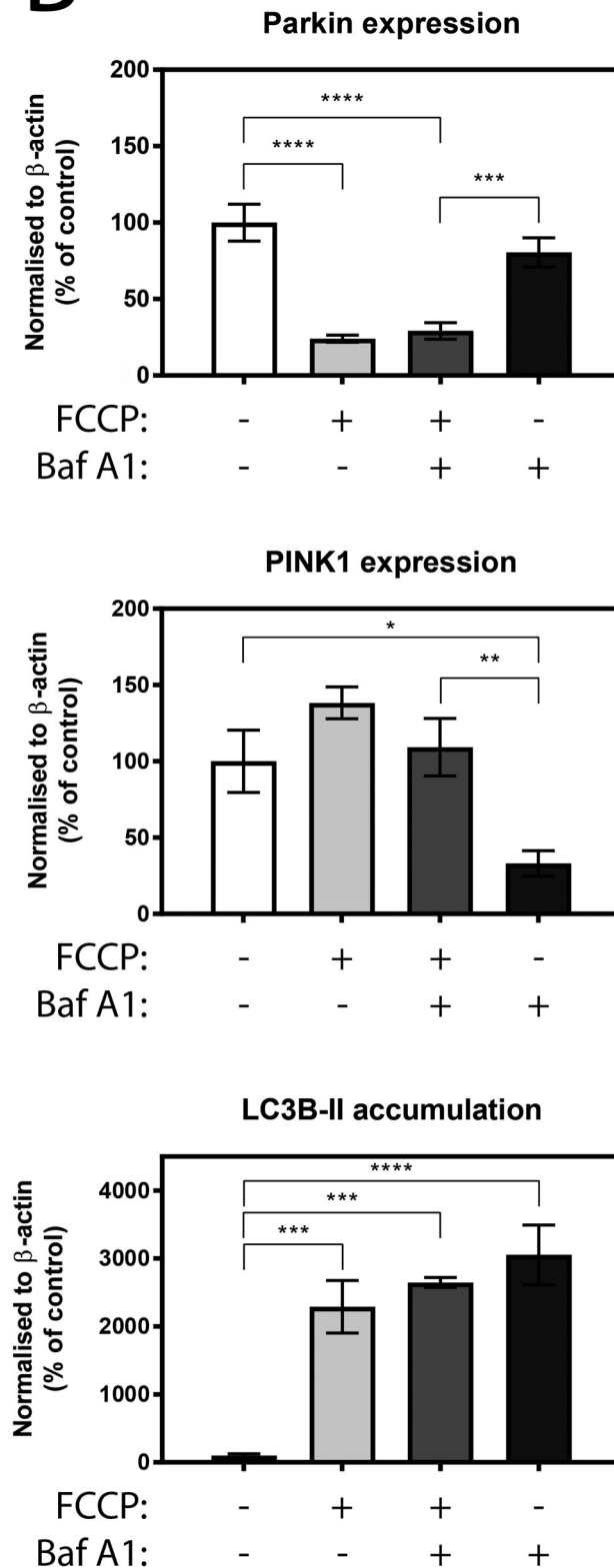
B

Figure 3.3.1 (B). FCCP induces mitophagy in SH-SY5Y cells. Parkin, PINK1, and LC3B-II densitometry normalised to corresponding β -actin levels. Densitometric analysis was pooled from the three independent experiments in panel A and data is shown as percentage of control. Error bars = SEM, one-way ANOVA, * $p < 0.05$, ** $p < 0.01$, *** $p < 0.001$, **** $p < 0.0001$.

RT-qPCR revealed both Parkin and PINK1 mRNA expression were increased upon FCCP treatment (Figure 3.3.1 C). A time course showed that mRNA expression increased over time, however, a decrease in mRNA expression was seen at 16 hours of FCCP treatment, after which mRNA expression increased even further.

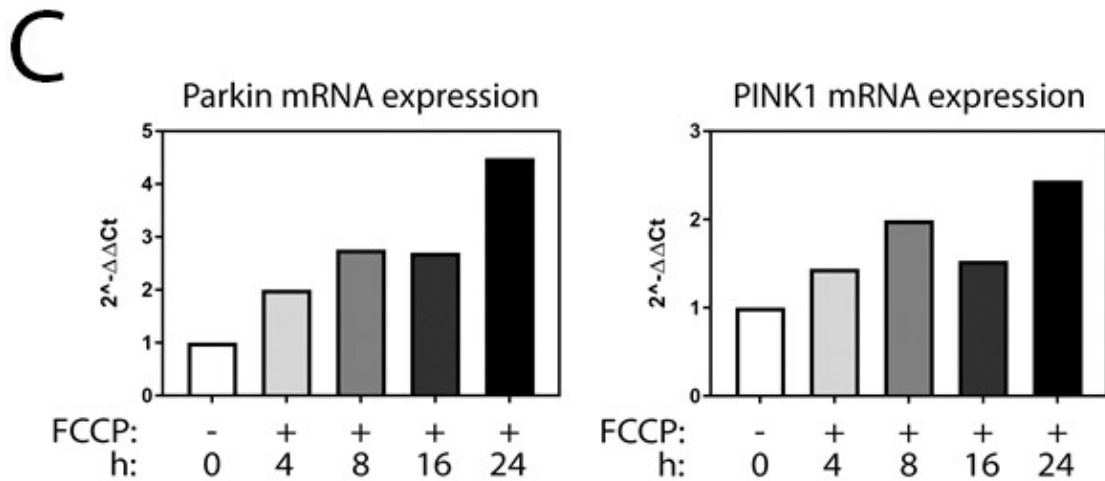


Figure 3.3.1 (C). *FCCP induces mitophagy in SH-SY5Y cells.* Induction of mitophagy is concomitant with increased Parkin and PINK1 mRNA expression. SH-SY5Y cells were treated with 5 μ M FCCP for indicated time points after which RNA was isolated. Parkin and PINK1 mRNA expression levels were normalised to the housekeeping gene 18s and are depicted as fold increase ($2^{-\Delta\Delta Ct}$). Data represents one experiment.

Mitophagy is not only characterised by decreased Parkin and PINK1 accumulation, but also by degradation of mitochondrial marker proteins. To determine the extent of mitochondrial degradation, SH-SY5Y cells were treated with 5 μ M FCCP for different time points. FCCP treatment led to degradation of mitochondrial markers TOM20 and TIM23 over time, with TIM23 showing the greatest decrease (Figure 3.3.2 A). The mitochondrial marker VDAC1, on the other hand, showed increased expression at 24 hours of FCCP treatment despite being degraded at earlier time points.

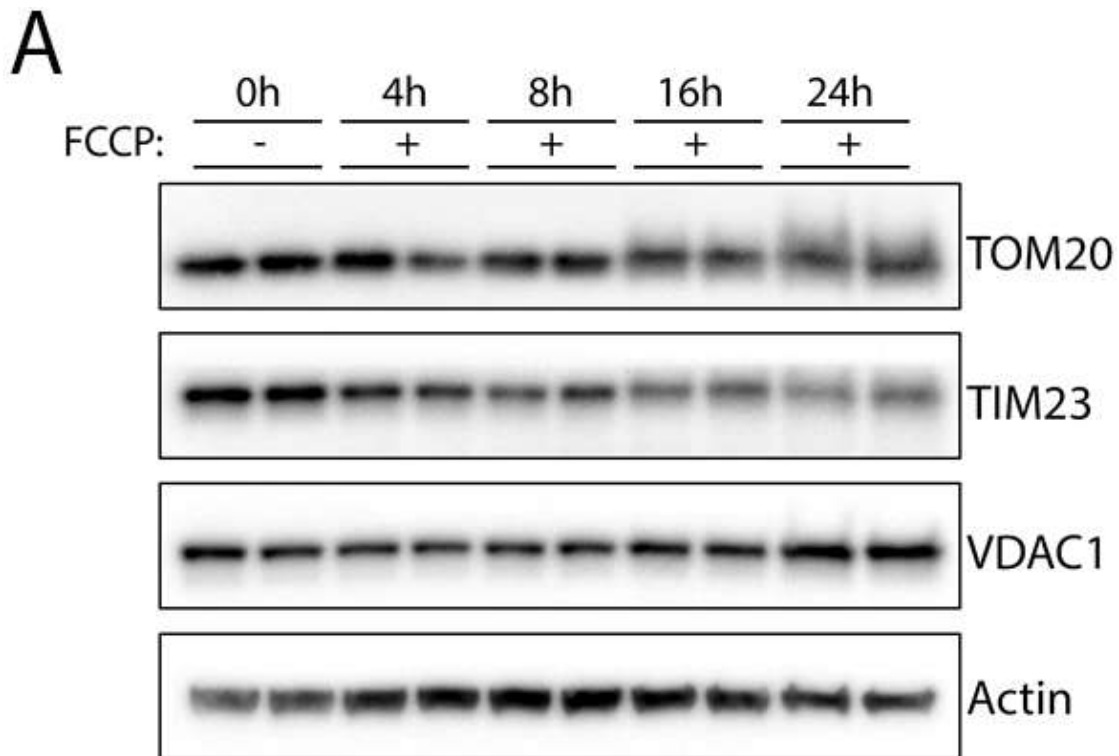


Figure 3.3.2 (A). *SH-SY5Y* cells show degradation of mitochondrial markers upon FCCCP treatment. Treatment of *SH-SY5Y* cells with FCCCP causes degradation of the mitochondrial markers TOM20, TIM23, and VDAC1 over time, although VDAC1 expression increased at 24 hours of treatment. *SH-SY5Y* cells were treated with 5 μ M FCCCP for indicated time points. Protein lysates (20 μ g) were probed for mitochondrial marker proteins TOM20, TIM23, and VDAC1. β -actin was used as loading control. Data represents one out of a total of three independent experiments.

Densitometric analysis confirmed that TIM23 ($p < 0.01$ at 4 hours, $p < 0.001$ at 8 and 16 hours, and $p < 0.05$ at 24 hours) was decreased upon FCCCP treatment (Figure 3.3.2 B). It also showed that TOM20 expression was increased at 16 and 24 hours of FCCCP treatment, which was likely caused by smearing of the protein bands (see Figure 3.3.2 A). Nevertheless, TIM23, although significantly decreased compared to control ($p < 0.05$), was increased after 24 hours of FCCCP treatment too and diffuse protein bands were not observed on the immunoblot (Figure 3.3.2 B). VDAC1 was significantly increased at 24 hours of FCCCP treatment ($p < 0.001$), suggesting VDAC1 could either be recycled or synthesised.

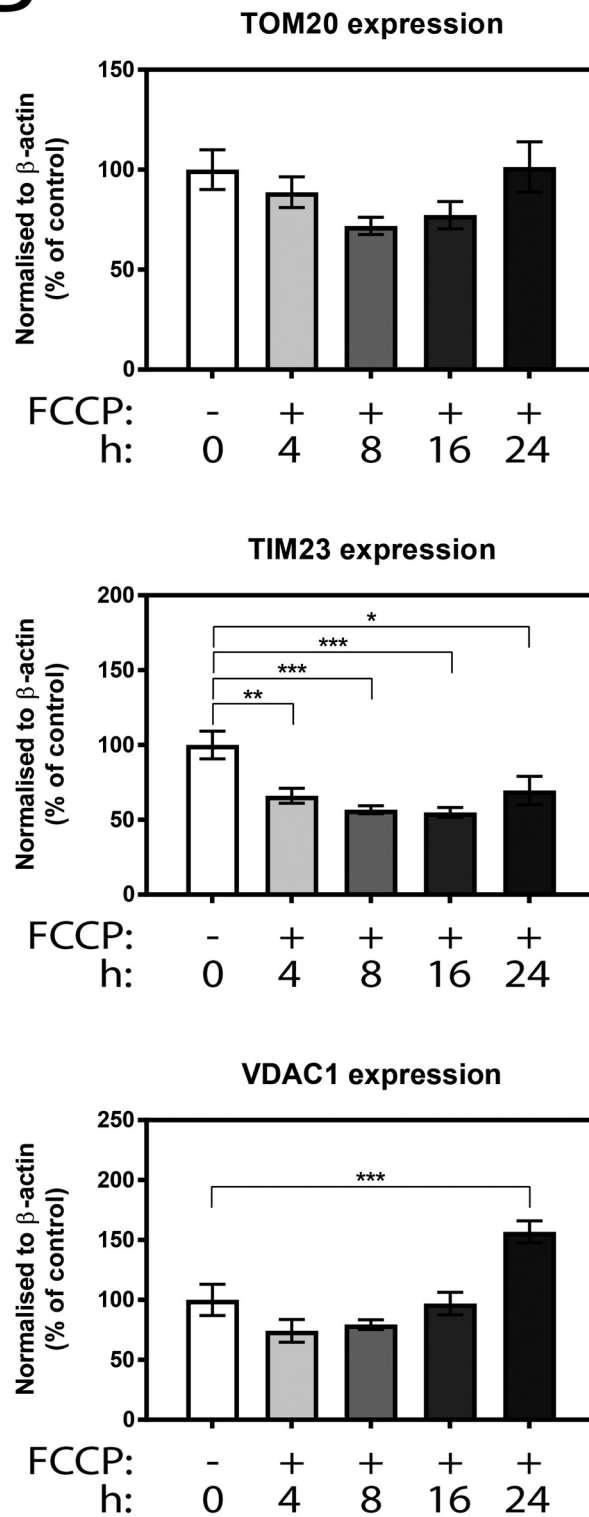
B

Figure 3.3.2 (B). *SH-SY5Y* cells show degradation of mitochondrial markers upon FCCP treatment. TOM20, TIM23, and VDAC1 densitometry normalised to corresponding β -actin levels. Densitometric analysis was pooled from the three independent experiments in panel A and data is shown as percentage of control. Error bars = SEM, one-way ANOVA, * $p < 0.05$, ** $p < 0.01$, *** $p < 0.001$.

3.4 Proteasomal inhibition prevents FCCP-induced Parkin degradation and mitophagy

After establishing FCCP activated mitophagy in SH-SY5Y cells, the involvement of proteasomal degradation during mitophagy was investigated. Parkin, an E3 ubiquitin ligase, is responsible for ubiquitination of proteins on the MOM during mitophagy, as well as for the activation of the ubiquitin-proteasome system (UPS), suggesting proteins ubiquitinated by Parkin could be proteasomally degraded instead of via the autophagic pathway (Narendra et al., 2010a, Chan et al., 2011).

To examine if mitochondrial proteins are proteasomally degraded when cells are undergoing mitophagy, early (E) and late (L) passage SH-SY5Y cells were challenged with 20 μ M of the proteasome inhibitor MG132. As shown in previous sections, FCCP treatment led to degradation of Parkin and the mitochondrial markers TOM20 and TIM23, as well as activation of autophagy seen by increased LC3B turnover and *de novo* synthesis of p62 (Figure 3.4.1 A). Proteasomal inhibition led to a further accumulation of both LC3B-II, which could result from upregulation of autophagy as a response to increased levels of ubiquitinated proteins, and p62, which, apart from being degraded by the autophagic pathway, can be proteasomally degraded as well (Song et al., 2016). Proteasomal inhibition also increased the expression of TOM20, TIM23, and VDAC1. When co-treated with FCCP, degradation of Parkin was prevented by proteasomal inhibition, with FCCP-induced mitophagy being inhibited as a consequence. PINK1 was immunoblotted too but did not result in any detectable signal.

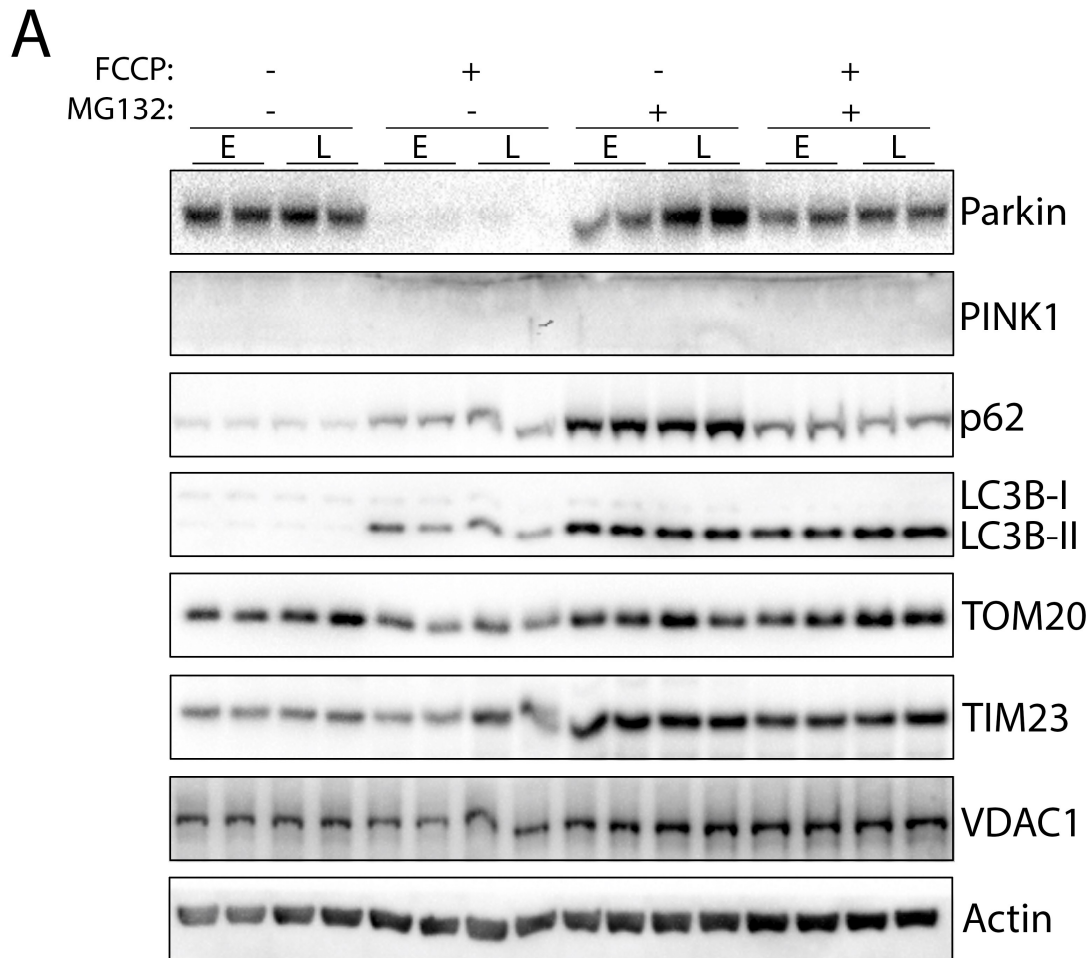


Figure 3.4.1 (A). *Inhibition of the proteasome prevents FCCP-induced degradation of Parkin and mitophagy.* Proteasomal inhibition leads to LC3B-II accumulation, increases p62, TOM20, TIM23, and VDAC1 expression and also prevents FCCP-induced Parkin degradation, leading to inhibition of mitophagy. Early (E) and late (L) passage SH-SY5Y cells were treated with either 5 μ M FCCP, 20 μ M MG132, or both, for 24 hours. Protein lysates (20 μ g) were probed for mitophagy marker proteins Parkin and PINK1, autophagy marker proteins p62 and LC3B, and mitochondrial marker proteins TOM20, TIM23, and VDAC1. β -actin was used as loading control. Data represents one out of a total of three independent experiments.

Densitometry showed that TOM20 (early = $p < 0.01$, late = $p < 0.05$) was significantly degraded upon FCCP treatment (Figure 3.4.1 B). Proteasomal inhibition increased expression of TIM23 (early = $p < 0.05$), suggesting it was proteasomally degraded under basal conditions. Induction of mitophagy upon proteasomal inhibition resulted in increased expression of TOM20 (late = $p < 0.05$), TIM23 (early = $p < 0.05$), and

VDAC1 (early = $p < 0.05$, late = $p < 0.01$) when compared to control. The significant increased TOM20 (early = $p < 0.05$, late = $p < 0.001$), TIM23 (early = $p < 0.001$, late = $p < 0.05$) and VDAC1 (early = $p < 0.001$, late = $p < 0.01$) expression when FCCP and co-treatment of FCCP with MG132 were compared indicates that the proteasome is involved in their degradation upon FCCP-induced damage.

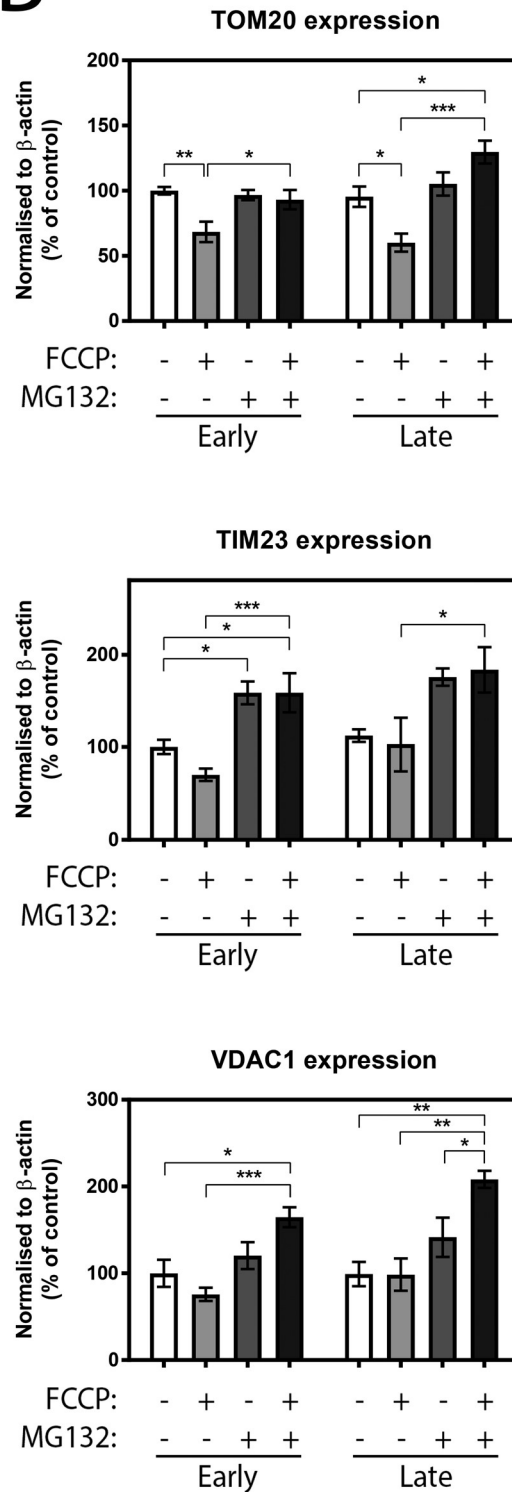
B

Figure 3.4.1 (B). *Inhibition of the proteasome prevents FCCCP-induced degradation of Parkin and mitophagy.* Densitometry of TOM20, TIM23, and VDAC1 normalised to corresponding β -actin levels. Densitometric analysis was pooled from three independent experiments in panel A and data is shown as percentage of control. Error bars = SEM, one-way ANOVA, * $p < 0.05$, ** $p < 0.01$, *** $p < 0.001$.

3.5 Discussion

This study demonstrates that the mitochondrial uncoupler FCCP is capable of activating autophagy in SH-SY5Y cells, which is an event that has been observed in several cell lines (Sandoval et al., 2008, Ma et al., 2011). Activation of autophagy by FCCP was established by examination of mTORC1 signalling. Inhibition of the mTORC1 complex is the first step in the induction of canonical autophagy and leads to activation of ULK1 (Russell et al., 2014). mTORC1 inhibition upon FCCP treatment was confirmed by decreased levels of phosphorylated S6K1 (Figure 3.1.2 A & B), another downstream target of mTORC1 responsible for protein synthesis, and increased phosphorylation of ERK1/2 (Esclatine et al., 2009, Laplante and Sabatini, 2009, Chen et al., 2013, Melemedjian et al., 2013) (Figure 3.1.4 A & B). The effect of PD184352 on mitophagy was not explored, but induction of ERK1/2 phosphorylation was inhibited by FCCP, suggesting that induction of mitochondrial damage activates the Ras pathway while concomitantly inhibiting the mTORC1 pathway, leading to activation of canonical autophagy processes. Literature confirmed involvement of the ERK signalling pathway in mitophagy since inhibition of MEK, the upstream kinase of ERK, blocked degradation of membrane proteins and mitochondrial matrix upon MPP⁺ poisoning in SH-SY5Y cells (Zhu et al., 2007).

Activation of autophagy was further confirmed by measuring the autophagic flux upon FCCP treatment. Autophagic flux can be measured by fluctuations in p62 expression and LC3B-II accumulation, whereby decreased p62 expression and increased conversion of LC3B-I to LC3B-II indicate activation of autophagy. FCCP treatment gave rise to increased LC3B turnover, but also increased, as opposed to decreased, p62 expression (Figure 3.2.1). p62 binds to ubiquitinated proteins and

brings them into the autophagosome by binding directly to LC3B, leading to p62 degradation when autophagy is activated (Pankiv et al., 2007). Increased p62 expression would therefore suggest a blockade of autophagy. Obstruction of the late phase of autophagy by preventing fusion between autophagosomes and lysosomes by Baf A1 showed a further increase in p62 levels (as well as LC3B-II), indicating autophagy was not inhibited. Inhibition of protein synthesis by CHX showed that FCCP caused *de novo* synthesis of p62, suggesting increased amounts of p62 could be needed to keep up with the increasing demand of removal of ubiquitinated proteins (Figure 3.2.3 A & B). These observations were supported by a recently published study showing that treatment of SH-SY5Y cells with CCCP for 18 hours resulted in increased p62 mRNA and protein expression levels, which led the authors to propose that increased p62 protein levels were observed because of *de novo* protein expression rather than inhibition of autophagy (Ivankovic et al., 2016), which is in agreement with the data presented herein.

Mitophagy, which is the selective removal of superfluous and damaged mitochondria (Narendra et al., 2010b), was induced by FCCP in SH-SY5Y cells also. One of the characteristics of mitophagy is decreased Parkin and increased PINK1 expression, which was induced by FCCP-mediated mitochondrial depolarisation in SH-SY5Y cells (Figure 3.3.1 A & B). FCCP treatment led to degradation of the mitochondrial markers TOM20, TIM23, and VDAC1, showing mitophagy was successfully induced (Figure 3.3.2 A & B). Visualisation of the mitochondrial network indicated that FCCP caused mitochondrial fragmentation and increased LC3B puncta formation that represent autophagosomes (Figure 3.2.4 C), which was reported previously (Legros et al., 2002, Cereghetti et al., 2010, Geisler et al., 2010, Cheng et al., 2016). LC3B

puncta and mitochondrial TOM20 staining did not overlap, suggesting that damaged mitochondria were not present inside autophagosomes or that TOM20 is already recycled before damaged mitochondria enter into autophagosomes. Chan and colleagues demonstrated that autophagy-deficient Parkin-expressing ATG3-null MEF failed to undergo mitophagy, but that cells still showed loss of TOM20 staining (Chan et al., 2011), which is in agreement with the data presented in this chapter.

Induction of autophagy and especially increase in LC3B puncta upon FCCP treatment suggests autophagy plays a considerable part in successful implementation of mitophagy. However, proteasomal inhibition in SH-SY5Y cells prevented Parkin degradation and inhibited FCCP-induced degradation of the mitochondrial markers TOM20, TIM23, and VDAC1 (Figure 3.4.1 A & B). Literature confirmed that inhibition of the ubiquitin-proteasome system (UPS) in SH-SY5Y cells completely abrogated mitophagy, showing the importance of proteasomal degradation when it comes to mitochondrial degradation (Chan et al., 2011). In addition, CCCP-mediated degradation of proteins on the MOM (among others TOM20) in autophagy defective MEFs was blocked by addition of the proteasomal inhibitors epoxomicin (Chan et al., 2011) or lactacystin (Yoshii et al., 2011).

Chapter 4

Effects of autophagic inhibition on mitophagy in SH-SY5Y cells

4.0 Introduction

The majority of mitophagy related research has been focussed on regulation of PINK1 and Parkin, and not autophagy related proteins, during mitophagy. Autophagy can begin following inhibition of mTORC1, leading to de-repression and the release of ULK1 from the mTORC1 inhibitory complex, leading to the subsequent activation of the PIK3C3 complex, which is required for nucleation of the autophagosome membrane (Russell et al., 2014). Processing of cytosolic LC3B into LC3B-I and conjugation of PE to form the membrane bound LC3B-II marks one of the final stages of autophagy.

ULK1 is a serine/threonine protein kinase that plays a key role in the induction of canonical autophagy (Russell et al., 2014). ULK1 is repressed by mTORC1 by means of phosphorylation during nutrient-rich conditions, whereas starvation leads to dissociation of mTORC1 from the ULK1 complex (consisting of ULK1, ULK2, FIP200, ATG13, and ATG101), leading to dephosphorylation of ULK1 and trans-phosphorylation of ATG13 and FIP200, which results in activation of the ULK1 complex (Hara et al., 2008, Ganley et al., 2009, Hosokawa et al., 2009a, Hosokawa et al., 2009b, Jung et al., 2009, Mercer et al., 2009). Blocking ULK1 activity effectively inhibits canonical autophagy, illustrating its importance for autophagy (Chan et al., 2007, Ganley et al., 2009, Jung et al., 2009). Nevertheless, it was also found that LC3B conversion following starvation was not affected in ULK1-deficient MEF (Kundu et al., 2008, Cheong et al., 2011, Lee and Tournier, 2011). Further research showed that combined deletion of ULK1 and ULK2 inhibited the autophagy response to nutrient starvation and that mice deficient for both *ULK1* and *ULK2* died shortly after birth, whereas mice deficient in either one of these genes were viable and did not

show any obvious developmental defects, suggesting ULK2 can compensate loss of ULK1 (Kundu et al., 2008, Cheong et al., 2011, Lee and Tournier, 2011).

After its activation, ULK1 phosphorylates Beclin1, which is together with hVps15, UVRAG, and ATG14L part of the PIK3C3 (class III phosphatidylinositol (PtdIns) 3-kinase) complex (Kim et al., 2013, Russell et al., 2013, Russell et al., 2014). While this complex is normally tethered to the cytoskeleton, phosphorylation of AMBRA1 through ULK1 localises it to the phagophore (Di Bartolomeo et al., 2010, Itakura and Mizushima, 2010, Matsunaga et al., 2010, Fan et al., 2011). The PIK3C3 complex is responsible for phosphorylation of PtdIns to PtdIns(3)P, thereby generating the lipid signal necessary for autophagosome biogenesis, which can be differentially regulated at different points in the autophagy pathway depending on proteins recruited by Beclin1 (Petiot et al., 2000, He and Levine, 2010, Wirth et al., 2013). The two main complexes involve either ATG14L or UVRAG, but Beclin1 was also found to interact with several other co-factors including Rubicon, Bif-1, or ROCK1, that are all involved in regulating PIK3C3 complex activity (Liang et al., 2006, Takahashi et al., 2007, Matsunaga et al., 2009, Zhong et al., 2009, Gurkar et al., 2013). ATG14L can induce autophagosome formation by upregulating PIK3C3 activity (Matsunaga et al., 2009, Zhong et al., 2009), whereas UVRAG can promote both autophagosome biogenesis and maturation (Liang et al., 2006, Liang et al., 2008). ATG14L and UVRAG bind directly to Beclin1 while Rubicon inhibits and Bif-1 stimulates PIK3C3 activity by interacting with Beclin1 through UVRAG (Takahashi et al., 2007, Matsunaga et al., 2009, Zhong et al., 2009).

It is known that ULK1 is also involved in the selective clearing of mitochondria during maturation of reticulocytes since ULK1-knockout mice showed defects in this process (Kundu et al., 2008). Involvement of ULK1 in mitochondrial clearance is implicated in MEF as well, showing that this is not restricted to reticulocytes (Itakura et al., 2012). More importantly, MEF deficient in FIP200 or MEF with reduced ATG13 activity, which are both part of the ULK1 complex, showed no activation of autophagy following starvation, however, they were still able to show a reduced rate of LC3B lipidation upon induction of mitochondrial damage by the mitochondrial proton gradient uncoupler CCCP, suggesting that non-canonical autophagy could have been activated (Chen et al., 2013).

The PIK3C3 complex was also reported to be dispensable for photodamage-induced mitophagy in hepatocytes (Kim and Lemasters, 2011b). Phosphoinositide 3-kinase (PI3K) inhibitors successfully blocked sequestration of mitochondria during starvation, but not upon photodamage-induced mitophagy. Furthermore, knockdown of either Beclin1 or its partner ATG14L did not diminish LC3B puncta formation or LC3B turnover (Chen et al., 2013). This is particularly interesting since Beclin1 was shown to interact with both Parkin and PINK1. Interaction between full-length PINK1 and Beclin1 significantly enhanced basal and starvation-induced autophagy, which was reduced by knocking down either Beclin1 or PIK3C3 expression (Michiorri et al., 2010). Loss of Beclin1 led to inhibition of CCCP-induced Parkin translocation to mitochondria and prevented Parkin-mediated mitophagy (Choubey et al., 2014).

Both LC3B and p62 are implicated in mitophagy, with LC3B being involved in the clearance of damaged mitochondria since it was shown that nutrient deprivation, as

well as mitochondrial depolarisation by photo irradiation, led to LC3B-labelled autophagosomes containing mitochondria (Kim and Lemasters, 2011a, Kim and Lemasters, 2011b). p62 was linked to mitophagy too, however, its requirement for effective execution of mitophagy is still unclear and further research is needed. On one hand, p62 knockdown was reported to significantly decrease mitochondrial clearance (Ding et al., 2010, Geisler et al., 2010, Lee et al., 2010), while on the other hand no changes in mitophagy were observed in p62-knockout cells (Narendra et al., 2010b, Okatsu et al., 2010).

Current research hints that CCCP-mediated mitochondrial damage and subsequent mitochondrial clearance might not completely depend on the autophagy pathway, or at least not on the canonical pathway. However, more research on this topic is needed, especially in a neuronal setting since that has been barely investigated. Therefore, involvement of the ULK1 and PIK3C3 complexes in FCCP-induced mitophagy in SH-SY5Y cells will be utilised. The effects of ULK1 or PIK3C3 inhibition on PINK1 and Parkin expression, as well as degradation of the mitochondrial markers TOM20, TIM23, and VDAC1, were analysed upon co-treatment with FCCP.

4.1 SH-SY5Y cells do not respond to different modulators of autophagy

SH-SY5Y cells were treated with different activators (rapamycin (Rap), EBSS) and different inhibitors (chloroquine (CQ), the effects of Baf A1 were shown in Chapter 3) of autophagy alongside FCCP for 24 hours to see their effects on expression levels of autophagy related proteins. Treatment with 5 μ M FCCP led to decreased Parkin and increased PINK1 expression, concomitant with LC3B-II accumulation and *de novo* synthesis of p62, indicating induction of autophagy and mitophagy (Figure 4.1.1 A; see Chapter 3). Rapamycin treatment (0.1 μ M), which relieves cells from mTORC1 inhibition and thereby activates autophagy, did not result in changes in expression levels of immunoblotted mitophagy and autophagy marker proteins. Amino acid deprivation by EBSS showed increased Parkin and PIK3C3 expression. Degradation of p62 suggests autophagic activity, but since neither LC3B-I nor LC3B-II were detected, it is not known if this was accompanied by increased LC3B turnover. Inhibition of autophagy by 5 μ M CQ, which prevents lysosomal protein degradation and fusion of autophagosomes with lysosomes by raising the lysosomal pH, led to a small decrease in Parkin expression and possibly an increase in PINK1 expression, suggesting that it could lead to induction of mitophagy, but did not result in increased p62 expression or LC3B-II accumulation. Collectively, these results suggest that SH-SY5Y cells do not respond to the used activators and inhibitors of autophagy in the classical way.

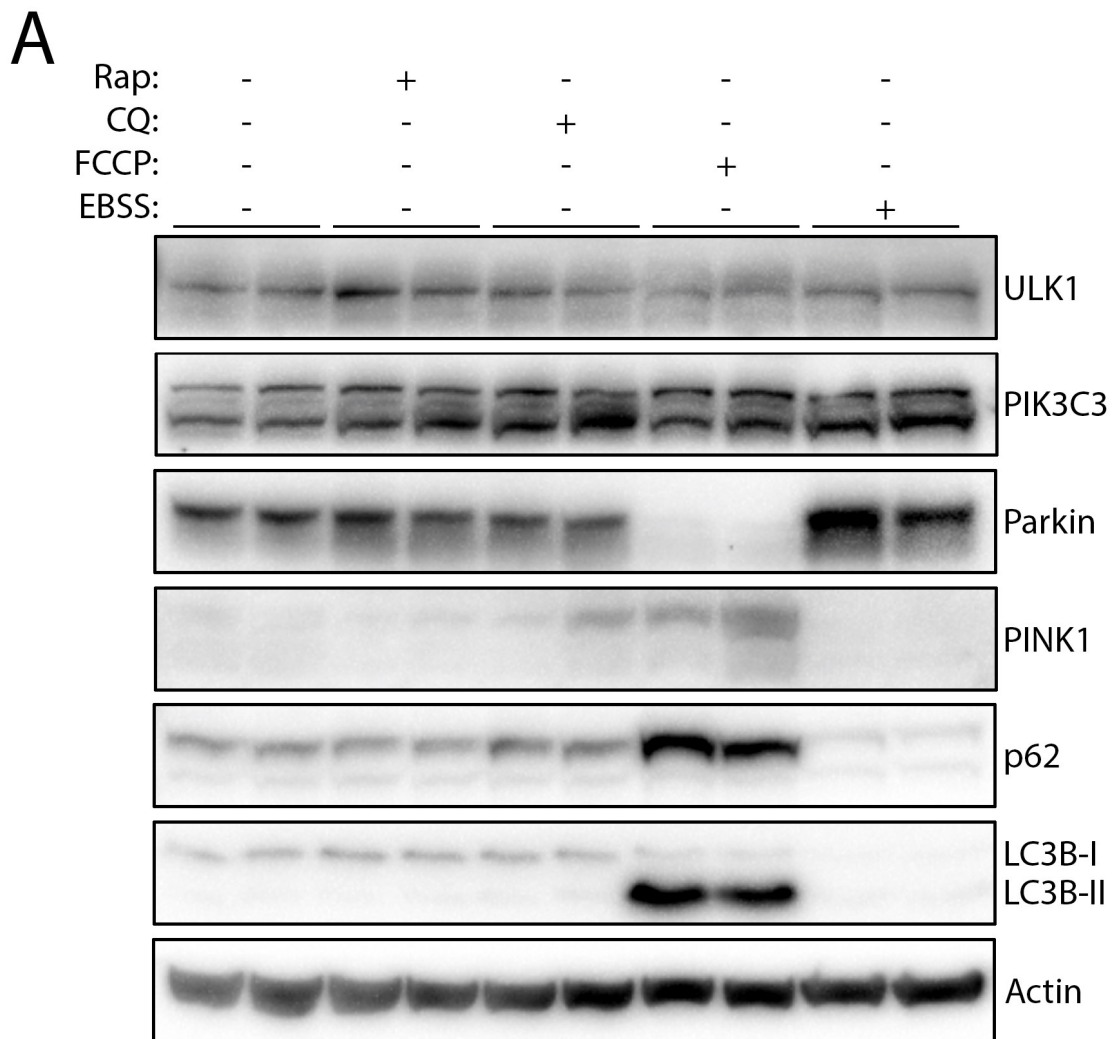


Figure 4.1.1 (A). *SH-SY5Y cells do not show signs of autophagic activity or inhibition upon treatment with different autophagy activators and an inhibitor.* When treated with autophagic activators (rapamycin (Rap), EBSS) or an inhibitor (CQ), SH-SY5Y cells do not show classical signs of autophagic activation or inhibition on protein level, whereas FCCP treatment leads to activation of autophagy and mitophagy. SH-SY5Y cells were treated with either 0.1 μ M rapamycin, 5 μ M CQ, 5 μ M FCCP, or were starved with EBSS, for 24 hours. Protein lysates (20 μ g) were probed for mitophagy marker proteins Parkin and PINK1, and autophagy marker proteins ULK1, PIK3C3, p62, and LC3B. β -actin was used as loading control. Data represents one out of a total of three independent experiments.

Densitometry showed that when protein expression levels were normalised to corresponding β -actin expression, rapamycin ($p < 0.05$) and EBSS ($p < 0.05$) treatment led to p62 degradation, but that this was not accompanied by LC3B-II accumulation

(Figure 4.1.1 B). FCCP induced *de novo* protein synthesis of p62 ($p < 0.001$) and it also led to accumulation of LC3B-II ($p < 0.001$).

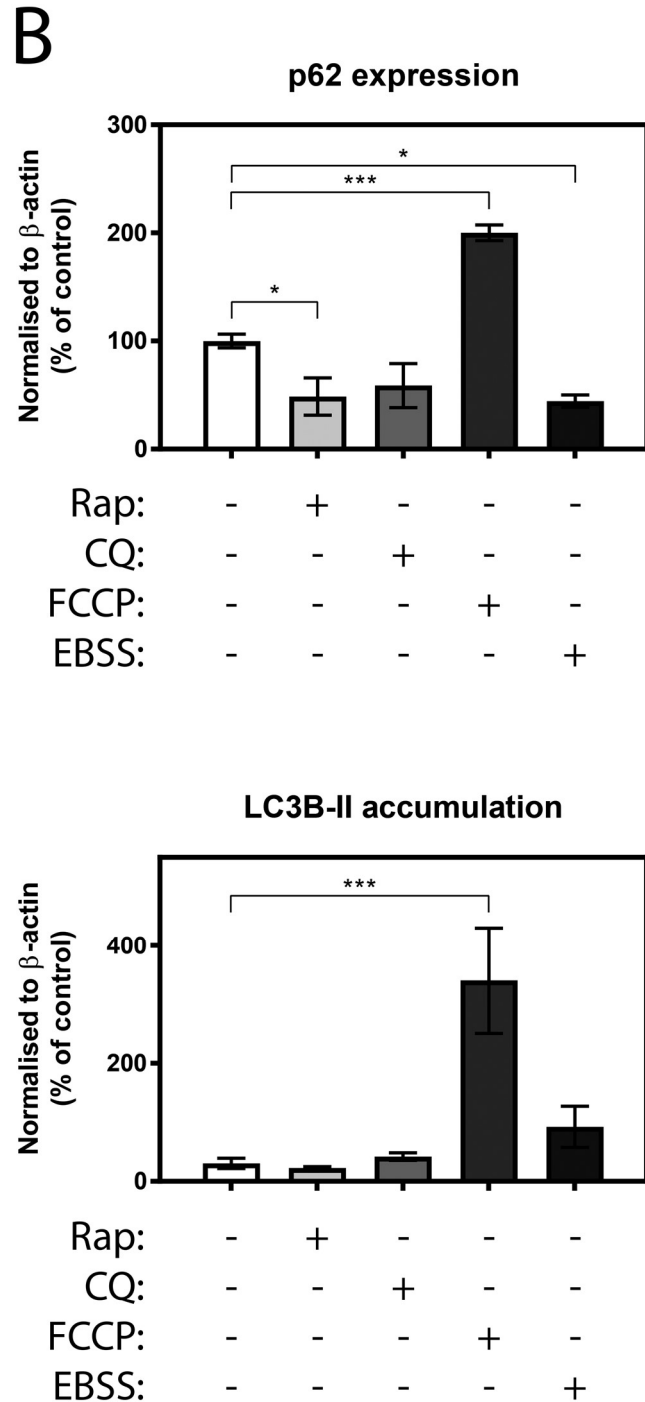


Figure 4.1.1 (B). *SH-SY5Y* cells do not show signs of autophagic activity or inhibition upon treatment with different autophagy activators and an inhibitor. p62 and LC3B-II densitometry normalised to corresponding β -actin levels. Densitometric analysis was pooled from three independent experiments in panel A and data is shown as percentage of control. Error bars = SEM, one-way ANOVA, * $p < 0.05$, *** $p < 0.001$.

4.2 ULK1 inhibition induces PINK1 expression and Parkin degradation

The first step in activation of canonical autophagy is inhibition of the mTORC1 complex (Russell et al., 2014). Under nutrient-rich conditions, the mTORC1 complex binds to and inhibits the ULK1 complex that regulates the downstream autophagy initiation machinery. mTORC1 inhibition leads to dissociation and therefore activation of ULK1, marking the next step in canonical autophagy. To investigate the effects of ULK1 inhibition on mitophagy induction and FCCP-mediated removal of mitochondrial markers, SH-SY5Y cells were challenged with 10 μ M of a small molecule inhibitor of ULK1 (iULK1) for 24 hours. ULK1 inhibition did not result in increased ULK1 expression, which has been observed previously (unpublished data from Ewelina Rozycka, see Appendix I) (Figure 4.2.1 A). In non-neuronal cells, inhibition of ULK1 usually leads to accumulation of p62 and LC3B-II, indicating a blockade of autophagy (Appendix II). Conversely, in SH-SY5Y cells, ULK1 inhibition induced p62 and LC3B-II degradation. It also resulted in loss of PIK3C3 expression, which could indicate a disruption of the PIK3C3 complex. Increased PINK1 expression and Parkin degradation suggests mitophagy was induced, however, VDAC1 expression was increased. Inhibition of ULK1 during FCCP induced mitophagy did not affect Parkin degradation or PINK1 expression, but it did further promote the degradation of p62, which normally accumulates during FCCP treatment, and VDAC1, as well as causing accumulation of LC3B-II, implicating inhibition of canonical autophagy.

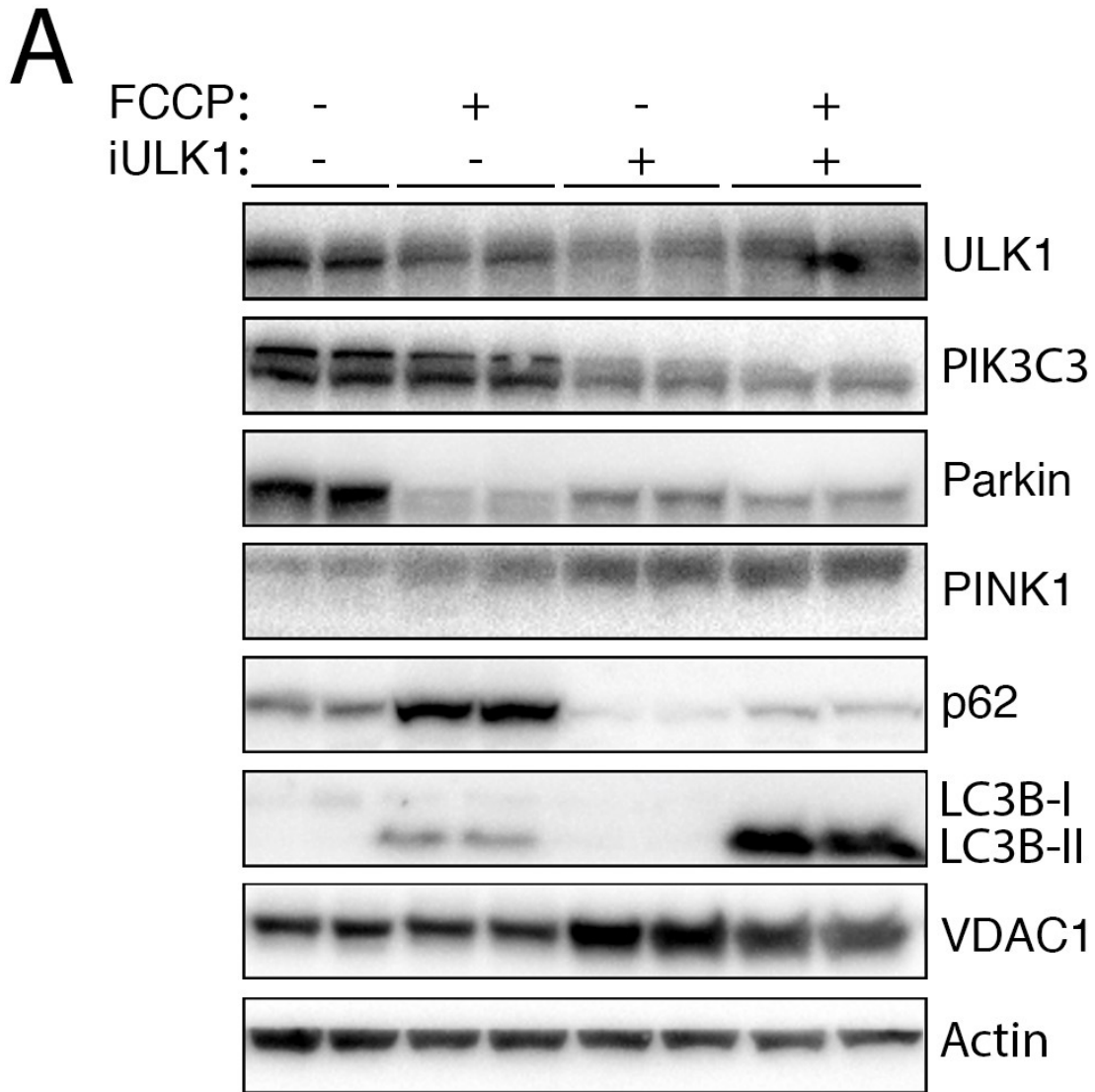


Figure 4.2.1 (A). *ULK1 inhibition induces PINK1 expression and Parkin degradation.* Inhibition of ULK1 with a small molecule inhibitor (iULK1) increases PINK1 expression, leads to Parkin degradation and does not affect Parkin degradation or PINK1 expression upon co-treatment with FCCP. ULK1 inhibition does not induce p62 and LC3B-II accumulation as seen in non-neuronal cells and promotes further degradation of p62 and causes LC3B-II accumulation when combined with FCCP. (A) SH-SY5Y cells were treated with either 5 μ M FCCP, 10 μ M iULK1, or both, for 24 hours. Protein lysates (20 μ g) were probed for mitophagy marker proteins Parkin and PINK1, autophagy marker proteins ULK1, PIK3C3, p62, LC3B, and the mitochondrial marker protein VDAC1. β -actin was used as loading control. Data represents one out of a total of three independent experiments.

All treatments resulted in a significant decrease in Parkin expression ($p < 0.001$) (Figure 4.2.1 B). FCCP-induced *de novo* expression of p62 ($p < 0.0001$) was abolished when ULK1 was inhibited simultaneously ($p < 0.0001$). iULK1 treatment led to decreased p62 expression ($p < 0.01$), regardless of addition of FCCP ($p < 0.05$). LC3B-II accumulation was increased upon FCCP treatment ($p < 0.0001$) and increased further when ULK1 was inhibited too ($p < 0.0001$), which is suggestive for autophagic inhibition. Combined treatment of FCCP and iULK1 also led to LC3B-II accumulation when compared with either FCCP ($p < 0.0001$) or iULK1 ($p < 0.0001$) treatment. VDAC1 expression was increased upon ULK1 inhibition ($p < 0.05$), while it was significantly decreased upon co-treatment with FCCP ($p < 0.01$).

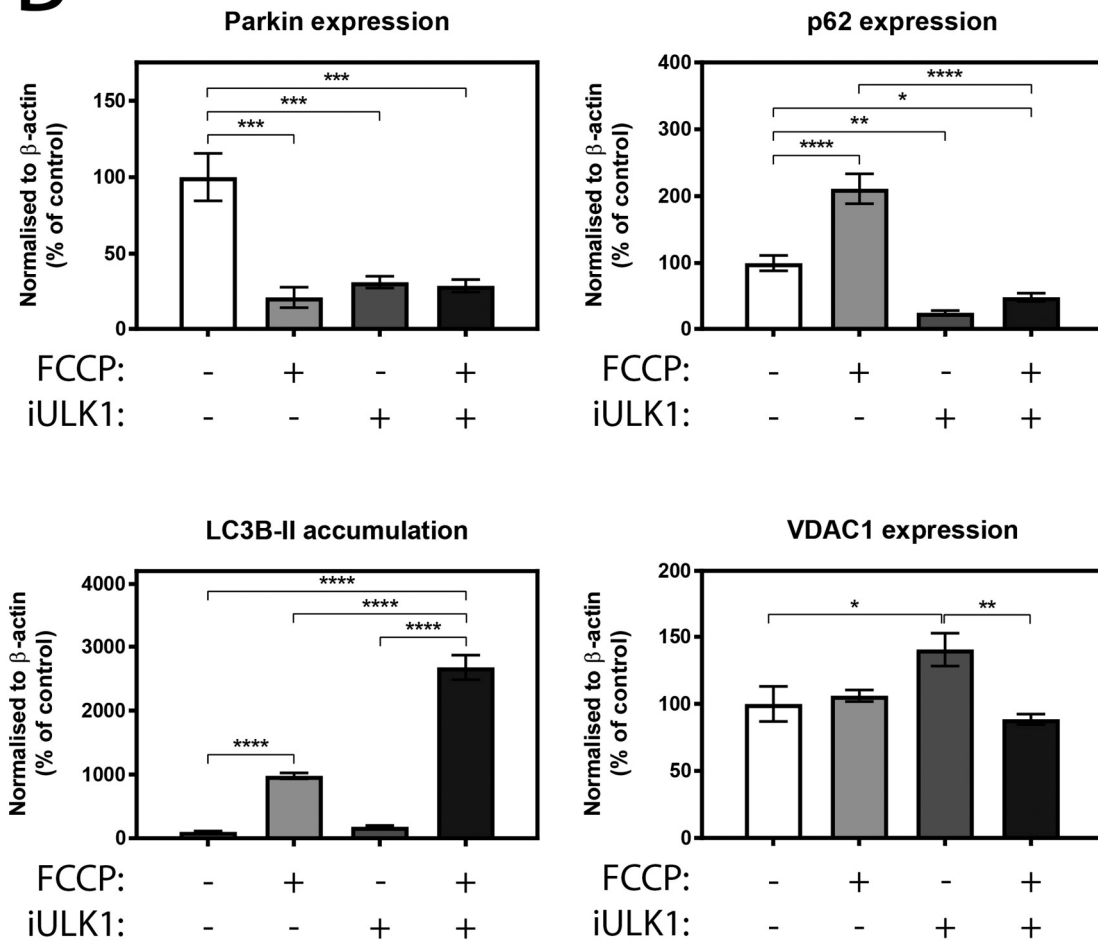
B

Figure 4.2.1 (B). *ULK1* inhibition induces *PINK1* expression and *Parkin* degradation. *Parkin*, *p62*, *LC3B-II*, and *VDAC1* densitometry normalised to corresponding β -actin levels. Densitometric analysis was pooled from three independent experiments in panel A and data is shown as percentage of control. Error bars = SEM, one-way ANOVA, * $p < 0.05$, ** $p < 0.01$, *** $p < 0.001$, **** $p < 0.0001$.

A time course of co-treatment of *iULK1* and *FCCCP* showed that besides increased *Parkin* expression and increased conversion of *LC3B-I* to *LC3B-II*, there were no changes in expression levels of the immunoblotted proteins in the first 8 hours of treatment (Figure 4.2.2 A). Decreased *Parkin* and increased *PINK1* expression was observed at 16 hours of treatment, indicating that mitophagy could be activated, however, increased *VDAC1* expression suggests mitochondria were not degraded. *LC3B-II* accumulation was increased even further from 16 hours of treatment

onwards, likely indicating an autophagic blockade. p62 expression increased at 4 and 8 hours of treatment, but returned to basal levels at later time points. Decrease in p62, ULK1, and PIK3C3 expression at 24 hours of treatment was not as clear as seen previously (see Figure 4.2.1 A).

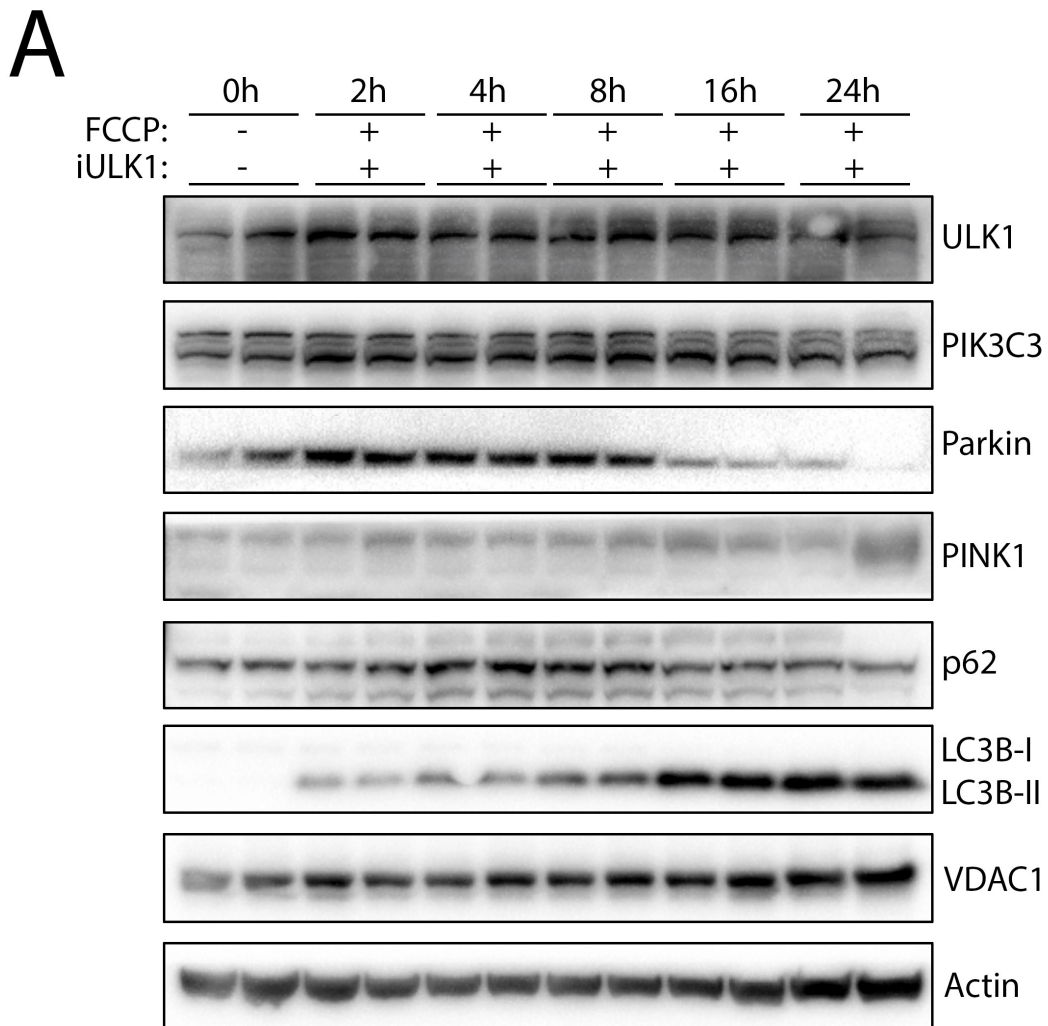


Figure 4.2.2 (A). FCCP-induced Parkin degradation and PINK1 accumulation are not affected by ULK1 inhibition. Parkin degradation and PINK1 accumulation are induced over time upon combined treatment of FCCP and an ULK1 inhibitor (iULK1), which also leads to increased VDAC1 expression. LC3B-II accumulation from 16 hours onwards could indicate that autophagy is blocked. (A) SH-SY5Y cells were treated with 5 μ M FCCP and 10 μ M iULK1 for indicated time points. Protein lysates (20 μ g) were probed for mitophagy marker proteins Parkin and PINK1, autophagy marker proteins ULK1, PIK3C3, p62, and LC3B, and the mitochondrial marker protein VDAC1. β -actin was used as loading control. Data represents one out of a total of three independent experiments.

Contrary to previous obtained results (see Figure 4.2.1 B), densitometry showed that p62 was not degraded and VDAC1 was significantly increased at all time points (2 and 24 hours $p<0.01$, 4 hours $p<0.0001$, 8 and 16 hours $p<0.001$) of FCCP and iULK1 treatment (Figure 4.2.2 B). LC3B-II accumulation showed a continuous significant increase over time (2 hours $p<0.05$, 4 hours $p<0.001$, 8, 16 and 24 hours $p<0.0001$) with its peak at 16 hours of treatment. Parkin expression was decreased, which was statistically significant at 24 hours of treatment ($p<0.05$).

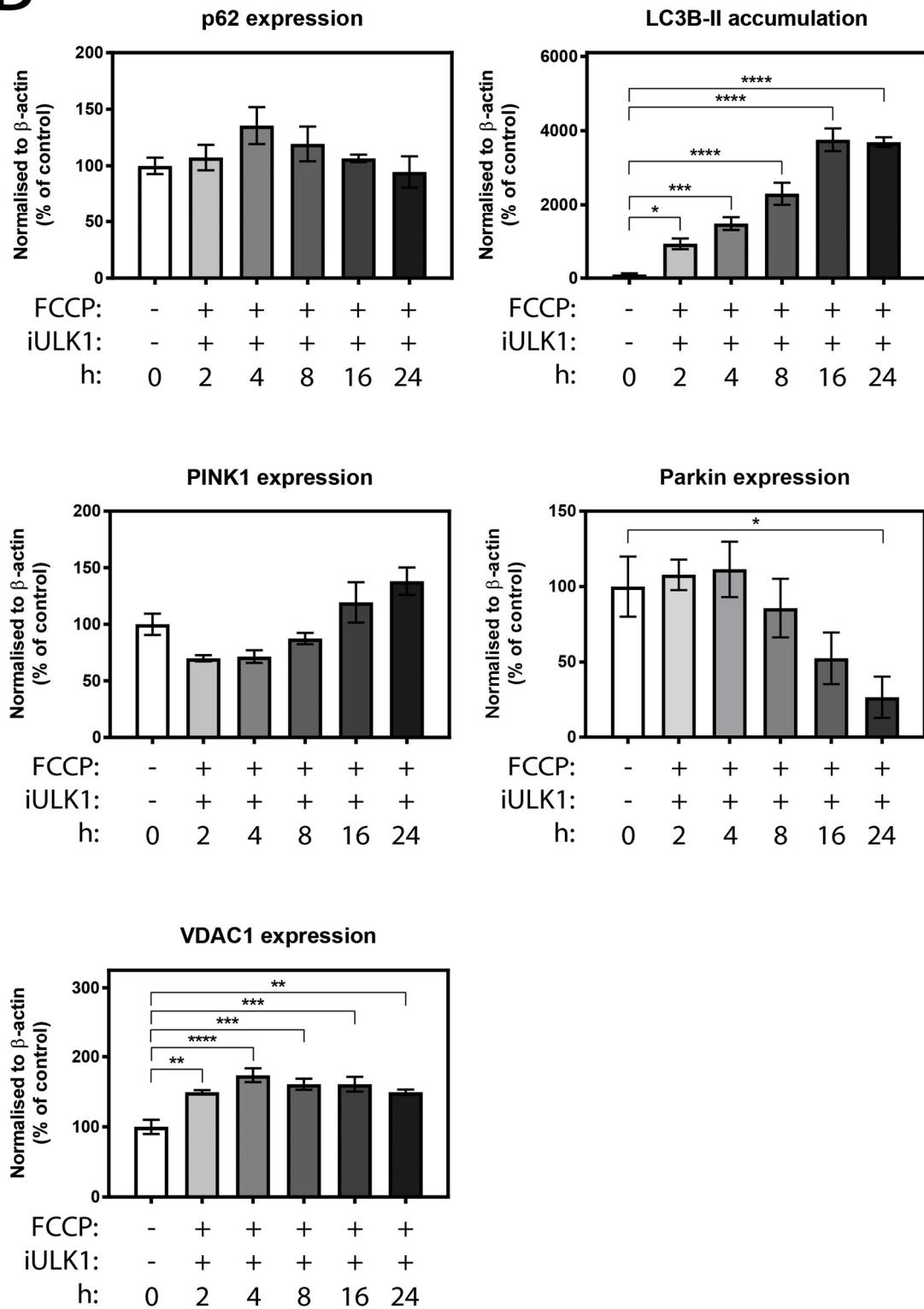
B

Figure 4.2.2 (B). FCCCP-induced Parkin degradation and PINK1 accumulation are not affected by ULK1 inhibition. p62, LC3B-II, PINK1, Parkin, and VDAC1 densitometry normalised to corresponding β -actin levels. Densitometric analysis was pooled from three independent experiments in panel A and data is shown as percentage of control. Error bars = SEM, one-way ANOVA, * $p < 0.05$, ** $p < 0.01$, *** $p < 0.001$, **** $p < 0.0001$.

The observation that ULK1 inhibition resulted in decreased Parkin and increased PINK1 expression suggested that inhibiting ULK1 may mimic damage to mitochondria and induce mitophagy. Thus, mitochondria were visualised by TOM20 staining to examine their morphology. A FCCP time course (5 μ M) led, as shown in Chapter 3, to dispersed TOM20 staining that progressed over time, indicating mitochondrial fragmentation (Figure 4.2.3). ULK1 inhibition (10 μ M) resulted in dispersed TOM20 staining too, however, TOM20 stained mitochondrial fragments appeared to be larger compared to FCCP treated cells (Figure 4.2.4). Mitochondrial fragmentation was also observed when SH-SY5Y cells were co-treated with FCCP and iULK1 (Figure 4.2.5). Enlarged images of TOM20 staining at 2 hours of FCCP, iULK1, or combined treatment of FCCP and iULK1, are shown in Figure 4.2.6.

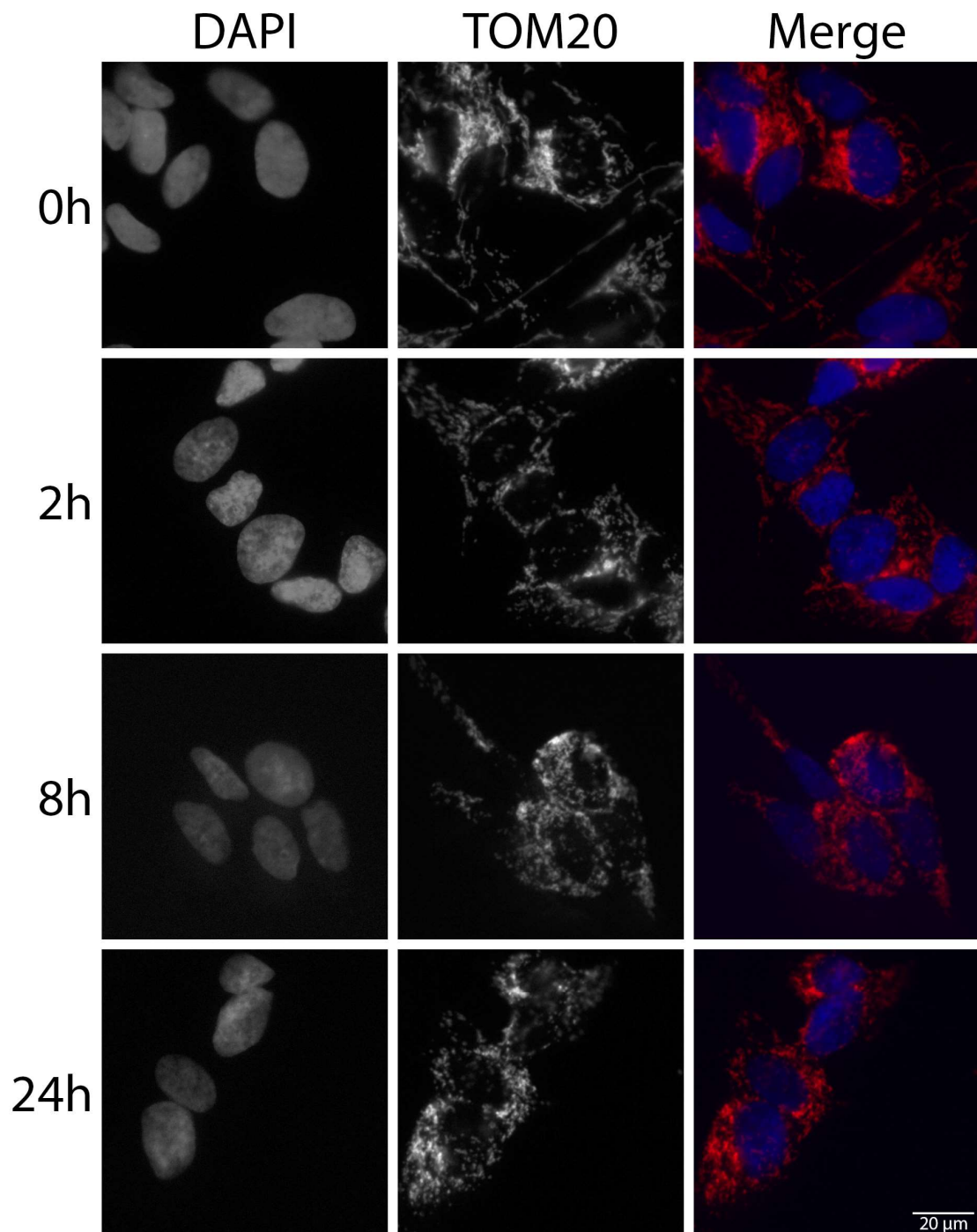


Figure 4.2.3. *FCCP induces mitochondrial fragmentation.* FCCP induces mitochondrial fragmentation in SH-SY5Y cells as seen by dispersed TOM20 staining. The amount of mitochondrial fragmentation increases the longer cells have been treated. SH-SY5Y cells were treated with 5 μ M FCCP for indicated time points before fixation of the cells. Mitochondria were visualised by TOM20 staining (red) and nuclei are labelled with DAPI (blue). Data represents one experiment. Magnification = 60x, scale bar = 20 μ m.

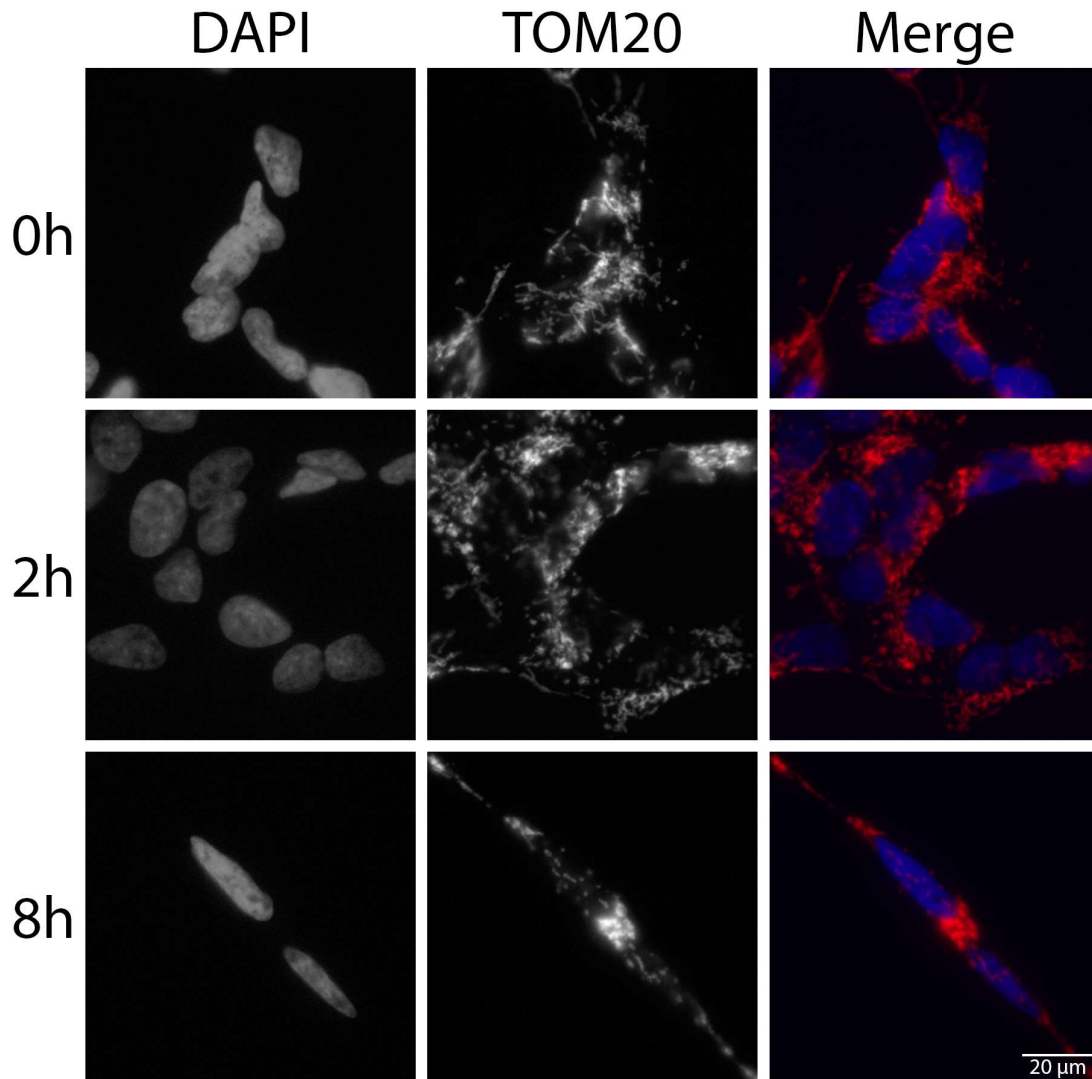


Figure 4.2.4. *ULK1 inhibition induces mitochondrial fragmentation.* ULK1 inhibition induces mitochondrial fragmentation in SH-SY5Y cells as seen by dispersed TOM20 staining. TOM20 stained mitochondrial fragments are larger than observed upon FCCP treatment. SH-SY5Y cells were treated with 10 μ M iULK1 for indicated time points before fixation of the cells. Mitochondria were visualised by TOM20 staining (red) and nuclei are labelled with DAPI (blue). Data represents one experiment. Magnification = 60x, scale bar = 20 μ m.

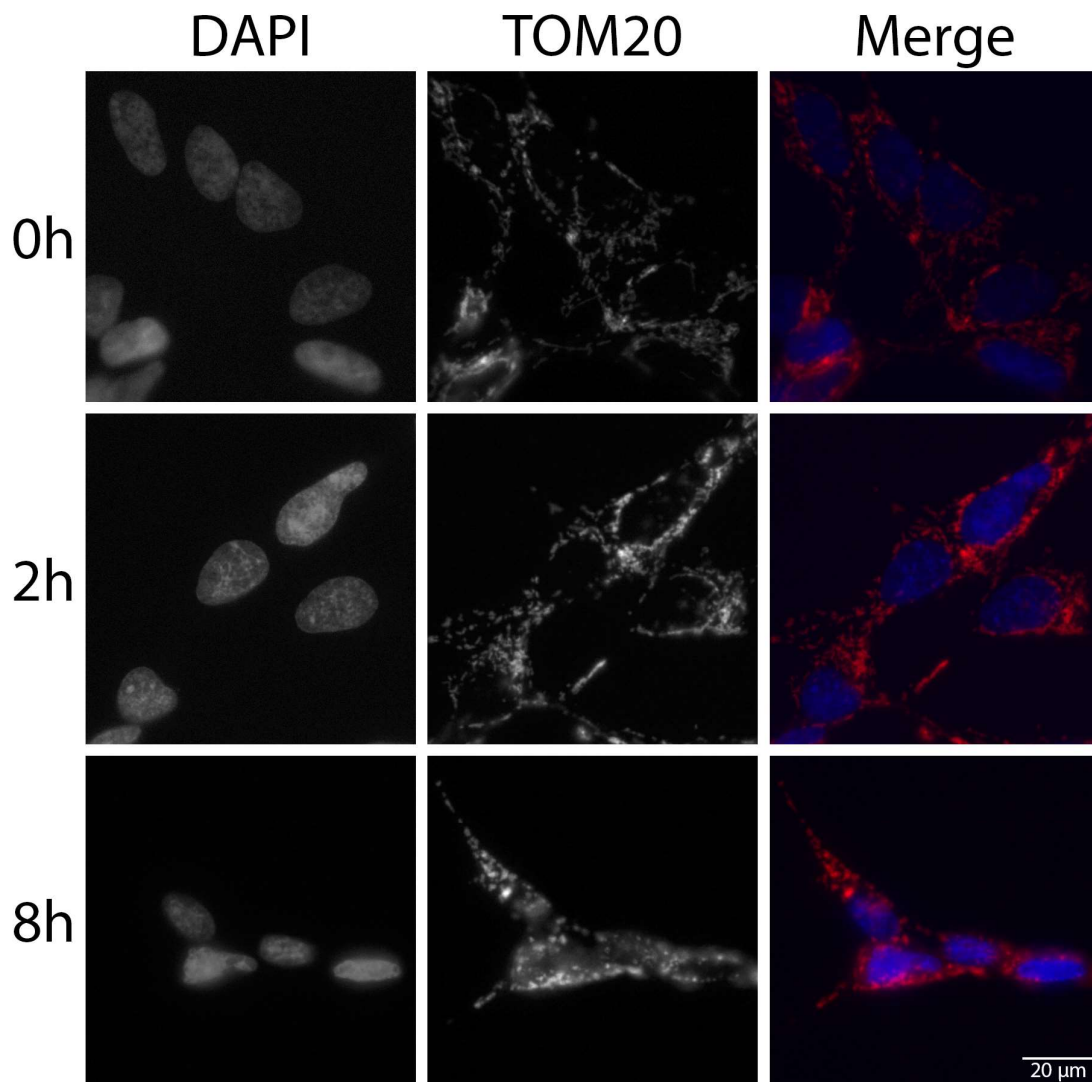
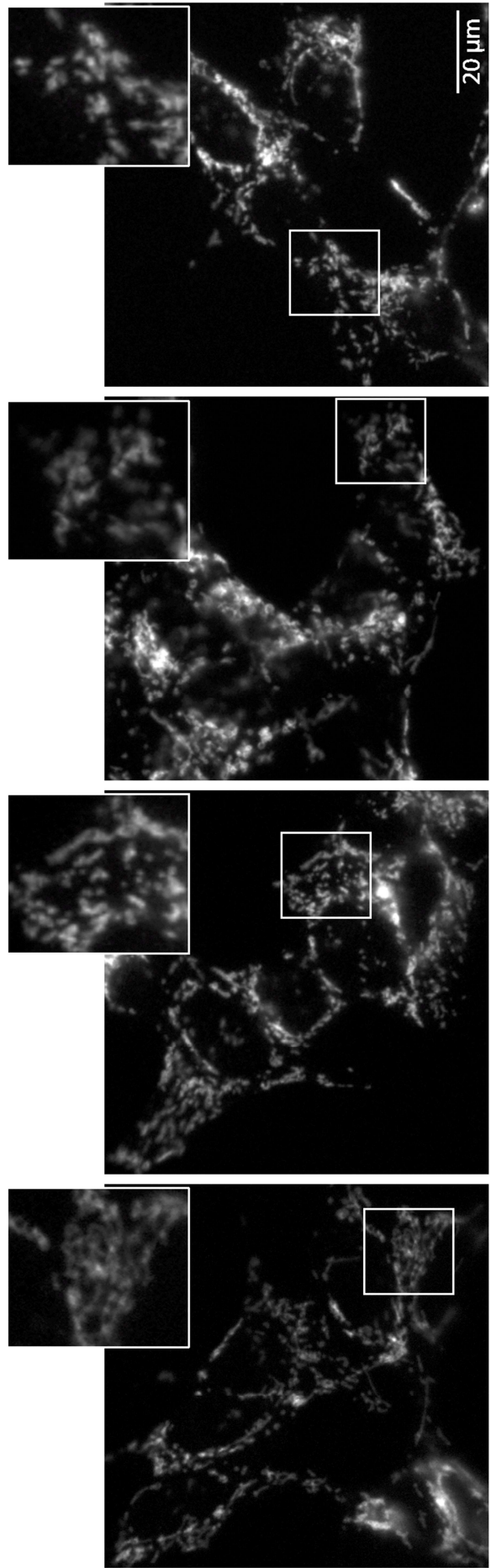


Figure 4.2.5. Mitochondrial fragmentation is induced by combined treatment of FCCP and *iULK1*. FCCP treatment upon ULK1 inhibition leads to dispersed TOM20 staining in SH-SY5Y cells, which is indicative of mitochondrial fragmentation. SH-SY5Y cells were treated with 5 μ M FCCP and 10 μ M *iULK1* for indicated time points before fixation of the cells. Mitochondria were visualised by TOM20 staining (red) and nuclei are labelled with DAPI (blue). Data represents one experiment. Magnification = 60x, scale bar = 20 μ m.



FCCCP + iULK1

iULK1

FCCCP

Ctr

Previous page: Figure 4.2.6. *Mitochondrial fragmentation is induced by FCCP, iULK1, or combined treatment of FCCP and iULK1.* Dispersed TOM20 staining, indicating mitochondrial fragmentation, is observed upon FCCP, iULK1, or combined treatment of FCCP and iULK1, in SH-SY5Y cells. Selected regions (small yellow box) are enlarged and are shown in the top right corner of the respective images (big yellow box). SH-SY5Y cells were treated with either 5 μ M FCCP, 10 μ M iULK1, or both, for 2 hours before fixation of the cells. Mitochondria were visualised by TOM20 staining. Data represents one experiment. Magnification = 60x, scale bar = 20 μ m.

4.3 PIK3C3 inhibition does not affect removal of FCCP damaged mitochondria

Downstream of ULK1 functions the PIK3C3 complex, which is the effector complex that is critical for autophagosome formation. To determine if this complex is involved in the removal of damaged mitochondria in early (E) and late (L) passage SH-SY5Y cells, PIK3C3 was inhibited for 24 hours with 1 μ M of a novel small molecule inhibitor, SAR405, which has been shown to prevent autophagy (Ronan et al., 2014). Inhibition of PIK3C3 led to ULK1, PIK3C3, and p62 accumulation, which is indicative of an autophagic blockade (Figure 4.3.1). Conversion of LC3B-I to LC3B-II was not observed since PtdIns(3)P that are necessary for the expansion of the phagophore are not generated upon PIK3C3 inhibition, meaning that LC3B is not processed and targeted to the phagophore (Russell et al., 2014).

Combined treatment of 5 μ M FCCP and 1 μ M SAR405 resulted in ULK1 and PIK3C3 degradation and accumulation of LC3B-II, which is more prevalent in the early passage cells, suggesting that PIK3C3 inhibition led to a blockade in autophagy flux.

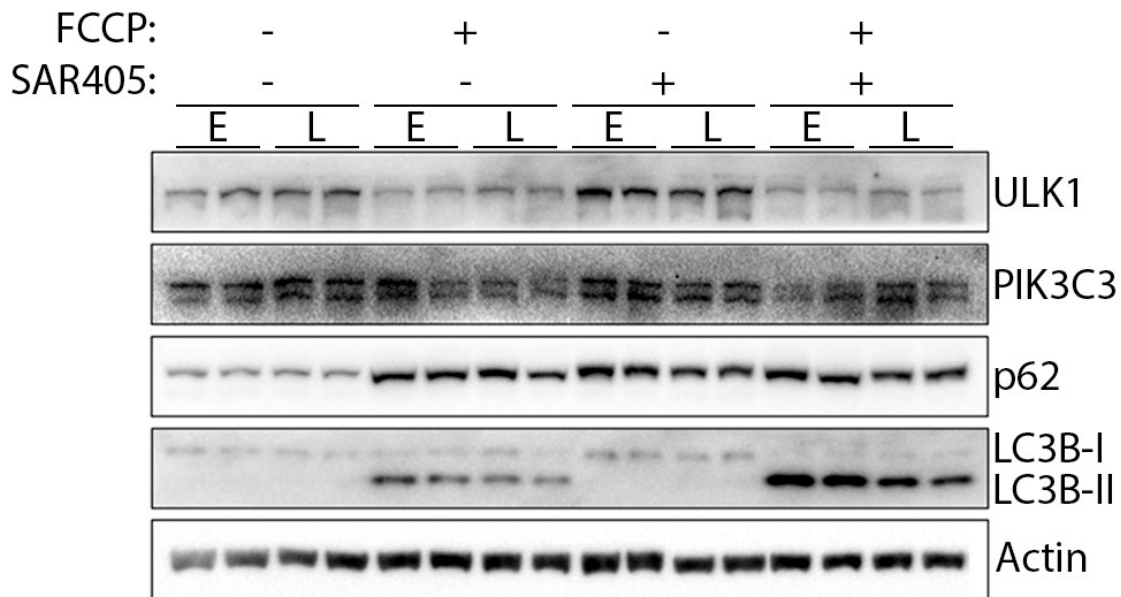


Figure 4.3.1. *PIK3C3* inhibition successfully blocks autophagy by prevention of LC3B conversion in SH-SY5Y cells. Autophagy is hindered by inhibition of PIK3C3 as seen by increased ULK, PIK3C3, and p62 expression and no LC3B conversion. SH-SY5Y cells show LC3B-II accumulation when co-treated with FCCP and SAR405, which suggests that PIK3C3 inhibition led to a blockade in autophagy flux. Early (E) and late (L) passage SH-SY5Y cells were treated with either 5 μ M FCCP, 1 μ M SAR405, or both, for 24 hours. Protein lysates (20 μ g) were probed for autophagy marker proteins ULK1, PIK3C3, p62, and LC3B. β -actin was used as loading control. Data represents one out of a total of three independent experiments.

When the effects of PIK3C3 inhibition on mitophagy were investigated, it was found that accumulation of Parkin was promoted, but that FCCP-mediated Parkin degradation was not prevented (Figure 4.3.2 A). This indicates that Parkin is not targeted to the lysosome, which supports the earlier made observation that Parkin is proteasomally degraded (see Chapter 3). SAR405 treatment reduced TIM23 and increased VDAC1 expression, while there was no change in TOM20 expression. TOM20 and TIM23 showed signs of FCCP-mediated degradation upon PIK3C3 inhibition, suggesting activity of the PIK3C3 complex is not necessary for degradation of these mitochondrial markers.

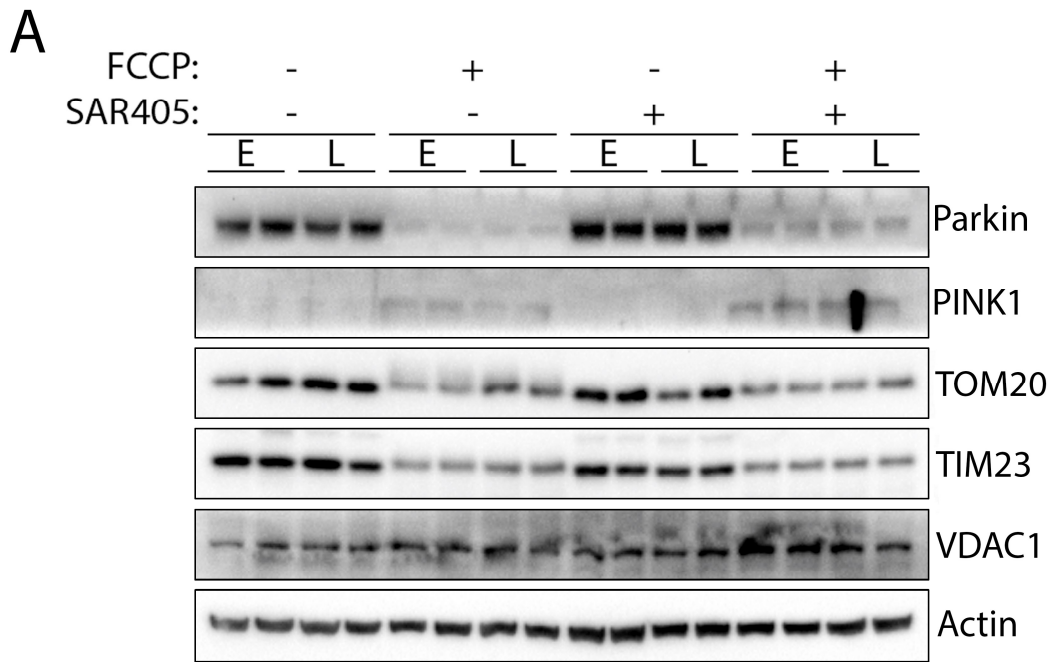


Figure 4.3.2 (A). *PIK3C3* inhibition does not prevent FCCP-mediated degradation of mitochondrial markers. Inhibition of *PIK3C3* increases Parkin expression, but does not affect FCCP-induced degradation of Parkin, TOM20, and TIM23. Early (E) and late (L) passage SH-SY5Y cells were treated with either 5 μ M FCCP, 1 μ M SAR405, or both, for 24 hours. Protein lysates (20 μ g) were probed for mitophagy marker proteins Parkin and PINK1, and mitochondrial marker proteins TOM20, TIM23, and VDAC1. β -actin was used as loading control. Data represents one out of a total of three independent experiments.

Densitometry pointed out that 5 μ M FCCP treatment led to significantly decreased TOM20 (early = $p < 0.05$) and TIM23 (early = $p < 0.01$, late = $p < 0.0001$) expression as shown previously (Figure 4.3.2 B). *PIK3C3* inhibition caused degradation of TOM20 (late = $p < 0.05$) and TIM23 (late = $p < 0.001$) too and did not block FCCP-induced degradation of both TOM20 ($p < 0.05$) and TIM23 (early = $p < 0.001$, late = $p < 0.0001$). In both early ($p < 0.01$) and late ($p < 0.001$) passage cells, TIM23 expression was significantly reduced when cells were co-treated with FCCP and SAR405 compared to SAR405 treatment alone.

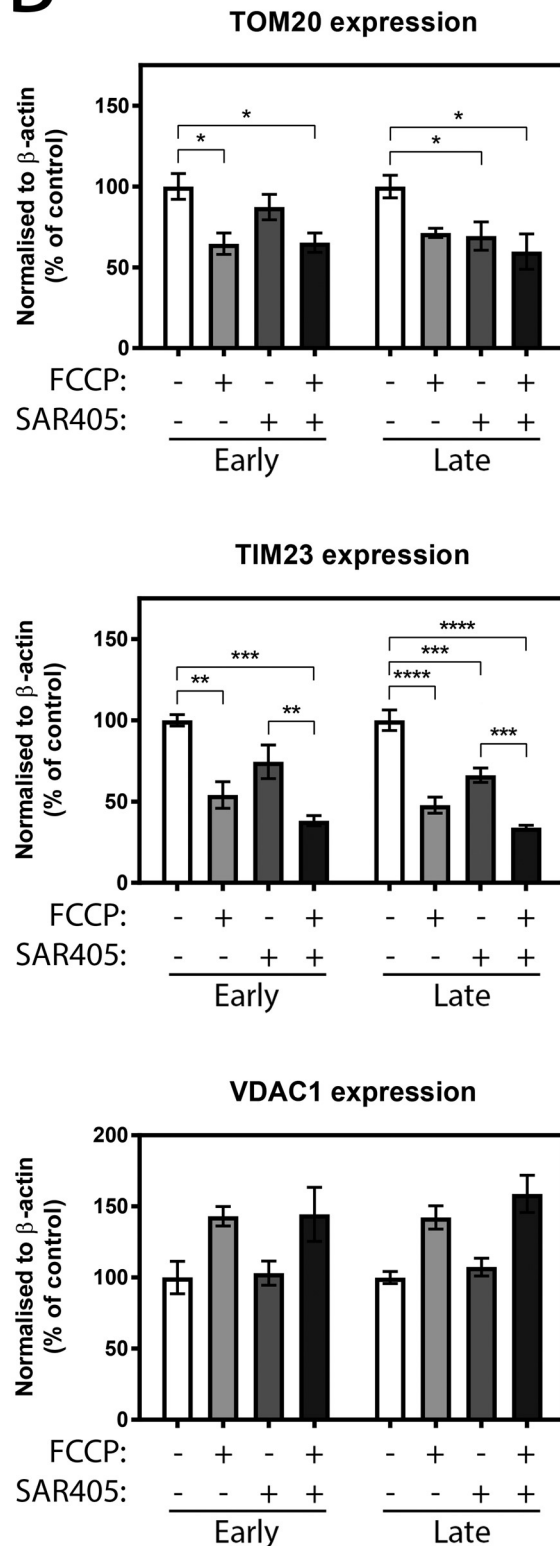
B

Figure 4.3.2 (B). *PIK3C3* inhibition does not prevent FCCCP-mediated degradation of mitochondrial markers. Densitometry of TOM20, TIM23, and VDAC1 normalised to corresponding β -actin levels. Densitometric analysis was pooled from three independent experiments in panel A and data is shown as percentage of control. Error bars = SEM, one-way ANOVA, * $p < 0.05$, ** $p < 0.01$, *** $p < 0.001$, **** $p < 0.0001$.

The effects of another PIK3C3 inhibitor, V34-IN1, on mitophagy induction and mitochondrial degradation was also investigated in early passage SH-SY5Y cells. V34-IN1 is reportedly a more selective PIK3C3 inhibitor than SAR405 since it does not inhibit class I and class II PI3Ks lipid kinases (Bago et al., 2014). Cells were also challenged with the proteasomal inhibitor MG132 to see the effects on FCCP-induced mitophagy when both PIK3C3 and proteasomal degradation were simultaneously inhibited.

p62 expression was increased and LC3B-II accumulated upon 5 μ M FCCP treatment (Figure 4.3.3). MG132 treatment (20 μ M) led to increased p62 expression and LC3B-II accumulation too, as well as increased ULK1 expression. Similar to results obtained with SAR405, V34-IN1 (1 μ M) caused increased ULK1, PIK3C3, and p62 expression and no LC3B turnover, while ULK1 and PIK3C3 degradation and LC3B-II accumulation were observed upon combined FCCP and V34-IN1 treatment when compared to V34-IN1 treatment on its own. Co-treatment of FCCP and MG132 resulted in decreased ULK1 and p62 expression as opposed to MG132 treatment. Proteasomal inhibition combined with FCCP treatment did not show any differences compared to FCCP treatment besides increased LC3B turnover. When cells were treated with both MG132 and V34-IN1, a small increase in LC3B turnover was observed, as well as increased ULK1 and p62 expression. Addition of FCCP led to a further accumulation of LC3B-II and decreased p62 expression.

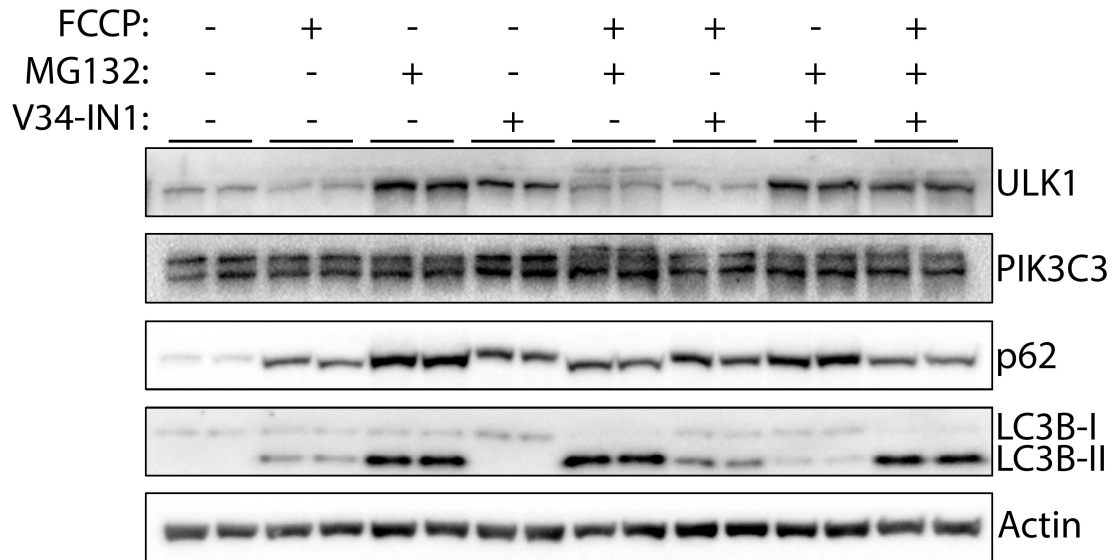


Figure 4.3.3. *PIK3C3* and proteasomal inhibition upon FCCP treatment leads to LC3B-II accumulation. Decreased ULK1 expression and *de novo* p62 synthesis combined with LC3B turnover suggest FCCP activates autophagy, whereas PIK3C3 inhibition leads to an autophagic blockade, as seen by increased ULK, PIK3C3, and p62 expression and no LC3B conversion. Co-treatment of FCCP, MG132, and V34-IN1 leads to LC3B-II accumulation. SH-SY5Y cells were treated with either 5 μ M FCCP, 20 μ M MG132, 1 μ M V34-IN1, or a combination, for 24 hours. Protein lysates (20 μ g) were probed for autophagy marker proteins ULK1, PIK3C3, p62, and LC3B. β -actin was used as loading control. Data represents one out of a total of three independent experiments.

FCCP-induced mitophagy was not as potent as seen previously since PINK1 expression was not increased and only TIM23 degradation was observed (Figure 4.3.4 A). MG132 treatment increased Parkin expression and led to TOM20 accumulation, indicating proteasomal inhibition affected basal turnover of TOM20. V34-IN1 treatment resulted in increased expression of both Parkin and PINK1, of which the latter was not increased upon SAR405 treatment (see Figure 4.3.2 A). Co-treatment of FCCP and MG132 increased the expression of Parkin and the mitochondrial markers TOM20, TIM23, and VDAC1, as shown previously (see Chapter 3), whereas these mitochondrial markers were degraded upon co-treatment of FCCP and V34-IN (Figure 4.3.4 A). Combined inhibition of both the proteasome and PIK3C3 increased

the expression of Parkin, PINK1, and the mitochondrial markers, which was not affected by the addition of FCCP.

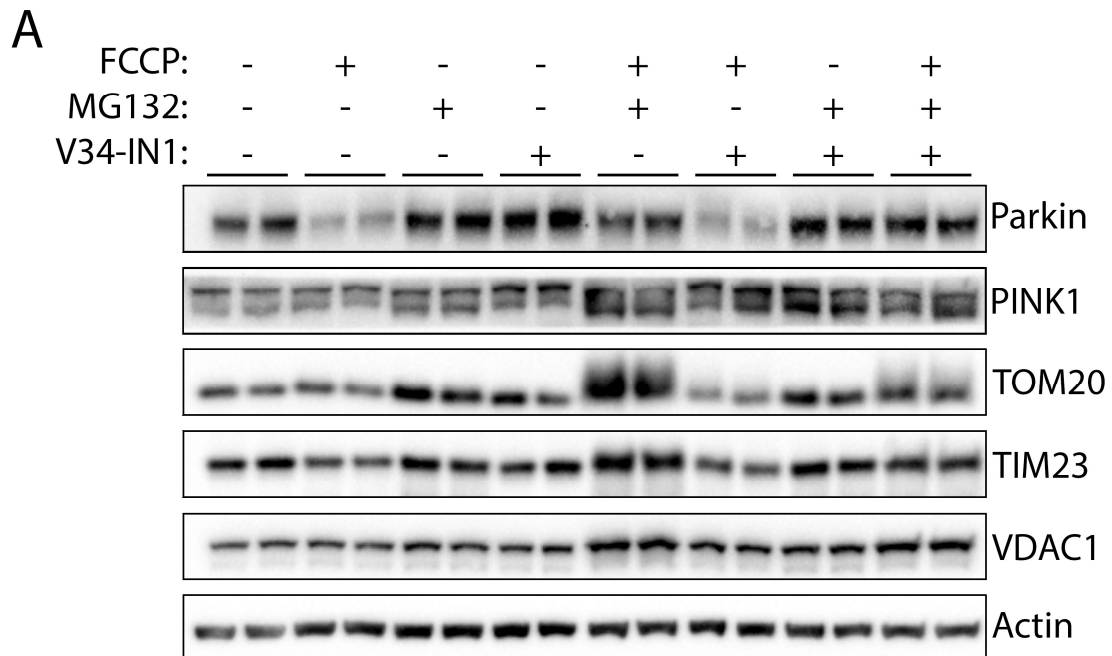


Figure 4.3.4 (A). Mitochondrial markers show FCCP-mediated selective proteasomal degradation irrespective of PIK3C3 inhibition. FCCP-mediated degradation of the mitochondrial markers TOM20 and TIM23 is not affected by PIK3C3 inhibition, whereas their degradation is prevented by a proteasomal blockade. Combined V34-IN1 and MG132 treatment illustrates that TOM20 and TIM23 show FCCP-mediated selective proteasomal degradation irrespective of PIK3C3 inhibition. (A) SH-SY5Y cells were treated with either 5 μ M FCCP, 20 μ M MG132, 1 μ M V34-IN1, or a combination, for 24 hours. Protein lysates (20 μ g) were probed for mitophagy marker proteins Parkin and PINK1, and mitochondrial marker proteins TOM20, TIM23, and VDAC1. β -actin was used as loading control. Data represents one out of a total of three independent experiments.

Densitometry showed that combined treatment of FCCP and MG132 ($p < 0.0001$) led to the biggest increase in TOM20 expression, which was partially reversed by V34-IN1 treatment ($p < 0.0001$) (Figure 4.3.4 B). TOM20 expression was also significantly increased upon combined treatment of FCCP, MG132, and V34-IN1 ($p < 0.05$) when

compared to control and FCCP and MG132 ($p < 0.0001$) when compared to FCCP treatment on its own.

Similarly to TOM20, the biggest increase in TIM23 expression was observed upon combined treatment of FCCP and MG132 ($p < 0.05$). Proteasomal inhibition reduced FCCP-mediated TIM23 degradation ($p < 0.0001$), which was not affected by V34-IN1. Co-treatment of FCCP, MG132, and V34-IN1 increased TIM23 expression when compared to FCCP ($p < 0.001$) or combined FCCP and V34-IN1 treatment ($p < 0.001$).

Combined treatment of FCCP and MG132 also increased VDAC1 expression when compared to either control ($p < 0.0001$) or FCCP treatment on its own ($p < 0.05$), which was irrespective of V34-IN1 ($p < 0.001$ compared to control, $p < 0.05$ compared to FCCP).

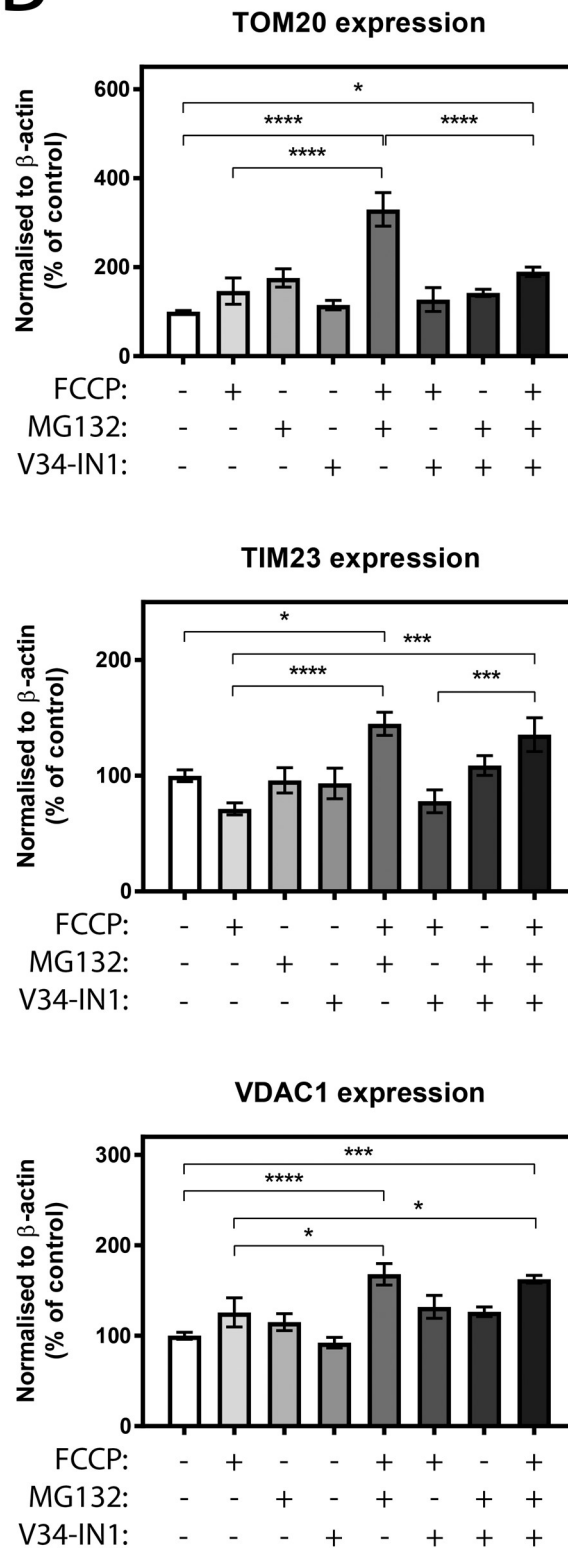
B

Figure 4.3.4 (B). Mitochondrial markers show FCCP-mediated selective proteasomal degradation irrespective of PIK3C3 inhibition. Densitometry of TOM20, TIM23, and VDAC1 normalised to corresponding β -actin levels. Densitometric analysis was pooled from three independent experiments in panel A and data is shown as percentage of control. Error bars = SEM, one-way ANOVA, * $p < 0.05$, *** $p < 0.001$, **** $p < 0.0001$.

4.4 PIK3C3 inhibition partially prevents FCCP cytotoxicity

To address the cytotoxicity of the different autophagy inhibitors utilised in this study, a cell viability assay was carried out. Phase contrast microscopy showed that 5 μM FCCP treated SH-SY5Y cells were smaller and detached at 24 hours of treatment (Figure 4.4.1). However, detachment was partially prevented by the addition of 1 μM SAR405 or 1 μM V34-IN1. MG132 (20 μM) treated cells detached as well, which was worsened by the addition of V34-IN1. Co-treatment of FCCP and MG123 resulted in increased cytotoxicity. SAR405 or V34-IN1 treatment did not have any visible effects on cell morphology. ULK1 inhibition (10 μM) mediated the formation of clumps, which was aggravated by the addition of FCCP. Combined treatment of FCCP, MG132, and V34-IN1 proved to be the most cytotoxic condition.

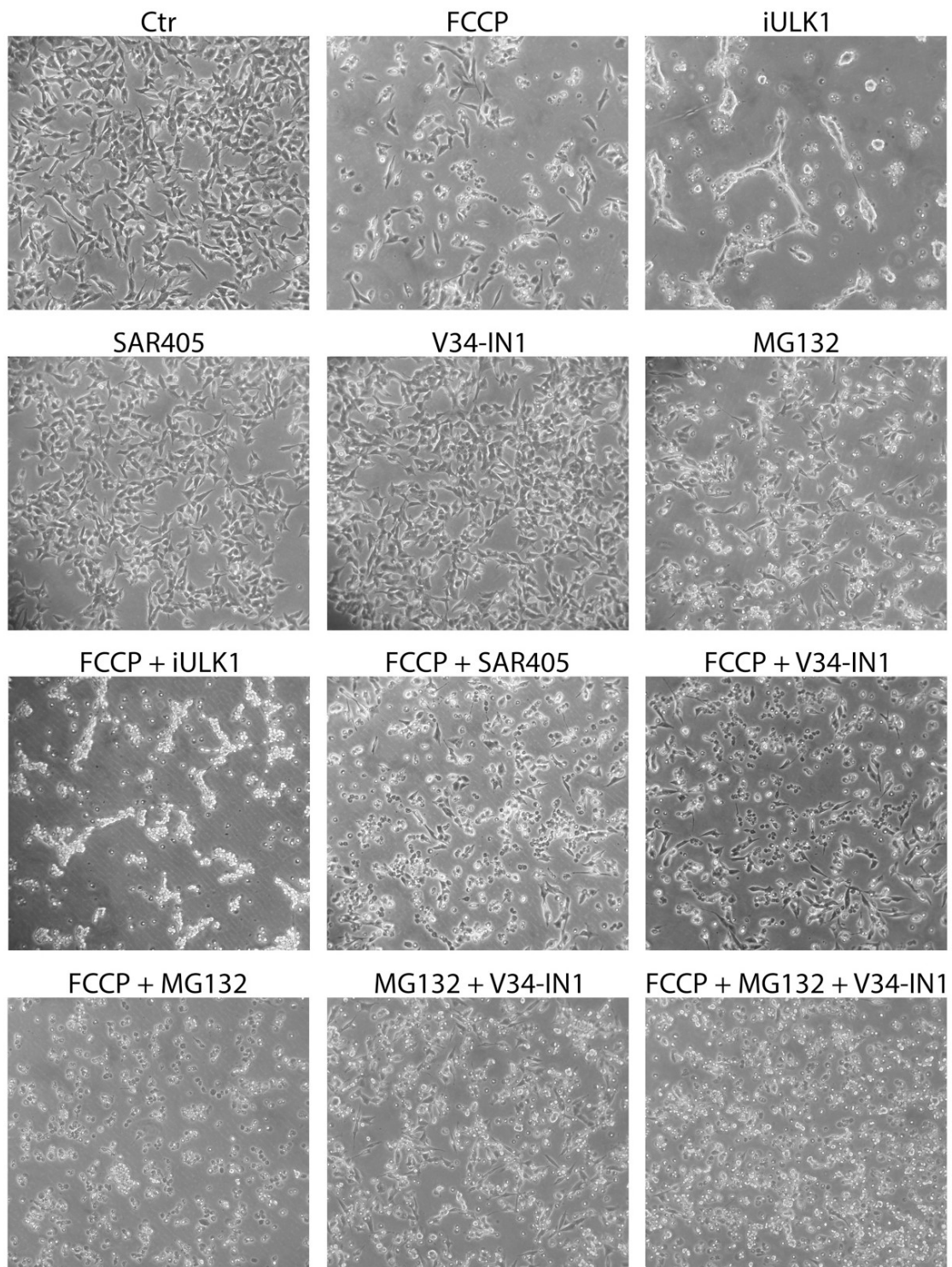


Figure 4.4.1. *PIK3C3* inhibition partially prevents cellular detachment of SH-SY5Y cells upon FCCP treatment. FCCP, iULK1, and MG132 treatment and combinations thereof are cytotoxic to SH-SY5Y cells. SAR405 or V34-IN1 partially prevent detachment of SH-SY5Y cells when co-treated with FCCP. SH-SY5Y cells were treated with either 5 μ M FCCP, 10 μ M iULK1, 1 μ M SAR405, 1 μ M V34-IN1, 20 μ M MG132, or a combination, for 24 hours. Phase contrast images were taken at 24 hours using a Nikon TMS microscope, magnification = 10x. Data represents one out of a total of three independent experiments.

The cell viability assay pointed out that all different treatments, except SAR405 or V34-IN1, led to cytotoxicity ($p < 0.0001$, not marked in Figure) (Figure 4.4.2). V34-IN1 partially rescued FCCP-mediated cytotoxicity ($p < 0.05$), regardless of the addition of MG132 ($p < 0.01$). The other inhibitors did not significantly affect FCCP-mediated cytotoxicity.

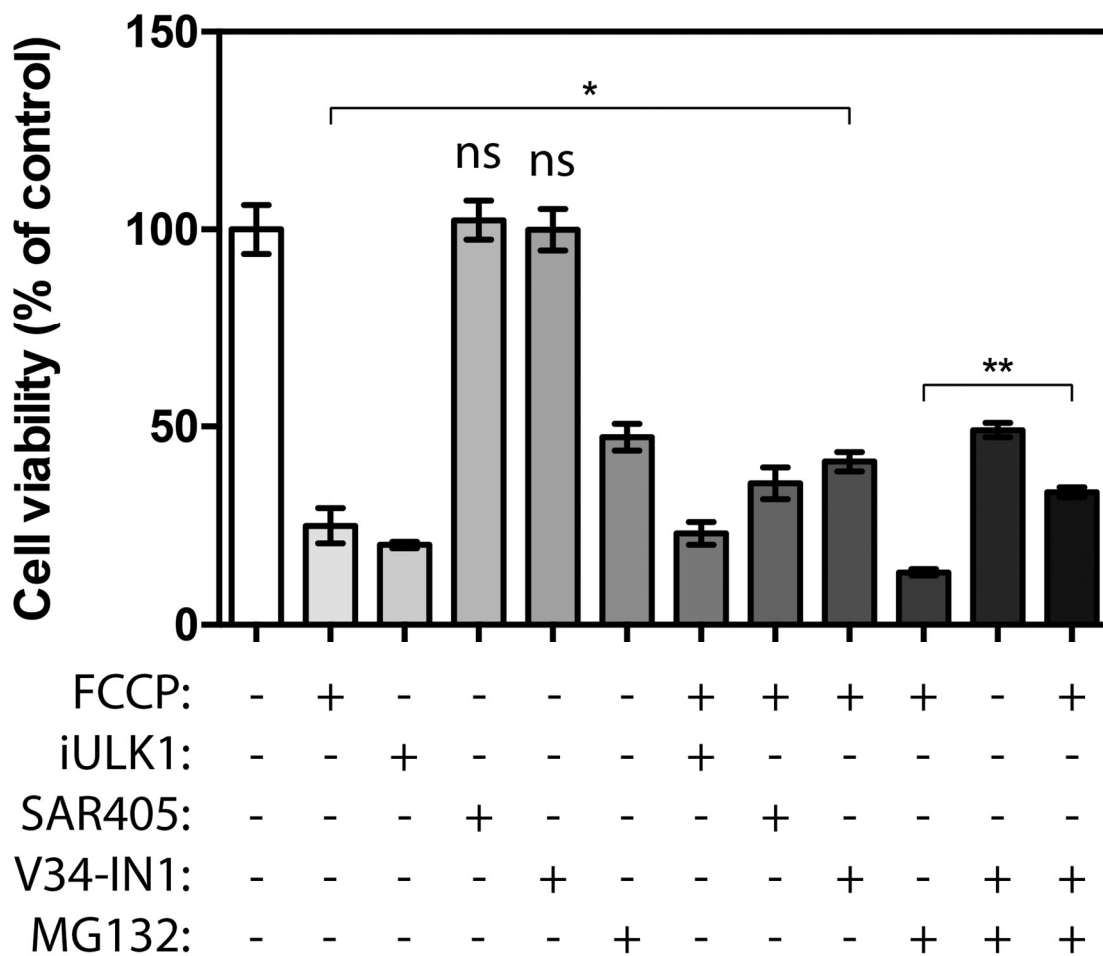


Figure 4.4.2. *PIK3C3* inhibition partially prevents FCCP cytotoxicity in SH-SY5Y cells. Inhibition of *PIK3C3* partially prevents FCCP, and FCCP + MG132 mediated cytotoxicity in SH-SY5Y cells. Note that all different treatments, except SAR405 and V34-IN1 (non-significant (ns)), led to cytotoxicity ($p < 0.0001$). SH-SY5Y cells were treated with 5 μ M FCCP, 10 μ M iULK1, 1 μ M SAR405, 1 μ M V34-IN1, 20 μ M MG132, or a combination, for 24 hours. Data is shown as percentage of control and was pooled from three independent experiments. Error bars = SEM, one-way ANOVA, $p > 0.05$ = ns, $*p < 0.05$, $**p < 0.01$.

4.5 ULK1 inhibition promotes Beclin1 phosphorylation

As described earlier in this chapter, ULK1 inhibition led to decreased PIK3C3 expression, which could indicate a disruption of the PIK3C3 complex (see Figure 4.2.1 A). PIK3C3 activity is regulated by both ULK1 and Beclin1, the latter being part of the PIK3C3 complex itself (Russell et al., 2014). Unpublished data from the Murray lab (Ewelina Rozycka, manuscript in preparation) showed that ULK1 can regulate Beclin1 phosphorylation at serine 30 (Ser30). Knockdown of ULK1 decreased the amount of Ser30 phosphorylated Beclin1 in two different cell lines, although ULK1 was not the responsible kinase for direct phosphorylation. Recently, the glycolytic enzyme phosphoglycerate kinase 1 (PGK1) was found to directly phosphorylate Beclin1 on Ser30 (Qian et al., 2017), suggesting that there is an intimate link between the glycolytic pathway and control of cellular autophagy.

In order to investigate whether the PIK3C3 complex would be disassembled in SH-SY5Y cells upon ULK1 inhibition, Beclin1 total and Ser30 phosphorylated Beclin1 were immunoblotted. Interestingly, 10 μ M iULK1 treatment led to increased Ser30 phosphorylation on Beclin1, indicating Beclin1 activation and suggesting that the PIK3C3 complex could still be active upon ULK1 inhibition, regardless of decreased PIK3C3 expression (Figure 4.5.1). ULK1 inhibition did not lead to increased ULK1 expression as observed previously.

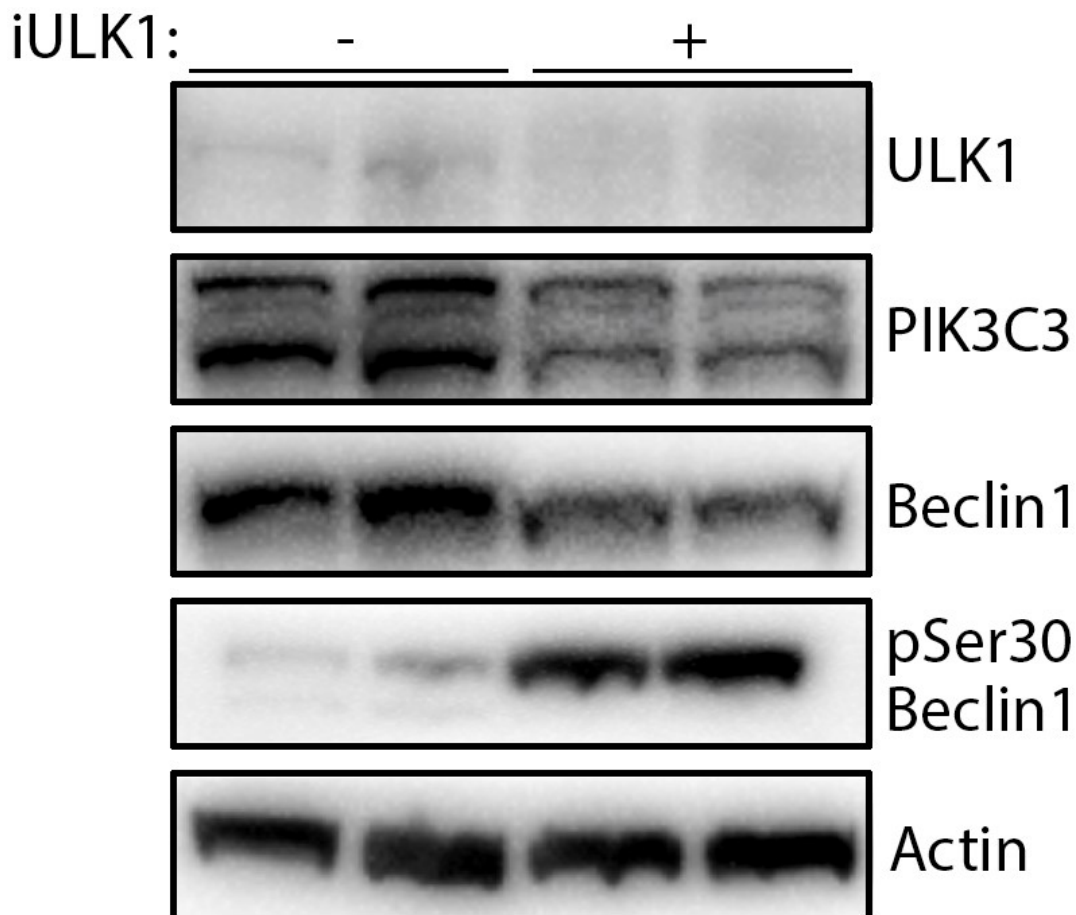


Figure 4.5.1. *ULK1 inhibition promotes Beclin1 phosphorylation in neuronal cells.* Inhibition of ULK1 promotes phosphorylation of Beclin1 at Ser30 and decreases ULK1 and PIK3C3 expression in SH-SY5Y cells. SH-SY5Y cells were treated with 10 μ M iULK1 for 24 hours. Protein lysates (20 μ g) were probed for autophagy marker proteins ULK1, PIK3C3, Beclin1, and Ser30 Beclin1. β -actin was used as loading control. Data represents one out of a total of three independent experiments.

To further investigate the effect of ULK1 inhibition on PIK3C3, both Beclin1 and PIK3C3 were immunoprecipitated (IP). ULK1 inhibition resulted in decreased Beclin1 expression, but did not have an effect on the amount of Ser30 phosphorylated Beclin1 or PIK3C3 expression (Figure 4.5.2 A). Expression of both UVRAG and hVps15, other proteins associated with the Beclin1-PIK3C3 complex, increased upon ULK1 inhibition. PIK3C3 IP showed that its expression, as well as Beclin1, Ser30 phosphorylated Beclin1 and possibly UVRAG, decreased upon ULK1 inhibition. The

effects of ULK1 inhibition on hVps15 remained unknown since duplicates did not match. Under control conditions, PIK3C3 was not associated with high amounts of Ser30 phosphorylated Beclin1. ULK1 inhibition lowered PIK3C3 expression, which, in turn, was associated with less (Ser30 phosphorylated) Beclin1.

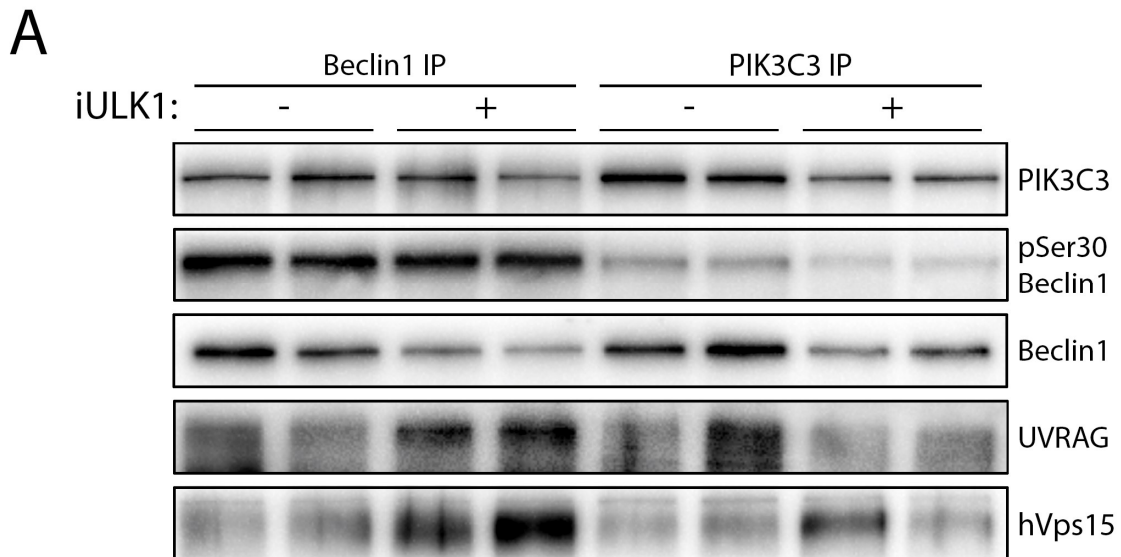


Figure 4.5.2 (A). *ULK1 inhibition does not affect expression of Ser30 phosphorylated Beclin1 associated with the PIK3C3 complex.* Beclin1 and PIK3C3 IP shows that ULK1 inhibition decreases Beclin1 expression, but that it does not inhibit Ser30 phosphorylated Beclin1 expression in SH-SY5Y cells. (A) SH-SY5Y cells were treated with 10 μ M iULK1 for 24 hours. Protein lysates (1.1 mg) were incubated overnight with appropriate antibodies to immunoprecipitate Beclin1 and PIK3C3. Samples were probed for members of the Beclin1-PIK3C3 complex, namely Beclin1, Ser30 phosphorylated Beclin1, PIK3C3, UVRAG, and hVps15. Data represents one out of a total of three independent experiments.

Beclin1 IP showed a small reduction, which was not statistically significant, in Ser30 phosphorylated Beclin1 expression upon ULK1 inhibition when Ser30 phosphorylated Beclin1 expression was normalised to corresponding Beclin1 expression (Figure 4.5.2 B). PIK3C3 IP showed an increase in Ser30 phosphorylated Beclin1, confirming that ULK1 inhibition did not lead to decreased Beclin1 phosphorylation at Ser30 as seen in non-neuronal cells

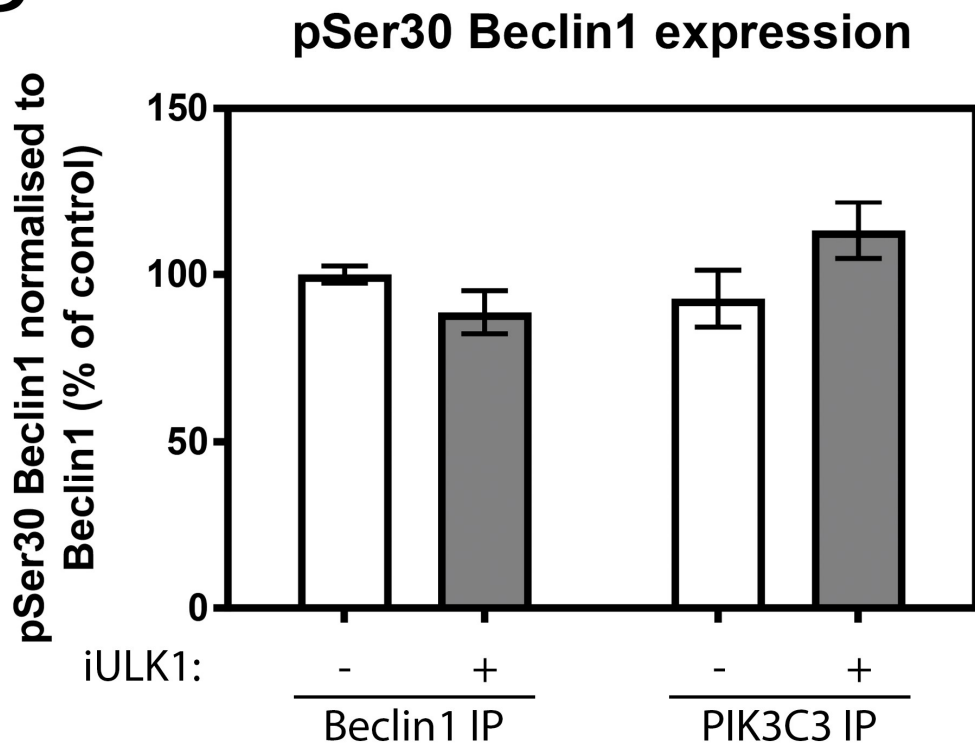
B

Figure 4.5.2 (B). *ULK1 inhibition does not affect expression of Ser30 phosphorylated Beclin1 associated with the PIK3C3 complex.* Densitometry of Ser30 phosphorylated Beclin1 normalised to corresponding Beclin1 levels. Densitometric analysis was pooled from three independent experiments in panel A and data is shown as percentage of control. Error bars = SEM, unpaired t-test. IP = immunoprecipitation.

When assessing the ratio of PIK3C3 bound to Beclin1 in the Beclin1 IP, an increase in the amount of interactions between Beclin1 and PIK3C3 was found upon iULK1 treatment ($p < 0.05$), despite a decrease in both Beclin1 and PIK3C3 expression (Figure 4.5.2 C).

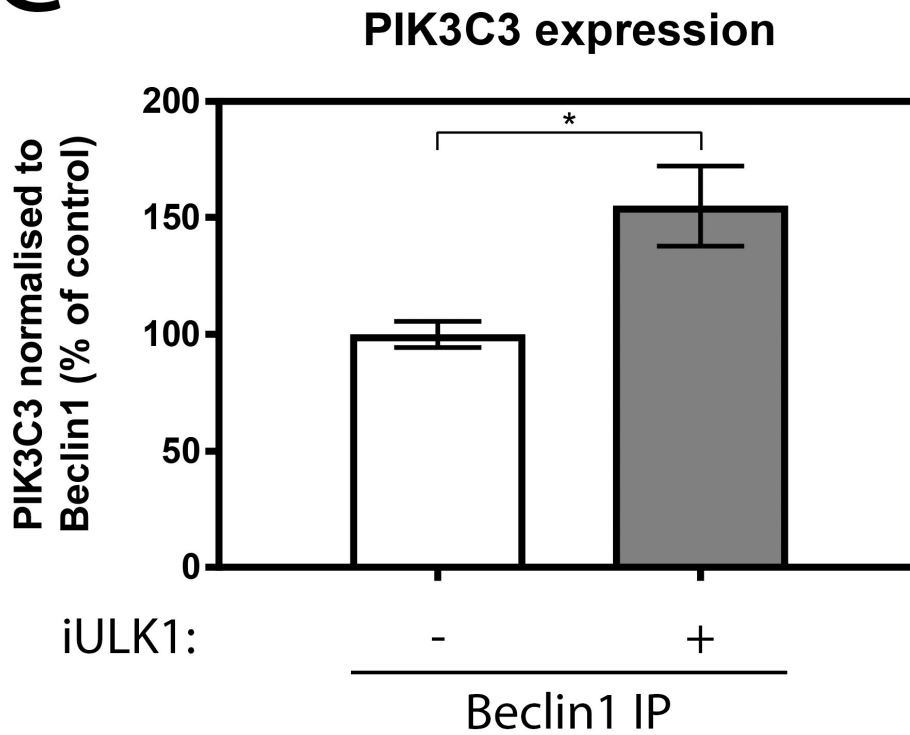
C

Figure 4.5.2 (C). *Beclin1* IP shows an increased amount of *Beclin1* and *PIK3C3* interactions upon *ULK1* inhibition. Densitometry of *PIK3C3* normalised to corresponding *Beclin1* levels. Densitometric analysis was pooled from three independent experiments in panel A and data is shown as percentage of control. Error bars = SEM, unpaired t-test, * $p < 0.05$. IP = immunoprecipitation.

4.6 Discussion

Mitophagy is considered to be a specialised type of autophagy, implying autophagy related proteins assist the mitophagic process. ULK1 is activated upon mTORC1 inhibition and its activation is important for the regulation of autophagy initiation (Russell et al., 2014). Inhibition of ULK1 led to mitochondrial fragmentation, increased PINK1 and decreased Parkin expression in SH-SY5Y cells, suggesting that mitophagy was induced (Figure 4.2.1 A & B, Figure 4.2.4). Both p62 and LC3B-II were degraded, which contradicts results obtained in non-neuronal cells that show that ULK1 inhibition leads to a blockade of autophagy flux as observed by accumulation of p62 and LC3B-II (Appendix II). Thus, ULK1 inhibition appears to have different effects in different cell types. FCCP-induced mitophagy or mitochondrial fragmentation was not affected by inhibition of ULK1, however, expression of the mitochondrial marker VDAC1 was increased, implying ULK1 inhibition affects degradation of damaged mitochondria (Figure 4.2.2 A & B). Nevertheless, it must be noted that FCCP-induced mitochondrial degradation upon ULK1 inhibition was only assessed by monitoring VDAC1 expression, which turned out to be not reliable for measuring mitochondrial degradation since VDAC1 was not always degraded during FCCP-induced mitophagy and VDAC1 could be recycled, instead of being degraded (Chapter 3). Therefore, more experiments need to be done, such as monitoring degradation of TOM20 and TIM23 and monitoring changes in mitochondrial mass, to establish the involvement of ULK1 in FCCP-induced degradation of mitochondria in SH-SY5Y cells.

In agreement with the results described herein, ULK1 was found to be necessary for mitophagy to be carried out successfully. In MEF, structures containing ULK1 were

recruited to CCCP-depolarised mitochondria and were required for mobilisation of downstream ATG proteins to carry out mitophagy (Itakura et al., 2012), while *ULK1*^{-/-} MEF did not recruit Parkin to CCCP-depolarised mitochondria, leading to defects in mitochondrial clearance upon CCCP treatment (Joo et al., 2011). Also in primary hepatocytes, loss of ULK1 led to defective mitophagy (Egan et al., 2011). On the contrary, however, Kundu and colleagues found that culturing reticulocytes obtained from ULK1-knockout mice, which show defects in the clearance of mitochondria during maturation, overcame impaired mitochondrial clearance in the presence of CCCP (Kundu et al., 2008). This suggests that mitochondrial depolarisation can lead to activation of ULK1-independent pathways that are responsible for clearance of damaged mitochondria. Another study supported the findings of Kundu and co-workers by showing that MEF deficient in or with reduced activity of different components of the ULK1 complex, namely FIP200 and ATG13, did not activate autophagy following starvation, but did show a reduced rate of LC3B lipidation upon induction of mitochondrial damage by CCCP, suggesting non-canonical autophagy could have been activated (Chen et al., 2013). It was suggested that ULK2 could compensate for loss of ULK1, since only combined deletion of ULK1 and ULK2 inhibited the autophagy response to nutrient starvation, but this is likely cell type specific (Cheong et al., 2011, Lee and Tournier, 2011, McAlpine et al., 2013). In addition, these studies also showed that mice deficient for both *ULK1* and *ULK2* died shortly after birth, whereas mice deficient in either one of these genes were viable and did not show any obvious developmental defects (Kundu et al., 2008, Cheong et al., 2011). The observed discrepancies between the different studies indicate that the precise role of ULK1 in mitophagy is unclear and that further research on this topic is needed.

Downstream of ULK1 functions the PIK3C3 complex, which is the effector complex that is critical for autophagosome formation (Russell et al., 2014). Inhibition of PIK3C3 by two different specific inhibitors (SAR405 and V34-IN1) successfully blocked autophagy, but did not have an effect on FCCP-mediated degradation of the mitochondrial markers TOM20 and TIM23, indicating a non-canonical autophagy pathway could be involved (Figure 4.3.1, Figure 4.3.2 A & B, Figure 4.3.3, Figure 4.3.4 A & B). These findings were supported by work done in hepatocytes in which the PIK3C3 complex was reported to be dispensable for photodamage-induced mitophagy (Kim and Lemasters, 2011b). Phosphatidylinositol 3-kinase (PI3K) inhibitors successfully blocked sequestration of mitochondria during starvation, but not upon photodamage-induced mitophagy, again suggesting mitochondrial depolarisation can lead to activation of non-canonical autophagy. Furthermore, knockdown of partners of the PIK3C3 complex, namely Beclin1 or ATG14L, did not diminish LC3B puncta formation or LC3B turnover (Chen et al., 2013). In addition, induction of mitochondrial degradation by the parkinsonian neurotoxin MPP⁺ and autophagy activated by ROS, of which FCCP is a potent inducer, was shown to be independent of Beclin1 in primary dopaminergic neurons and SH-SY5Y cells (Chu et al., 2007, Zhu et al., 2007). Conversely, loss of Beclin1 led to inhibition of CCCP-induced Parkin translocation to mitochondria in PC12 cells, which suppressed mitochondrial fragmentation since no Parkin-induced MFN2 loss was observed (Choubey et al., 2014). However, the authors did not investigate the effects of Beclin1 loss on mitochondrial degradation and therefore it is unclear if loss of Beclin1 led to impaired mitophagy in PC12 cells.

Activity of the PIK3C3 complex is regulated by Beclin1, which in turn is controlled by ULK1 (Russell et al., 2014). Previous obtained results in the Murray lab showed that ULK1 can phosphorylate Beclin1 at Ser30 and that ULK1 inhibition led to decreased Ser30 phosphorylated Beclin1 expression in non-neuronal cells. However, ULK1 inhibition increased Ser30 phosphorylated Beclin1 expression in SH-SY5Y cells, indicating that ULK1-dependent Ser30 phosphorylation of Beclin1 in cancer cells of epithelial origin is distinct to neuronally-derived cells (Figure 4.5.1). A recent study showed that Beclin1 phosphorylation at Ser30 could be induced in non-neuronal cells by PGK1 (Qian et al., 2017). Experiments need to be done to test whether PGK1 functions downstream of ULK1 and perhaps differential regulation of PGK1 explains the differences across cells from different tissue origins. This could be related to control of glycolysis, since PGK1 is a glycolytic enzyme, and a possible mechanism of supporting continued glycolysis, if glycolytic flux drops, is by mobilising the autophagy pathway to provide additional pre-cursors to support energy production. Nevertheless, it still remains to be determined which protein is responsible for Ser30 Beclin1 phosphorylation in SH-SY5Y cells.

ULK1 inhibition by iULK1 also led to decreased PIK3C3 expression, which could indicate disruption of the PIK3C3 complex (Figure 4.5.1), possibly through altered binding to Beclin1, which is partially supported by the immunoprecipitation data in Figure 4.5.2 C, where the ratio of PIK3C3 bound to Beclin1 in Beclin1 immunoprecipitates increased from 1 to 1.5, indicating that despite a decrease in both Beclin1 and PIK3C3 expression, there was an increase in interactions, although the associated increase in Ser30 phosphorylation is not likely to be associated with PIK3C3:Beclin1 interactions, since this IP may contain predominantly monomeric

Beclin1 and also in the PIK3C3 IP's there was no enrichment of Beclin1 or increased Ser30 abundance. PIK3C3 IP demonstrated that ULK1 inhibition resulted in lower expression levels of PIK3C3, Beclin1, and Ser30 phosphorylated Beclin1, implying ULK1 inhibition leads to a decrease in the amount of PIK3C3 complexes (Figure 4.5.2 A & B). IP also showed that upon ULK1 inhibition, PIK3C3 is not associated with increased Ser30 phosphorylated Beclin1 expression, suggesting a pool of Ser30 phosphorylated Beclin1 is not associated with the PIK3C3 complex. This pool of Ser30 phosphorylated Beclin1 might be involved in other cellular processes or it could be the pool that is associated with PINK1 or Parkin, linking it to mitophagy.

Even though the involvement of ULK1 in mitophagy needs to be investigated further, observed FCCP-induced TOM20 and TIM23 degradation upon PIK3C3 inhibition hints that canonical autophagy might be dispensable for FCCP-induced mitophagy in SH-SY5Y cells, which is supported by the finding that proteasomal inhibition causes a blockade in degradation of the mitochondrial markers (Figure 4.3.4 A & B, Chapter 3). In fibroblasts, it was reported that proteins on the outer mitochondrial membrane, such as TOM20, are mainly proteasomally degraded, whereas proteins on the inner mitochondrial membrane, like TIM23, are mainly degraded via auto/mitophagy, of which the latter is contradictory to described results (Yoshii et al., 2011). Therefore, the effects of autophagic and proteasomal inhibition on FCCP-induced mitophagy should be investigated on additional mitochondrial marker proteins and differences in mitochondrial mass, to monitor mitochondrial degradation, should be taken into account to investigate if the described results hold up.

Chapter 5

Effects of FCCP on mitophagy and autophagy in stem cell models

5.0 Introduction

Mitochondrial damage and mitochondrial defects have been observed in the brains of deceased PD patients. To date, it is not known whether this is the primary cause of pathogenesis or a consequence of damaged neurons. The current hypothesis is that mitochondrial dysfunction may lie at the basis of PD, which is strengthened by the fact that many of the genes involved in familial forms of PD are related to mitochondria or their function. To test this hypothesis, it is important to utilise appropriate cell models. Nevertheless, most research concerning this topic is carried out with cell types other than neurons and the outcomes might not reflect neuronal processes. Neurons are a specialised cell type with different mitochondrial dynamics and selective removal of (damaged) mitochondria by mitophagy could be regulated in a different manner. PD is characterised by progressive loss of dopamine (DA) neurons in the substantia nigra (SN) and therefore DA neurons should ideally be used to study PD (Exner et al., 2012). DA neurons can be generated from both embryonic stem cells (ESC) and human induced pluripotent stem cells (hiPSC), which are thus a suitable cellular model for PD related studies (Park et al., 2004).

Mitochondria have been extensively studied in mammalian cells, giving rise to great insights in mitochondrial structure and function. However, knowledge of mitochondria in ESC is limited (Lonergan et al., 2007). Electron microscopy revealed that in undifferentiated mouse and human ESC lines only few mitochondria are present that have poorly developed cristae, the site where oxidative phosphorylation takes place. In line with this observation, glycolysis was found to be the major contributor of energy production in ESC (Kondoh et al., 2007). Concomitant with low mitochondrial levels, low levels of mitochondrial mass and mitochondrial DNA

(mtDNA) were also reported (Lonergan et al., 2007). Inhibition of complex I of the respiratory chain resulted in mitophagy, whereas mild inhibition of complex III enhanced the pluripotency of ESC, suggesting that proper maintenance of mitochondrial function is important for ESC (Varum et al., 2009, Guan et al., 2013). Differentiation of ESC increased the mitochondrial number resulting in increased mitochondrial mass, mtDNA, and ATP production, giving rise to a mitochondrial pool that is large enough to study mitophagy (Cho et al., 2006, Lonergan et al., 2007).

Little is known about mitophagy and its regulation in ESC. Mitophagy can be induced in ESC by inhibition of complex I of the respiratory chain, while downregulation of growth factor *erv1*-like (*Gfer*) also resulted in elimination of damaged mitochondria by mitophagy, with the latter being restricted to undifferentiated ESC (Varum et al., 2009, Todd et al., 2010, Guan et al., 2013). Damaging mitochondria with CCCP led to changes in ATP and ROS levels and undifferentiated ESC were shown to proliferate slowly (Mandal et al., 2011).

While ESC are an appropriate cell model to study PD, ethical concerns and the fact that these cells are not disease-related make hiPSC the preferred cell line to study PD. hiPSC are a novel cell source that have numerous advantages over the use of immortalised cell lines. Given their self-renewability and their potential to give rise to almost all somatic cell types of the human body, hiPSC can provide an unlimited source for generation of disease-related specific cell types (Li et al., 2015). Not only the disease, but also early onset molecular changes during disease progression, can be studied with the use of hiPSC generated from patient somatic cells since it was found that neurodegeneration caused by either *PINK1* or *PARK2* loss in humans can already

been seen at the age of three (Whitworth and Pallanck, 2017). Furthermore, hiPSC can also be used as a model system for drug screening and drug toxicity tests, thereby reducing the use of animals, and could even open doors towards personalised drug discovery. PD patients, for example, show variations in therapeutic outcomes that are likely caused by differences in genetic background and epigenetic modifications between the patients (Liu et al., 2013). hiPSC generated from these patients will have their genetic background and likely respond to drugs in a similar way as the patient itself, making them a great asset for personalised drug screening (Ko and Gelb, 2014). Lastly, hiPSC could be used for autologous transplantation purposes as well, which was shown to result in a much lower immune response compared to allogeneic transplantation (Li et al., 2015).

Generation of iPSC by reprogramming of somatic cells into an embryonic-like state by introduction of four transcription factors, Octamer-binding transcription factor 3/4 (Oct3/4), Sex determining region Y (SRY)-box 2 (Sox2), C-myc, and Kruppel-like factor 4 (Klf4), into mouse embryonic fibroblasts was first described in 2006 (Takahashi and Yamanaka, 2006). However, this approach also marks one of the major drawbacks of these cells. Use of viruses to reprogram cells gives rise to safety concerns and limits potential clinical use, as described previously, of hiPSC-derived cells in future. Progress has been made to optimise protocols for both hiPSC generation and subsequent differentiation, of which efficient protocols are also still lacking, but many problems still exist despite improvements that have been made (Li et al., 2015).

Given the recent discovery of hiPSC and lack of good protocols for both generation and differentiation of hiPSC, which is also a time consuming process, few studies have been published that explore the effects of *PINK1* and *PARK2* mutations in hiPSC-derived DA neurons from PD patients (Valente et al., 2004). The advantage of these cells is that they present a more direct view of how these proteins function and dysfunction in disease compared to immortalised cell lines in which PINK1 and Parkin are either knocked down or in which disease-associated mutations are overexpressed.

DA neurons derived from PINK1 mutant hiPSC showed that loss of PINK1 function likely intrinsically damaged mitochondria since increased ROS production and increased rate of basal oxygen consumption and proton leakage were observed, as well as increased sensitivity to cell death (Cooper et al., 2012). Furthermore, PINK1 mutant hiPSC-derived neurons presented with decreased mitochondrial membrane potential and mitochondrial complex I activity (Morais et al., 2014). Mitochondrial depolarisation did not lead to a reduction in mtDNA as observed in control hiPSC, suggesting that mitophagy did not take place (Seibler et al., 2011). This was confirmed by the observation that recruitment of lentivirally expressed Parkin to mitochondria was impaired upon mitochondrial depolarisation, which was restored upon lentiviral overexpression of wildtype (WT) PINK1, showing the importance of functionally active PINK1 in mitophagy.

Whereas *PINK1* mutations lead to mitochondrial dysfunction and lack of mitophagy, mutations in *PARK2* are associated with numerous pathologies. Neurons derived from Parkin mutated hiPSC had abnormal mitochondrial morphology, impaired

mitochondrial homeostasis and increased levels of oxidative stress (Imaizumi et al., 2012). Abnormal mitochondrial morphology was confirmed by another study, in which reduced mitochondrial volume and reduced amount of differentiated DA neurons was also found (Shaltouki et al., 2015). Decreased DA uptake and increased spontaneous DA release was observed too, which could be rescued by lentiviral expression of WT Parkin (Jiang et al., 2012). In addition, mutant Parkin iPSC-derived DA neurons had destabilised microtubules, leading to reduced neurite length and complexity, which could be rescued by overexpression of WT Parkin as well (Ren et al., 2015). Recently, it was shown that DA neurons derived from mutated Parkin hiPSC had defective mitophagy and that they had increased cleavage of caspase 3, suggesting that Parkin defects lead to increased levels of apoptosis (Suzuki et al., 2017). Lastly, Parkin mutant neurons demonstrated increased expression and abnormal accumulation of α -synuclein, downregulation of the proteasome and anti-oxidative pathways, which was accompanied by increased oxidative stress, and increased susceptibility to mitochondrial toxins (Chang et al., 2016, Chung et al., 2016). Taken together, these studies show that Parkin is involved in different processes in DA neurons besides mitophagy.

In this chapter, the effects of the mitochondrial uncoupler FCCP on mitophagy and autophagy in undifferentiated ESC, presumptive neuronal precursor cells (NPC), and NPC differentiated into DA neurons (presumptively) of a control and PD hiPSC line containing a *SNCA* triplication will be explored. Activation of autophagy and induction of mitophagy upon FCCP treatment was examined, as well as presence of FCCP-induced mitochondrial degradation and the effects of both autophagic and proteasomal inhibition on removal of FCCP-damaged mitochondria.

5.1 Undifferentiated mESC respond to autophagic activators and inhibitors

Undifferentiated 46C mouse ESC (mESC) were treated with either activators (rapamycin (Rap), EBSS) or inhibitors (chloroquine (CQ), iULK1) of autophagy, as well as FCCP, for 24 hours and the effects on autophagy were analysed. Activation of autophagy by 0.1 μ M rapamycin increased ULK1 and PIK3C3 expression and led to p62 degradation and increased LC3B turnover, indicative of autophagic activity (Figure 5.1.1 A). Starvation of undifferentiated 46C mESC with EBSS was toxic to the cells and protein expression levels were too low to detect on immunoblots. PINK1 expression did not change upon autophagy activation and Parkin was not detected (data not shown).

Inhibition of autophagy by 5 μ M CQ increased ULK1 expression and was characterised by p62 accumulation, as well as LC3B-II accumulation, indicative of an autophagy flux blockade. iULK1 treatment (10 μ M) led to decreased ULK1 and PIK3C3 expression, p62 degradation, and normal conversion of LC3B-I to LC3B-II, suggesting autophagy was not inhibited. Lastly, 50 μ M FCCP led to decreased PIK3C3 expression and increased p62 expression while LC3B conversion was similar to control conditions. Decreased PINK1 expression was observed upon CQ treatment whereas the effects of iULK1 and FCCP on PINK1 expression are inconclusive.

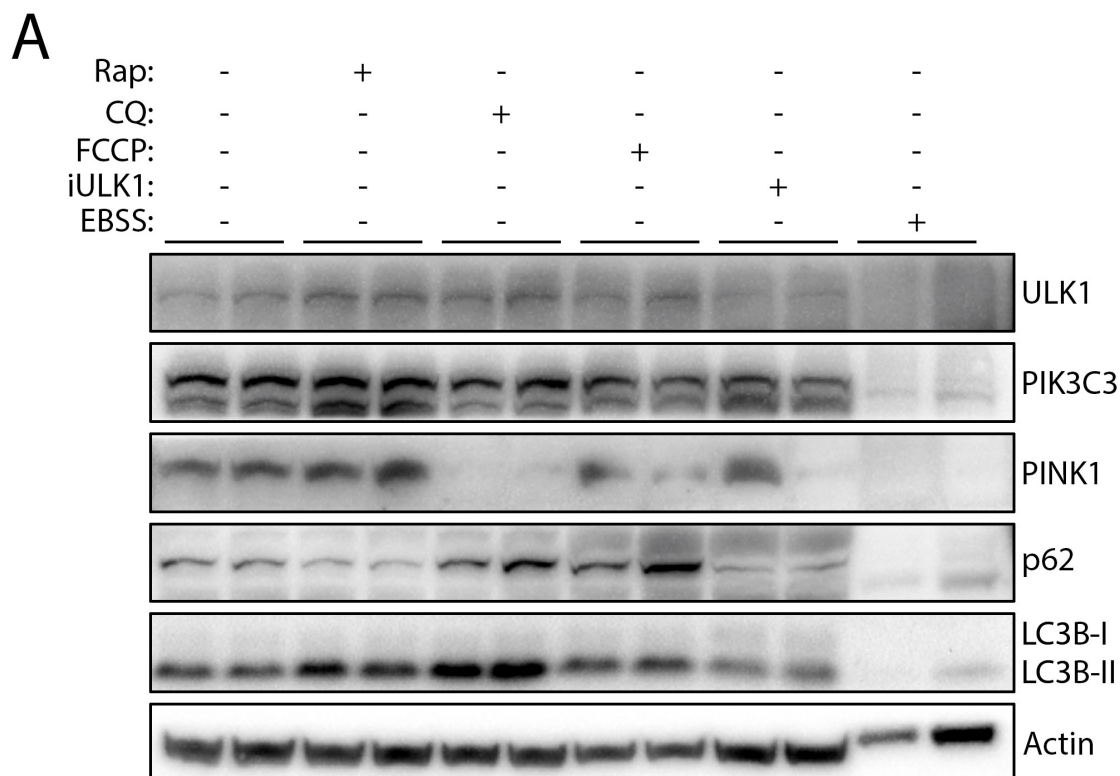


Figure 5.1.1 (A). *Undifferentiated 46C mESC respond to autophagic activators and inhibitors.* Activation of autophagy by rapamycin (Rap) decreases p62 expression and induces LC3B-II accumulation, whereas EBSS treatment is toxic to cells. Inhibition of autophagy by chloroquine (CQ) causes p62 and LC3B-II accumulation, while this is not the case upon iULK1 treatment. FCCP leads to increased p62 expression and its effects on PINK1 expression are inconclusive. Undifferentiated 46C mESC were treated with either 0.1 μ M rapamycin, 5 μ M chloroquine, 50 μ M FCCP, 10 μ M iULK1, or were starved with EBSS, for 24 hours. Protein lysates (20 μ g, \pm 3 μ g for EBSS only) were probed for autophagy marker proteins ULK1, PIK3C3, p62, and LC3B, and the mitophagy marker protein PINK1. β -actin was used as loading control. Data represent one out of a total of two independent experiments.

Densitometry showed that activation or inhibition of autophagy did not lead to a statistically significant increase or decrease in expression of immunoblotted proteins (Figure 5.1.1 B). Besides iULK1 treatment, both activation and inhibition of autophagy led to a small increase in ULK1 expression. iULK1 treatment also caused a small decrease in PIK3C3 expression while PIK3C3 expression was not affected by the other conditions. Autophagy activation by rapamycin resulted in p62 degradation

and increased LC3B conversion, whereas autophagic inhibition led to p62 and LC3B-II accumulation. FCCP treatment increased ULK1 and p62 expression, and also caused LC3B-II accumulation, but did not affect expression of PIK3C3. EBSS data was not analysed since protein expression of the immunoblotted proteins was too low.

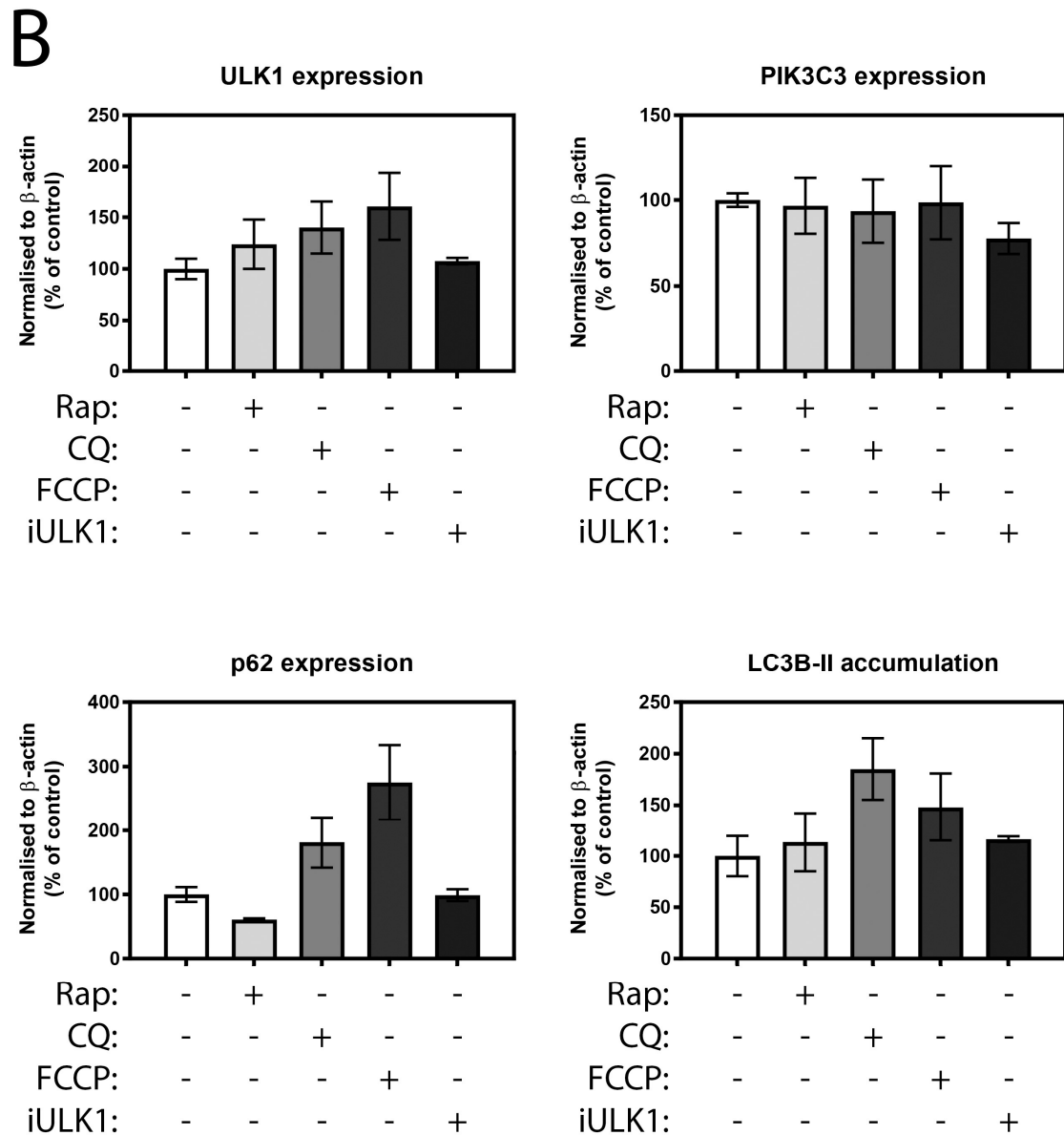


Figure 5.1.1 (B). Undifferentiated 46C mESC respond to autophagic activators and inhibitors. ULK1, PIK3C3, p62, and LC3B-II densitometry normalised to corresponding β -actin levels. Densitometric analysis was pooled from two independent experiments and data is shown as percentage of control. Error bars = SEM.

5.2 FCCP induces PINK1 expression in undifferentiated mESC

To examine the effects of FCCP on Parkin and PINK1 expression in undifferentiated 46C mESC, a time course was carried out. Preliminary data showed that 50 μ M FCCP treatment led to an increase in PINK1 expression for the duration of the experiment (Figure 5.2.1 A). Conversion of LC3B-I to LC3B-II was increased at 4 hours of FCCP treatment and is reminiscent of an autophagy flux blockade. Nevertheless, undifferentiated 46C mESC were able to overcome this blockade at later time points. The Parkin immunoblot showed a faint band at the predicted molecular weight of Parkin, however, it is not known if this was due to specific binding of the antibody.

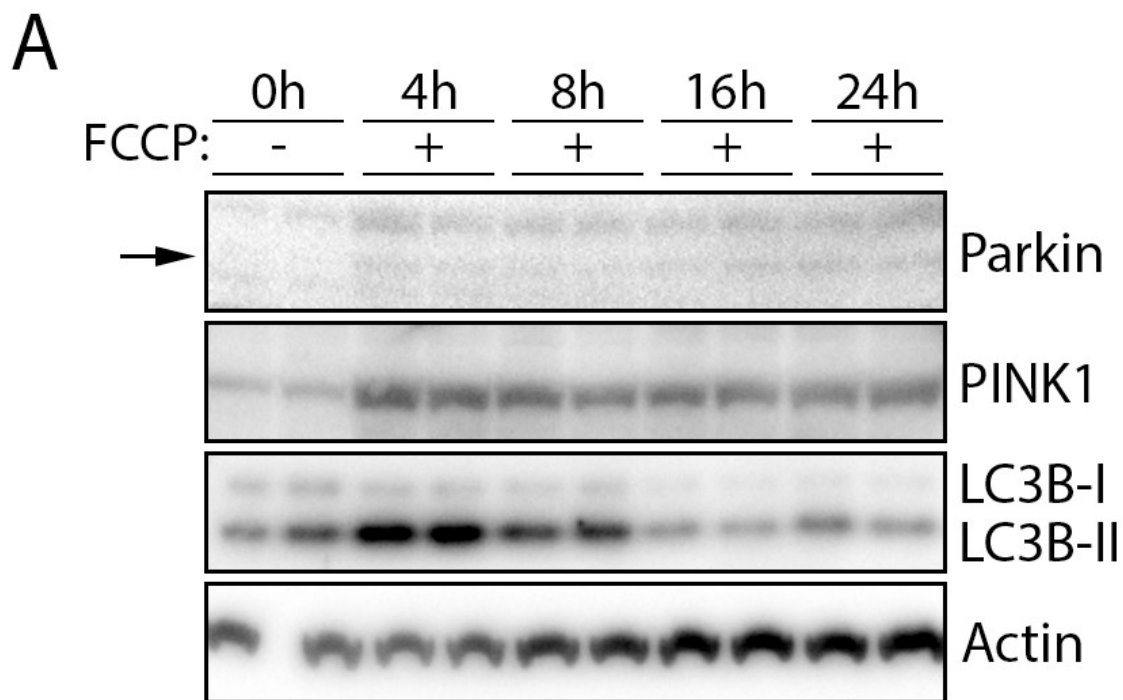


Figure 5.2.1 (A). *FCCP induces PINK1 expression in undifferentiated 46C mESC.* PINK1 expression is induced upon FCCP treatment in undifferentiated 46C mESC. LC3B-II accumulates at 4 hours, which is reminiscent of an autophagic blockade, but LC3B conversion decreases at later time points. Undifferentiated 46C mESC were treated with 50 μ M FCCP for indicated time points. Protein lysates (20 μ g) were probed for mitophagy marker proteins Parkin and PINK1, and the autophagy marker protein LC3B. β -actin was used as loading control. Arrow indicates possible Parkin expression. Data represents one experiment.

Densitometric analysis confirmed that PINK1 expression was increased upon FCCP treatment at all time points, with its peak at 4 hours of treatment (Figure 5.2.1 B). FCCP increased conversion of LC3B-I into LC3B-II at 4 hours of treatment, however, LC3B-II was degraded at later time points.

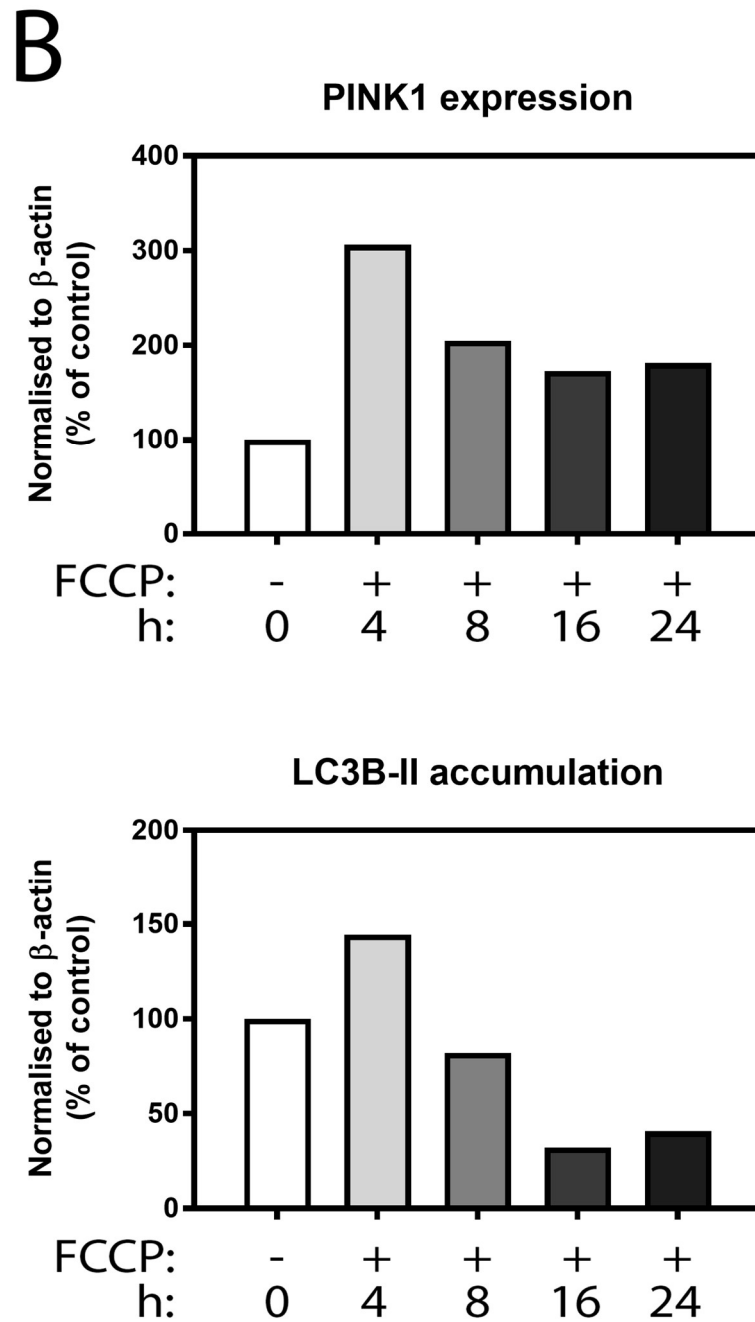


Figure 5.2.1 (B). *FCCP induces PINK1 expression in undifferentiated 46C mESC.* PINK1 and LC3B-II densitometry normalised to corresponding β -actin levels. Data is shown as percentage of control and represents one experiment.

5.3 ULK1 inhibition induces PINK1 expression in undifferentiated mESC

To assess how Parkin and PINK1 expression in undifferentiated 46C mESC are affected by ULK1 inhibition over time, ULK1 was inhibited with the small molecule inhibitor iULK1 for different time points. Preliminary data showed that 10 μ M iULK1 treatment induced ULK1 degradation and led to a big increase in LC3B-II, which is indicative of autophagic inhibition (Figure 5.3.1 A). This is in contrast with previous obtained data showing no changes in LC3B conversion at 24 hours of iULK1 treatment (see Figure 5.1.1 A & B). ULK1 inhibition increased PINK1 expression at 4 hours of treatment, which was increased further at 24 hours. Parkin expression was difficult to detect and it is not clear how its expression was affected by iULK1.

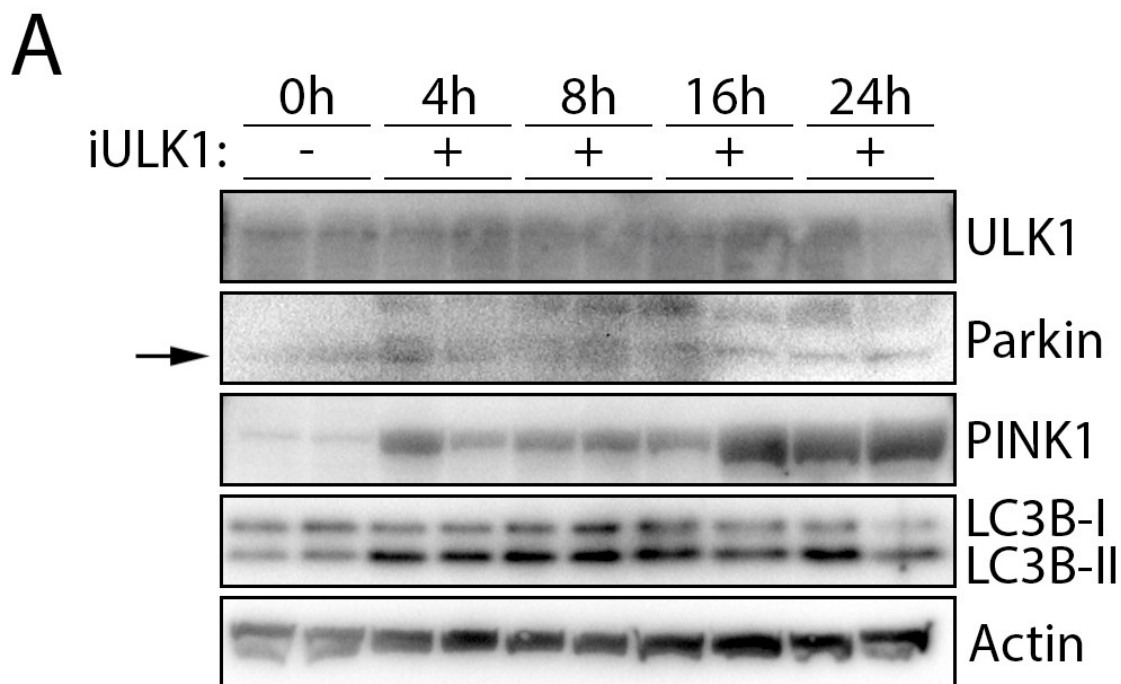


Figure 5.3.1 (A). *ULK1 inhibition induces PINK1 expression in undifferentiated 46C mESC.* ULK1 inhibition leads to increased PINK1 expression and LC3B-II accumulation, whereas ULK1 was possibly degraded. Undifferentiated 46C mESC were treated with 10 μ M iULK1 for indicated time points. Protein lysates (20 μ g) were probed for mitophagy marker proteins Parkin and PINK1, and autophagy marker proteins ULK1 and LC3B. β -actin was used as loading control. Arrow indicates possible Parkin expression. Data represents one experiment.

As shown by densitometry, PINK1 expression was continuously increased at all time points upon iULK1 treatment (Figure 5.3.1 B). LC3B-II accumulation was increased at 4 hours and 8 hours of ULK1 inhibition before being degraded. However, LC3B-I to LC3B-II conversion was still increased at 16 hours and 24 hours of ULK1 inhibition compared to control.

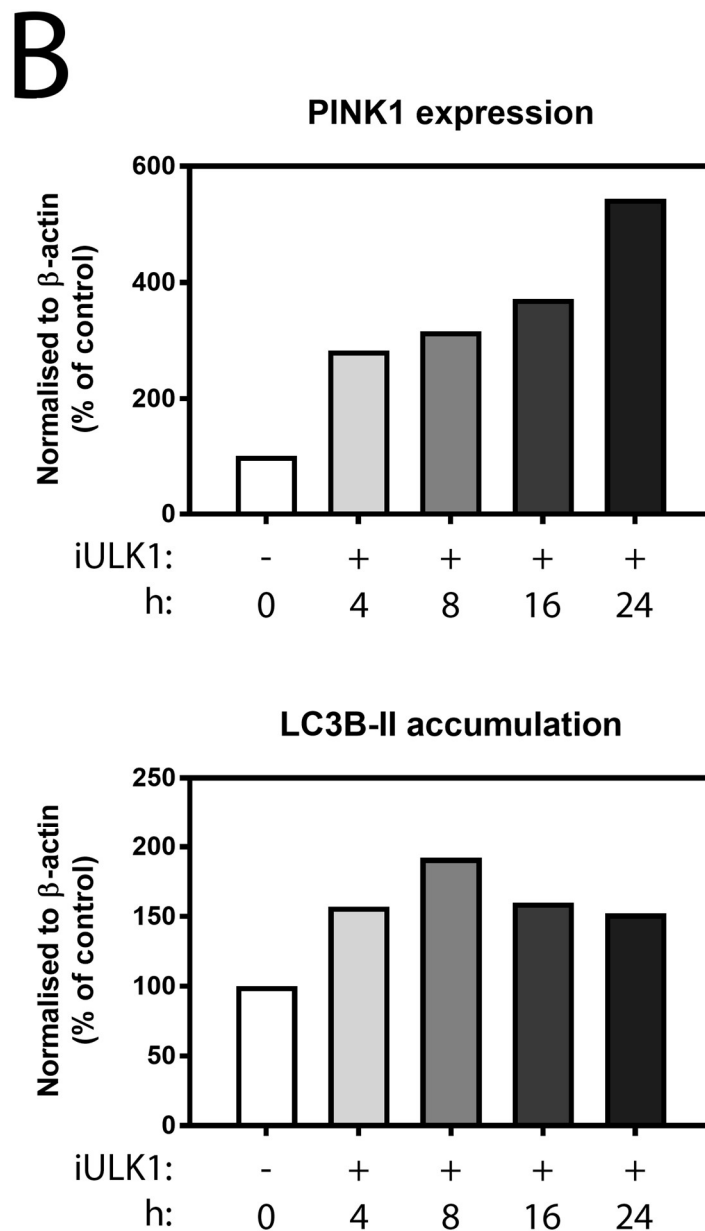


Figure 5.3.1 (B). *ULK1* inhibition induces *PINK1* expression in undifferentiated 46C mESC. *PINK1* and LC3B-II densitometry normalised to corresponding β -actin levels. Data is shown as percentage of control and represents one experiment.

5.4 ULK1 inhibition affects basal turnover of the mitochondrial marker VDAC1 in undifferentiated mESC

ULK1, which is activated in the early stages of autophagy, regulates the downstream autophagy initiation machinery (Russell et al., 2014). To investigate how ULK1 inhibition affects FCCP-mediated mitophagy, undifferentiated 46C mESC were treated with FCCP and iULK1 for 24 hours. FCCP treatment (50 μ M) led to Parkin degradation and PINK1 accumulation, suggesting mitophagy was induced (Figure 5.4.1 A). However, expression of the mitochondrial marker VDAC1 was not affected. p62 expression was decreased, which is contrary to previous obtained results (see Figure 5.1.1 A & B), while increased LC3B-I into LC3B-II conversion was observed. iULK1 (10 μ M) treatment had a similar effect on expression of immunoblotted proteins as FCCP, except p62 was degraded further and VDAC1 expression increased. Induction of mitophagy as seen by Parkin degradation and PINK1 accumulation was not affected by combined treatment of FCCP and iULK1, but it did lead to increased VDAC1 expression. The effects of combined treatment on LC3B-II accumulation are inconclusive, however, the amount of immunoblotted LC3B-I was decreased. ULK1 degradation was observed upon all treatments.

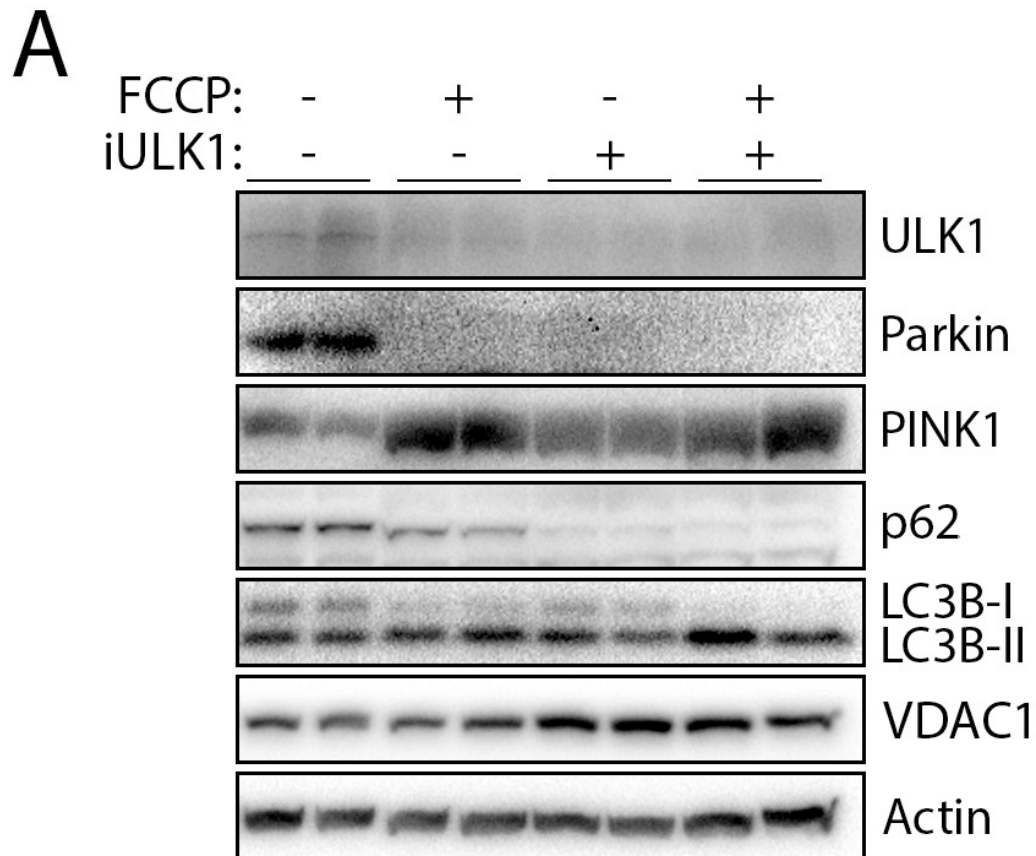


Figure 5.4.1 (A). *ULK1 inhibition affects basal turnover of the mitochondrial marker VDAC1 in undifferentiated 46C mESC.* Both FCCP and iULK1 treatment cause ULK1 and p62 degradation and increase LC3B-I into LC3B-II conversion. Parkin degradation and PINK1 accumulation suggest induction of mitophagy, however, VDAC1 was not degraded. ULK1 accumulation suggests induction of mitophagy, however, VDAC1 was not degraded. ULK1 inhibition affects the basal turnover of VDAC1 in undifferentiated 46C mESC, which is not affected by the addition of FCCP. Undifferentiated 46C mESC were treated with 50 μ M FCCP, 10 μ M iULK1, or both, for 24 hours. Protein lysates (20 μ g) were probed for mitophagy marker proteins Parkin and PINK1, the mitochondrial marker protein VDAC1, and autophagy marker proteins ULK1, p62, and LC3B. β -actin was used as loading control. Data represents one out of a total of three independent experiments.

ULK1 inhibition increased VDAC1 expression ($p < 0.001$), indicating autophagy could play a role in the basal turnover of VDAC1 (Figure 5.4.1 B). Co-treatment of FCCP and iULK1 decreased VDAC1 expression when compared to iULK1 treatment ($p < 0.01$), whereas VDAC1 expression was increased when compared to FCCP treatment ($p < 0.05$).

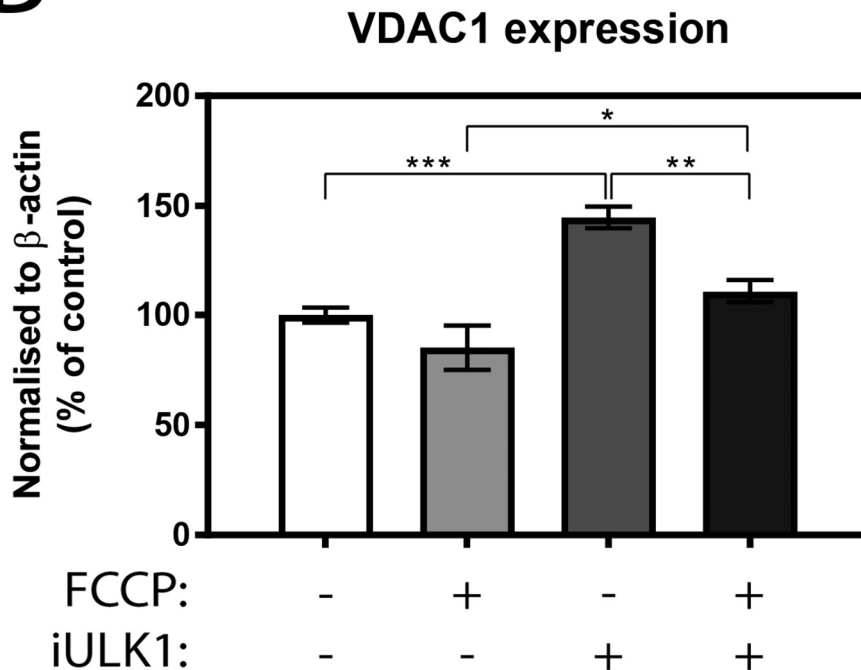
B

Figure 5.4.1 (B). *ULK1 inhibition affects basal turnover of the mitochondrial marker VDAC1 in undifferentiated 46C mESC.* Densitometry of VDAC1 normalised to corresponding β -actin levels. Data is shown as percentage of control and was pooled from three independent experiments. Error bars = SEM, one-way ANOVA, * $p < 0.05$, ** $p < 0.01$, *** $p < 0.001$.

Unfortunately, mESC data was inconsistent and cell culturing difficulties were experienced, which led to the decision to not differentiate the mESC and to terminate the research using these cells. However, when hiPSC became available, research concerning FCCP-induced mitophagy and effects of proteasomal and autophagic inhibition on FCCP-induced mitophagy was continued. The hiPSC data will be described in the remainder of this chapter.

5.5 Differentiation of hiPSC into presumptive dopaminergic neurons

Differentiation of hiPSC into presumptive DA neurons is a time consuming process. A schematic representation of the differentiation process describing the different steps is depicted in Figure 5.5.1.

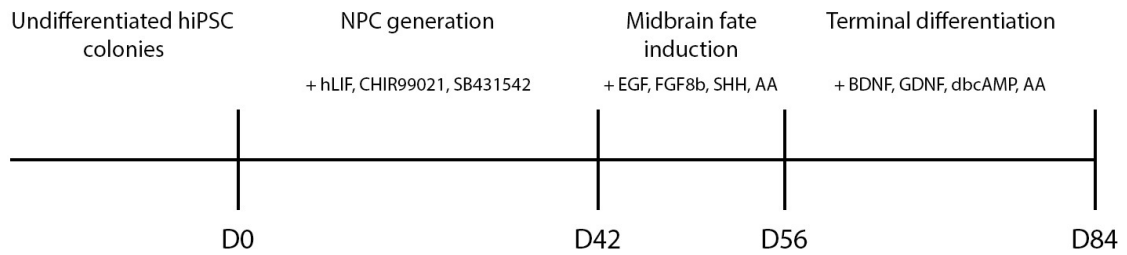


Figure 5.5.1. *Schematic overview of hiPSC differentiation process into presumptive dopamine neurons.* This schematic overview shows the time needed to induce NPC generation (presumptively) from undifferentiated hiPSC colonies and differentiation of NPC into presumptive DA neurons. AA = ascorbic acid, BDNF = brain-derived neurotrophic factor, dbcAMP = dibutyryladenine 3', 5'-cyclic monophosphate sodium salt, EGF = epidermal growth factor, FGF8b = fibroblast growth factor 8b, GDNF = glial cell line-derived neurotrophic factor, hiPSC = human induced pluripotent stem cells, hLIF = human leukaemia inhibitory factor, NPC = neuronal precursor cells, SHH = Sonic Hedgehog.

In order to maintain the undifferentiated and pluripotent state of undifferentiated hiPSC, colonies were grown on a feeder layer of MEF first (Yue et al., 2012). Colonies grew on top of the MEF and MEF were seen surrounding the colonies (Figure 5.5.2 A). However, hiPSC cannot be differentiated when maintained on feeder cells and need to be cultured feeder free to do so. Undifferentiated colonies were manually picked and transferred to Matrigel coated plates. To diminish the risk of contamination of hiPSC, colonies maintained on Matrigel were picked and replated on fresh Matrigel coated plates to get rid of any remaining MEF. Feeder free cultured hiPSC colonies displayed well defined borders unlike colonies grown on MEF (Figure 5.5.2 B).

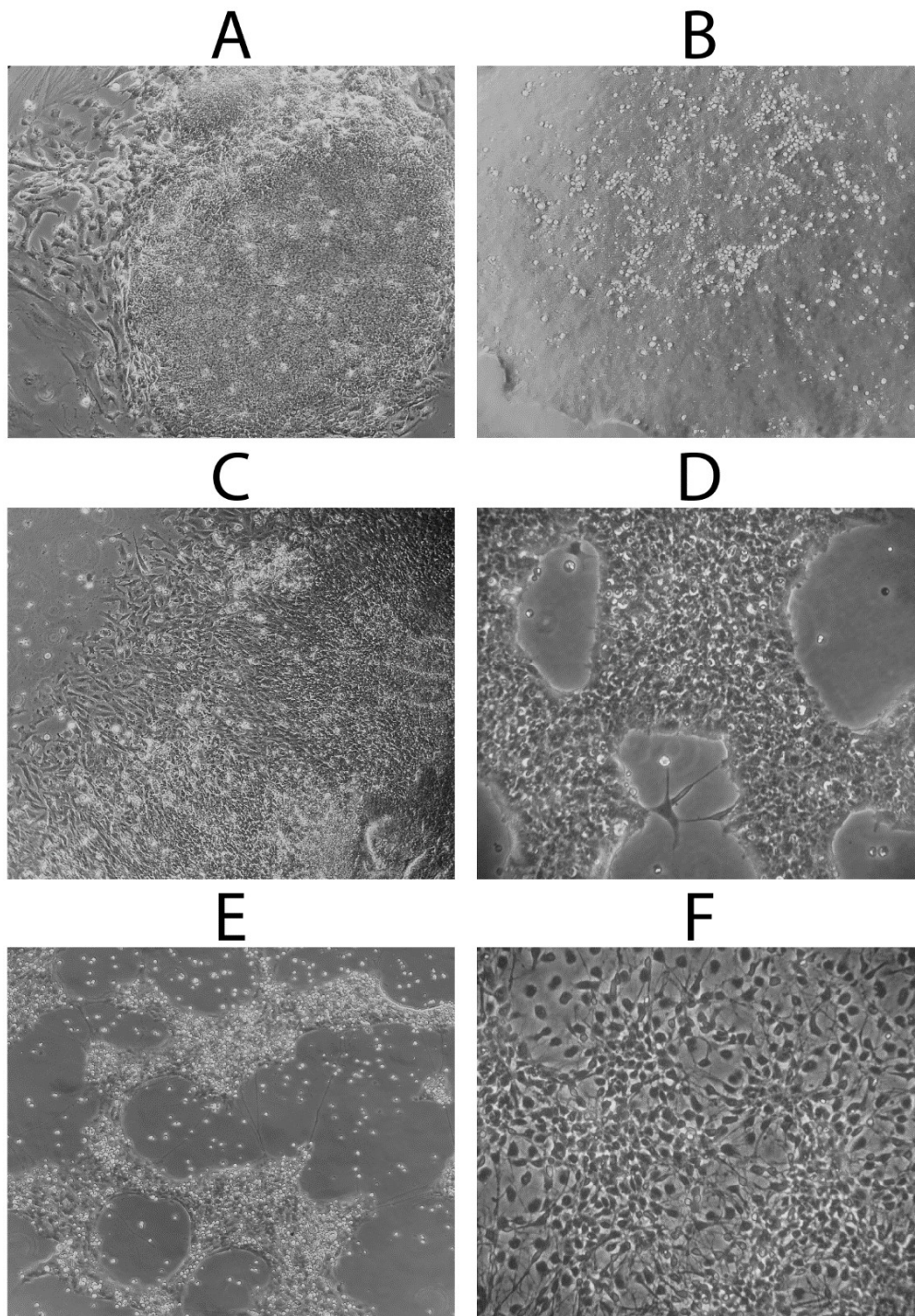


Figure 5.5.2. *Differentiation of hiPSC into presumptive dopaminergic neurons.* Undifferentiated hiPSC can be differentiated into presumptive DA neurons by following a specific protocol. (A) Undifferentiated PD hiPSC colony on MEF. (B) Undifferentiated PD hiPSC colony on Matrigel. (C) Induction of PD NPC (presumptively) after 1 week. (D) Fully matured PD NPC (presumptively). (E) Midbrain phenotype induction of presumptive NPC after 2 weeks. (F) Terminally differentiated presumptive dopaminergic PD neurons. Phase contrast images were taken using a Nikon TMS microscope, magnification = 10x. Data represents one out of a total of three independent experiments.

Undifferentiated hiPSC colonies are labour intensive and have the potential to differentiate spontaneously. Fortunately, undifferentiated hiPSC colonies can be differentiated into a more stable line, namely NPC. NPC can develop into subtype-specific neuronal identities and maintain their broad differentiation potential and high neurogenic propensity even after repeated passaging and long-term expansion (Li et al., 2011). Induction of presumptive NPC was carried out by treating undifferentiated hiPSC colonies with a combined treatment of hLIF, known for its ability to suppress spontaneous differentiation, a glycogen synthase kinase 3 (GSK3) inhibitor (CHIR99021) that can activate canonical Wnt signalling, and a transforming growth factor β (TGF- β) inhibitor (SB431542) for 6 weeks. A clear transition from colony to the formation of single cells could already be seen after 1 week of presumptive NPC induction (Figure 5.5.2 C). Fully matured presumptive NPC were maintained on Matrigel and were subcultured once a week (Figure 5.5.2 D).

Differentiation of presumptive NPC into presumptive dopaminergic neurons was carried out as described by Kriks and colleagues with some adaptations (Kriks et al., 2011). Presumptive NPC were driven towards a midbrain phenotype by culturing them in the presence of human epidermal growth factor (EGF), human fibroblast growth factor 8b (FGF8b), Sonic Hedgehog (SHH), and ascorbic acid (AA). hiPSC displayed a clear change from presumptive NPC to a more neuronlike state with the development of axons after 2 weeks of midbrain phenotype induction (Figure 5.5.2 E). Terminal differentiation into presumptive DA neurons was carried out by removal of the earlier used growth factors after 2 weeks and introduction of the cells to human brain-derived neurotrophic factor (BDNF), glial cell line-derived neurotrophic factor (GDNF), dibutyryladenosine 3',5'-cyclic monophosphate sodium salt (dbcAMP), and

AA for 4 weeks. This led to the transformation of presumptive NPC into mature looking neurons with axons that should express the dopaminergic markers dopamine transporter (DAT) and tyrosine hydroxylase (TH) (Figure 5.5.2 F).

Given the long differentiation period of hiPSC, the majority of the experiments as described in this chapter were carried out using presumptive NPC. NPC represent a neuronal cell population and therefore similarities in findings are expected between presumptive NPC and presumptive NPC differentiated into presumptive DA neurons.

5.6. FCCP induces autophagy, but not mitophagy, in presumptive NPC

To investigate how autophagy and mitophagy are regulated upon FCCP treatment in presumptive NPC generated from a healthy patient (will be called control NPC in remainder of thesis) and presumptive NPC generated from a PD patient, a time course was carried out. Control and PD presumptive NPC presented with a similar phenotype and prolonged 5 μ M FCCP treatment did not lead to changes in cell morphology or detachment of cells (Figure 5.6.1).

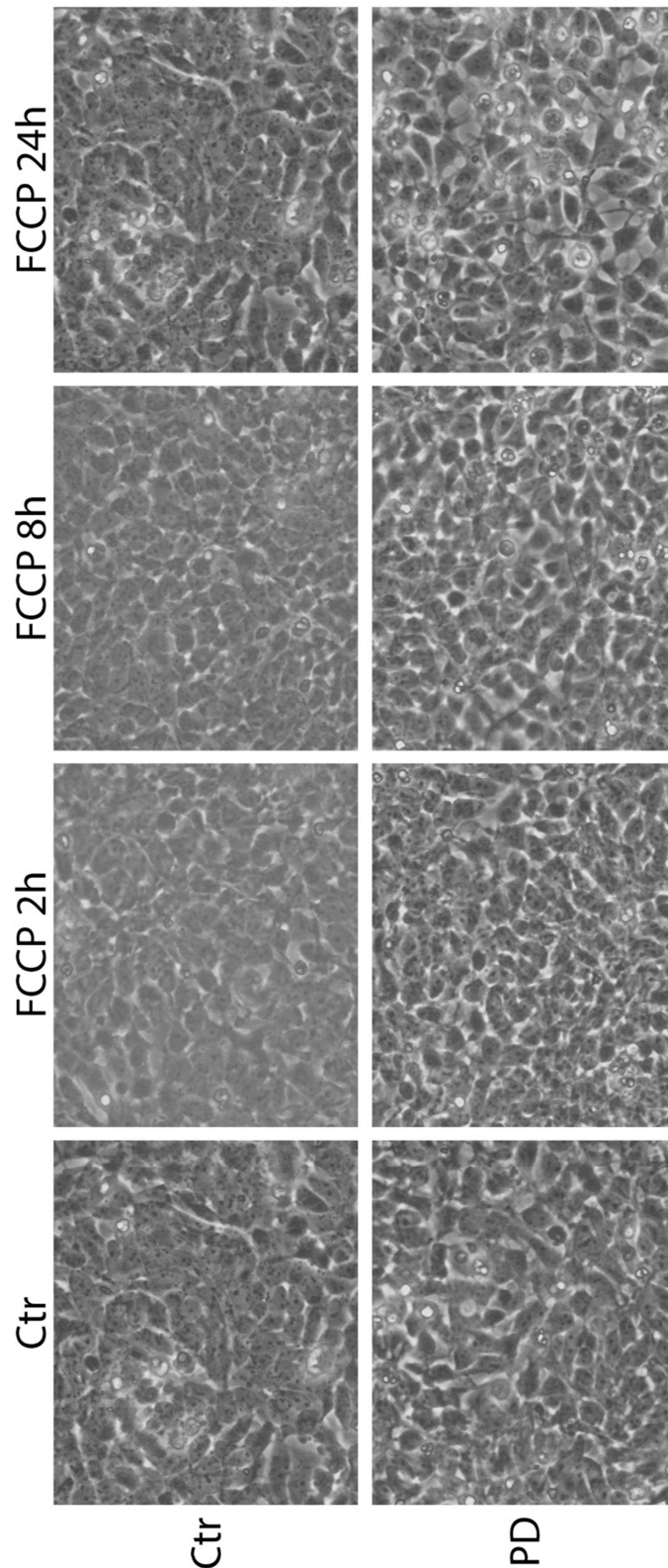


Figure 5.6.1. *FCCP exposure does not affect presumptive NPC morphology.* FCCP treatment does not lead to cell detachment or changes in cell morphology of control (Ctr) and PD presumptive NPC. Presumptive NPC were treated with 5 μ M FCCP and phase contrast images were taken at indicated time points using a Nikon TMS microscope, magnification = 20x. Data represents one out of a total of three independent experiments.

Preliminary RT-qPCR data showed that 5 μ M FCCP increased Parkin mRNA expression over time in control presumptive NPC (Figure 5.6.2, white bars). On the contrary, PD presumptive NPC had reduced Parkin mRNA expression at 2 hours of FCCP treatment, which did not return to control levels, even after 24 hours.

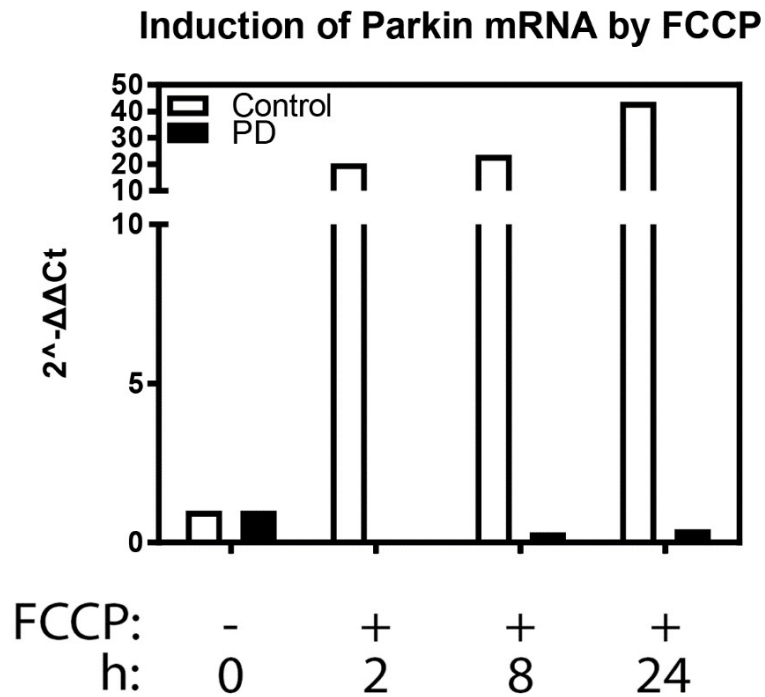


Figure 5.6.2. FCCP-mediated effects on Parkin mRNA expression differs between control and PD presumptive NPC. FCCP treatment leads to increased Parkin mRNA expression over time in control presumptive NPC, whereas PD presumptive NPC have reduced Parkin mRNA expression. Control and PD presumptive NPC were treated with 5 μ M FCCP for indicated time points after which RNA was isolated. Parkin mRNA expression levels were normalised to the housekeeping gene 18s and are depicted as fold increase ($2^{-\Delta\Delta Ct}$). Data represents one experiment.

At the protein level, both control and PD presumptive NPC showed increased Parkin expression at 2 hours of 5 μ M FCCP treatment, which, except for PD presumptive NPC at 24 hours displaying Parkin degradation, decreased to basal levels at later time points (Figure 5.6.3 A). FCCP also induced a small increase in PINK1 expression

throughout the time course, however, it is unknown whether FCCP induced mitophagy in presumptive NPC since Parkin was not clearly degraded.

PD presumptive NPC had a higher basal expression of p62 (arrow) compared to control presumptive NPC, which was degraded upon FCCP treatment. This was accompanied by a small increase in LC3B-II accumulation and therefore suggests activation of autophagy. Control presumptive NPC showed p62 accumulation at 8 hours of FCCP treatment, which was followed by a decrease at 24 hours, but there was no degradation. Increased p62 expression was associated with reduced LC3B-II accumulation and p62 reduction resulted in increased LC3B turnover, suggesting FCCP induced autophagy that was temporarily blocked at 8 hours of treatment. Lysosomal associated membrane protein 1 (LAMP1) was degraded in both control and PD presumptive NPC, however, PD presumptive NPC showed higher rates of degradation at 8 and 24 hours of FCCP treatment.

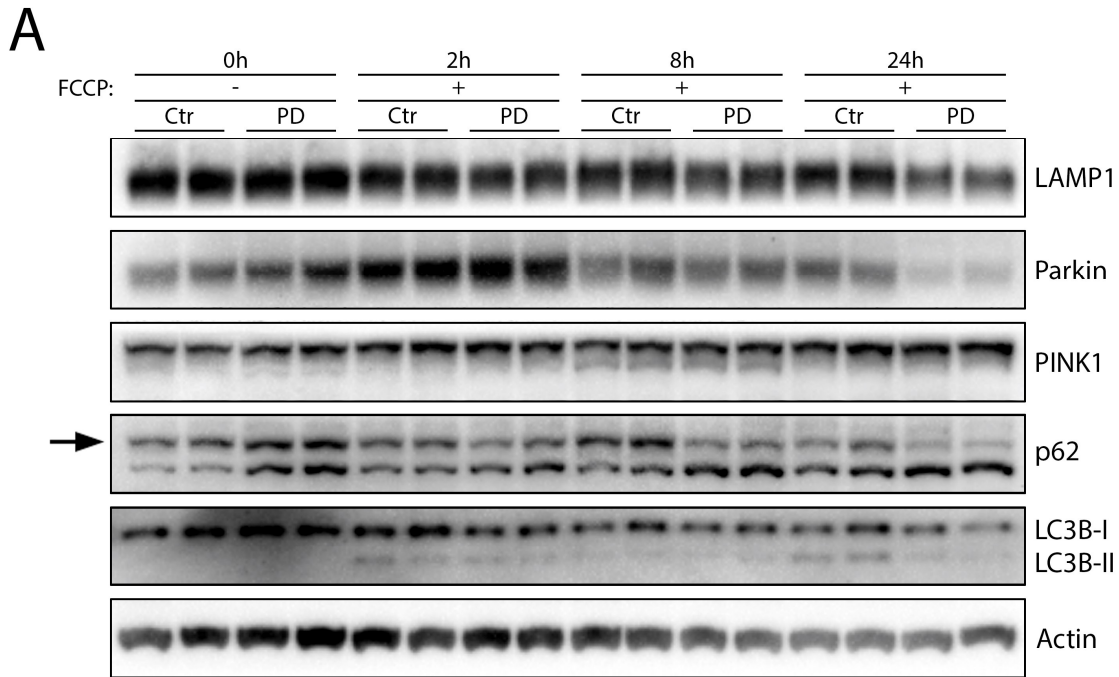


Figure 5.6.3 (A). *FCCP induces autophagy in presumptive NPC.* FCCP induces autophagy in both control (Ctrl) and PD presumptive NPC, based on p62 degradation and increased LC3B turnover, whereas it is unclear whether it induces mitophagy as well since Parkin is not clearly degraded besides the observed Parkin degradation in PD presumptive NPC at 24 hours of FCCP treatment. Presumptive NPC were treated with 5 μ M FCCP for indicated time points. Protein lysates (30 μ g) were probed for the mitophagy marker proteins Parkin and PINK1, and autophagy marker proteins LAMP1, p62, and LC3B. β -actin was used as loading control. p62 expression is indicated by the arrow. Data represents one out of a total of three independent experiments.

After normalising protein expression to corresponding β -actin levels, no increase was observed in Parkin expression at 2 hours of FCCP treatment in both control and PD presumptive NPC (Figure 5.6.3 B). Parkin was stably expressed in control presumptive NPC besides being degraded at 8 hours of treatment. In PD presumptive NPC, on the other hand, a small decrease in Parkin expression was seen. LC3B-II accumulation was significantly increased at 8 hours of FCCP treatment in both control and PD presumptive NPC ($p < 0.05$).

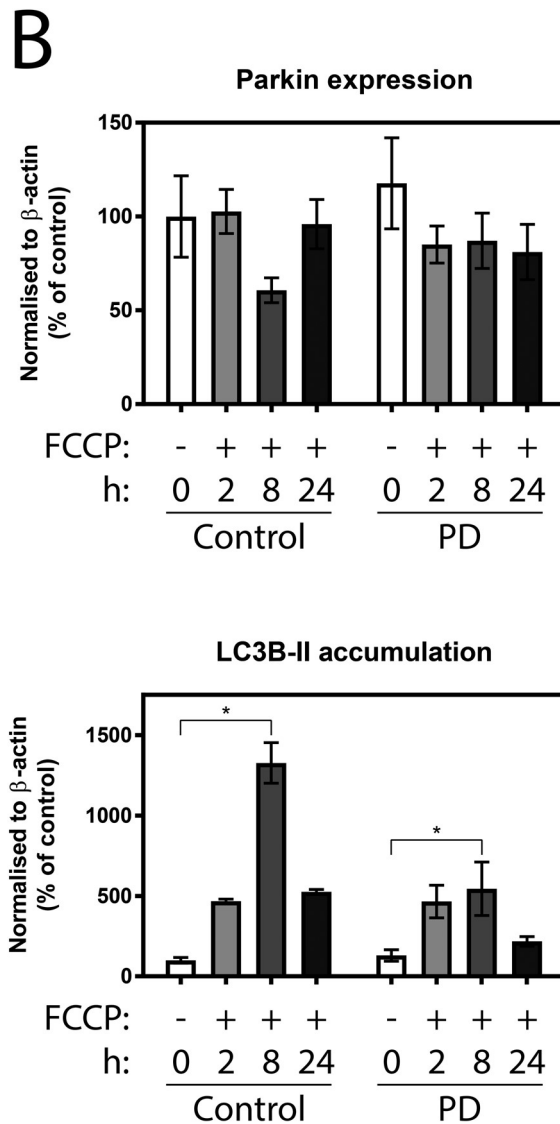


Figure 5.6.3 (B). *FCCP induces autophagy in presumptive NPC.* Parkin and LC3B-II densitometry normalised to corresponding β -actin levels. Densitometric analysis was pooled from three independent experiments and data is shown as percentage of control. Error bars = SEM, one-way ANOVA, * $p < 0.05$.

To determine whether FCCP was capable of inducing mitochondrial degradation in presumptive NPC, expression of mitochondrial markers was investigated. In control presumptive NPC, TOM20 was degraded only at 24 hours of 5 μ M FCCP treatment, whereas TOM20 was degraded in PD presumptive NPC at all time points (Figure 5.6.4 A). Similar to TOM20, TIM23 was only degraded at 24 hours of FCCP treatment in control presumptive NPC, while TIM23 expression was reduced at 2

hours and 8 hours, before reaching basal levels at 24 hours of treatment, in PD presumptive NPC. Interestingly, PD presumptive NPC had higher basal TIM23 expression compared to control presumptive NPC. VDAC1 expression was increased in both control and PD presumptive NPC upon FCCP treatment with the biggest increase at 8 hours. PD presumptive NPC had a higher increase in VDAC1 expression than control presumptive NPC.

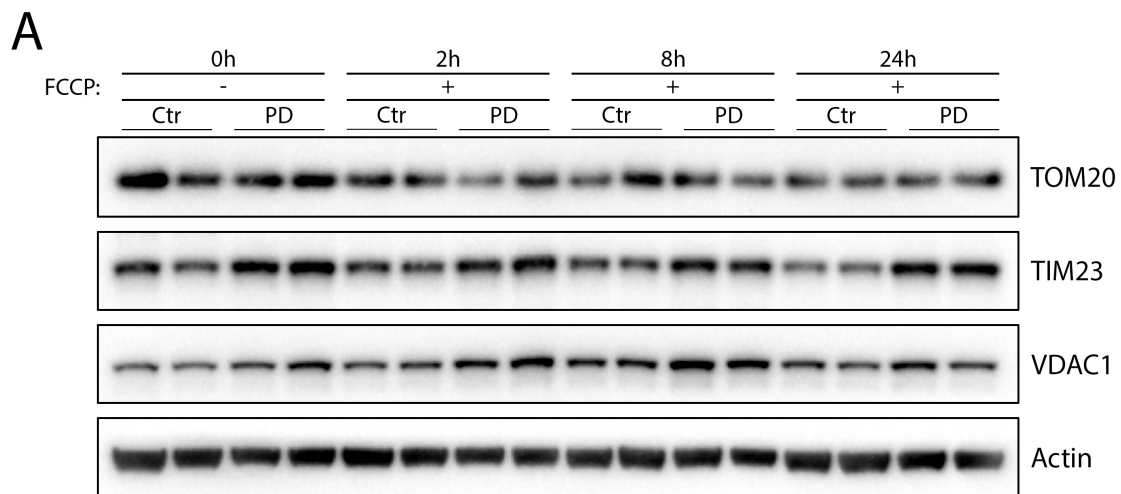


Figure 5.6.4 (A). FCCP does not induce mitochondrial degradation in presumptive NPC. FCCP treatment does not lead to degradation of the mitochondrial markers TOM20, TIM23, and VDAC1 in control (Ctr) and PD presumptive NPC. Note that PD presumptive NPC had higher basal expression of TIM23 and VDAC1. Presumptive NPC were treated with 5 μ M FCCP for indicated time points. Protein lysates (30 μ g) were probed for mitochondrial marker proteins TOM20, TIM23, and VDAC1. β -actin was used as loading control. Data represents one out of a total of three independent experiments.

Densitometry showed that only VDAC1 expression was affected by FCCP treatment in control presumptive NPC (Figure 5.6.4 B). VDAC1 expression was significantly increased at 8 hours ($p < 0.05$) and 24 hours ($p < 0.01$) of FCCP treatment.

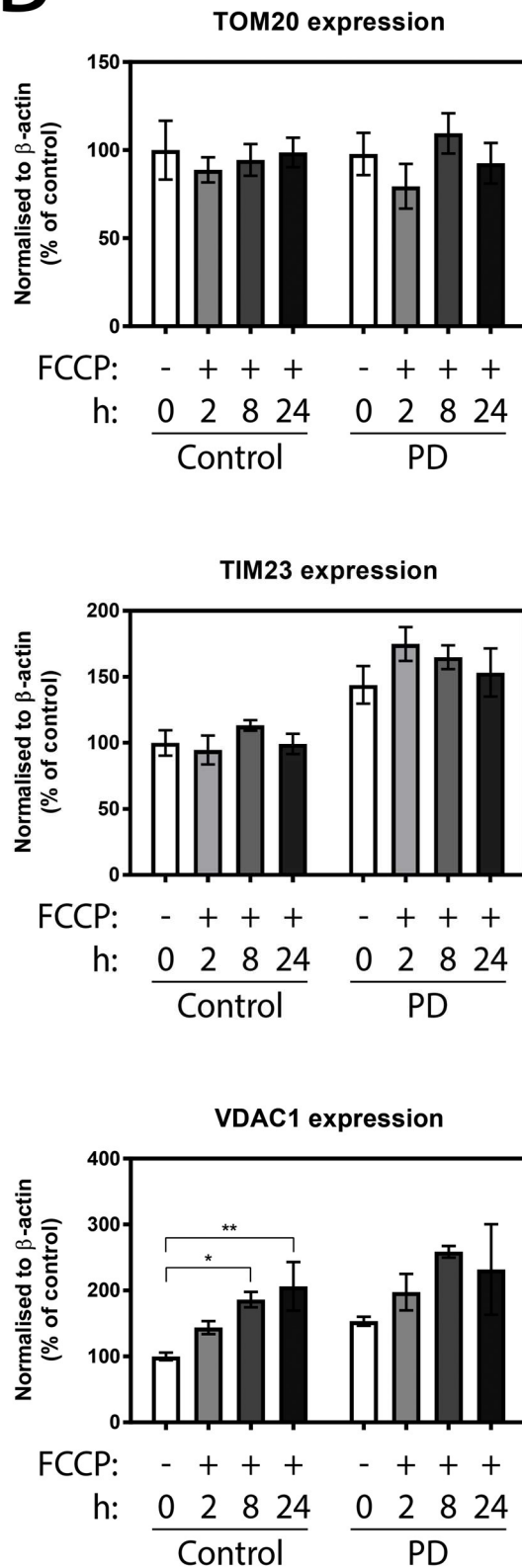
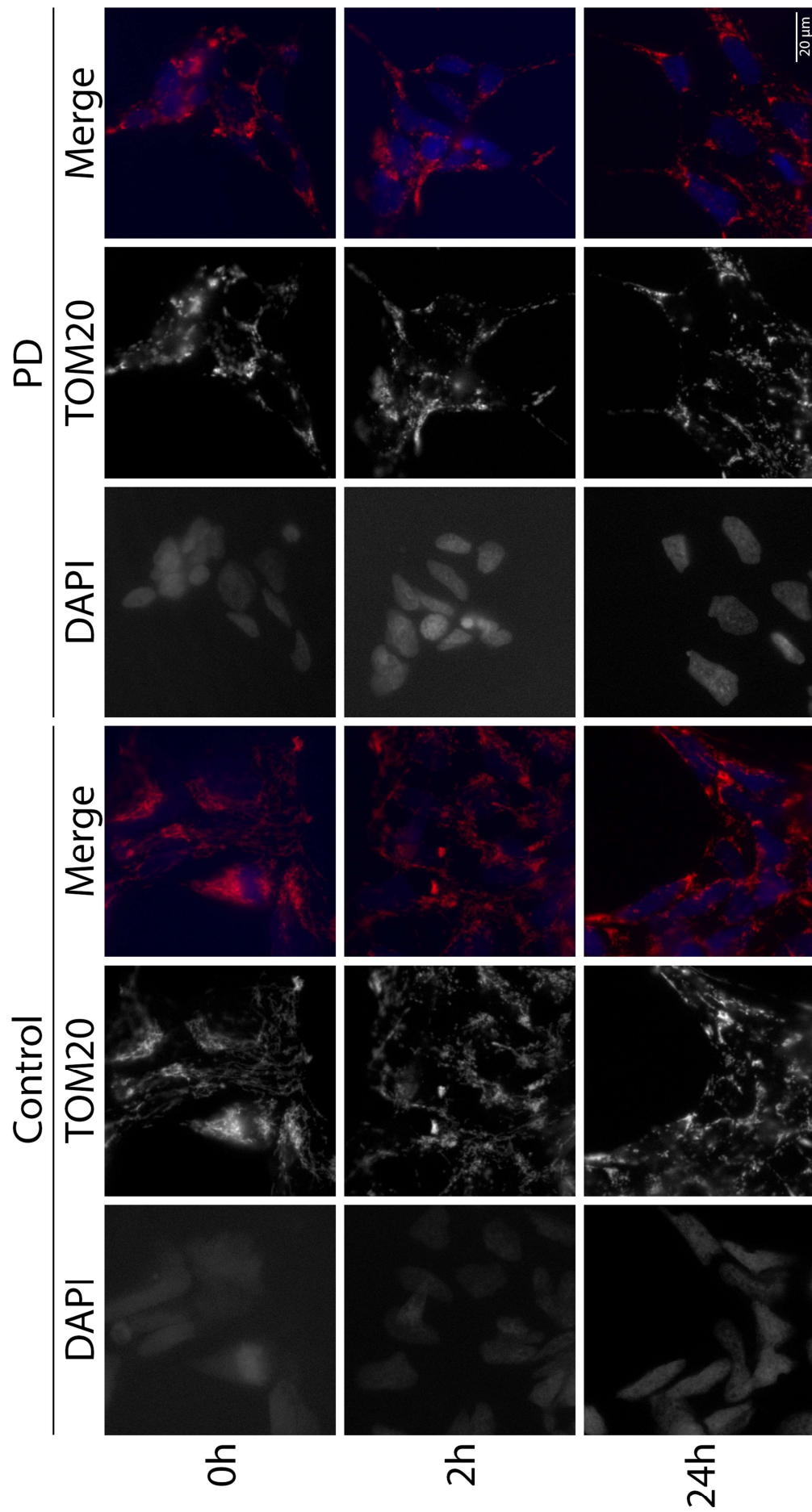
B

Figure 5.6.4 (B). FCCCP does not induce mitochondrial degradation in presumptive NPC. TOM20, TIM23, and VDAC1 densitometry normalised to corresponding β -actin levels. Densitometric analysis was pooled from three independent experiments and data is shown as percentage of control. Error bars = SEM, one-way ANOVA, *p<0.05, **p<0.01.

To investigate whether FCCP was capable of inducing mitochondrial fragmentation in presumptive NPC, mitochondria were visualised by epifluorescence microscopy. Dispersed TOM20 staining revealed that mitochondria were fragmented in control presumptive NPC upon 5 μ M FCCP treatment (Figure 5.6.5). Fragmentation was observed at 2 hours of FCCP treatment and was increased at 24 hours. PD presumptive NPC already presented with dispersed TOM20 staining under basal conditions, which was worsened upon FCCP treatment.



Previous Page: Figure 5.6.5. *Mitochondria fragment upon FCCP treatment.* FCCP treatment leads to dispersed TOM20 staining, indicating fragmentation of mitochondria, in both control and PD presumptive NPC with increased amounts of mitochondrial fragmentation seen at later time points. Note that PD presumptive NPC already show dispersed TOM20 staining under basal conditions. Presumptive NPC were treated with 5 μ M FCCP for indicated time points before fixation of the cells. Mitochondria were visualised by TOM20 staining (red) and nuclei are labelled with DAPI (blue). Data represents one experiment. Magnification = 60x, scale bar = 20 μ m.

5.7 Inhibition of lysosomal degradation affects basal turnover of TOM20 and VDAC1 in presumptive NPC

The effects of autophagic inhibition on expression of autophagy related proteins and mitochondrial markers were also investigated in presumptive NPC. Autophagy was inhibited by Baf A1 treatment (100 nM), which did not lead to a change in cell morphology or cellular detachment in control and PD presumptive NPC (Figure 5.7.1).

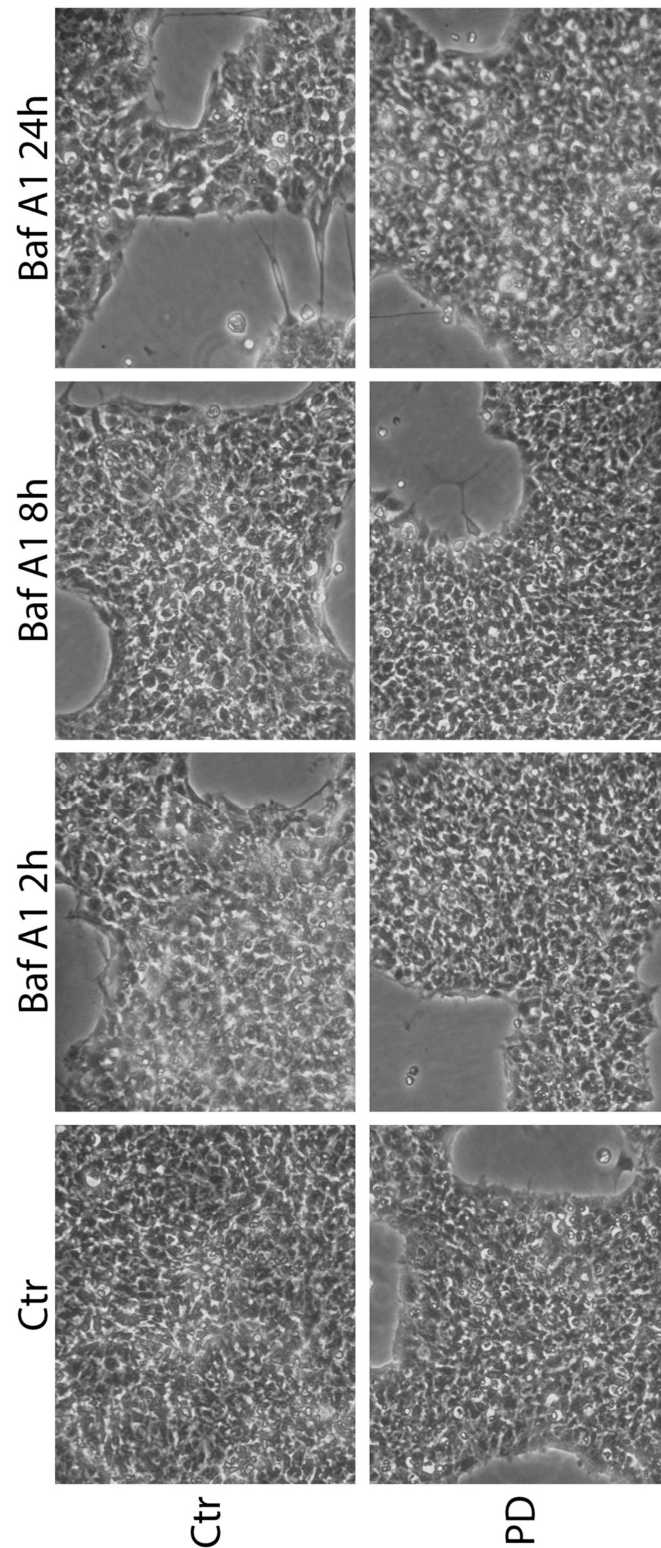


Figure 5.7.1. *Prevention of lysosomal degradation does not change presumptive NPC cell morphology.* Inhibition of autophagy by prevention of autophagic cargo degradation by Baf A1 does not alter cell morphology nor does it lead to detachment of control (Ctr) and PD presumptive NPC. Control and PD presumptive NPC were treated with 100 nM Baf A1. Phase contrast images were taken at indicated time points using a Nikon TMS microscope, magnification = 10x. Data represents one out of a total of four independent experiments.

A Baf A1 time course showed that the late stage of autophagy was effectively inhibited as seen by p62 and LC3B-II accumulation in both control and PD presumptive NPC (Figure 5.7.2). p62 accumulation was observed at an earlier time point (2 hours) in PD presumptive NPC than in control presumptive NPC (8 hours). Increased conversion of LC3B-I to LC3B-II took place at 8 hours and peaked at 24 hours of treatment. Increased LAMP1 expression upon Baf A1 treatment suggests that the population of lysosomes increased upon autophagic inhibition. Parkin expression in control presumptive NPC fluctuated from a small reduction at 2 hours and 24 hours of treatment to basal levels at 8 hours. PD presumptive NPC displayed a small increase in Parkin expression at observed time points. PINK1 expression was decreased over time in both control and PD presumptive NPC.

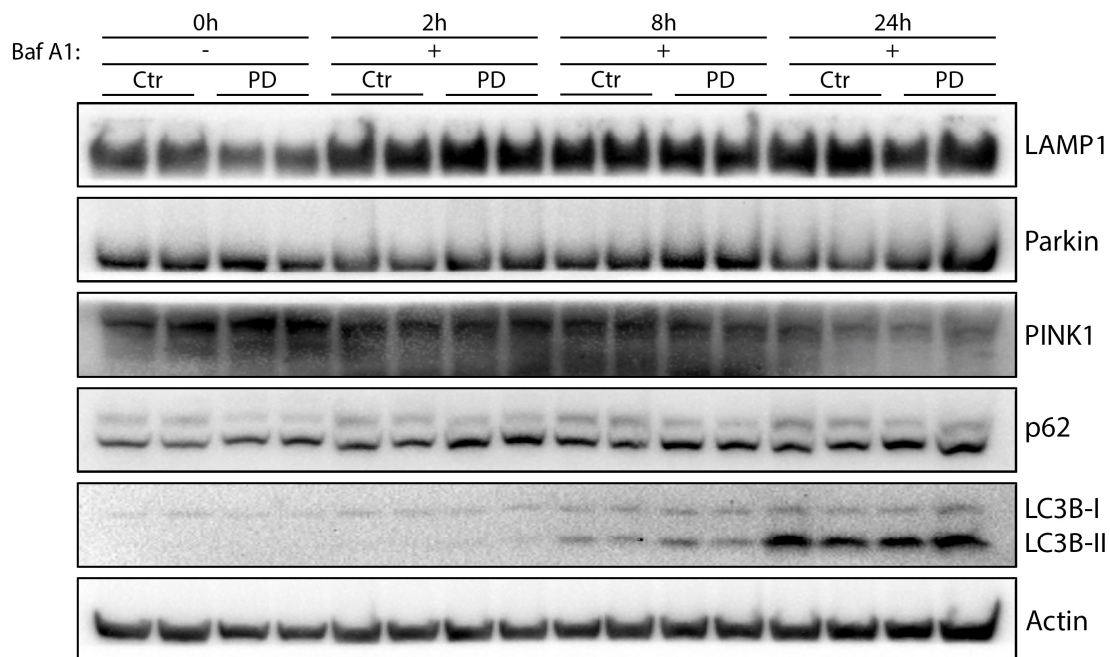


Figure 5.7.2. *Baf A1 inhibits autophagy in presumptive NPC.* Baf A1 treatments leads to p62 and LC3B-II accumulation in both control and PD presumptive NPC, indicating autophagy is inhibited. Baf A1 also increases LAMP1 expression, decreases PINK1 expression and leads to fluctuations in Parkin expression. Presumptive NPC were treated with 100 nM Baf A1 for indicated time points. Protein lysates (30 μ g) were probed for mitophagy marker proteins Parkin and PINK1, and autophagy marker proteins LAMP1, p62, and LC3B. β -actin was used as loading control. Data represents one out of a total of four independent experiments.

TOM20 expression increased upon Baf A1 treatment in control presumptive NPC, while in PD presumptive NPC, TOM20 expression was only increased at 2 hours of treatment and decreased to basal expression levels at later time points (Figure 5.7.3 A). TIM23 expression was unaffected by Baf A1 treatment in both control and PD presumptive NPC, whereas VDAC1 accumulated over time.

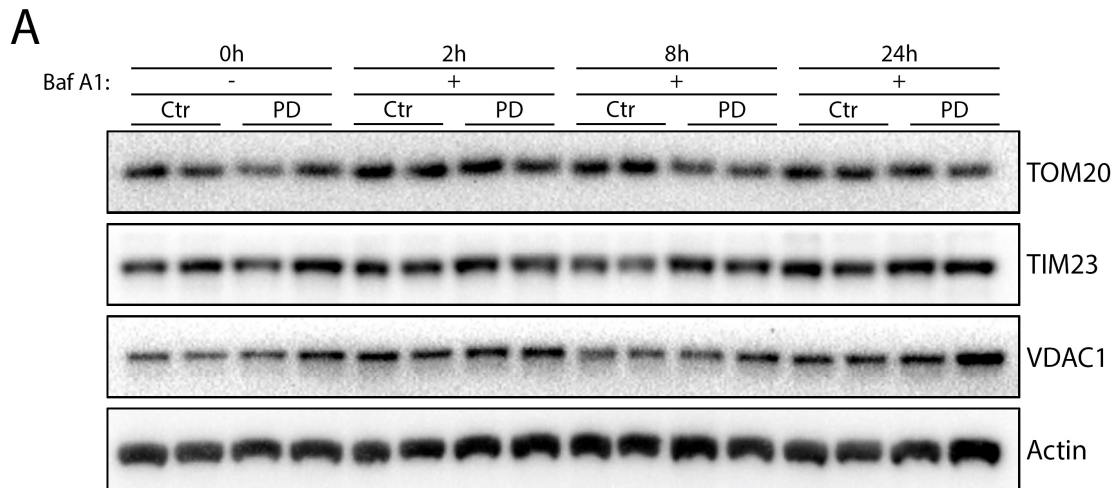


Figure 5.7.3 (A). *Baf A1 inhibits basal turnover of TOM20 and VDAC1.* Inhibition of autophagic degradation by Baf A1 inhibits basal turnover of TOM20 in both control and PD presumptive NPC and VDAC1 in control presumptive NPC only. VDAC1 was degraded in PD presumptive NPC at 24 hours of treatment, whereas TIM23 expression was not affected by Baf A1. Presumptive NPC were treated with 100 nM Baf A1 for indicated time points. Protein lysates (30 μ g) were probed for mitochondrial marker proteins TOM20, TIM23, and VDAC1. β -actin was used as loading control. Data represents one out of a total of four independent experiments.

Densitometric analysis revealed that TOM20 expression was significantly increased at 8 hours ($p < 0.01$) and 24 hours ($p < 0.05$) of Baf A1 treatment in control presumptive NPC (Figure 5.7.3 B). VDAC1 was accumulated in control presumptive NPC at 2 hours of treatment ($p < 0.05$), after which its expression returned to basal levels.

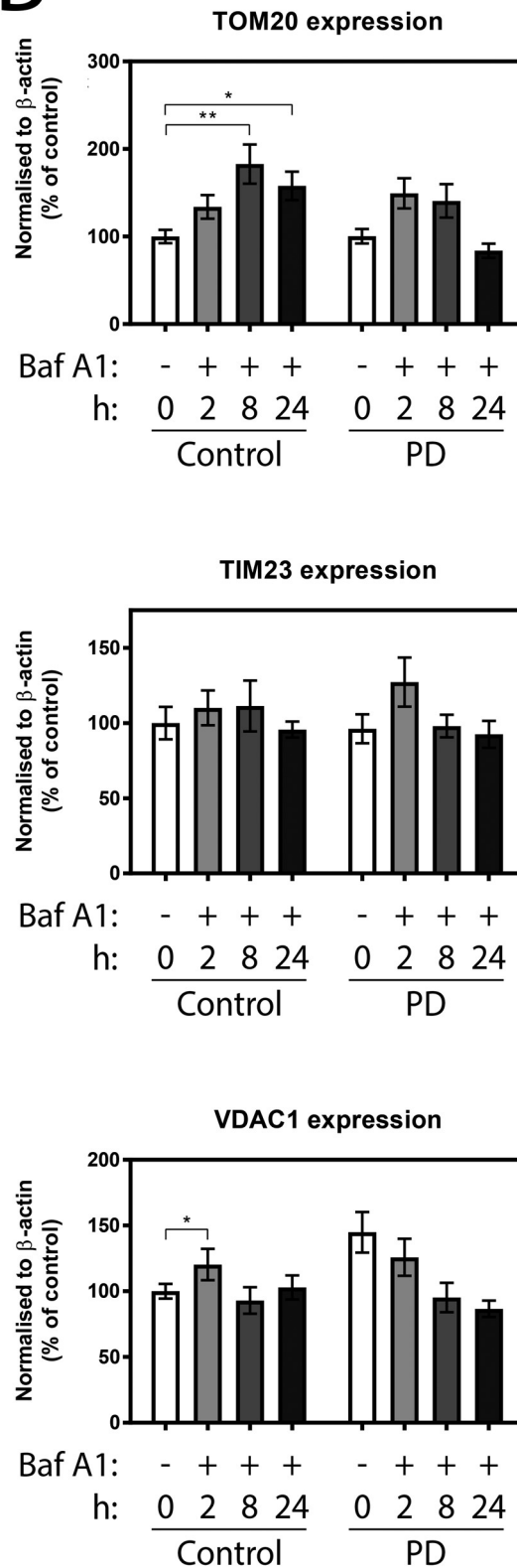
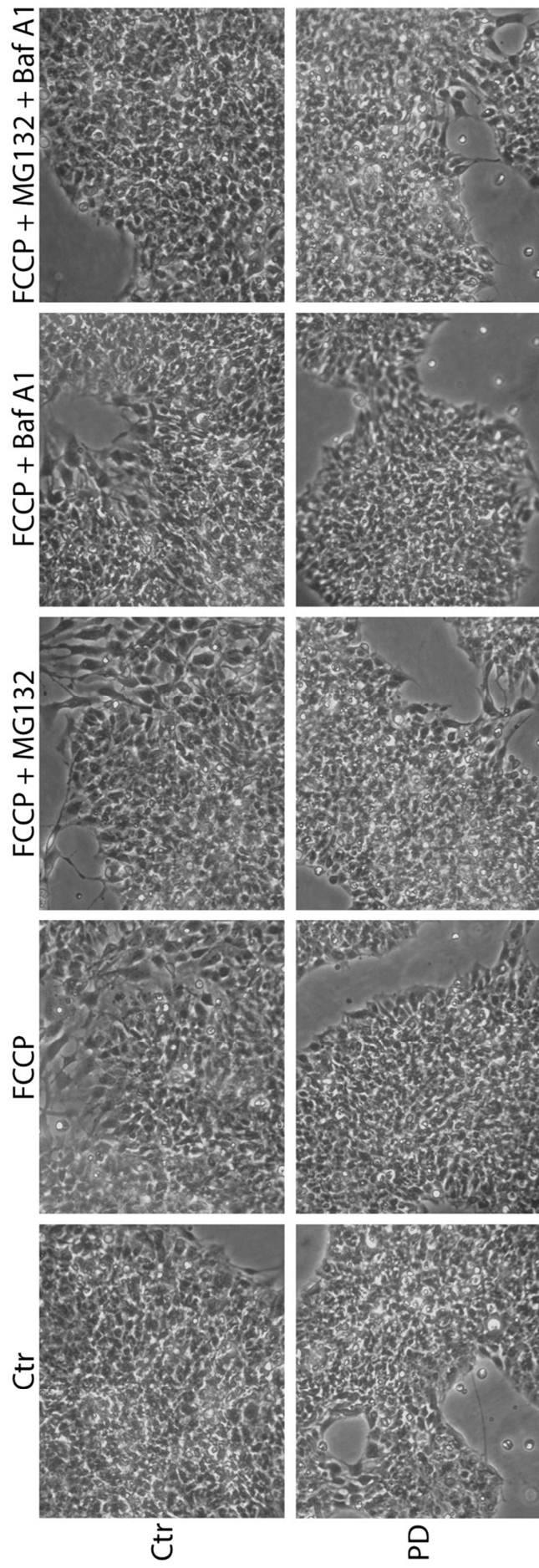
B

Figure 5.7.3 (B). *Baf A1* inhibits basal turnover of *TOM20* and *VDAC1*. *TOM20*, *TIM23*, and *VDAC1* densitometry normalised to corresponding β -actin levels. Densitometric analysis was pooled from four independent experiments and data is shown as percentage of control. Error bars = SEM, one-way ANOVA, * $p < 0.05$, ** $p < 0.01$.

5.8 Proteasomal or autophagic inhibition does not affect expression of mitochondrial markers upon FCCP treatment

Combined treatment of FCCP, MG132, and Baf A1 was carried out to see if FCCP-induced effects are attributable to the autophagy or the proteasomal pathway. Different combinations of the reagents did not lead to morphological differences or detachment of control and PD presumptive NPC (Figure 5.8.1).

FCCP treatment (5 μ M) for 8 hours did not result in Parkin degradation nor PINK1 accumulation as observed previously (Figure 5.8.2). PD presumptive NPC had a higher basal expression of Parkin and higher Parkin expression upon FCCP treatment, but Parkin expression was increased in control presumptive NPC upon FCCP treatment as well. p62 expression (arrow) was decreased in both control and PD presumptive NPC, suggesting activation of autophagy, however, this was not associated with LC3B turnover. Combined treatment of 5 μ M FCCP and 20 μ M MG132 decreased Parkin expression in both control and PD presumptive NPC when compared to FCCP treatment, whereas MG132 did not affect expression of the other immunoblotted proteins. Co-treatment of 5 μ M FCCP and 100 nM Baf A1 increased LAMP1 expression in both control and PD presumptive NPC, but did not result in p62 and LC3B-II accumulation. There was, however, accumulation of LC3B-I. Both Parkin and PINK1 were degraded in control and PD presumptive NPC when compared to FCCP treatment. A combination of FCCP, MG132, and Baf A1 did not affect the expression of the immunoblotted proteins when compared to FCCP and Baf A1 co-treatment besides increased p62 expression in control presumptive NPC.



Previous Page: Figure 5.8.1. *Autophagic or proteasomal inhibition upon FCCP treatment does not affect cell morphology nor does it lead to detachment of presumptive NPC.* Proteasomal inhibition by MG132 or blockade of autophagic cargo degradation by Baf A1 does not alter cell morphology nor does it lead to detachment of control (Ctr) and PD presumptive NPC. Presumptive NPC were treated with a combination of 5 μ M FCCP, 20 μ M MG132, or 100 nM Baf A1, for 8 hours. Phase contrast images were taken using a Nikon TMS microscope, magnification 10x. Data represents one out of a total of three independent experiments.

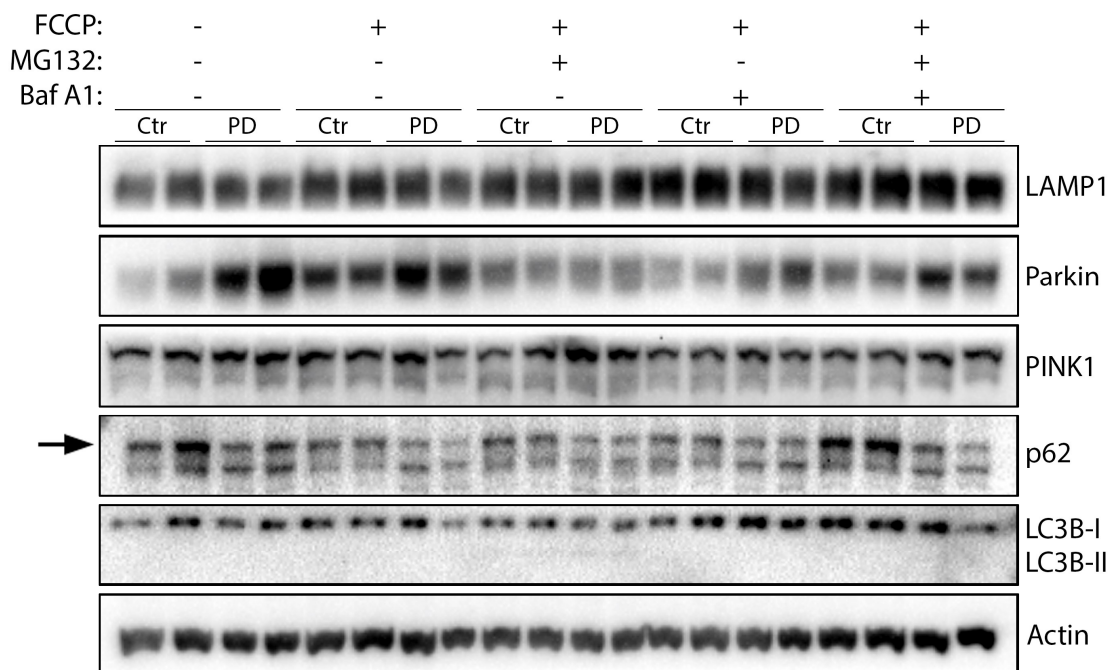


Figure 5.8.2. *Treatment of FCCP with or without MG132 does not lead to LC3B-II accumulation in presumptive NPC.* Compared to FCCP treatment, combined treatment of FCCP and MG132 decreases Parkin expression, whereas LAMP1 and LC3B-I expression are increased upon FCCP and Baf A1 treatment. Mitophagy is likely not induced since Parkin is not degraded and PINK1 expression is not increased upon FCCP treatment. Presumptive NPC were treated with either 5 μ M FCCP, 20 μ M MG132, 100 nM Baf A1, or a combination, for 8 hours. Protein lysates (30 μ g) were probed for mitophagy marker proteins Parkin and PINK1, and autophagy marker proteins LAMP1, p62, and LC3B. β -actin was used as loading control. p62 expression is indicated by the arrow. Data represents one out of a total of two independent experiments.

After repeating the experiment, it became evident that protein expression of immunoblotted proteins differed (Figure 5.8.3). FCCP treatment resulted in LC3B lipidation that was increased upon co-treatment with MG132. LAMP1 was increased in both control and PD presumptive NPC upon FCCP treatment, which did not change when co-treated with MG132. Decreased LAMP1 expression was found in PD presumptive NPC upon combined treatment with FCCP and Baf A1, and in both control and PD presumptive NPC when MG132 was added as well. Basal Parkin expression was not increased in PD presumptive NPC, but did degrade upon FCCP treatment.

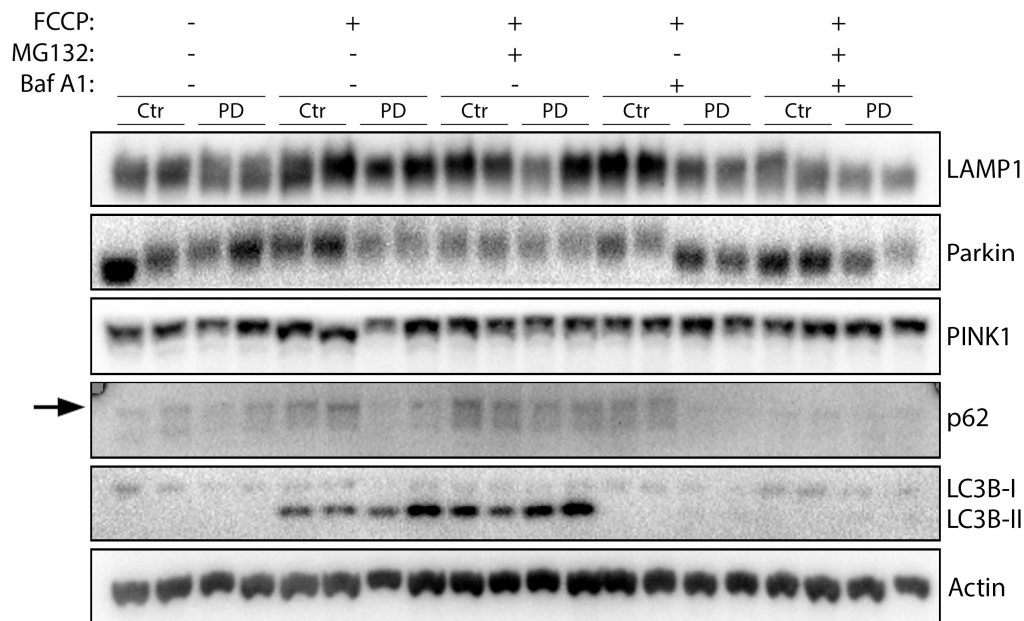


Figure 5.8.3. Treatment of FCCP with or without MG132 leads to LC3B-II accumulation in presumptive NPC. Regardless of MG132, FCCP treatment results in LC3B-II accumulation and increased LAMP1 expression in control and PD presumptive NPC. Parkin expression increases in PD presumptive NPC upon FCCP treatment, while addition of Baf A1 decreases LAMP1 expression when compared to FCCP treatment. Note that the described results differ from Figure 5.8.2. Presumptive NPC were treated with either 5 μ M FCCP, 20 μ M MG132, 100 nM Baf A1, or a combination, for 8 hours. Protein lysates (30 μ g) were probed for mitophagy marker proteins Parkin and PINK1, and autophagy marker proteins LAMP1, p62, and LC3B. β -actin was used as loading control. p62 expression is indicated by the arrow. Data represents one experiment.

Densitometric analysis of protein expression normalised to corresponding β -actin levels shows that LAMP1 expression followed a similar pattern in control and PD presumptive NPC (Figure 5.8.4). All treatments led to increased LAMP1 expression. Similar to LAMP1, Parkin expression was increased by all treatments in control presumptive NPC. In PD presumptive NPC, on the other hand, Parkin expression was decreased by the different treatments. PD presumptive NPC also had a higher basal expression of Parkin. LC3B-II accumulation was increased by all conditions in both control and PD presumptive NPC.

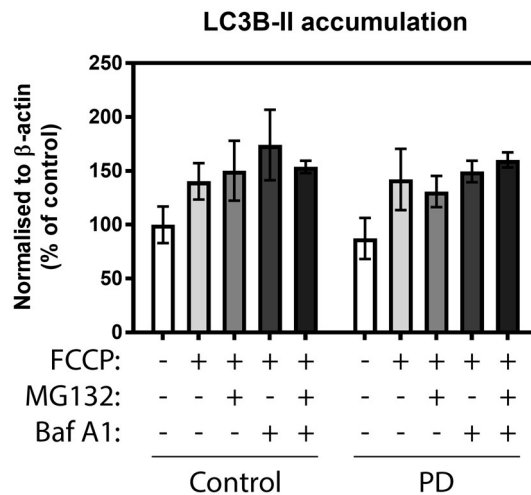
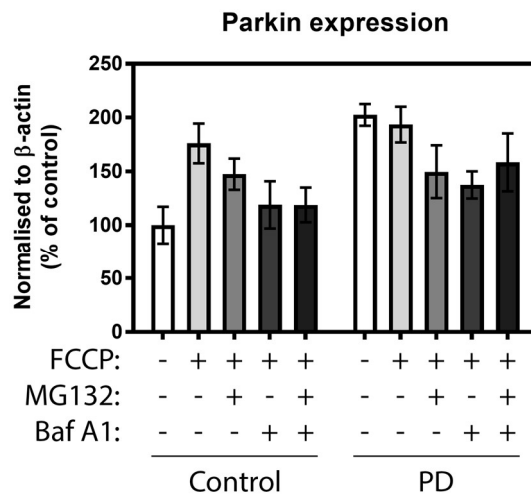
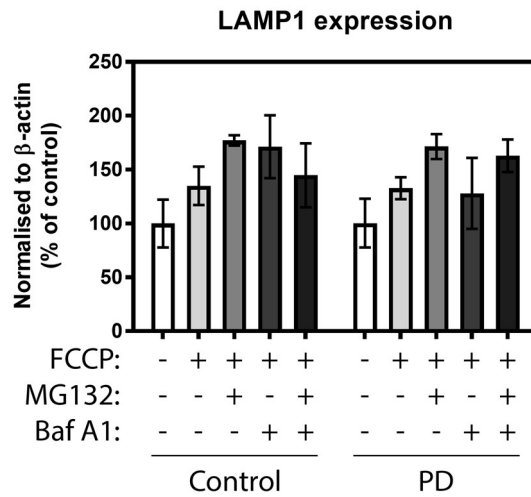


Figure 5.8.4. Parkin is degraded in PD presumptive NPC upon co-treatment of FCCP and either MG132, Baf A1, or both. LAMP1, Parkin, and LC3B-II densitometry normalised to corresponding β -actin levels. Densitometric analysis was pooled from two independent experiments as shown in Figure 5.8.2 and data is shown as percentage of control. Error bars = SEM.

As shown previously, FCCP treatment did not lead to degradation of the mitochondrial markers TOM20, TIM23, and VDAC1 in both control and PD presumptive NPC (Figure 5.8.5 A). TOM20 showed a further accumulation in both control and PD presumptive NPC upon co-treatment with either MG132, Baf A1, or both. Co-treatment of FCCP with either Baf A1 or Baf A1 and MG132 led to TIM23 degradation in control presumptive NPC, whereas TIM23 expression was decreased in all conditions in PD presumptive NPC. FCCP and MG132 co-treatment led to VDAC1 degradation in PD presumptive NPC, however, VDAC1 expression was unaffected by the other treatments in both control and PD presumptive NPC.

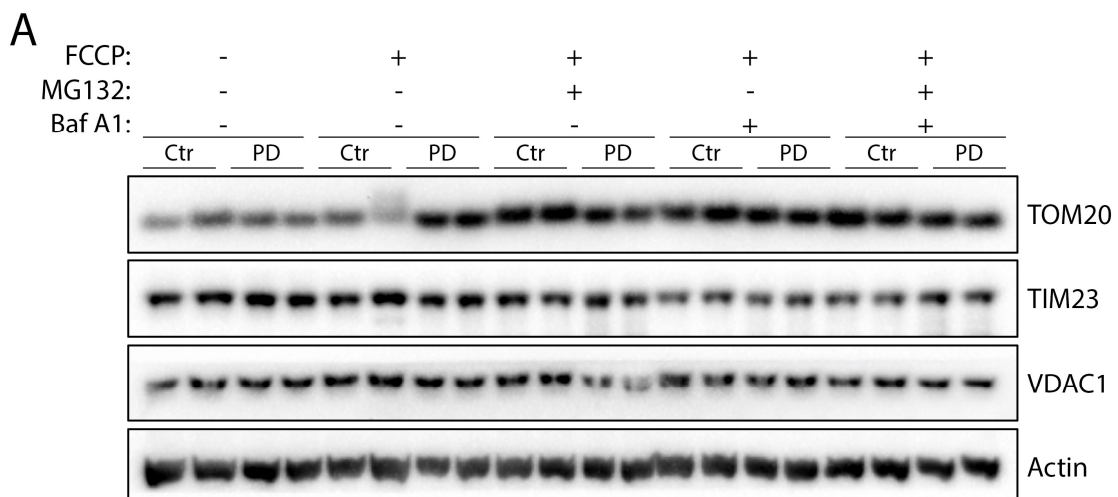


Figure 5.8.5 (A). *Proteasomal or autophagic inhibition does not affect FCCP-induced changes in expression of mitochondrial markers.* FCCP treatment does not lead to degradation of the mitochondrial markers TOM20, TIM23, and VDAC1. Proteasomal inhibition by MG132 or blockade of autophagic cargo degradation by Baf A1 do not have substantial effects on the expression of the mitochondrial markers. Presumptive NPC were treated with either 5 μ M FCCP, 20 μ M MG132, 100 nM Baf A1, or a combination, for 8 hours. Protein lysates (30 μ g) were probed for mitochondrial marker proteins TOM20, TIM23, and VDAC1. β -actin was used as loading control. Data represents one out of a total of three independent experiments.

Densitometry showed that TOM20, TIM23, and VDAC1 expression were not significantly affected by the different treatments in both control and PD presumptive NPC (Figure 5.8.5 B).

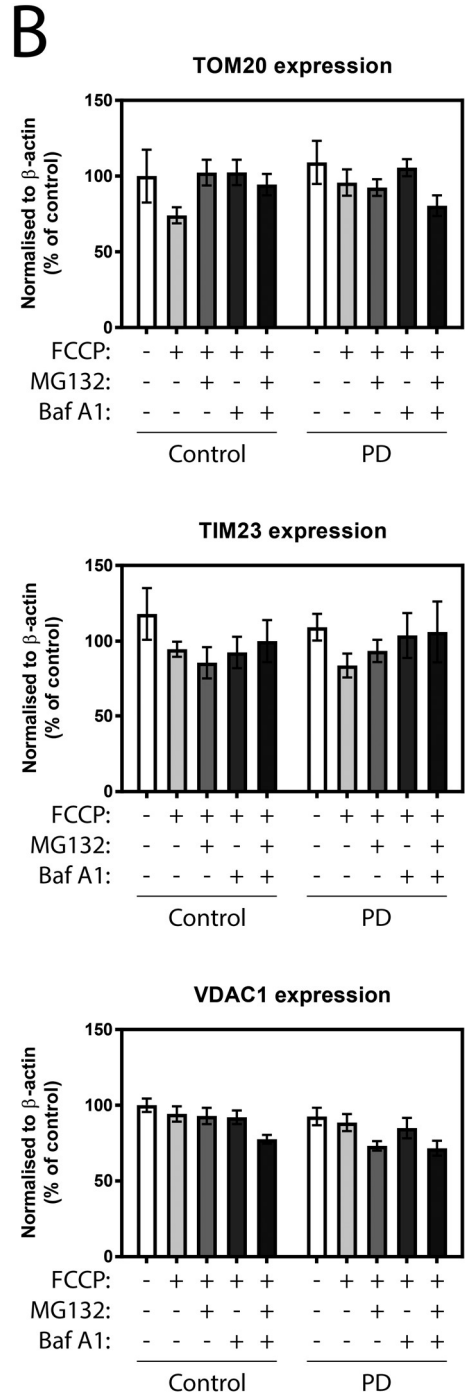


Figure 5.8.5 (B). Proteasomal or autophagic inhibition does not affect FCCP-induced changes in expression of mitochondrial markers. TOM20, TIM23, and VDAC1 densitometry normalised to corresponding β -actin levels. Densitometric analysis was pooled from three independent experiments and data is shown as percentage of control. Error bars = SEM, one-way ANOVA.

5.9 Preliminary analysis of FCCP-mediated degradation of mitochondrial markers in presumptive dopaminergic neurons

Control and PD presumptive NPC were differentiated into presumptive DA neurons and were treated with either FCCP or Baf A1 for 6 hours to examine their effects on autophagy and mitochondrial degradation. Preliminary data showed that Parkin nor PINK1 expression in control presumptive DA neurons was affected by 5 μ M FCCP treatment, suggesting mitophagy was not induced (Figure 5.9.1 A). Decreased LAMP1 and p62 expression, and LC3B lipidation, suggests FCCP activated autophagy. Baf A1 treatment (100 nM) did not lead to p62 and LC3B-II accumulation, which could be due to low protein expression based on β -actin expression levels.

FCCP treatment was cytotoxic to PD presumptive DA neurons and therefore resulted in low protein expression. Baf A1 treatment increased Parkin and PINK1 expression and no build-up of LC3B-II and p62 degradation, rather than accumulation, suggests autophagy was not inhibited. Note that control presumptive DA neurons have higher levels of cleaved PINK1 (lower band) compared to PD presumptive DA neurons.

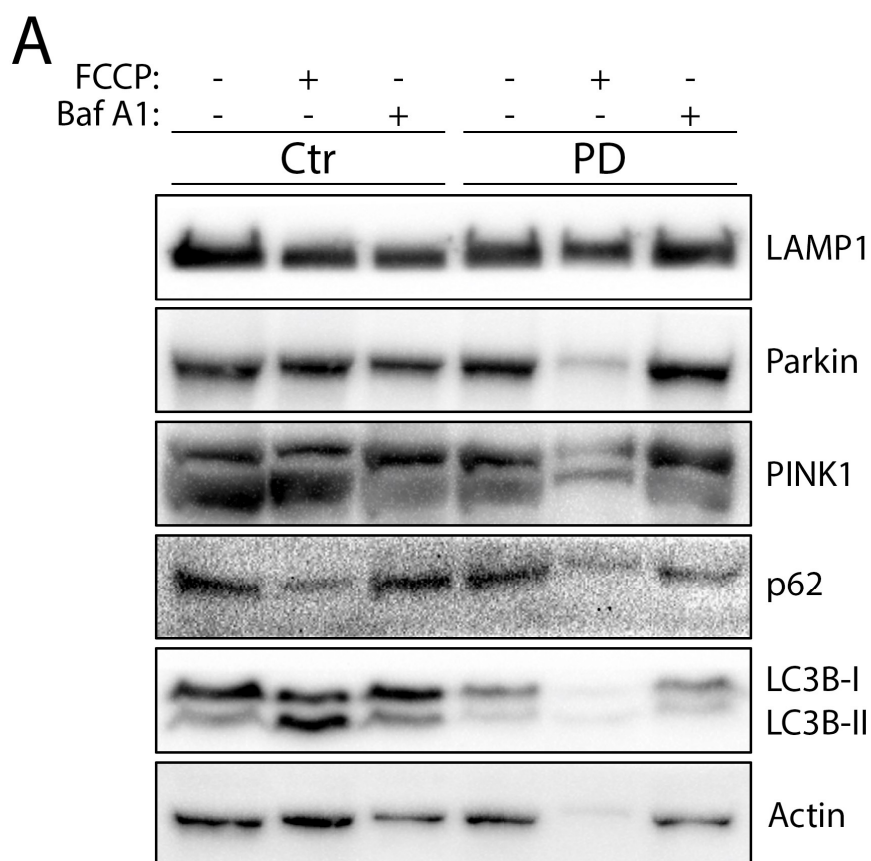


Figure 5.9.1 (A). *FCCP induces autophagy in control presumptive dopaminergic neurons.* FCCP treatment does not decrease Parkin or increase PINK1 expression and might therefore not induce mitophagy in control and PD presumptive DA neurons. Decreased p62 expression and increased LC3B-II accumulation shows that FCCP activates autophagy in control presumptive DA neurons. Baf A1 treatment might not inhibit autophagy in both control and PD presumptive DA neurons. Presumptive NPC were differentiated for 8 weeks to induce presumptive DA neuron formation. Presumptive DA neurons were treated with 5 μ M FCCP or 100 nM Baf A1 for 6 hours. Protein lysates (30 μ g) were probed for mitophagy marker proteins Parkin and PINK1, and autophagy marker proteins LAMP1, p62, and LC3B. β -actin was used as loading control. Data represents one experiment.

Densitometric analysis showed that Baf A1 treatment caused increased p62 expression and LC3B-II accumulation in control presumptive DA neurons, indicating it did inhibit autophagy, whereas PD presumptive DA neurons were unaffected by Baf A1 (Figure 5.9.1 B). FCCP-mediated LC3B-II accumulation in control presumptive DA neurons was similar to Baf A1-induced LC3B-II accumulation. PD presumptive DA

neurons had increased p62 and LC3B-II expression upon FCCP treatment, indicating autophagy could be inhibited in these cells.

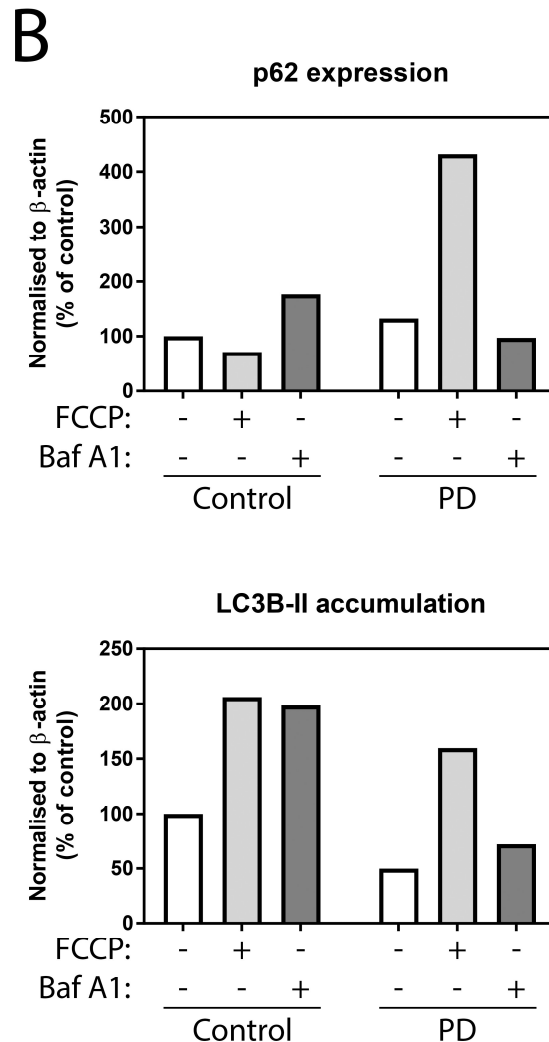


Figure 5.9.1 (B). *FCCP induces autophagy in control presumptive dopaminergic neurons.* p62 and LC3B-II densitometry normalised to corresponding β -actin levels. Data is shown as percentage of control and represents one experiment.

Despite the lack of Parkin degradation and PINK1 accumulation, mitophagy was induced in control presumptive DA neurons by FCCP treatment (Figure 5.9.2 A). TOM20, TIM23, and VDAC1 all showed FCCP-induced degradation, whereas Baf A1 treatment likely increased their expression when low β -actin levels are taken into account. The effects of FCCP on degradation of the mitochondrial markers in PD

presumptive DA neurons is not clear, but inhibition of autophagic cargo degradation by Baf A1 increased TIM23 expression.

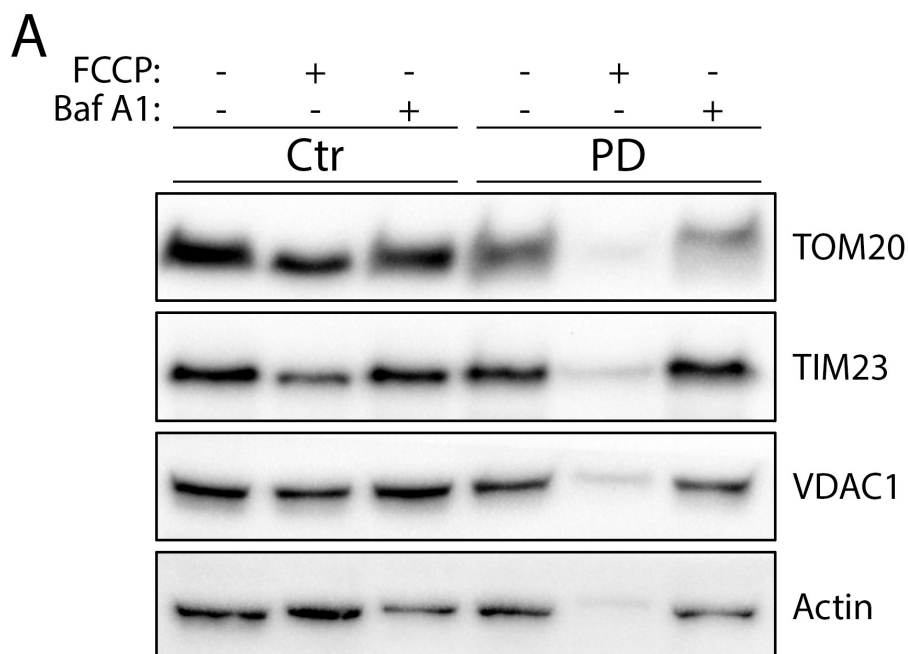


Figure 5.9.2 (A). Control presumptive dopaminergic neurons show FCCP-mediated degradation of mitochondrial markers. Control, and not PD, presumptive DA neurons show FCCP-mediated degradation of TOM20, TIM23, and VDAC1. Prevention of autophagic cargo degradation by Baf A1 blocks basal turnover of the mitochondrial markers. Presumptive NPC were differentiated for 8 weeks to induce presumptive DA neuron formation. Presumptive DA neurons were treated with 5 μ M FCCP or 100 nM Baf A1 for 6 hours. Protein lysates (30 μ g) were probed for mitochondrial markers TOM20, TIM23, and VDAC1. Same β -actin blot from Figure 5.9.1 A was used since these were the same extracts. Data represents one experiment.

FCCP-mediated degradation of TOM20, TIM23, and VDAC1 in control presumptive DA neurons was confirmed by densitometric analysis (Figure 5.9.2 B). Densitometry also showed that basal turnover of these proteins was blocked by Baf A1. On the other hand, PD presumptive DA neurons had increased TOM20, TIM23, and VDAC1 expression upon FCCP treatment. Baf A1 treatment did not induce accumulation of TOM20, but did accumulate TIM23 and VDAC1.

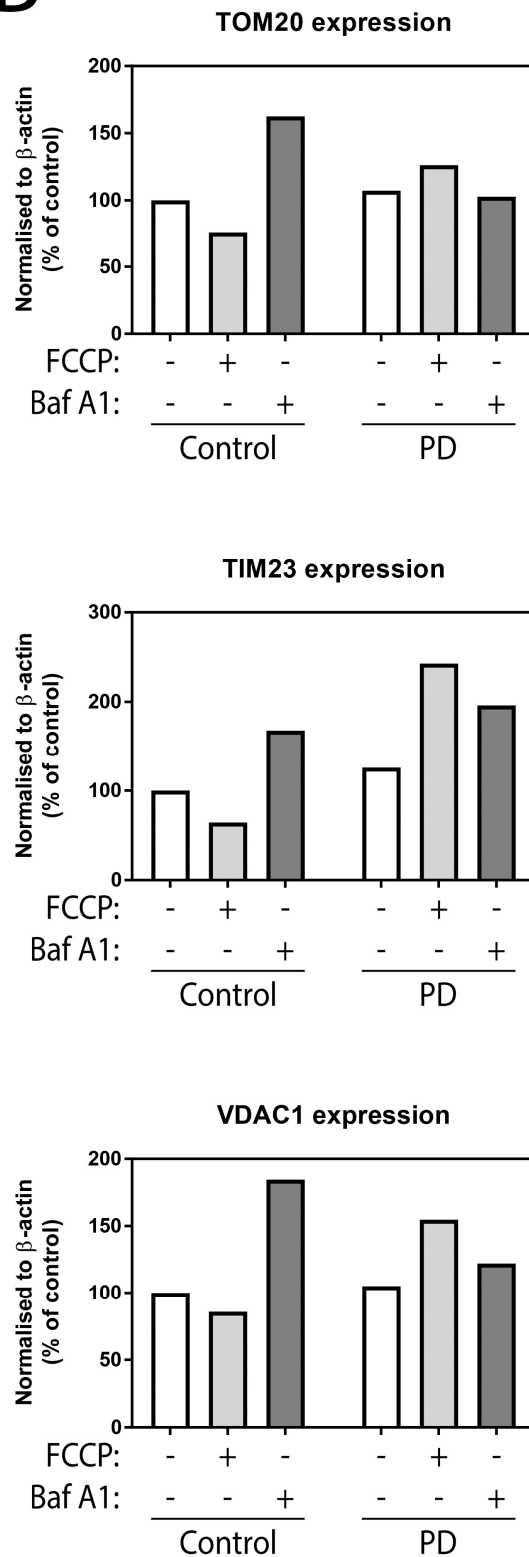
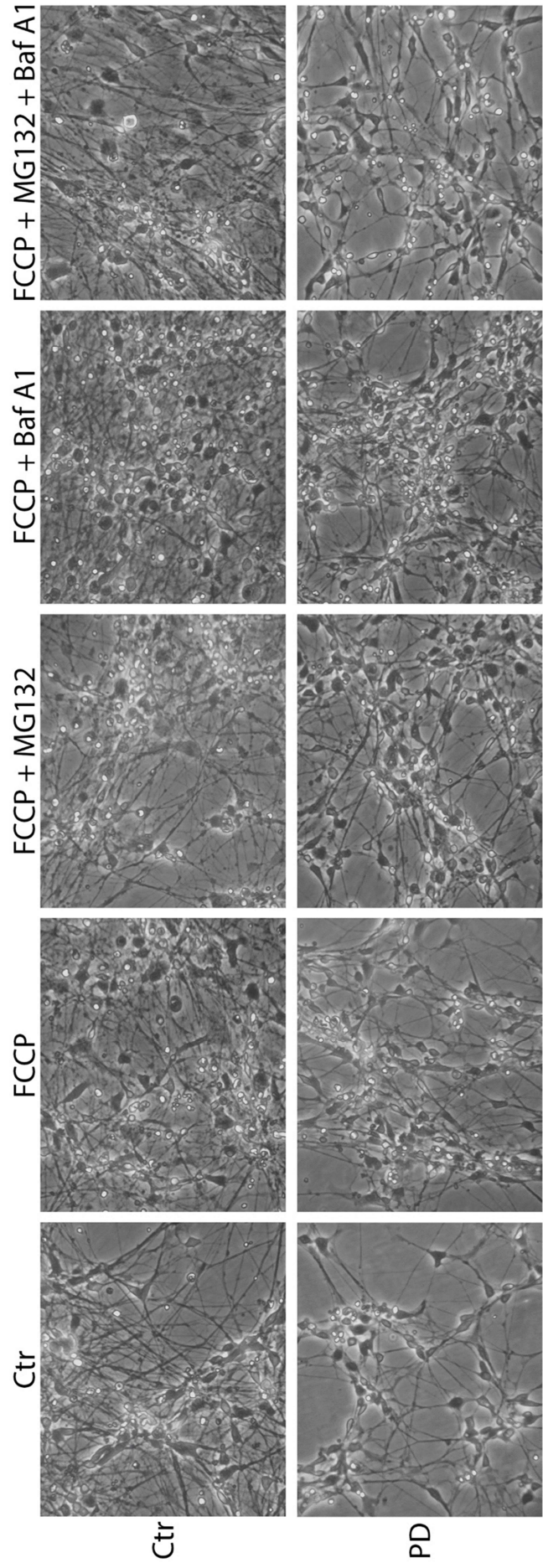
B

Figure 5.9.2 (B). Control presumptive dopaminergic neurons show FCCP-mediated degradation of mitochondrial markers. TOM20, TIM23, and VDAC1 densitometry normalised to corresponding β -actin levels. Data is shown as percentage of control and represents one experiment.

5.10 Preliminary analysis of proteasomal and autophagic inhibition shows partial rescue of FCCP-induced TOM20 and TIM23 degradation in PD presumptive dopaminergic neurons

To investigate if the proteasomal or autophagic pathway are involved in FCCP-mediated degradation of mitochondrial markers in control presumptive DA neurons and to determine whether inhibition affects accumulation of mitochondrial markers in PD presumptive DA neurons, control and PD presumptive DA neurons were treated with FCCP, MG123 and/or Baf A1 for 8 hours. PD presumptive DA neurons had a more organised looking neuronal network upon different treatments than control presumptive DA neurons (Figure 5.10.1). Treatments resulted in a small increase in cellular detachment of both control and PD presumptive DA neurons, however, most neurons looked unaffected.



Previous Page: Figure 5.10.1. *Autophagic or proteasomal inhibition upon FCCP treatment increases detachment of presumptive dopaminergic neurons.* Proteasomal inhibition by MG132 or blockade of the late phase of autophagy by Baf A1 leads to a small increase in cellular detachment of control (Ctr) and PD presumptive DA neurons. Presumptive NPC were differentiated for 5 weeks to induce presumptive DA neuron formation. Presumptive DA neurons were treated with a combination of 5 μ M FCCP, 20 μ M MG132, or 100 nM Baf A1, for 8 hours. Phase contrast images were taken using a Nikon TMS microscope, magnification = 10x. Data represents one experiment.

Preliminary results show that control presumptive DA neurons had higher basal LAMP1 expression, Parkin expression, and increased LC3B conversion compared to PD presumptive DA neurons (Figure 5.10.2 A). FCCP (5 μ M) caused Parkin degradation and PINK1 accumulation in control presumptive DA neurons. Degradation of LAMP1 and possible degradation of p62 together with LC3B lipidation indicates activation of autophagy. Co-treatment with 20 μ M MG132 prevented PINK1 accumulation, but did not affect Parkin degradation or activation of autophagy. Co-treatment of FCCP and 100 nM Baf A1 also prevented increased PINK1 expression, but did not inhibit autophagy since p62 and LC3B-II did not accumulate. Combined MG132 and Baf A1 treatment affected FCCP-mediated Parkin degradation and PINK accumulation, but no inhibitory effects on autophagy were observed.

In PD presumptive DA neurons, FCCP treatment led to increased Parkin expression, whereas PINK1 results are inconclusive. p62 expression and LC3B turnover differed between duplicates, making it difficult to observe the effects of FCCP on autophagy. Co-treatment with either MG132 or Baf A1 decreased FCCP-induced Parkin accumulation, but did not affect expression of other immunoblotted proteins. Combined treatment of FCCP, MG132, and Baf A1 led to Parkin and PINK1

degradation, but no changes were seen in either p62 or LC3B expression compared to control conditions. LAMP1 expression was unaffected by the different treatments.

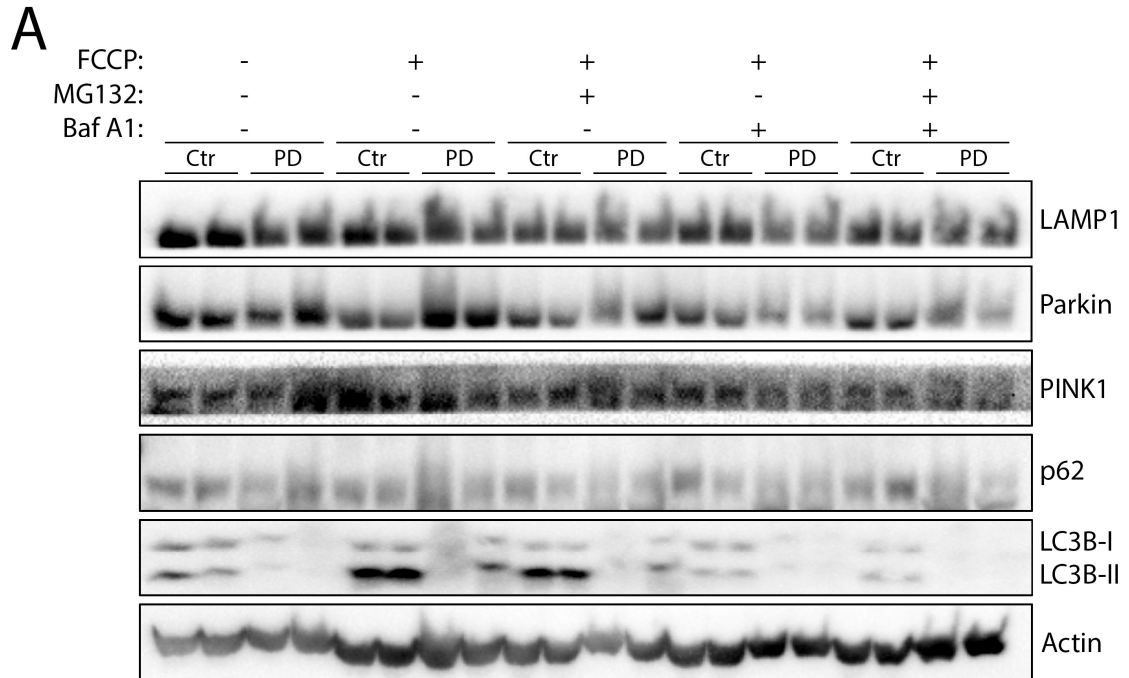


Figure 5.10.2 (A). Control and PD presumptive dopaminergic neurons respond differently to proteasomal or autophagic inhibition upon FCCCP treatment. Differences in protein expression of the immunoblotted proteins upon co-treatment of FCCCP with either MG132, Baf A1, or both, are found between control and PD presumptive DA neurons. Presumptive NPC were differentiated for 5 weeks to induce presumptive DA neuron formation. Presumptive DA neurons were treated with a combination of 5 μ M FCCCP, 20 μ M MG132, or 100 nM Baf A1, for 8 hours. Protein lysates (20 μ g) were probed for mitophagy marker proteins Parkin and PINK1, and autophagy marker proteins LAMP1, p62, and LC3B. β -actin was used as loading control. Data represents one experiment.

According to densitometric analysis, Parkin was degraded upon FCCCP treatment in control presumptive DA neurons and this decrease was not affected by co-treatment with either MG132 and/or Baf A1 (Figure 5.10.2 B). In PD presumptive DA neurons, on the other hand, Parkin expression was not affected by FCCCP or co-treatment of FCCCP and MG132, while it was decreased upon co-treatment of either FCCCP and Baf A1 or FCCCP, Baf A1, and MG132. Contrary to PD presumptive DA neurons, FCCCP-

mediated p62 degradation was not affected by co-treatment with MG132 and/or Baf A1 in control presumptive DA neurons. The largest decrease in p62 expression in PD presumptive DA neurons was upon combined treatment of FCCP, MG132, and Baf A1, showing that proteasomal inhibition and prevention of autophagic cargo degradation did not induce p62 accumulation. LC3B-II accumulation was increased upon FCCP treatment and co-treatment of FCCP and MG132 in both control and PD presumptive DA neurons. Co-treatment of FCCP and Baf A1 resulted in decreased, rather than increased, LC3B-II accumulation. Simultaneous treatment with MG132 further increased LC3B-II degradation.

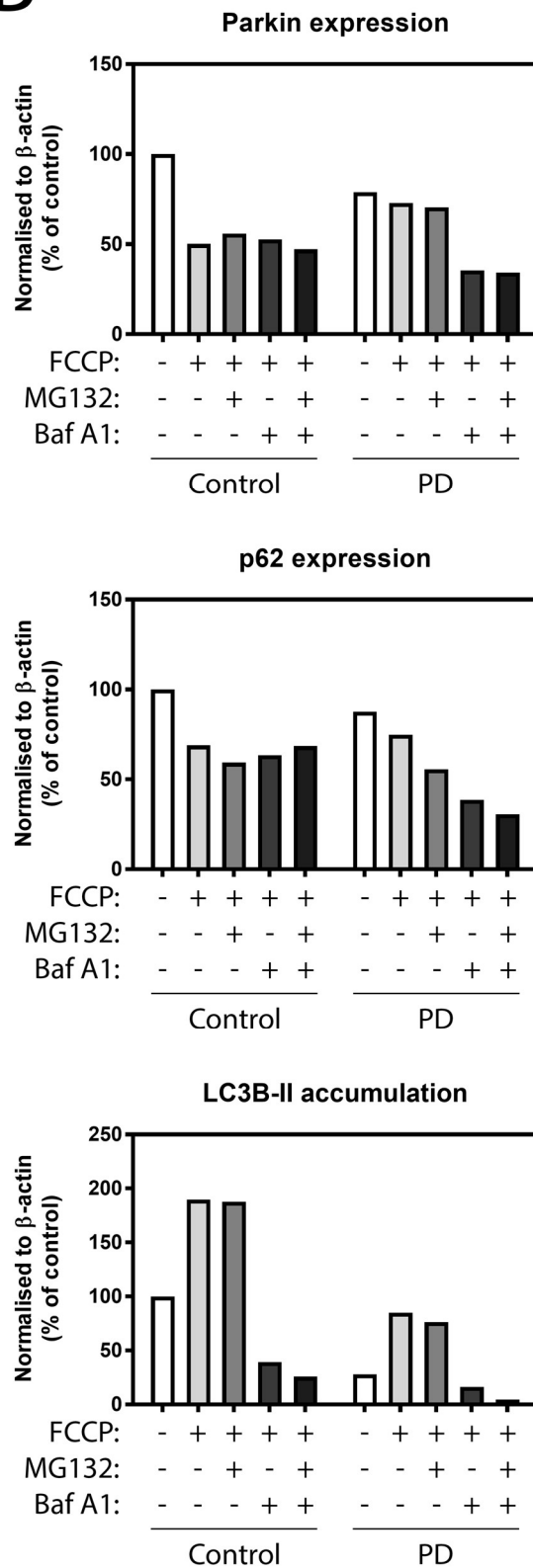
B

Figure 5.10.2 (B). Control and PD presumptive dopaminergic neurons respond differently to proteasomal or autophagic inhibition upon FCCP treatment. Parkin, p62, and LC3B-II densitometry normalised to corresponding β -actin levels. Data is shown as percentage of control and represents one experiment.

In control presumptive DA neurons, FCCP treatment potentially induced TOM20 accumulation, whereas TOM20 expression was decreased upon combined treatment of FCCP with either MG132, Baf A1, or both (Figure 5.10.3 A). TIM23 expression was decreased upon FCCP and Baf A1 treatment, regardless of the addition of MG132. The effects of the different treatments on TOM20 and TIM23 expression in PD presumptive DA neurons is unknown since no protein bands were observed on the immunoblot.

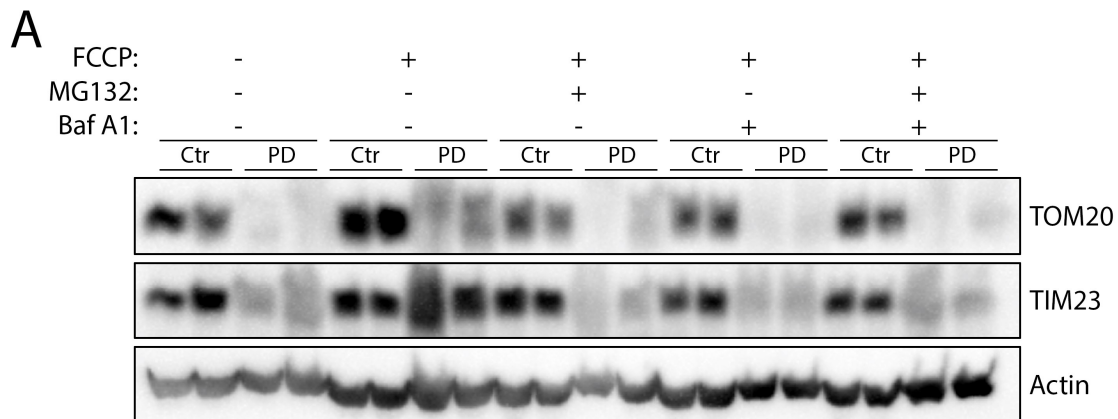


Figure 5.10.3 (A). *FCCP induces TIM23, but not TOM20, degradation in control presumptive dopaminergic neurons.* TIM23 is degraded upon FCCP treatment in control presumptive DA neurons and proteasomal and/or late autophagy inhibition leads to reduced TOM20 and TIM23 expression. The effects of the different treatments on TOM20 and TIM23 expression in PD presumptive DA neurons is unknown. Presumptive NPC were differentiated for 5 weeks to induce presumptive DA neuron formation. Presumptive DA neurons were treated with a combination of 5 μ M FCCP, 20 μ M MG132, or 100 nM Baf A1, for 8 hours. Protein lysates (20 μ g) were probed for mitochondrial marker proteins TOM20 and TIM23. Same β -actin blot from Figure 5.10.2 A was used since these were the same extracts. Data represents one experiment.

Densitometry showed that when protein expression was normalised to corresponding β -actin levels, TOM20 was degraded in control presumptive DA neurons upon all treatments except FCCP (Figure 5.10.3 B). FCCP led to TIM23 degradation,

regardless of inhibition of autophagic cargo degradation by Baf A1. MG132 reduced FCCP-induced TIM23 degradation, but this was abolished by Baf A1. PD presumptive DA results were not analysed by densitometry since no protein bands were observed on the immunoblot (see Figure 5.10.3 A).

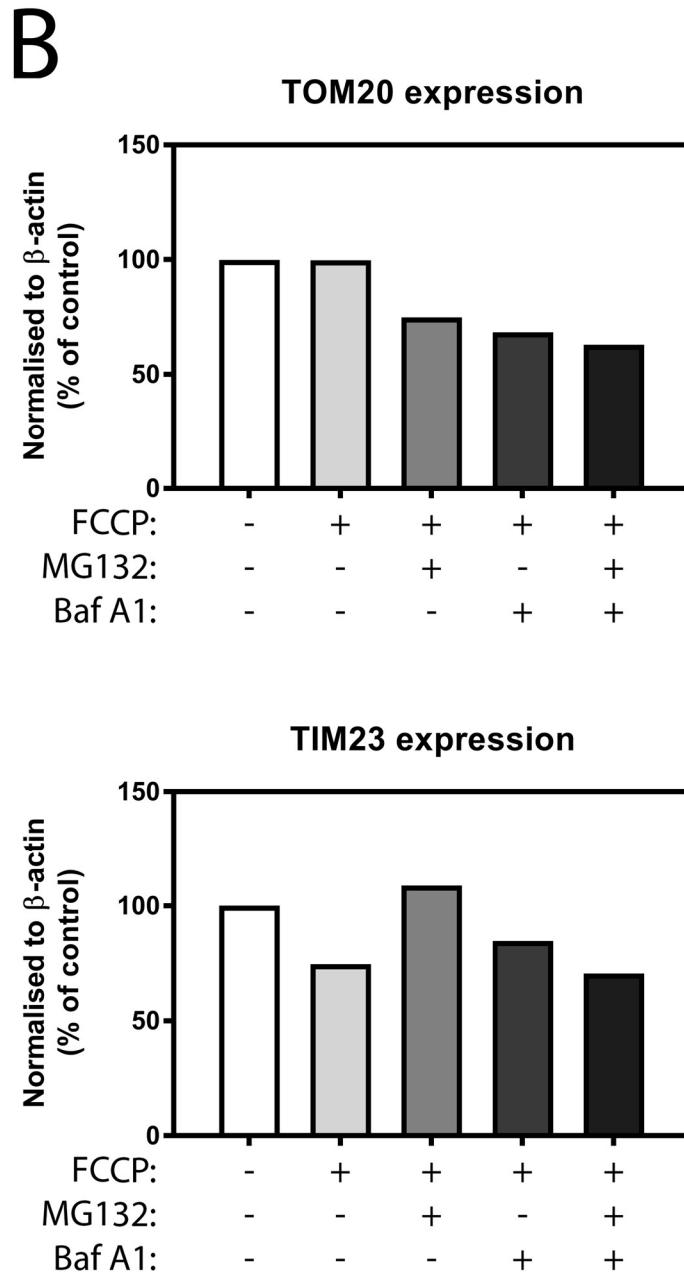


Figure 5.10.3 (B). FCCP induces TIM23, but not TOM20, degradation in control presumptive dopaminergic neurons. TOM20 and TIM23 densitometry of control presumptive DA neurons normalised to corresponding β -actin levels. Data is shown as percentage of control and represents one experiment.

5.11 Discussion

Little research has been done so far regarding mitophagy and autophagy in mESC (Guan et al., 2013). Results described herein show that autophagy can be successfully induced or inhibited with commonly used reagents in undifferentiated mESC (Figure 5.1.1 A & B), which is in accordance with a study using human ESC (Tra et al., 2011). Besides being important for turnover of cellular proteins, autophagy in ESC is likely important for self-renewal, pluripotency, differentiation, and quiescence of ESC (Phadwal et al., 2013).

A time course showed that autophagy was inhibited upon 4 hours of FCCP treatment, but that undifferentiated mESC were able to overcome this blockade at later time points (Figure 5.2.1 A & B). p62 expression increased upon FCCP treatment (Figure 5.1.1 A & B), raising the question if FCCP induced *de novo* p62 synthesis as seen in SH-SY5Y cells (see Chapter 3). Mitochondrial depolarisation led to increased PINK1 expression and possibly reduced Parkin expression, however, Parkin expression was difficult to detect (Figure 5.2.1 A, Figure 5.4.1 A). It is possible that mESC have low endogenous Parkin expression or that the used antibody was not sensitive enough, which resulted in difficulties in its detection.

Increased PINK1 and potentially decreased Parkin expression upon FCCP treatment suggests mitophagy was induced. Nevertheless, FCCP treatment did not lead to degradation of the mitochondrial marker VDAC1, which could indicate that mitochondria were not broken down or that mitophagy was not activated (Figure 5.4.1 A & B). Mitochondrial VDAC1 is a target of Parkin-dependent ubiquitination and is normally degraded when mitophagy is active (Geisler et al., 2010, Sun et al., 2012). A

potential explanation could be that low endogenous Parkin expression in undifferentiated mESC might not be sufficient to induce VDAC1 degradation. However, VDAC1 could also not be a good marker for monitoring mitochondrial degradation as seen in SH-SY5Y cells (see Chapter 3).

It is not clear if inhibition of ULK1, which is important for initiation of autophagy, led to an autophagic blockade in undifferentiated mESC. Similar to SH-SY5Y cells, ULK1 inhibition led to decreased ULK1, PIK3C3, and p62 expression (Figure 5.1.1 A, Figure 5.4.1 A). LC3B results were inconclusive since LC3B turnover was either unaffected or increased (Figure 5.1.1 A, Figure 5.3.1 A & B). PINK1 expression was increased, whereas Parkin was only decreased at late time points, suggesting ULK1 inhibition mimicked mitochondrial damage and led to activation of mitophagy, but only after a long incubation period. Basal turnover of VDAC1 was affected by ULK1 inhibition and its expression was not affected by simultaneous FCCP treatment. The involvement of ULK1 has been investigated in mitophagy, which suggests that ULK1 is required for successful execution of mitophagy, but not in basal turnover of mitochondria. Studies done in MEF showed that structures containing ULK1 were recruited to depolarised mitochondria and that they were required for recruitment of downstream ATG proteins to carry out mitophagy and that *ULK1^{-/-}* MEF did not recruit Parkin to depolarised mitochondria, leading to defects in mitochondrial clearance upon CCCP treatment (Joo et al., 2011, Itakura et al., 2012). These studies indicate that ULK1 and autophagy are necessary for removal of damaged mitochondria and might therefore also be essential for basal turnover of mitochondria.

It was difficult to observe if FCCP induced mitophagy in undifferentiated mESC, however, it did show the importance of ULK1 for basal turnover of VDAC1. mESC only have few mitochondria that are poorly developed, making it difficult to monitor mitochondrial processes, which could explain difficulties in monitoring mitophagy (Lonergan et al., 2007). Another potential explanation could be the observation that PINK1 levels decreased in response to low ATP levels, leading to inactivation of Parkin-mediated mitophagy (Lee et al., 2015). Differentiation of ESC would have led to increased mitochondrial numbers, giving rise to a mitochondrial pool that is large enough to study mitophagy, however, mESC were not differentiated because of inconsistent results and culturing difficulties (Cho et al., 2006, Lonergan et al., 2007). An explanation for these contradictory results could be spontaneous differentiation of the mESC, which was difficult to control for. As a result, human inducible pluripotent stem cells (hiPSC) obtained from normal and PD diseased patients were employed instead.

Similarly to mESC, mitophagy and autophagy have not been extensively studied in NPC and differentiated neurons. Obtained data showed that mitochondria were fragmented upon FCCP treatment (Figure 5.6.5), but that FCCP did not lead to a clear reduction of Parkin (Figure 5.6.3 A & B). Nevertheless, FCCP led to a small reduction in the expression levels of the mitochondrial markers TOM20, TIM23, and VDAC1 in presumptive NPC (Figure 5.8.5 A & B). Preliminary results showed that control presumptive NPC differentiated into presumptive DA neurons might degrade mitochondrial markers upon FCCP treatment, but this is not the case in PD presumptive DA neurons (Figure 5.9.2 A & B, Figure 5.10.3 A & B). Literature indicates that the mitochondrial poison valinomycin was not successful in induction of

detectable mitophagy in hiPS-derived neurons, which could not be rescued by overexpression of Parkin (Rakovic et al., 2013). It is possible that PINK1/Parkin mitophagy is not carried out in hiPSC, but defects in both PINK1 and Parkin in hiPSC have been associated with altered mitochondrial morphology, abnormalities in bioenergetics, increased oxidative stress, and no mitochondrial DNA reduction upon mitochondrial depolarisation, making it more likely that FCCP and valinomycin were not successful inducers of mitophagy (Exner et al., 2007b, Grünewald et al., 2009, Seibler et al., 2011, Imaizumi et al., 2012).

Even though FCCP was not a potent inducer of mitophagy, it did activate autophagy in presumptive NPC (Figure 5.6.3 A & B), which could be successfully inhibited by Baf A1 (Figure 5.7.2). Indeed, it was shown that autophagosomes accumulated in NPC upon Baf A1 treatment (Walls et al., 2010). Inhibition of the late phase of autophagy showed that it is involved in the basal turnover of the mitochondrial markers TOM20 and VDAC1 in control presumptive NPC and TOM20 in PD presumptive NPC (Figure 5.7.3 A & B). In presumptive DA neurons, on the other hand, autophagy was activated by FCCP in control presumptive DA neurons, but was potentially inhibited in PD presumptive DA neurons (Figure 5.9.1 A & B). Inhibition of autophagy led to accumulation of TOM20, TIM23, and VDAC1 in control presumptive DA neurons and accumulation of TIM23 and VDAC1 in PD presumptive DA neurons, indicating autophagy is involved in this process in presumptive DA neurons too (Figure 5.9.2 A & B). Degradation of the mitochondrial markers was observed upon prevention of autophagic cargo degradation by Baf A1, which was exacerbated by proteasomal inhibition by MG132 (Figure 5.10.3 A & B). A possible

explanation for this observation could be that the inhibitors induced cytotoxicity, which could lead to the release of intracellular contents (Peter et al., 2010).

In short, the hiPSC data showed that differences in response to different treatments were observed between control and PD hiPSC. Mitochondria in PD presumptive NPC were fragmented and FCCP cytotoxicity was more pronounced in PD presumptive DA neurons. Moreover, mitochondrial markers that were degraded in control presumptive DA neurons were not degraded in PD presumptive DA neurons upon FCCP treatment. This suggests that mitochondria were already affected in PD hiPSC and that removal of damaged mitochondria was impaired.

Results were highly variable, which is an inherent difficulty with using the hiPSC system. This was most clear in presumptive NPC treated with a combination of FCCP, Baf A1, or MG132. LC3B-II expression was not detected on some immunoblots, while it was on others (Figure 5.8.2, Figure 5.8.3). This was not due to differences in culture age, but could be caused by differences that exist between individual hiPSC clones. It was reported that hiPSC clones generated from the same individual in the same reprogramming experiment had dissimilar characteristics influencing the cells performances for which a solution has not been found yet (Hu et al., 2010).

Use of hiPSC lines comes with several caveats that should be taken into account. The two hiPSC lines used in this study were generated from two individuals, meaning that generated results cannot be compared with one another since cell lines have a different genetic background that might be accountable for observed differences. This could possibly be minimised by the use of healthy age-matched individuals, however, these

individuals could potentially develop PD or another neurodegenerative disease later on in life that could lead to misleading results (Zhao et al., 2014). A better method would be to correct PD gene mutations with zinc finger nucleases (ZFN), transcription activator-like effector nucleases (TALEN), or clustered regularly interspaced short palindromic repeats associated nuclease Cas9 (CRISPR-Cas9), which has already been used successfully to correct PD-associated gene mutations in hiPSC (Gaj et al., 2013, Zhao et al., 2014). However, this method also has its drawbacks since off-target effects were reported and lengthy cell expansion could lead to instability of hiPSC (Gupta et al., 2011, Laurent et al., 2011, Fu et al., 2013). Furthermore, it can only be used when mutations causing the disease are known. Thus, taking the above into consideration, it would have been better to correct the PD mutation in order to use the same cells for control, but even though cells used in this study were obtained from two individuals, significant discrepancies in obtained results could suggest that the disease could be liable for detected differences.

The PD hiPSC line used for this study contained a triplication of the α -synuclein gene (*SNCA*) that is known to cause early-onset PD (Singleton et al., 2003). hiPSC were not characterised due to lack of time, and therefore NPC and DA neurons used in this study are presumptive, but research has shown that PD NPC carrying the *SNCA* triplication presented with normal cellular and mitochondrial morphology (Flierl et al., 2014). Nevertheless, altered mitochondrial membrane potential, reduced ATP levels, altered mitochondrial bioenergetics, and increased ROS production were observed, which could be rescued by knockdown of α -synuclein. Indeed, α -synuclein has been found to influence mitochondrial performance on several occasions (Nakamura, 2013). Furthermore, NPC displayed an increased amount of aggregate

formation, delayed protein import into mitochondria and peroxisomes, increased levels of cellular stress, and changes in growth and viability upon starvation or mitochondrial damage of NPC. Differentiation of these NPC into DA neurons led to accumulation of double the amount of α -synuclein, secretion of more α -synuclein, and increased susceptibility to oxidative stress and oxidative stress induced cell death (Byers et al., 2011, Devine et al., 2011). A more recent study illustrated that hiPSC with *SNCA* triplication showed impaired neuronal differentiation and maturation, reduced neurite outgrowth, and impaired electrophysiological properties, which was not reported in previously described papers (Oliveira et al., 2015). A possible explanation for observed differences could be use of different protocols and growth factors.

The protocol used for differentiation of presumptive NPC into presumptive dopaminergic neurons should give rise to neurons expressing neuron specific class III β -tubulin (Tuj-1), tyrosine hydroxylase (TH), which is the rate-limiting enzyme in synthesis of DA, and Nuclear Receptor Related 1 (NURR1) that is associated with DA neuron function and expression of postmitotic DA neuron markers (Kriks et al., 2011, Decressac et al., 2013). These studies also showed that generated cultures only had few gamma-aminobutyric acid (GABA)- and serotonin-positive neurons and that DA neurons were capable of long-term in vitro survival. Furthermore, these neurons showed extensive fibre outgrowth, synthesised DA and its metabolites 3, 4-dihydroxy-phenylacetic acid (DOPAC) and homovanillic acid (HVA), and had robust expression of mature neuronal markers including dopamine transporter (DAT) and synapsin.

Chapter 6

General discussion

6.0 General discussion

6.0.1 FCCP activates autophagy and induces clearance of mitochondrial markers in SH-SY5Y cells

Mitophagy describes the selective removal of superfluous and damaged mitochondria and is a specialised form of autophagy (Narendra et al., 2010b). PINK1 and Parkin are the main proteins involved in mitophagy that detect and clear damaged mitochondria as follows. The serine/threonine kinase PINK1 is responsible for sensing damaged mitochondria and is under normal conditions imported into all mitochondria by the TOM complex on the MOM and the TIM complex on the MIM (Valente et al., 2004, Neupert and Herrmann, 2007, Schmidt et al., 2010, Becker et al., 2012). There PINK1 is cleaved by MPP and PARL, generating a 52-kDa form of PINK1 that can exit mitochondria (Jin et al., 2010, Meissner et al., 2011). Once cleaved PINK1 is released into the cytosol, it is rapidly degraded by the proteasome and thus PINK1 is maintained at very low levels (Yamano and Youle, 2013, Fedorowicz et al., 2014). Loss of mitochondrial membrane potential leads to PINK1 accumulation on the MOM since it cannot be processed by MPP or PARL anymore, inhibiting PINK1 degradation (Jin et al., 2010, Narendra et al., 2010b). From there, PINK1 selectively recruits the E3-ligase Parkin and activates it by phosphorylation of Parkin and Ub on Ser65 (Kim et al., 2008, Kondapalli et al., 2012, Shiba-Fukushima et al., 2012, Iguchi et al., 2013, Kane et al., 2014, Kazlauskaitė et al., 2014, Koyano et al., 2014, Ham et al., 2016, Zhuang et al., 2016, Aguirre et al., 2017). Parkin mainly ubiquitinates MOM proteins to cause their degradation, which is likely facilitated by autophagy (Sarraf et al., 2013).

Firstly, mitophagy was characterised in SH-SY5Y cells. Damaging mitochondria with

the mitochondrial uncoupler FCCP led to increased PINK1 and decreased Parkin expression. Degradation of the mitochondrial markers TOM20, TIM23, and VDAC1 indicated mitophagy was successfully induced. Moreover, visualisation of the mitochondrial network showed that FCCP caused mitochondrial fragmentation and increased LC3B puncta formation, resembling autophagosomes, which was reported previously (Legros et al., 2002, Cereghetti et al., 2010, Geisler et al., 2010, Cheng et al., 2016).

Formation of LC3B puncta upon FCCP-induced mitochondrial damage suggests activation of autophagy. Indeed, FCCP was a potent inducer of autophagy in SH-SY5Y cells, which can be observed in other cell types too (Sandoval et al., 2008, Ma et al., 2011). FCCP inhibited mTORC1 signalling, which is the master regulator of autophagy (Russell et al., 2014). Under nutrient-rich conditions, mTORC1 signalling is stimulated by growth factors, leading to phosphorylation of S6K1, which is responsible for protein synthesis, thus promoting cell growth (Laplanche and Sabatini, 2009). ERK1/2 regulates tuberous sclerosis complex (TSC) 2, which in turn negatively regulates mTORC1 signalling (Ma et al., 2005). ERK1/2 increases phosphorylation of TSC2, leading to its inactivation and subsequent activation of mTORC1. Thus, decreased S6K1 and increased ERK1/2 phosphorylation both implicate inhibition of mTORC1 signalling and activation of canonical autophagy, which was shown to take place in SH-SY5Y cells upon FCCP treatment. Moreover, FCCP treatment led to increased conversion of LC3B-I to LC3B-II and increased formation of LC3B puncta. Cytosolic LC3B is targeted to the isolation membrane where it is processed into LC3B-I and subsequently conjugated to PE to form the membrane bound LC3B-II, indicating that increased LC3B-II levels represent

increased formation of autophagosomes and thus activation of autophagy (Kabeya et al., 2000, Mizushima et al., 2001, Fujita et al., 2008b). The final confirmation of autophagy activation upon FCCP treatment was given by examining the ubiquitin binding protein p62, which binds to ubiquitinated proteins destined for degradation and delivers them to the autophagosome by direct binding to LC3B, thereby being degraded itself as well (Pankiv et al., 2007). FCCP treatment led to increased, as opposed to decreased, expression of p62, however, inhibition of protein synthesis by cycloheximide (CHX) showed that FCCP caused *de novo* p62 synthesis, suggesting that more p62 could be needed to keep up with the increasing demand of removal of ubiquitinated proteins, which was in line with a recently published study (Ivankovic et al., 2016).

6.0.2 Removal of FCCP-damaged mitochondrial markers might not depend on canonical autophagy in SH-SY5Y cells

After establishing autophagy was activated upon FCCP treatment, involvement of different proteins deemed necessary for successful execution of autophagy in FCCP-mediated mitochondrial removal was investigated. ULK1 is the first protein to be activated upon mTORC1 inhibition and its activation is important for regulation of the downstream autophagy initiation machinery (Russell et al., 2014). In SH-SY5Y cells, ULK1 inhibition led to mitochondrial fragmentation, PINK1 accumulation, and Parkin degradation, suggesting mitophagy was induced. It has to be noted that observed effects of ULK1 inhibition on mitophagy and mitochondria could be due to side effects of the used inhibitor and not because of ULK1 inhibition self, since effects of the inhibitor were not fully characterised and off-target effects might be observed, including inhibition of cell cycle-regulating kinases, receptor and non-receptor

tyrosine kinases (unpublished results Murray lab, Appendix III).

When examining the effects of ULK1 inhibition on FCCP-induced mitophagy, onset of mitophagy was not affected, however, VDAC1 was accumulated. Unfortunately, TOM20 and TIM23 expression was not investigated. VDAC1 did not always show degradation upon FCCP treatment and is likely recycled, indicating that it does not give an appropriate view of mitochondrial degradation. Even though involvement of ULK1 in mitochondrial clearance has been implicated in mitophagy (Egan et al., 2011, Joo et al., 2011, Itakura et al., 2012), other studies showed non-canonical autophagy could have been activated (Kundu et al., 2008, Chen et al., 2013) and that neither ULK1 nor its homologue ULK2 were required for Parkin-mediated mitochondrial clearance in MEF, suggesting a similar mechanism could be present in SH-SY5Y cells (Hammerling et al., 2017).

Of note, when investigating the effects of ULK1 inhibition on FCCP-induced mitophagy in SH-SY5Y cells, decreased PIK3C3 expression was observed, which could indicate disruption of the PIK3C3 complex. The PIK3C3 complex, consisting of Beclin1, hVps15, UVRAG, and ATG14L, lies downstream of the ULK1 complex and is responsible for autophagosome formation (Kim et al., 2013, Russell et al., 2013, Russell et al., 2014). Immunoprecipitation pointed out that ULK1 inhibition led to Beclin1 and PIK3C3 degradation and that increased Ser30 phosphorylated Beclin1 levels were not associated with the PIK3C3 complex, suggesting a pool of Ser30 phosphorylated Beclin1 might be involved in other cellular processes.

The observation that ULK1 inhibition increased Ser30 phosphorylated Beclin1 levels was contradictory to previous results obtained in the Murray lab showing that ULK1 phosphorylated Beclin1 at Ser30 and that ULK1 inhibition therefore decreased Ser30 phosphorylated Beclin1 levels, suggesting that this process could be cell type specific. Recently, phosphoglycerate kinase 1 (PGK1) was shown to mediate Beclin1 Ser30 phosphorylation upon glutamine deprivation- and hypoxia-induced autophagy, however, it is not known if this happens during mitophagy, and FCCP-induced mitophagy in SH-SY5Y cells, as well (Qian et al., 2017).

The effects of PIK3C3 inhibition on FCCP-induced mitochondrial degradation was investigated too. Two specific PIK3C3 inhibitors were utilised and successfully inhibited autophagy in SH-SY5Y cells, however, basal or FCCP-mediated turnover of mitochondrial markers TOM20 and TIM23 were not affected, suggesting non-canonical autophagy could be involved or that proteasomal degradation of these markers was increased. Combined inhibition of PIK3C3 and the proteasome showed increased accumulation of the mitochondrial markers, suggesting the proteasome plays an important role in mitochondrial degradation, even though induction of autophagy and especially increase in LC3B puncta upon FCCP treatment suggest autophagy plays a considerable part in successful implementation of mitophagy.

6.0.3 The proteasome is involved in FCCP-induced degradation of mitochondrial markers in SH-SY5Y cells

Lastly, effects of proteasomal inhibition on FCCP-induced mitochondrial degradation in SH-SY5Y cells was investigated. Proteasomal inhibition prevented Parkin degradation and inhibited FCCP-induced mitophagy as observed by TOM20, TIM23,

and VDAC1 accumulation, indicating the ubiquitin-proteasome system (UPS) plays an important role in mitophagy, which was confirmed by other studies (Chan et al., 2011, Yoshii et al., 2011). Research has shown that Parkin is able to induce both K48-linked and K63-linked polyubiquitination on mitochondria upon CCCP treatment (Chan et al., 2011, Narendra et al., 2014), with K48-linked polyubiquitination being responsible for UPS activation (Ciechanover and Brundin, 2003), and K63-linked polyubiquitination being responsible for triggering autophagy by recruitment of Ub binding factors (Ding et al., 2010, Geisler et al., 2010, Lee et al., 2010), indicating both autophagy and the UPS are activated upon mitochondrial damage, with the UPS being more important for degradation of the mitochondrial markers in SH-SY5Y cells. Interplay between UPS and autophagy was further confirmed by a recent study showing that fragmented and dysfunctional mitochondria accumulated upon continued proteasomal dysfunction, leading to autophagy induction that was ultimately impaired upon prolonged proteasome dysfunction (Ugun-Klusek et al., 2017).

The majority of research as described herein was carried out with SH-SY5Y cells, but mESC and hiPSC were utilised as well. The obtained mESC results will not be taken into account since it was difficult to observe if FCCP induced mitophagy and since mESC did not represent a neuronal population because they were not differentiated as a result of inconsistent results and culturing difficulties.

6.0.4 Control and PD hiPSC respond differently to FCCP treatment

hiPSC generated from a healthy and PD affected individual were first differentiated into presumptive NPC, which represent a neuronal precursor cell line that can develop into subtype-specific neuronal identities (Li et al., 2011). Mitochondria did fragment

upon FCCP treatment, but there was no clear reduction of Parkin. Nevertheless, a small reduction in the expression levels of the mitochondrial markers was observed upon FCCP treatment. FCCP activated autophagy in presumptive NPC too as seen by increased lipidation of LC3B-I to LC3B-II and p62 degradation. Inhibition of autophagy with Baf A1, a potent inhibitor of the late phase of autophagy by inhibiting fusion between autophagosomes and lysosomes, thereby preventing maturation of autophagic vacuoles (Yamamoto et al., 1998), led to TOM20 and VDAC1 accumulation in control presumptive NPC and TOM20 accumulation in PD presumptive NPC, indicating autophagy is involved in the basal turnover of these mitochondrial markers.

Differentiation of presumptive NPC into presumptive DA neurons, the main affected cell type in PD patients, showed similar results as obtained with presumptive NPC. FCCP treatment induced autophagy and degradation of mitochondrial markers in control presumptive DA neurons, however, it did potentially inhibit autophagy in PD presumptive DA neurons, in which no mitochondrial marker degradation was observed. Baf A1 treatment led to accumulation of mitochondrial markers in both control and PD derived presumptive DA neurons too. Mitochondria were already fragmented in PD presumptive NPC and FCCP cytotoxicity was more pronounced in PD presumptive DA neurons, suggesting mitochondria were intrinsically damaged. Degradation of the mitochondrial markers was observed upon inhibition of autophagy, which was exacerbated by proteasomal inhibition. A possible explanation for this observation could be that the used inhibitors induced cytotoxicity that could lead to the release of intracellular contents (Peter et al., 2010).

Inability to induce mitophagy in hiPSC-derived neurons was also reported in literature. The mitochondrial poison valinomycin did not induce detectable mitophagy in hiPSC-derived neurons, which led the authors to speculate that PINK1/Parkin mediated mitophagy is not carried out in hiPSC (Rakovic et al., 2013). A hypothesis why neurons might not show PINK1/Parkin-mediated mitophagy or why they do not show any mitochondrial loss upon CCCP/FCCP treatment is the fact that these cells rely heavily on OXPHOS for energy production, whereas cancerous cells, in which most PINK1/Parkin-mediated mitophagy studies have been carried out, rely on glycolysis and could potentially tolerate substantial loss of mitochondria (Bolaños, 2016, Whitworth and Pallanck, 2017). This hypothesis was confirmed by a study showing that PINK1/Parkin-mediated mitophagy was greatly inhibited upon loss of mitochondrial membrane potential in cells forced to rely on OXPHOS (MacVicar and Lane, 2014). This suggests that SH-SY5Y cells could be highly glycolytic since PINK1/Parkin-mediated mitophagy can be induced and loss of mitochondrial proteins is observed. It is not known if SH-SY5Y cells used for this thesis were glycolytic or not, however, research indicates that SH-SY5Y cells rely on glycolysis (Xun et al., 2012).

6.0.5 Caveats of the study

Regarding use of hiPSC, several factors need to be taken into account. Firstly, besides the fact that used hiPSC lines were obtained from different individuals and therefore have a different genetic background, leading to different results, even hiPSC clones generated from the same individual in the same reprogramming experiment can have dissimilar characteristics, which influences cell performances and could lead to variable outcomes (Hu et al., 2010). Secondly, considering the mutation of the PD

hiPSC line used for this study is known, this mutation could have been corrected by either ZFN, TALEN, or CRISPR-Cas9, generating a new hiPSC line with the same genetic background that could have been used as control (Gaj et al., 2013, Zhao et al., 2014). However, this method also has its drawbacks since off-target effects were reported and required lengthy cell expansion could lead to instability of hiPSC (Gupta et al., 2011, Laurent et al., 2011, Fu et al., 2013). Lastly, differentiation of hiPSC is a time consuming process and optimal protocols are yet to be generated. Different protocols lead to differences in the efficiency of generation of desired cell type, however, the efficiency could even change between different batches of cells using the same protocol, showing one of the difficulties of working with hiPSC (Hu et al., 2010). For this study, hiPSC were differentiated into presumptive DA neurons since those neurons are affected in PD patients (Exner et al., 2012), however, it is unknown how efficient the differentiation protocol was and therefore it is unclear how many presumptive DA neurons were generated. The hiPSC were possibly differentiated in multiple neuronal lineages and obtained results likely reflect changes in a pool of different types of neurons (Hu et al., 2010, Zhao et al., 2014). It has to be noted that no protocols exist to date that offer near 100 % successful differentiation into the preferred cell type and the fact that it is difficult to only select the preferred cell type from the pool of differentiated cells indicates that obtained results will include processes happening in the other cell types as well.

Another issue needing to be addressed is use of mitochondrial uncouplers such as FCCP and CCCP for induction of mitophagy in cell models, since their effects do not resemble naturally occurring conditions. Mitochondrial uncouplers affect the entire mitochondrial population rather than a specific subgroup, which could even lead to

complete mitochondrial elimination upon prolonged treatments in some cell types (Narendra et al., 2008). FCCP was shown to be cytotoxic even at low concentrations that do not dissipate mitochondrial membrane potential and likely interferes with lysosomal degradation of autophagic cargo in the same way CCCP does (Tsiper et al., 2012, Padman et al., 2013). CCCP generates a lysosomal membrane potential by dissipating the pH gradient, leading to collapse of the lysosomal proton gradient. This dissipation of the lysosomal pH gradient led to a complete blockade in LC3B-positive autophagosome degradation, indicating CCCP inhibits autophagosome clearance and that it decreases autophagic flux (Padman et al., 2013). Furthermore, FCCP was reported to reduce cytosolic pH as well and this was important for mitophagy induction (Berezhnov et al., 2016). Low CCCP or FCCP concentrations completely abolish mitochondrial membrane potential, but do not induce mitophagy, which could be because low concentrations do not acidify cytosolic pH. High FCCP concentrations were ineffective in the induction of mitophagy when cytosolic pH was increased. However, on the other hand, it was proposed that PINK1 and Parkin might promote repair of less severely damaged mitochondria, which might be mediated by low FCCP concentrations, and does not lead to mitophagy. Localised translation of nuclear-encoded respiratory chain subunits at the mitochondrial surface is regulated by PINK1 and Parkin (Gehrke et al., 2015). Translocation of specific translationally repressed mRNAs from the cytosol to the MOM is mediated by PINK1, where it enables translation, in collaboration with Parkin, by displacement of translation inhibitors.

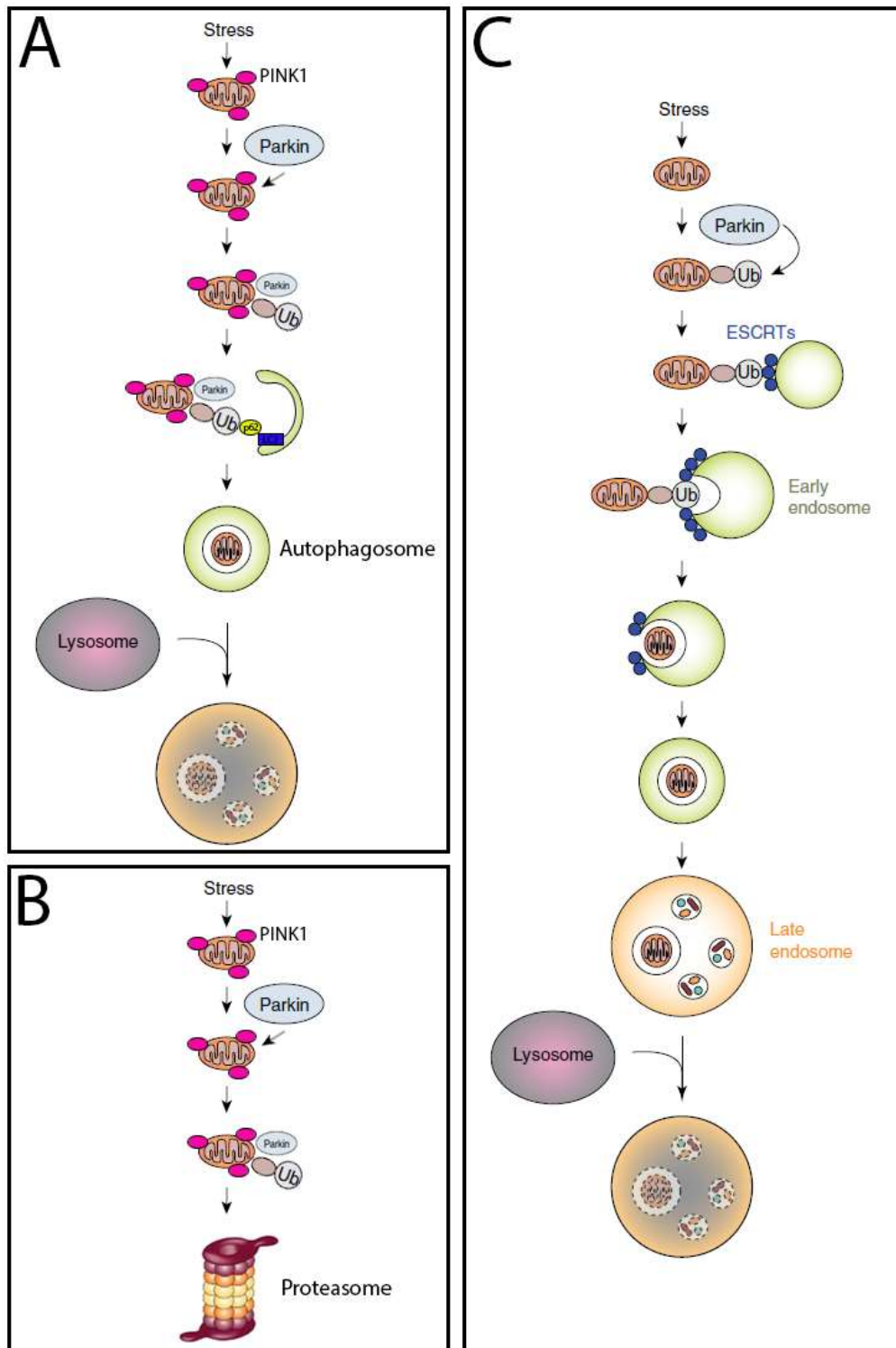
6.0.6 Updated model of PINK1/Parkin-mediated mitophagy

Based on results described herein and observations from literature, an adjusted pathway describing the selective removal of damaged mitochondria by PINK1 and

Parkin can be proposed. Mitochondrial damage induced by CCCP/FCCP leads to accumulation of PINK1 on damaged mitochondria and selective recruitment of Parkin, leading to ubiquitination of mitochondrial proteins and their elimination (Figure 6.0.6 A) (Gao et al., 2015, Berezhnov et al., 2016, Ivankovic et al., 2016).

Autophagy is activated upon CCCP/FCCP treatment (Sandoval et al., 2008, Ma et al., 2011), but is likely non-canonical. ULK1 or PIK3C3 inhibition did not lead to accumulation of FCCP-damaged mitochondria, however, proteasomal degradation was important for mitochondrial clearance (Figure 6.0.6 B, Chapter 3 & 4). Recent studies showed that CCCP activated ATG13-, which is part of the ULK1 complex, and PIK3C3-independent autophagy, but that LC3B lipidation was not affected (Jacquin et al., 2017). This LC3B lipidation was found to be endolysosomal, suggesting the endosomal pathway could be involved. Moreover, it was recently demonstrated that mitochondria underwent Parkin-dependent sequestration into Rab5-positive early endosomes via the endosomal sorting complexes required for transport (ESCRT) machinery that delivered mitochondria to lysosomes for degradation following maturation (Figure 6.0.6 C) (Hammerling et al., 2017). This endosomal pathway is activated by stressors that also induce autophagy, however, endosomal-mediated mitochondrial clearance is initiated before autophagy. Abrogation of Rab5 activity increased autophagic activity, suggesting autophagy compensates for impaired endosomal activity. Interestingly, Beclin1 regulates Rab5 activation and Beclin1 was shown to be required for neuron viability and regulation of endosomal pathways via the PIK3C3 complex (McKnight et al., 2014, Hammerling et al., 2017), while Rab5 was found to inhibit mTORC1 activity (Li et al., 2010) and to be important for the formation of the PIK3C3 complex (Ravikumar et al., 2008), indicating a cross-talk

between autophagy and the endosomal pathway. Rab5 knockdown, or functional inhibition, resulted in accumulation of stressed mitochondria and increased susceptibility to cell death, suggesting that Rab5-associated complexes are required for mitochondrial clearance (Hammerling et al., 2017).



Previous page: Figure 6.0.6. *Mitophagy can take place via different mechanisms.* Mitochondrial damage induces PINK1 accumulation and Parkin translocation. Parkin induces ubiquitination of mitochondrial proteins after which either (A) ubiquitinated proteins are recognised by p62 that binds to LC3B on the phagophore, leading to encapsulation of the damaged mitochondrion and subsequent degradation after the formed autophagosomes fuses with a lysosome, or (B) ubiquitinated proteins are degraded by the proteasome. (C) Mitochondrial proteins are ubiquitinated by Parkin that is recruited to mitochondria upon damage after which it is captured by endosomal sorting complexes required for transport (ESCRT) complexes on the early endosome that induce invagination and subsequent scission of the endosome membrane, leading to internalisation of the mitochondrion and its degradation after fusing with a lysosome. Figure adapted from (Hammerling et al., 2017).

Thus, after PINK1 accumulation and Parkin recruitment, dysfunctional mitochondria are rapidly taken up into endosomes that act as a first line of defence since early endosomes are continuously synthesised and exist in a network in cells (Figure 6.0.6 C) (Zeigerer et al., 2012). Simultaneously, Parkin also causes degradation of mitochondrial markers by the proteasome (Figure 6.0.6 B) (Chan et al., 2011, Yoshii et al., 2011, Sarraf et al., 2013). Finally, activation of non-canonical autophagy is responsible for clearance of the remainder of damaged mitochondria (Figure 6.0.6 A). Autophagosomes are synthesised *de novo* on demand and therefore cells need to utilise other degradative pathways to be able to remove damaged mitochondria immediately (Rubinsztein et al., 2012). Cells are likely to switch between endosomal-, proteasomal-, and autophagic degradation when one of these systems either gets overloaded or becomes impaired. Beclin1 could be a potential regulator of activation and switch between the different pathways since it has been linked to PINK1, Rab5 activation, and autophagy activation. However, all these events were reported upon CCCP/FCCP-induced mitochondrial damage and it remains to be seen if these processes also take place under physiological conditions.

6.1 Conclusions

The research described herein shows that responses to FCCP treatment differs between cell lines. FCCP led to increased PINK1 and decreased Parkin expression in SH-SY5Y cells, induction of autophagy, which is possibly non-canonical, and degradation of mitochondrial markers. Similarly to SH-SY5Y cells, autophagy was activated and mitochondrial fragmentation upon FCCP treatment was observed in presumptive NPC, but there was no Parkin degradation nor degradation of mitochondrial markers. FCCP potentially induced autophagy and degradation of mitochondrial markers in control presumptive DA neurons, while autophagic inhibition and no mitochondrial marker degradation was observed in PD presumptive DA neurons. Mitochondrial fragmentation was found to be present in PD presumptive DA neurons under basal conditions and PD presumptive DA neurons were also more susceptible to FCCP cytotoxicity, suggesting mitochondria were intrinsically damaged.

Differences in observations between presumptive NPC and presumptive DA neurons implicate that presumptive DA neurons are more susceptible to PD and that its use is therefore preferred over the use of presumptive NPC. Combined with the finding that control and presumptive PD DA neurons respond differently to treatments, which could be caused by the disease, the importance of the use of appropriate cell models for PD related research is highlighted.

Chapter 7

Perspectives

7.0 Perspectives

During the course of research as described herein, new questions were raised that need to be addressed in future investigations.

- 1) Is mitophagy molecularly distinct from generic autophagy?** The process of mitophagy has been described to take place upon induction of substantial mitochondrial damage by uncouplers such as CCCP and FCCP that induce autophagy in cell lines. It is not known if activation of autophagy is merely a side effect of CCCP/FCCP treatment or if it is activated upon mitochondrial damage under physiological conditions too. Can mitophagy be seen as a process that is molecularly distinct from generic autophagy or are mitophagy and autophagy running side by side? More research needs to be done on finding different methods to induce mitophagy in cell lines that do not have off-target effects such as CCCP/FCCP, but it would also be important to monitor the extent of mitochondrial degradation in cell lines under control conditions to investigate if this process is molecularly distinct from autophagy. Using fluorescently-labelled mitochondrial probes, mitochondria can be tracked by live cell imaging and degradation can be monitored. Via this method the effects of autophagic inhibition on mitochondrial degradation under control conditions can be investigated, which will give a clue about whether or not mitophagy is molecularly distinct from autophagy.

- 2) Does ULK1 inhibition affect FCCP-induced TOM20/TIM23 degradation?**

The effects of ULK1 inhibition on FCCP-induced mitochondrial degradation need to be investigated further, even though ULK1 is likely not involved in

this process. Only VDAC1 expression was assessed upon ULK1 inhibition and this was not an appropriate marker for monitoring mitochondrial degradation. Effects of ULK1 inhibition on FCCP-induced TOM20 and TIM23 degradation should be examined, however, it is also worth investigating if FCCP induced changes in mitochondrial mass, which can be quantified by measuring citrate synthase spectrophotometrically, and if this is affected by ULK1 inhibition.

- 3) What kinase phosphorylates Beclin1 at Ser30 and what is the function of unbound Ser30 phosphorylated Beclin1 in SH-SY5Y cells?** Previous results obtained in the Murray lab showed that ULK1 phosphorylated Beclin1 and that ULK1 inhibition decreased Ser30 phosphorylated Beclin1 levels in cancerous cells, which is the opposite as observed in SH-SY5Y cells. Therefore, which kinase is responsible for Ser30 Beclin1 phosphorylation in SH-SY5Y cells? A recent study demonstrated that Beclin1 can be phosphorylated at Ser30 by PGK1, suggesting that PGK1 could also be responsible for Beclin1 phosphorylation in SH-SY5Y cells, but this needs to be investigated (Qian et al., 2017). Immunoprecipitation of Beclin1 followed by immunoblotting with an α -PGK1 antibody could confirm presence of PGK1 in the Beclin1 complex. However, if PGK1 is not detected, mass spectrometry analysis of immunoprecipitated Beclin1 can identify other kinases that could be responsible for Beclin1 phosphorylation.

Immunoprecipitation of Beclin1 and PIK3C3 upon ULK1 inhibition showed that a pool of Ser30 phosphorylated Beclin1 was not associated to the PIK3C3 complex. This suggests that unbound Ser30 phosphorylated Beclin1 could

have different (unknown) function(s) in cells that needs to be identified. Beclin1 has also been linked to mitophagy since it was associated with both PINK1 (Michiorri et al., 2010) and Parkin (Choubey et al., 2014). It would be interesting to investigate if the pool of Ser30 phosphorylated Beclin1 that is not associated with the PIK3C3 complex is the pool of Beclin1 that is linked with either PINK1 or Parkin. Immunoprecipitation of PINK1 or Parkin could identify if Beclin1 is directly associated with them and if a pool of Beclin1 is phosphorylated at Ser30.

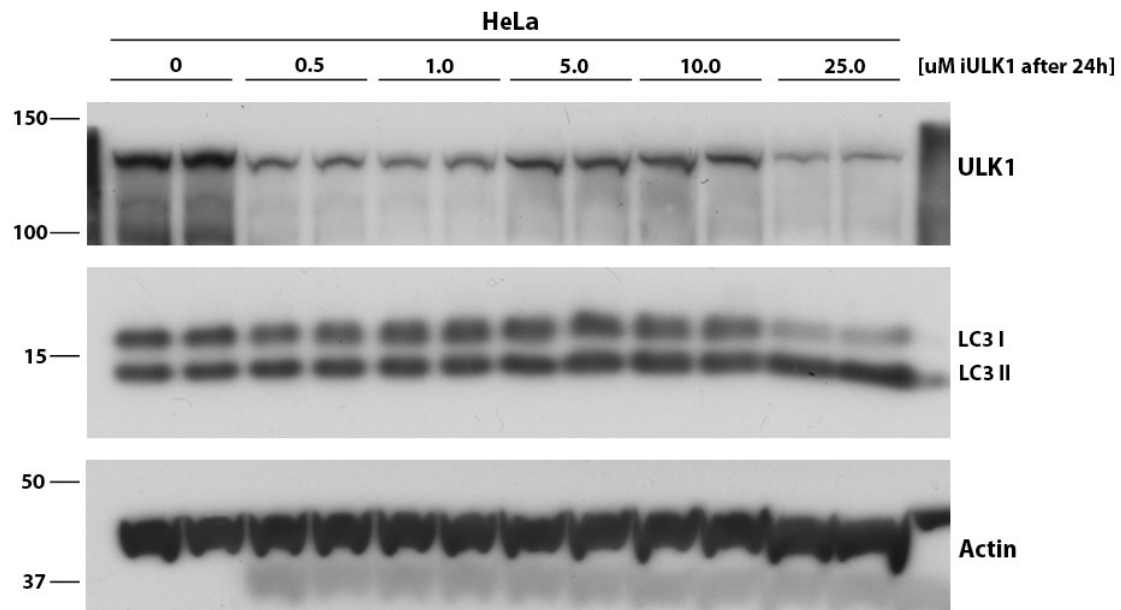
- 4) How can mitophagy be induced and how is it regulated in dopamine neurons generated from PD hiPSC?** Firstly, hiPSC lines utilised in this study were generated from two individuals, meaning that generated results cannot be compared with one another since cell lines have a different genetic background that might be accountable for observed differences. Therefore, to continue this line of research, it would be best to correct the mutation in the PD line, which can be done with the use of ZFN, TALEN, or CRISPR-Cas9 (Gaj et al., 2013, Zhao et al., 2014), to generate a control line with the same genetic background.

Preliminary results showed that FCCP did not induce mitochondrial degradation in presumptive DA neurons generated from hiPSC and therefore other methods need to be utilised to do so. Other mitochondrial poisons could be tested or FUNDC1 could be overexpressed since that was demonstrated to activate mitophagy in different cell lines (Ding and Yin, 2012). If this leads to successful induction of mitophagy and mitochondrial degradation in DA

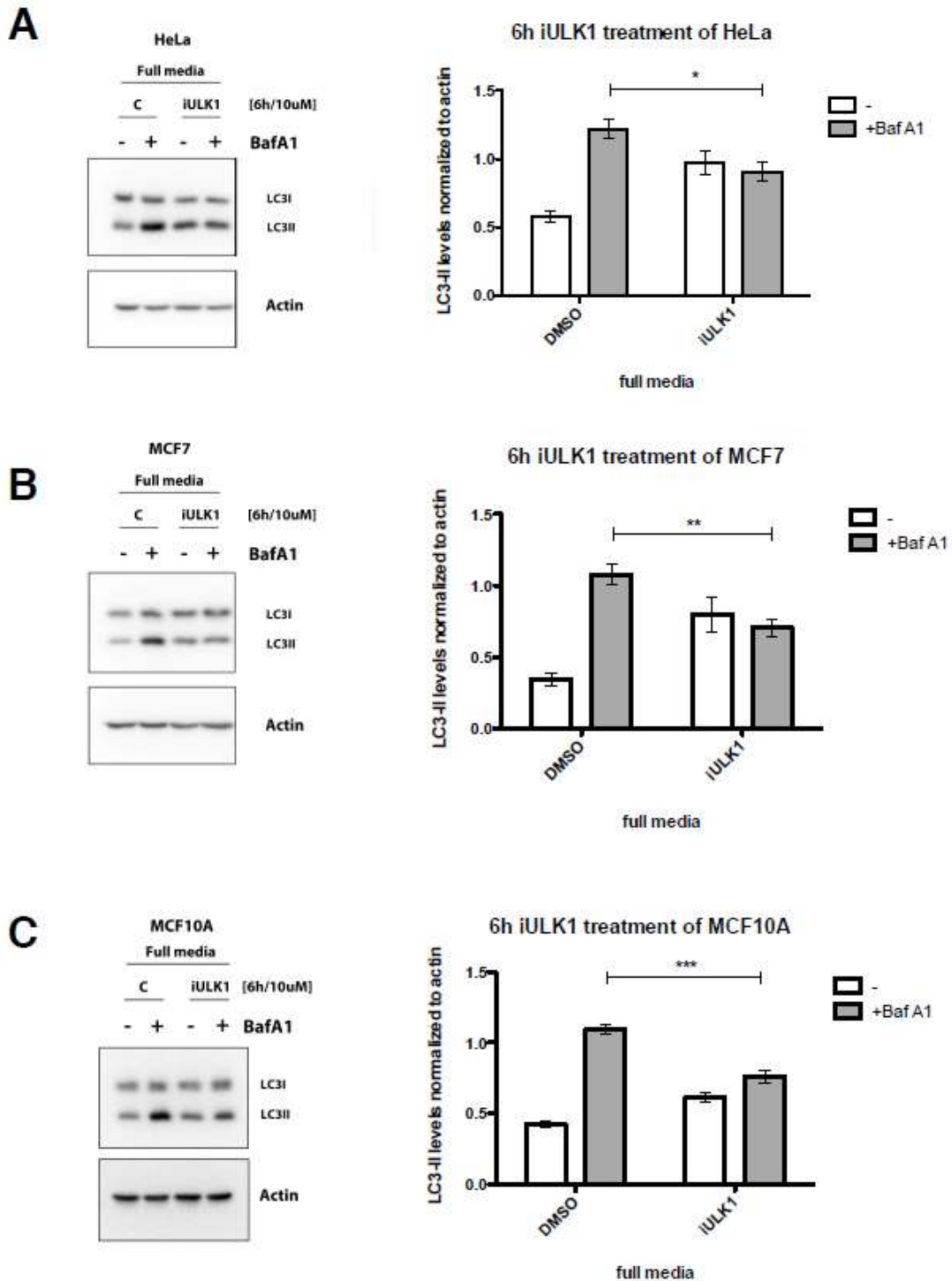
neurons, it would be interesting to find out if endosomal-, proteasomal-, and autophagic degradation pathways are involved in this process by inhibiting them and examining the effects on mitochondrial degradation by immunoblotting and live cell imaging. Ultimately, mechanisms in control and PD DA neurons could be compared to identify differences, which could give an answer as to why mitophagy related proteins are implicated in PD.

Chapter 8

Appendix



Appendix I: *iULK1 treatment of HeLa cells promotes degradation of ULK1.* HeLa cells were treated with up to 25 μ M of iULK1 for 24 hours in nutrient replete medium. Protein lysates were probed for autophagy marker proteins ULK1 and LC3B. β -actin was used as a loading control. Data represents three independent experiments. Taken from Ewelina Rozycka's PhD thesis.



Appendix II: *iULK1* promotes LC3B-II accumulation during basal autophagy in nutrient replete cells by preventing LC3B-II reaching the lysosome. HeLa (A), MCF7 (B), and MCF10A (C) cells were treated with 10 μ M *iULK1* in nutrient replete media for 4 hours before addition of 100 nM Baf A1 for a further 2 hours. Protein lysates were probed for the autophagy marker protein LC3B. Left panels illustrate immunoblots and corresponding densitometry normalised to corresponding β -actin levels is depicted in the right panels. Data represents three independent experiments. Error bars = SEM, unpaired t-test, * p <0.05, ** p <0.01, *** p <0.001. Taken from Ewelina Rozycka's PhD thesis.

Kinase	% Activity remaining	S.D. of replicates
ERK8	1	0
GSK3b	1	0
Aurora A	1	0
HIPK2	1	0
IGF-1R	1	0
CLK2	3	0
IR	3	1
HIPK1	4	1
HIPK3	4	0
Src	4	1
STK33	5	0
DYRK1A	5	0
MLK3	5	1
SYK	5	1
CDK2-Cyclin A	6	1
PAK4	6	0
GCK	6	1
TAK1	6	1
YES1	6	1
FGF-R1	6	6
CHK2	7	0
MARK3	7	1
NUAK1	7	2
JAK2	7	2
EPH-B1	7	1
EPH-B2	7	0
VEG-FR	7	3
RSK1	8	2
RIPK2	8	0
EPH-B4	8	0
PAK5	9	1
AMPK	10	2
TBK1	10	3
PIM3	10	2
MEKK1	10	2
TrkA	10	7
PRK2	11	1
DAPK1	11	0
DYRK2	11	1
BRK	11	3
EPH-A4	11	0
RSK2	12	1
BTK	12	1
CAMKKb	13	0
TAO1	13	1
Lck	13	3
ABL	13	0
MLK1	14	3
SGK1	15	1
BRSK2	15	2
IRR	16	4
PDK1	17	0
IKKe	17	5
TIE2	17	3
CHK1	18	1
MKK1	19	0
S6K1	19	1
MARK2	19	3
DYRK3	19	1

Kinase	% Activity remaining	S.D. of replicates
MKK2	20	7
CAMK1	20	1
PIM1	20	1
IRAK4	23	1
Aurora B	27	7
IKKb	27	1
PHK	28	4
SmMLCK	29	1
MELK	31	2
PAK6	31	3
MINK1	31	1
JNK3	34	0
MARK1	34	4
EPH-A2	34	1
JNK1	36	3
PKD1	36	1
MARK4	36	6
CSK	36	1
BRSK1	37	2
ROCK 2	39	1
HER4	39	1
MNK1	40	2
MST2	41	7
EPH-B3	42	1
PAK2	44	3
MST4	46	4
PKCγ	48	2
ASK1	50	2
TTK	50	2
MAPKAP-K2	56	9
ZAP70	58	7
MKK6	59	2
JNK2	61	11
PKA	61	4
NEK2a	61	7
MPSK1	63	9
MSK1	65	4
PIM2	66	7
CK2	67	4
LKB1	69	10
p38d MAPK	79	9
PKCa	79	3
PRAK	79	0
PKCz	80	3
MNK2	80	2
p38g MAPK	83	4
PLK1	83	3
ERK1	84	8
SRPK1	87	11
ERK2	88	5
PKBb	90	10
NEK6	90	6
p38b MAPK	91	3
p38a MAPK	93	8
MAPKAP-K3	93	6
EF2K	97	10
CK1	98	6
PKBa	104	0

Previous page: Appendix III: *Kinase selectivity panel of protein kinase activities tested with iULK1.* Results are shown as percentage of activity remaining in the presence of iULK1, as compared with the control conditions with iULK1 omitted.

Chapter 9

References

- Adams, K. A., Maida, J. M., Golden, J. A. and Riddle, R. D. (2000) 'The transcription factor *Lmx1b* maintains *Wnt1* expression within the isthmic organizer', *Development*, 127(9), pp. 1857-67.
- Agnihotri, S. K., Shen, R., Li, J., Gao, X. and Büeler, H. (2017) 'Loss of PINK1 leads to metabolic deficits in adult neural stem cells and impedes differentiation of newborn neurons in the mouse hippocampus', *FASEB J*, 31(7), pp. 2839-2853.
- Aguirre, J. D., Dunkerley, K. M., Mercier, P. and Shaw, G. S. (2017) 'Structure of phosphorylated UBL domain and insights into PINK1-orchestrated parkin activation', *Proc Natl Acad Sci U S A*, 114(2), pp. 298-303.
- Alavi, M. V. and Fuhrmann, N. (2013) 'Dominant optic atrophy, OPA1, and mitochondrial quality control: understanding mitochondrial network dynamics', *Mol Neurodegener*, 8, pp. 32.
- Albéri, L., Sgadò, P. and Simon, H. H. (2004) 'Engrailed genes are cell-autonomously required to prevent apoptosis in mesencephalic dopaminergic neurons', *Development*, 131(13), pp. 3229-36.
- Almeida, A., Almeida, J., Bolanos, J. P. and Moncada, S. (2001) 'Different responses of astrocytes and neurons to nitric oxide: the role of glycolytically generated ATP in astrocyte protection', *Proc Natl Acad Sci U S A*, 98(26), pp. 15294-9.
- Amadoro, G., Corsetti, V., Florenzano, F., Atlante, A., Bobba, A., Nicolini, V., Nori, S. L. and Calissano, P. (2014) 'Morphological and bioenergetic demands underlying the mitophagy in post-mitotic neurons: the pink-parkin pathway', *Front Aging Neurosci*, 6, pp. 18.
- Andersson, E., Tryggvason, U., Deng, Q., Friling, S., Alekseenko, Z., Robert, B., Perlmann, T. and Ericson, J. (2006) 'Identification of intrinsic determinants of midbrain dopamine neurons', *Cell*, 124(2), pp. 393-405.
- Andersson, E. R., Prakash, N., Cajanek, L., Minina, E., Bryja, V., Bryjova, L., Yamaguchi, T. P., Hall, A. C., Wurst, W. and Arenas, E. (2008) 'Wnt5a regulates ventral midbrain morphogenesis and the development of A9-A10 dopaminergic cells in vivo', *PLoS One*, 3(10), pp. e3517.
- Arenas, E., Denham, M. and Villaescusa, J. C. (2015) 'How to make a midbrain dopaminergic neuron', *Development*, 142(11), pp. 1918-36.
- Bach, M., Larance, M., James, D. E. and Ramm, G. (2011) 'The serine/threonine kinase ULK1 is a target of multiple phosphorylation events', *Biochem J*, 440(2), pp. 283-91.

- Baek, J. H., Hatakeyama, J., Sakamoto, S., Ohtsuka, T. and Kageyama, R. (2006) 'Persistent and high levels of Hes1 expression regulate boundary formation in the developing central nervous system', *Development*, 133(13), pp. 2467-76.
- Bago, R., Malik, N., Munson, M. J., Prescott, A. R., Davies, P., Sommer, E., Shpiro, N., Ward, R., Cross, D., Ganley, I. G. and Alessi, D. R. (2014) 'Characterization of VPS34-IN1, a selective inhibitor of Vps34, reveals that the phosphatidylinositol 3-phosphate-binding SGK3 protein kinase is a downstream target of class III phosphoinositide 3-kinase', *Biochem J*, 463(3), pp. 413-27.
- Bear, M. F., Connors, B. W. and Paradiso, M. A. (2007) *Neuroscience: Exploring the Brain*. 3 edn.: Lippincott Williams & Wilkins.
- Beck, R. W. (2008) *Functional Neurology for Practitioners of Manual Therapy*. Elsevier Limited.
- Becker, D., Richter, J., Tocilescu, M. A., Przedborski, S. and Voos, W. (2012) 'Pink1 kinase and its membrane potential (Deltapsi)-dependent cleavage product both localize to outer mitochondrial membrane by unique targeting mode', *J Biol Chem*, 287(27), pp. 22969-87.
- Bellot, G., Garcia-Medina, R., Gounon, P., Chiche, J., Roux, D., Pouyssegur, J. and Mazure, N. M. (2009) 'Hypoxia-induced autophagy is mediated through hypoxia-inducible factor induction of BNIP3 and BNIP3L via their BH3 domains', *Mol Cell Biol*, 29(10), pp. 2570-81.
- Berezhnov, A. V., Soutar, M. P., Fedotova, E. I., Frolova, M. S., Plun-Favreau, H., Zinchenko, V. P. and Abramov, A. Y. (2016) 'Intracellular pH Modulates Autophagy and Mitophagy', *J Biol Chem*, 291(16), pp. 8701-8.
- Berg, J. M., Tymoczko, J. L. and Stryer, L. (2002) *Biochemistry*. 5 edn. New York: W. H. Freeman.
- Bhujabal, Z., Birgisdottir, Å., Sjøttem, E., Brenne, H. B., Øvervatn, A., Habisov, S., Kirkin, V., Lamark, T. and Johansen, T. (2017) 'FKBP8 recruits LC3A to mediate Parkin-independent mitophagy', *EMBO Rep*, 18(6), pp. 947-961.
- Birsa, N., Norkett, R., Wauer, T., Mevissen, T. E., Wu, H. C., Foltynie, T., Bhatia, K., Hirst, W. D., Komander, D., Plun-Favreau, H. and Kittler, J. T. (2014) 'Lysine 27 ubiquitination of the mitochondrial transport protein Miro is dependent on serine 65 of the Parkin ubiquitin ligase', *J Biol Chem*, 289(21), pp. 14569-82.

- Bissonette, G. B. and Roesch, M. R. (2015) 'Development and function of the midbrain dopamine system: what we know and what we need to', *Genes Brain Behav.*
- Bolaños, J. P. (2016) 'Bioenergetics and redox adaptations of astrocytes to neuronal activity', *J Neurochem*, 139 Suppl 2, pp. 115-125.
- Bolaños, J. P., Almeida, A. and Moncada, S. (2010) 'Glycolysis: a bioenergetic or a survival pathway?', *Trends Biochem Sci*, 35(3), pp. 145-9.
- Braut, C., Levy, P. L. and Bartosch, B. (2013) 'Hepatitis C virus-induced mitochondrial dysfunctions', *Viruses*, 5(3), pp. 954-80.
- Byers, B., Cord, B., Nguyen, H. N., Schüle, B., Fenno, L., Lee, P. C., Deisseroth, K., Langston, J. W., Pera, R. R. and Palmer, T. D. (2011) 'SNCA triplication Parkinson's patient's iPSC-derived DA neurons accumulate α -synuclein and are susceptible to oxidative stress', *PLoS One*, 6(11), pp. e26159.
- Bäckman, C., Perlmann, T., Wallén, A., Hoffer, B. J. and Morales, M. (1999) 'A selective group of dopaminergic neurons express Nurr1 in the adult mouse brain', *Brain Res*, 851(1-2), pp. 125-32.
- Cai, Q., Zakaria, H. M., Simone, A. and Sheng, Z. H. (2012) 'Spatial parkin translocation and degradation of damaged mitochondria via mitophagy in live cortical neurons', *Curr Biol*, 22(6), pp. 545-52.
- Caudle, W. M., Richardson, J. R., Wang, M. Z., Taylor, T. N., Guillot, T. S., McCormack, A. L., Colebrooke, R. E., Di Monte, D. A., Emson, P. C. and Miller, G. W. (2007) 'Reduced vesicular storage of dopamine causes progressive nigrostriatal neurodegeneration', *J Neurosci*, 27(30), pp. 8138-48.
- Celardo, I., Martins, L. M. and Gandhi, S. (2014) 'Unravelling mitochondrial pathways to Parkinson's disease', *Br J Pharmacol*, 171(8), pp. 1943-57.
- Cereghetti, G. M., Costa, V. and Scorrano, L. (2010) 'Inhibition of Drp1-dependent mitochondrial fragmentation and apoptosis by a polypeptide antagonist of calcineurin', *Cell Death Differ*, 17(11), pp. 1785-94.
- Chan, D. C. (2006) 'Mitochondria: dynamic organelles in disease, aging, and development', *Cell*, 125(7), pp. 1241-52.
- Chan, D. C. (2012) 'Fusion and fission: interlinked processes critical for mitochondrial health', *Annu Rev Genet*, 46, pp. 265-87.

- Chan, E. Y., Kir, S. and Tooze, S. A. (2007) 'siRNA screening of the kinome identifies ULK1 as a multidomain modulator of autophagy', *J Biol Chem*, 282(35), pp. 25464-74.
- Chan, N. C., Salazar, A. M., Pham, A. H., Sweredoski, M. J., Kolawa, N. J., Graham, R. L., Hess, S. and Chan, D. C. (2011) 'Broad activation of the ubiquitin-proteasome system by Parkin is critical for mitophagy', *Hum Mol Genet*, 20(9), pp. 1726-37.
- Chang, K. H., Lee-Chen, G. J., Wu, Y. R., Chen, Y. J., Lin, J. L., Li, M., Chen, I. C., Lo, Y. S., Wu, H. C. and Chen, C. M. (2016) 'Impairment of proteasome and anti-oxidative pathways in the induced pluripotent stem cell model for sporadic Parkinson's disease', *Parkinsonism Relat Disord*, 24, pp. 81-8.
- Chen, D., Chen, X., Li, M., Zhang, H., Ding, W. X. and Yin, X. M. (2013) 'CCCP-Induced LC3 lipidation depends on Atg9 whereas FIP200/Atg13 and Beclin 1/Atg14 are dispensable', *Biochem Biophys Res Commun*, 432(2), pp. 226-30.
- Chen, H. and Chan, D. C. (2009) 'Mitochondrial dynamics--fusion, fission, movement, and mitophagy--in neurodegenerative diseases', *Hum Mol Genet*, 18(R2), pp. R169-76.
- Chen, M., Chen, Z., Wang, Y., Tan, Z., Zhu, C., Li, Y., Han, Z., Chen, L., Gao, R., Liu, L. and Chen, Q. (2016) 'Mitophagy receptor FUNDC1 regulates mitochondrial dynamics and mitophagy', *Autophagy*, 12(4), pp. 689-702.
- Chen, Y. and Dorn, G. W., 2nd (2013) 'PINK1-phosphorylated mitofusin 2 is a Parkin receptor for culling damaged mitochondria', *Science*, 340(6131), pp. 471-5.
- Cheng, M., Liu, L., Lao, Y., Liao, W., Liao, M., Luo, X., Wu, J., Xie, W., Zhang, Y. and Xu, N. (2016) 'MicroRNA-181a suppresses parkin-mediated mitophagy and sensitizes neuroblastoma cells to mitochondrial uncoupler-induced apoptosis', *Oncotarget*, 7(27), pp. 42274-42287.
- Cheong, H., Lindsten, T., Wu, J., Lu, C. and Thompson, C. B. (2011) 'Ammonia-induced autophagy is independent of ULK1/ULK2 kinases', *Proc Natl Acad Sci U S A*, 108(27), pp. 11121-11126.
- Chinta, S. J. and Andersen, J. K. (2008) 'Redox imbalance in Parkinson's disease', *Biochim Biophys Acta*, 1780(11), pp. 1362-7.
- Cho, Y. M., Kwon, S., Pak, Y. K., Seol, H. W., Choi, Y. M., Park do, J., Park, K. S. and Lee, H. K. (2006) 'Dynamic changes in mitochondrial biogenesis and

- antioxidant enzymes during the spontaneous differentiation of human embryonic stem cells', *Biochem Biophys Res Commun*, 348(4), pp. 1472-8.
- Choubey, V., Cagalinec, M., Liiv, J., Safiulina, D., Hickey, M. A., Kuum, M., Liiv, M., Anwar, T., Eskelinen, E. L. and Kaasik, A. (2014) 'BECN1 is involved in the initiation of mitophagy: it facilitates PARK2 translocation to mitochondria', *Autophagy*, 10(6), pp. 1105-19.
- Chu, C. T., Zhu, J. and Dagda, R. (2007) 'Beclin 1-independent pathway of damage-induced mitophagy and autophagic stress: implications for neurodegeneration and cell death', *Autophagy*, 3(6), pp. 663-6.
- Chung, S., Leung, A., Han, B. S., Chang, M. Y., Moon, J. I., Kim, C. H., Hong, S., Pruszk, J., Isacson, O. and Kim, K. S. (2009) 'Wnt1-lmx1a forms a novel autoregulatory loop and controls midbrain dopaminergic differentiation synergistically with the SHH-FoxA2 pathway', *Cell Stem Cell*, 5(6), pp. 646-58.
- Chung, S. Y., Kishinevsky, S., Mazzulli, J. R., Graziotto, J., Mrejeru, A., Mosharov, E. V., Puspita, L., Valiulahi, P., Sulzer, D., Milner, T. A., Taldone, T., Krainc, D., Studer, L. and Shim, J. W. (2016) 'Parkin and PINK1 Patient iPSC-Derived Midbrain Dopamine Neurons Exhibit Mitochondrial Dysfunction and α -Synuclein Accumulation', *Stem Cell Reports*, 7(4), pp. 664-677.
- Cianfanelli, V., De Zio, D., Di Bartolomeo, S., Nazio, F., Strappazzon, F. and Cecconi, F. (2015) 'Ambra1 at a glance', *J Cell Sci*, 128(11), pp. 2003-8.
- Ciechanover, A. and Brundin, P. (2003) 'The ubiquitin proteasome system in neurodegenerative diseases; sometimes the chicken, sometimes the egg', *Neuron*, 40, pp. 427-446.
- Clark, I. E., Dodson, M. W., Jiang, C., Cao, J. H., Huh, J. R., Seol, J. H., Yoo, S. J., Hay, B. A. and Guo, M. (2006) 'Drosophila pink1 is required for mitochondrial function and interacts genetically with parkin', *Nature*, 441(7097), pp. 1162-6.
- Clarke, D. D. and Sokoloff, L. (1999) *Basic Neurochemistry: Molecular, Cellular and Medical Aspects. Chapter 31: Circulation and Energy Metabolism of the Brain* 6 edn. Philadelphia: Lippincott-Raven.
- Cooper, O., Seo, H., Andrabi, S., Guardia-Laguarta, C., Graziotto, J., Sundberg, M., McLean, J. R., Carrillo-Reid, L., Xie, Z., Osborn, T., Hargus, G., Deleidi, M., Lawson, T., Bogetofte, H., Perez-Torres, E., Clark, L., Moskowitz, C.,

- Mazzulli, J., Chen, L., Volpicelli-Daley, L., Romero, N., Jiang, H., Uitti, R. J., Huang, Z., Opala, G., Scarffe, L. A., Dawson, V. L., Klein, C., Feng, J., Ross, O. A., Trojanowski, J. Q., Lee, V. M., Marder, K., Surmeier, D. J., Wszolek, Z. K., Przedborski, S., Krainc, D., Dawson, T. M. and Isacson, O. (2012) 'Pharmacological rescue of mitochondrial deficits in iPSC-derived neural cells from patients with familial Parkinson's disease', *Sci Transl Med*, 4(141), pp. 141ra90.
- Crossley, P. H. and Martin, G. R. (1995) 'The mouse *Fgf8* gene encodes a family of polypeptides and is expressed in regions that direct outgrowth and patterning in the developing embryo', *Development*, 121(2), pp. 439-51.
- Cui, K., Luo, X., Xu, K. and Ven Murthy, M. R. (2004) 'Role of oxidative stress in neurodegeneration: recent developments in assay methods for oxidative stress and nutraceutical antioxidants', *Prog Neuropsychopharmacol Biol Psychiatry*, 28(5), pp. 771-99.
- Cui, M., Tang, X., Christian, W. V., Yoon, Y. and Tieu, K. (2010) 'Perturbations in mitochondrial dynamics induced by human mutant PINK1 can be rescued by the mitochondrial division inhibitor mdivi-1', *J Biol Chem*, 285(15), pp. 11740-52.
- Dagda, R. K., Cherra, S. J., 3rd, Kulich, S. M., Tandon, A., Park, D. and Chu, C. T. (2009) 'Loss of PINK1 function promotes mitophagy through effects on oxidative stress and mitochondrial fission', *J Biol Chem*, 284(20), pp. 13843-55.
- Dai, J. X., Hu, Z. L., Shi, M., Guo, C. and Ding, Y. Q. (2008) 'Postnatal ontogeny of the transcription factor *Lmx1b* in the mouse central nervous system', *J Comp Neurol*, 509(4), pp. 341-55.
- Davis, C. A. and Joyner, A. L. (1988) 'Expression patterns of the homeo box-containing genes *En-1* and *En-2* and the proto-oncogene *int-1* diverge during mouse development', *Genes Dev*, 2(12B), pp. 1736-44.
- Decressac, M., Volakakis, N., Björklund, A. and Perlmann, T. (2013) 'NURR1 in Parkinson disease--from pathogenesis to therapeutic potential', *Nat Rev Neurol*, 9(11), pp. 629-36.
- Deng, Q., Andersson, E., Hedlund, E., Alekseenko, Z., Coppola, E., Panman, L., Millonig, J. H., Brunet, J. F., Ericson, J. and Perlmann, T. (2011) 'Specific and

- integrated roles of Lmx1a, Lmx1b and Phox2a in ventral midbrain development', *Development*, 138(16), pp. 3399-408.
- Denison, S. R., Wang, F., Becker, N. A., Schule, B., Kock, N., Phillips, L. A., Klein, C. and Smith, D. I. (2003) 'Alterations in the common fragile site gene Parkin in ovarian and other cancers', *Oncogene*, 22(51), pp. 8370-8.
- Detmer, S. A. and Chan, D. C. (2007a) 'Complementation between mouse Mfn1 and Mfn2 protects mitochondrial fusion defects caused by CMT2A disease mutations', *J Cell Biol*, 176(4), pp. 405-14.
- Detmer, S. A. and Chan, D. C. (2007b) 'Functions and dysfunctions of mitochondrial dynamics', *Nat Rev Mol Cell Biol*, 8(11), pp. 870-9.
- Devine, M. J., Ryten, M., Vodicka, P., Thomson, A. J., Burdon, T., Houlden, H., Cavaleri, F., Nagano, M., Drummond, N. J., Taanman, J. W., Schapira, A. H., Gwinn, K., Hardy, J., Lewis, P. A. and Kunath, T. (2011) 'Parkinson's disease induced pluripotent stem cells with triplication of the α -synuclein locus', *Nat Commun*, 2, pp. 440.
- Di Bartolomeo, S., Corazzari, M., Nazio, F., Oliverio, S., Lisi, G., Antonioli, M., Pagliarini, V., Matteoni, S., Fuoco, C., Giunta, L., D'Amelio, M., Nardacci, R., Romagnoli, A., Piacentini, M., Cecconi, F. and Fimia, G. M. (2010) 'The dynamic interaction of AMBRA1 with the dynein motor complex regulates mammalian autophagy', *J Cell Biol*, 191(1), pp. 155-68.
- Ding, W. X., Guo, F., Ni, H. M., Bockus, A., Manley, S., Stolz, D. B., Eskelinen, E. L., Jeaschke, H. and Yin, X. M. (2012) 'Parkin and mitofusins reciprocally regulate mitophagy and mitochondrial spheroid formation', *The Journal of Biological Chemistry*, 287(50), pp. 42379-42388.
- Ding, W. X., Ni, H. M., Li, M., Liao, Y., Chen, X., Stolz, D. B., Dorn, G. W., 2nd and Yin, X. M. (2010) 'Nix is critical to two distinct phases of mitophagy, reactive oxygen species-mediated autophagy induction and Parkin-ubiquitin-p62-mediated mitochondrial priming', *J Biol Chem*, 285(36), pp. 27879-90.
- Ding, W. X. and Yin, X. M. (2012) 'Mitophagy: mechanisms, pathophysiological roles, and analysis', *Biol Chem*, 393(7), pp. 547-64.
- Durcan, T. M., Tang, M. Y., Pérusse, J. R., Dashti, E. A., Aguilera, M. A., McLelland, G. L., Gros, P., Shaler, T. A., Faubert, D., Coulombe, B. and Fon, E. A. (2014) 'USP8 regulates mitophagy by removing K6-linked ubiquitin conjugates from parkin', *EMBO J*, 33(21), pp. 2473-91.

- Echelard, Y., Epstein, D. J., St-Jacques, B., Shen, L., Mohler, J., McMahon, J. A. and McMahon, A. P. (1993) 'Sonic hedgehog, a member of a family of putative signaling molecules, is implicated in the regulation of CNS polarity', *Cell*, 75(7), pp. 1417-30.
- Egan, D. F., Shackelford, D. B., Mihaylova, M. M., Gelino, S., Kohnz, R. A., Mair, W., Vasquez, D. S., Joshi, A., Gwinn, D. M., Taylor, R., Asara, J. M., Fitzpatrick, J., Dillin, A., Viollet, B., Kundu, M., Hansen, M. and Shaw, R. J. (2011) 'Phosphorylation of ULK1 (hATG1) by AMP-activated protein kinase connects energy sensing to mitophagy', *Science*, 331, pp. 456-461.
- Emelyanov, V. V. (2001) 'Rickettsiaceae, rickettsia-like endosymbionts, and the origin of mitochondria', *Biosci Rep*, 21(1), pp. 1-17.
- Erecinska, M., Nelson, D., Yudkoff, M. and Silver, I. A. (1994) 'Energetics of the nerve terminal in relation to central nervous system function', *Biochem Soc Trans*, 22, pp. 959-965.
- Ernster, L. and Schatz, G. (1981) 'Mitochondria: a historical review', *J Cell Biol*, 91(3), pp. 227s-255s.
- Esclatine, A., Chaumorcel, M. and Codogno, P. (2009) 'Macroautophagy signaling and regulation', *Curr Top Microbiol Immunol*, 335, pp. 33-70.
- Exner, N., Lutz, A. K., Haass, C. and Winklhofer, K. F. (2012) 'Mitochondrial dysfunction in Parkinson's disease: molecular mechanisms and pathophysiological consequences', *EMBO J*, 31(14), pp. 3038-62.
- Exner, N., Treske, B., Paquet, D., Holmstrom, K., Schiesling, C., Gispert, S., Carballo-Carbajal, I., Berg, D., Hoepken, H. H., Gasser, T., Kruger, R., Winklhofer, K. F., Vogel, F., Reichert, A. S., Auburger, G., Kahle, P. J., Schmid, B. and Haass, C. (2007a) 'Loss-of-function of human PINK1 results in mitochondrial pathology and can be rescued by parkin', *J Neurosci*, 27(45), pp. 12413-8.
- Exner, N., Treske, B., Paquet, D., Holmström, K., Schiesling, C., Gispert, S., Carballo-Carbajal, I., Berg, D., Hoepken, H. H., Gasser, T., Krüger, R., Winklhofer, K. F., Vogel, F., Reichert, A. S., Auburger, G., Kahle, P. J., Schmid, B. and Haass, C. (2007b) 'Loss-of-function of human PINK1 results in mitochondrial pathology and can be rescued by parkin', *J Neurosci*, 27(45), pp. 12413-8.

- Fahn, S. (2004) 'Levodopa and the progression of Parkinson's disease', *N Engl J Med*, 351(24), pp. 2498-508.
- Fan, W., Nassiri, A. and Zhong, Q. (2011) 'Autophagosome targeting and membrane curvature sensing by Barkor/Atg14(L)', *Proc Natl Acad Sci U S A*, 108(19), pp. 7769-7774.
- Fedorowicz, M. A., de Vries-Schneider, R. L. A., Rüb, C., Becker, D., Huang, Y., Zhou, C., Alessi Wolken, D. M., Voos, W., Liu, Y. and Przedborski, S. (2014) 'Cytosolic cleaved PINK1 represses Parkin translocation to mitochondria and mitophagy', *EMBO Rep*, 15(1), pp. 86-93.
- Fischer, F., Hamann, A. and Osiewacz, H. D. (2012) 'Mitochondrial quality control: an integrated network of pathways', *Trends Biochem Sci*, 37(7), pp. 284-92.
- Flierl, A., Oliveira, L. M., Falomir-Lockhart, L. J., Mak, S. K., Hesley, J., Soldner, F., Arndt-Jovin, D. J., Jaenisch, R., Langston, J. W., Jovin, T. M. and Schüle, B. (2014) 'Higher vulnerability and stress sensitivity of neuronal precursor cells carrying an alpha-synuclein gene triplication', *PLoS One*, 9(11), pp. e112413.
- Fogal, V., Richardson, A. D., Karmali, P. P., Scheffler, I. E., Smith, J. W. and Ruoslahti, E. (2010) 'Mitochondrial p32 protein is a critical regulator of tumor metabolism via maintenance of oxidative phosphorylation', *Mol Cell Biol*, 30(6), pp. 1303-18.
- Frezza, C., Cipolat, S., Martins de Brito, O., Micaroni, M., Beznoussenko, G. V., Rudka, T., Bartoli, D., Polishuck, R. S., Danial, N. N., De Strooper, B. and Scorrano, L. (2006) 'OPA1 controls apoptotic cristae remodeling independently from mitochondrial fusion', *Cell*, 126(1), pp. 177-89.
- Fu, Y., Foden, J. A., Khayter, C., Maeder, M. L., Reyon, D., Joung, J. K. and Sander, J. D. (2013) 'High-frequency off-target mutagenesis induced by CRISPR-Cas nucleases in human cells', *Nat Biotechnol*, 31(9), pp. 822-6.
- Fujita, N., Hayashi-Nishino, M., Fukumoto, H., Omori, H., Yamamoto, A., Noda, T. and Yoshimori, T. (2008a) 'An Atg4B mutant hampers the lipidation of LC3 paralogues and causes defects in autophagosome closure', *Mol Biol Cell*, 19(11), pp. 4651-9.
- Fujita, N., Itoh, T., Omori, H., Fukuda, M., Noda, T. and Yoshimori, T. (2008b) 'The Atg16L complex specifies the site of LC3 lipidation for membrane biogenesis in autophagy', *Mol Biol Cell*, 19(5), pp. 2092-100.

- Gaj, T., Gersbach, C. A. and Barbas, C. F. (2013) 'ZFN, TALEN, and CRISPR/Cas-based methods for genome engineering', *Trends Biotechnol*, 31(7), pp. 397-405.
- Ganley, I. G., Lam du, H., Wang, J., Ding, X., Chen, S. and Jiang, X. (2009) 'ULK1.ATG13.FIP200 complex mediates mTOR signaling and is essential for autophagy', *J Biol Chem*, 284(18), pp. 12297-305.
- Gao, F., Chen, D., Si, J., Hu, Q., Qin, Z., Fang, M. and Wang, G. (2015) 'The mitochondrial protein BNIP3L is the substrate of PARK2 and mediates mitophagy in PINK1/PARK2 pathway', *Hum Mol Genet*, 24(9), pp. 2528-38.
- Gates, M. A., Coupe, V. M., Torres, E. M., Fricker-Gates, R. A. and Dunnett, S. B. (2004) 'Spatially and temporally restricted chemoattractive and chemorepulsive cues direct the formation of the nigro-striatal circuit', *Eur J Neurosci*, 19(4), pp. 831-44.
- Gautier, C. A., Kitada, T. and Shen, J. (2008) 'Loss of PINK1 causes mitochondrial functional defects and increased sensitivity to oxidative stress', *Proc Natl Acad Sci U S A*, 105(32), pp. 11364-9.
- Gegg, M. E., Cooper, J. M., Chau, K. Y., Rojo, M., Schapira, A. H. and Taanman, J. W. (2010) 'Mitofusin 1 and mitofusin 2 are ubiquitinated in a PINK1/parkin-dependent manner upon induction of mitophagy', *Hum Mol Genet*, 19(24), pp. 4861-70.
- Gegg, M. E., Cooper, J. M., Schapira, A. H. and Taanman, J. W. (2009) 'Silencing of PINK1 expression affects mitochondrial DNA and oxidative phosphorylation in dopaminergic cells', *PLoS One*, 4(3), pp. e4756.
- Gehrke, S., Wu, Z., Klinkenberg, M., Sun, Y., Auburger, G., Guo, S. and Lu, B. (2015) 'PINK1 and Parkin control localized translation of respiratory chain component mRNAs on mitochondria outer membrane', *Cell Metab*, 21(1), pp. 95-108.
- Geisler, S., Holmström, K. M., Skujat, D., Fiesel, F. C., Rothfuss, O. C., Kahle, P. J. and Springer, W. (2010) 'PINK1/Parkin-mediated mitophagy is dependent on VDAC1 and p62/SQSTM1', *Nat Cell Biol*, 12(2), pp. 119-31.
- Greene, A. W., Grenier, K., Aguilera, M. A., Muise, S., Farazifard, R., Haque, M. E., McBride, H. M., Park, D. S. and Fon, E. A. (2012) 'Mitochondrial processing peptidase regulates PINK1 processing, import and Parkin recruitment', *EMBO Rep*, 13(4), pp. 378-85.

- Grenier, K., McLelland, G. L. and Fon, E. A. (2013) 'Parkin- and PINK1-Dependent Mitophagy in Neurons: Will the Real Pathway Please Stand Up?', *Front Neurol*, 4, pp. 100.
- Grünewald, A., Gegg, M. E., Taanman, J. W., King, R. H., Kock, N., Klein, C. and Schapira, A. H. (2009) 'Differential effects of PINK1 nonsense and missense mutations on mitochondrial function and morphology', *Exp Neurol*, 219(1), pp. 266-73.
- Guan, J. L., Simon, A. K., Prescott, M., Menendez, J. A., Liu, F., Wang, F., Wang, C., Wolvetang, E., Vazquez-Martin, A. and Zhang, J. (2013) 'Autophagy in stem cells', *Autophagy*, 9(6), pp. 830-49.
- Gupta, A., Meng, X., Zhu, L. J., Lawson, N. D. and Wolfe, S. A. (2011) 'Zinc finger protein-dependent and -independent contributions to the in vivo off-target activity of zinc finger nucleases', *Nucleic Acids Res*, 39(1), pp. 381-92.
- Gurkar, A. U., Chu, K., Raj, L., Bouley, R., Lee, S. H., Kim, Y. B., Dunn, S. E., Mandinova, A. and Lee, S. W. (2013) 'Identification of ROCK1 kinase as a critical regulator of Beclin1-mediated autophagy during metabolic stress', *Nat Commun*, 4, pp. 2189.
- Guzman, J. N., Sanchez-Padilla, J., Wokosin, D., Kondapalli, J., Ilijic, E., Schumacker, P. T. and Surmeier, D. J. (2010) 'Oxidant stress evoked by pacemaking in dopaminergic neurons is attenuated by DJ-1', *Nature*, 468(7324), pp. 696-700.
- Gwinn, D. M., Shackelford, D. B., Egan, D. F., Mihaylova, M. M., Mery, A., Vasquez, D. S., Turk, B. E. and Shaw, R. J. (2008) 'AMPK phosphorylation of raptor mediates a metabolic checkpoint', *Mol Cell*, 30(2), pp. 214-26.
- Haelterman, N. A., Yoon, W. H., Sandoval, H., Jaiswal, M., Shuiman, J. M. and Bellen, H. J. (2014) 'A mitocentric view of Parkinson's disease', *Annu Rev Neurosci*, 37, pp. 137-149.
- Ham, S. J., Lee, S. Y., Song, S., Chung, J. R., Choi, S. and Chung, J. (2016) 'Interaction between RING1 (R1) and the Ubiquitin-like (UBL) Domains Is Critical for the Regulation of Parkin Activity', *J Biol Chem*, 291(4), pp. 1803-16.
- Hammerling, B. C., Najor, R. H., Cortez, M. Q., Shires, S. E., Leon, L. J., Gonzalez, E. R., Boassa, D., Phan, S., Thor, A., Jimenez, R. E., Li, H., Kitsis, R. N., Dorn II, G. W., Sadoshima, J., Ellisman, M. H. and Gustafsson, Å. (2017) 'A

- Rab5 endosomal pathway mediates Parkin-dependent mitochondrial clearance', *Nat Commun*, 8, pp. 14050.
- Hanna, R. A., Quinsay, M. N., Orogo, A. M., Giang, K., Rikka, S. and Gustafsson, A. B. (2012) 'Microtubule-associated protein 1 light chain 3 (LC3) interacts with Bnip3 protein to selectively remove endoplasmic reticulum and mitochondria via autophagy', *J Biol Chem*, 287(23), pp. 19094-104.
- Hara, T., Takamura, A., Kishi, C., Iemura, S., Natsume, T., Guan, J. L. and Mizushima, N. (2008) 'FIP200, a ULK-interacting protein, is required for autophagosome formation in mammalian cells', *J Cell Biol*, 181(3), pp. 497-510.
- He, C. and Levine, B. (2010) 'The Beclin 1 interactome', *Curr Opin Cell Biol*, 22(2), pp. 140-9.
- Hegarty, S. V., Sullivan, A. M. and O'Keeffe, G. W. (2013) 'Midbrain dopaminergic neurons: a review of the molecular circuitry that regulates their development', *Dev Biol*, 379(2), pp. 123-38.
- Herrero-Mendez, A., Almeida, A., Fernandez, E., Maestre, C., Moncada, S. and Bolanos, J. P. (2009) 'The bioenergetic and antioxidant status of neurons is controlled by continuous degradation of a key glycolytic enzyme by APC/C-Cdh1', *Nat Cell Biol*, 11(6), pp. 747-52.
- Hirsch, E. C. and Hunot, S. (2009) 'Neuroinflammation in Parkinson's disease: a target for neuroprotection?', *Lancet Neurol*, 8, pp. 382-97.
- Hollenbeck, P. J. and Saxton, W. M. (2005) 'The axonal transport of mitochondria', *J Cell Sci*, 118(Pt 23), pp. 5411-9.
- Hosokawa, N., Hara, T., Kaizuka, T., Kishi, C., Takamura, A., Miura, Y., Iemura, S., Natsume, T., Takehana, K., Yamada, N., Guan, J. L., Oshiro, N. and Mizushima, N. (2009a) 'Nutrient-dependent mTORC1 association with the ULK1-Atg13-FIP200 complex required for autophagy', *Mol Biol Cell*, 20(7), pp. 1981-91.
- Hosokawa, N., Sasaki, T., Iemura, S., Natsume, T., Hara, T. and Mizushima, N. (2009b) 'Atg101, a novel mammalian autophagy protein interacting with Atg13', *Autophagy*, 5(7), pp. 973-979.
- Hu, B. Y., Weick, J. P., Yu, J., Ma, L. X., Zhang, X. Q., Thomson, J. A. and Zhang, S. C. (2010) 'Neural differentiation of human induced pluripotent stem cells

- follows developmental principles but with variable potency', *Proc Natl Acad Sci U S A*, 107(9), pp. 4335-40.
- Iguchi, M., Kujuro, Y., Okatsu, K., Koyano, F., Kosako, H., Kimura, M., Suzuki, N., Uchiyama, S., Tanaka, K. and Matsuda, N. (2013) 'Parkin-catalyzed ubiquitin-ester transfer is triggered by PINK1-dependent phosphorylation', *J Biol Chem*, 288(30), pp. 22019-32.
- Ikeda, Y., Shirakabe, A., Brady, C., Zablocki, D., Ohishi, M. and Sadoshima, J. (2015) 'Molecular mechanisms mediating mitochondrial dynamics and mitophagy and their functional roles in the cardiovascular system', *J Mol Cell Cardiol*, 78, pp. 116-22.
- Imaizumi, Y., Okada, Y., Akamatsu, W., Koike, M., Kuzumaki, N., Hayakawa, H., Nihira, T., Kobayashi, T., Ohyama, M., Sato, S., Takanashi, M., Funayama, M., Hirayama, A., Soga, T., Hishiki, T., Suematsu, M., Yagi, T., Ito, D., Kosakai, A., Hayashi, K., Shouji, M., Nakanishi, A., Suzuki, N., Mizuno, Y., Mizushima, N., Amagai, M., Uchiyama, Y., Mochizuki, H., Hattori, N. and Okano, H. (2012) 'Mitochondrial dysfunction associated with increased oxidative stress and alpha-synuclein accumulation in PARK2 iPSC-derived neurons and postmortem brain tissue', *Mol Brain*, 5, pp. 35.
- Inoki, K., Zhu, T. and Guan, K. L. (2003) 'TSC2 mediates cellular energy response to control cell growth and survival', *Cell*, 115, pp. 577-590.
- Itakura, E., Kishi-Itakura, C., Koyama-Honda, I. and Mizushima, N. (2012) 'Structures containing Atg9A and the ULK1 complex independently target depolarized mitochondria at initial stages of Parkin-mediated mitophagy', *J Cell Sci*, 125(Pt 6), pp. 1488-99.
- Itakura, E. and Mizushima, N. (2010) 'Characterization of autophagosome formation site by a hierarchical analysis of mammalian Atg proteins', *Autophagy*, 6(6), pp. 764-776.
- Ivankovic, D., Chau, K. Y., Schapira, A. H. and Gegg, M. E. (2016) 'Mitochondrial and lysosomal biogenesis are activated following PINK1/parkin-mediated mitophagy', *J Neurochem*, 136(2), pp. 388-402.
- Jacquín, E., Leclerc-Mercier, S., Judon, C., Blanchard, E., Fraïtag, S. and Florey, O. (2017) 'Pharmacological modulators of autophagy activate a parallel noncanonical pathway driving unconventional LC3 lipidation', *Autophagy*, 13(5), pp. 854-867.

- Jellinger, K. A. (2009) 'A critical evaluation of current staging of alpha-synuclein pathology in Lewy body disorders', *Biochim Biophys Acta*, 1792(7), pp. 730-40.
- Jiang, H., Ren, Y., Yuen, E. Y., Zhong, P., Ghaedi, M., Hu, Z., Azabdaftari, G., Nakaso, K., Yan, Z. and Feng, J. (2012) 'Parkin controls dopamine utilization in human midbrain dopaminergic neurons derived from induced pluripotent stem cells', *Nat Commun*, 3, pp. 668.
- Jiao, H., Su, G. Q., Dong, W., Zhang, L., Xie, W., Yao, L. M., Chen, P., Wang, Z. X., Liou, Y. C. and You, H. (2015) 'Chaperone-like protein p32 regulates ULK1 stability and autophagy', *Cell Death Differ*.
- Jin, S. M., Lazarou, M., Wang, C., Kane, L. A., Narendra, D. P. and Youle, R. J. (2010) 'Mitochondrial membrane potential regulates PINK1 import and proteolytic destabilization by PARL', *J Cell Biol*, 191(5), pp. 933-42.
- Jin, S. M. and Youle, R. J. (2012) 'PINK1- and Parkin-mediated mitophagy at a glance', *J Cell Sci*, 125(Pt 4), pp. 795-9.
- Johansen, T. and Lamark, T. (2011) 'Selective autophagy mediated by autophagic adapter proteins', *Autophagy*, 7(3), pp. 279-96.
- Joo, J. H., Dorsey, F. C., Joshi, A., Hennessy-Walters, K. M., Rose, K. L., McCastlain, K., Zhang, J., Iyengar, R., Jung, C. H., Suen, D. F., Steeves, M. A., Yang, C. Y., Prater, S. M., Kim, D. H., Thompson, C. B., Youle, R. J., Ney, P. A., Cleveland, J. L. and Kundu, M. (2011) 'Hsp90-Cdc37 chaperone complex regulates Ulk1- and Atg13-mediated mitophagy', *Mol Cell*, 43(4), pp. 572-85.
- Joselin, A. P., Hewitt, S. J., Callaghan, S. M., Kim, R. H., Chung, Y. H., Mak, T. W., Shen, J., Slack, R. S. and Park, D. S. (2012) 'ROS-dependent regulation of Parkin and DJ-1 localization during oxidative stress in neurons', *Hum Mol Genet*, 21(22), pp. 4888-903.
- Jung, C. H., Jun, C. B., Ro, S. H., Kim, Y. M., Otto, N. M., Cao, J., Kundu, M. and Kim, D. H. (2009) 'ULK-Atg13-FIP200 complexes mediate mTOR signaling to the autophagy machinery', *Mol Biol Cell*, 20(7), pp. 1992-2003.
- Kabeya, Y., Mizushima, N., Ueno, T., Yamamoto, A., Kirisako, T., Noda, T., Kominami, E., Ohsumi, Y. and Yoshimori, T. (2000) 'LC3, a mammalian homologue of yeast Apg8p, is localized in autophagosome membranes after processing', *EMBO J*, 19(21), pp. 5720-8.

- Kabeya, Y., Mizushima, N., Yamamoto, A., Oshitani-Okamoto, S., Ohsumi, Y. and Yoshimori, T. (2004) 'LC3, GABARAP and GATE16 localize to autophagosomal membrane depending on form-II formation', *J Cell Sci*, 117(Pt 13), pp. 2805-12.
- Kageyama, Y., Zhang, Z., Roda, R., Fukaya, M., Wakabayashi, J., Wakabayashi, N., Kensler, T. W., Reddy, P. H., Iijima, M. and Sesaki, H. (2012) 'Mitochondrial division ensures the survival of postmitotic neurons by suppressing oxidative damage', *J Cell Biol*, 197(4), pp. 535-51.
- Kane, L. A., Lazarou, M., Fogel, A. I., Li, Y., Yamano, K., Sarraf, S. A., Banerjee, S. and Youle, R. J. (2014) 'PINK1 phosphorylates ubiquitin to activate Parkin E3 ubiquitin ligase activity', *J Cell Biol*, 205(2), pp. 143-53.
- Kawajiri, S., Saiki, S., Sato, S., Sato, F., Hatano, T., Eguchi, H. and Hattori, N. (2010) 'PINK1 is recruited to mitochondria with parkin and associates with LC3 in mitophagy', *FEBS Lett*, 584(6), pp. 1073-9.
- Kazlauskaite, A., Kondapalli, C., Gourlay, R., Campbell, D. G., Ritorto, M. S., Hofmann, K., Alessi, D. R., Knebel, A., Trost, M. and Muqit, M. M. (2014) 'Parkin is activated by PINK1-dependent phosphorylation of ubiquitin at Ser65', *Biochem J*, 460(1), pp. 127-39.
- Kim, I. and Lemasters, J. J. (2011a) 'Mitochondrial degradation by autophagy (mitophagy) in GFP-LC3 transgenic hepatocytes during nutrient deprivation', *Am J Physiol Cell Physiol*, 300(2), pp. C308-17.
- Kim, I. and Lemasters, J. J. (2011b) 'Mitophagy selectively degrades individual damaged mitochondria after photoirradiation', *Antioxid Redox Signal*, 14(10), pp. 1919-28.
- Kim, J., Kim, Y. C., Fang, C., Russell, R. C., Kim, J. H., Fan, W., Liu, R., Zhong, Q. and Guan, K. L. (2013) 'Differential regulation of distinct Vps34 complexes by AMPK in nutrient stress and autophagy', *Cell*, 152(1-2), pp. 290-303.
- Kim, J., Kundu, M., Viollet, B. and Guan, K. L. (2011) 'AMPK and mTOR regulate autophagy through direct phosphorylation of Ulk1', *Nat Cell Biol*, 13(2), pp. 132-41.
- Kim, Y., Park, J., Kim, S., Song, S., Kwon, S. K., Lee, S. H., Kitada, T., Kim, J. M. and Chung, J. (2008) 'PINK1 controls mitochondrial localization of Parkin through direct phosphorylation', *Biochem Biophys Res Commun*, 377(3), pp. 975-80.

- Ko, H. C. and Gelb, B. D. (2014) 'Concise review: drug discovery in the age of the induced pluripotent stem cell', *Stem Cells Transl Med*, 3(4), pp. 500-9.
- Kondapalli, C., Kazlauskaitė, A., Zhang, N., Woodroof, H. I., Campbell, D. G., Gourlay, R., Burchell, L., Walden, H., Macartney, T. J., Deak, M., Knebel, A., Alessi, D. R. and Muqit, M. M. (2012) 'PINK1 is activated by mitochondrial membrane potential depolarization and stimulates Parkin E3 ligase activity by phosphorylating Serine 65', *Open Biol*, 2(5), pp. 120080.
- Kondoh, H., Leonart, M. E., Nakashima, Y., Yokode, M., Tanaka, M., Bernard, D., Gil, J. and Beach, D. (2007) 'A high glycolytic flux supports the proliferative potential of murine embryonic stem cells', *Antioxid Redox Signal*, 9(3), pp. 293-9.
- Konovalova, E. V., Lopacheva, O. M., Grivennikov, I. A., Lebedeva, O. S., Dashinimaev, E. B., Khaspekov, L. G., Fedotova, E. Y. and Illarioshkin, S. N. (2015) 'Mutations in the Parkinson's Disease-Associated PARK2 Gene Are Accompanied by Imbalance in Programmed Cell Death Systems', *Acta Naturae*, 7(4), pp. 146-9.
- Koshiba, T., Detmer, S. A., Kaiser, J. T., Chen, H., McCaffery, J. M. and Chan, C. H. (2004) 'Structural basis of mitochondrial tethering by mitofusin complexes', *Science*, 305, pp. 858-862.
- Koyano, F., Okatsu, K., Ishigaki, S., Fujioka, Y., Kimura, M., Sobue, G., Tanaka, K. and Matsuda, N. (2013) 'The principal PINK1 and Parkin cellular events triggered in response to dissipation of mitochondrial membrane potential occur in primary neurons', *Genes Cells*, 18(8), pp. 672-81.
- Koyano, F., Okatsu, K., Kosako, H., Tamura, Y., Go, E., Kimura, M., Kimura, Y., Tsuchiya, H., Yoshihara, H., Hirokawa, T., Endo, T., Fon, E. A., Trempe, J. F., Saeki, Y., Tanaka, K. and Matsuda, N. (2014) 'Ubiquitin is phosphorylated by PINK1 to activate parkin', *Nature*, 510(7503), pp. 162-6.
- Kriks, S., Shim, J. W., Piao, J., Ganat, Y. M., Wakeman, D. R., Xie, Z., Carrillo-Reid, L., Auyeung, G., Antonacci, C., Buch, A., Yang, L., Beal, M. F., Surmeier, D. J., Kordower, J. H., Tabar, V. and Studer, L. (2011) 'Dopamine neurons derived from human ES cells efficiently engraft in animal models of Parkinson's disease', *Nature*, 480(7378), pp. 547-51.
- Kundu, M., Lindsten, T., Yang, C. Y., Wu, J., Zhao, F., Zhang, J., Selak, M. A., Ney, P. A. and Thompson, C. B. (2008) 'Ulk1 plays a critical role in the autophagic

- clearance of mitochondria and ribosomes during reticulocyte maturation', *Blood*, 112(4), pp. 1493-502.
- Lahti, L., Peltopuro, P., Piepponen, T. P. and Partanen, J. (2012) 'Cell-autonomous FGF signaling regulates anteroposterior patterning and neuronal differentiation in the mesodiencephalic dopaminergic progenitor domain', *Development*, 139(5), pp. 894-905.
- Laplante, M. and Sabatini, D. M. (2009) 'mTOR signaling at a glance', *J Cell Sci*, 122(Pt 20), pp. 3589-94.
- Laurent, L. C., Ulitsky, I., Slavin, I., Tran, H., Schork, A., Morey, R., Lynch, C., Harness, J. V., Lee, S., Barrero, M. J., Ku, S., Martynova, M., Semechkin, R., Galat, V., Gottesfeld, J., Izpisua Belmonte, J. C., Murry, C., Keirstead, H. S., Park, H. S., Schmidt, U., Laslett, A. L., Muller, F. J., Nievergelt, C. M., Shamir, R. and Loring, J. F. (2011) 'Dynamic changes in the copy number of pluripotency and cell proliferation genes in human ESCs and iPSCs during reprogramming and time in culture', *Cell Stem Cell*, 8(1), pp. 106-18.
- Lazarou, M., Jin, S. M., Kane, L. A. and Youle, R. J. (2012) 'Role of PINK1 binding to the TOM complex and alternate intracellular membranes in recruitment and activation of the E3 ligase Parkin', *Dev Cell*, 22(2), pp. 320-33.
- Lazarou, M., Narendra, D. P., Jin, S. M., Tekle, E., Banerjee, S. and Youle, R. J. (2013) 'PINK1 drives Parkin self-association and HECT-like E3 activity upstream of mitochondrial binding', *J Cell Biol*, 200(2), pp. 163-72.
- Lazarou, M., Sliter, D. A., Kane, L. A., Sarraf, S. A., Wang, C., Burman, J. L., Sideris, D. P., Fogel, A. I. and Youle, R. J. (2015) 'The ubiquitin kinase PINK1 recruits autophagy receptors to induce mitophagy', *Nature*, 524(7565), pp. 309-314.
- Lee, E. J. and Tournier, C. (2011) 'The requirement of uncoordinated 51-like kinase 1 (ULK1) and ULK2 in the regulation of autophagy', *Autophagy*, 7(7), pp. 689-95.
- Lee, J. Y., Nagano, Y., Taylor, J. P., Lim, K. L. and Yao, T. P. (2010) 'Disease-causing mutations in parkin impair mitochondrial ubiquitination, aggregation, and HDAC6-dependent mitophagy', *J Cell Biol*, 189(4), pp. 671-9.
- Lee, S., Sterky, F. H., Mourier, A., Terzioglu, M., Cullheim, S., Olson, L. and Larsson, N. G. (2012) 'Mitofusin 2 is necessary for striatal axonal projections of midbrain dopamine neurons', *Hum Mol Genet*, 21(22), pp. 4827-35.

- Lee, S., Zhang, C. and Liu, X. (2015) 'Role of glucose metabolism and ATP in maintaining PINK1 levels during Parkin-mediated mitochondrial damage responses', *J Biol Chem*, 290(2), pp. 904-17.
- Lee, Y. J., Jeong, S. Y., Karbowski, M., Smith, C. L. and Youle, R. J. (2004) 'Roles of the mammalian mitochondrial fission and fusion mediators Fis1, Drp1, and Opa1 in apoptosis', *Mol Biol Cell*, 15(11), pp. 5001-11.
- Legros, F., Lombès, A., Frachon, P. and Rojo, M. (2002) 'Mitochondrial fusion in human cells is efficient, requires the inner membrane potential, and is mediated by mitofusins', *Mol Biol Cell*, 13(12), pp. 4343-54.
- Lemasters, J. J. (2014) 'Variants of mitochondrial autophagy: Types 1 and 2 mitophagy and micromitophagy (Type 3)', *Redox Biol*, 2, pp. 749-54.
- Li, H., Chen, Y., Jones, A. F., Sanger, R. H., Collis, L. P., Flannery, R., McNay, E. C., Yu, T., Schwarzenbacher, R., Bossy, B., Bossy-Wetzell, E., Bennett, M. V., Pypaert, M., Hickman, J. A., Smith, P. J., Hardwick, J. M. and Jonas, E. A. (2008) 'Bcl-xL induces Drp1-dependent synapse formation in cultured hippocampal neurons', *Proc Natl Acad Sci U S A*, 105(6), pp. 2169-74.
- Li, L., Kim, E., Yuan, H., Inoki, K., Goraksha-Hicks, P., Schiesher, R. L., Neufeld, T. P. and Guan, K. L. (2010) 'Regulation of mTORC1 by the Rab and Arf GTPases', *J Biol Chem*, 285(26), pp. 19705-9.
- Li, W., Chen, S. and Li, J. Y. (2015) 'Human induced pluripotent stem cells in Parkinson's disease: A novel cell source of cell therapy and disease modeling', *Prog Neurobiol*, 134, pp. 161-77.
- Li, W., Sun, W., Zhang, Y., Wei, W., Ambasudhan, R., Xia, P., Talantova, M., Lin, T., Kim, J., Wang, X., Kim, W. R., Lipton, S. A., Zhang, K. and Ding, S. (2011) 'Rapid induction and long-term self-renewal of primitive neural precursors from human embryonic stem cells by small molecule inhibitors', *Proc Natl Acad Sci U S A*, 108(20), pp. 8299-304.
- Li, Z., Okamoto, K., Hayashi, Y. and Sheng, M. (2004) 'The importance of dendritic mitochondria in the morphogenesis and plasticity of spines and synapses', *Cell*, 119(6), pp. 873-87.
- Liang, C., Feng, P., Ku, B., Dotan, I., Canaani, D., Oh, B. H. and Jung, J. U. (2006) 'Autophagic and tumour suppressor activity of a novel Beclin1-binding protein UVRAG', *Nat Cell Biol*, 8(7), pp. 688-99.

- Liang, C., Lee, J. S., Inn, K. S., Gack, M. U., Li, Q., Roberts, E. A., Vergne, I., Deretic, V., Feng, P., Akazawa, C. and Jung, J. U. (2008) 'Beclin1-binding UVRAG targets the class C Vps complex to coordinate autophagosome maturation and endocytic trafficking', *Nat Cell Biol*, 10(7), pp. 776-87.
- Lin, W., Metzakopian, E., Mavromatakis, Y. E., Gao, N., Balaskas, N., Sasaki, H., Briscoe, J., Whitsett, J. A., Goulding, M., Kaestner, K. H. and Ang, S. L. (2009) 'Foxa1 and Foxa2 function both upstream of and cooperatively with Lmx1a and Lmx1b in a feedforward loop promoting mesodiencephalic dopaminergic neuron development', *Dev Biol*, 333(2), pp. 386-96.
- Liu, L., Feng, D., Chen, G., Chen, M., Zheng, Q., Song, P., Ma, Q., Zhu, C., Wang, R., Qi, W., Huang, L., Xue, P., Li, B., Wang, X., Jin, H., Wang, J., Yang, F., Liu, P., Zhu, Y., Sui, S. and Chen, Q. (2012) 'Mitochondrial outer-membrane protein FUNDC1 mediates hypoxia-induced mitophagy in mammalian cells', *Nat Cell Biol*, 14(2), pp. 177-85.
- Liu, W., Deng, Y., Liu, Y., Gong, W. and Deng, W. (2013) 'Stem cell models for drug discovery and toxicology studies', *J Biochem Mol Toxicol*, 27(1), pp. 17-27.
- Lodish, H., Berk, A., Zipursky, S. L., Matsudaira, P., Baltimore, D. and Darnell, J. (2000) *Molecular Cell Biology*. 4 edn. New York: W. H. Freeman.
- Lonergan, T., Bavister, B. and Brenner, C. (2007) 'Mitochondria in stem cells', *Mitochondrion*, 7(5), pp. 289-96.
- Lutz, A. K., Exner, N., Fett, M. E., Schlehe, J. S., Kloos, K., Lammermann, K., Brunner, B., Kurz-Drexler, A., Vogel, F., Reichert, A. S., Bouman, L., Vogt-Weisenhorn, D., Wurst, W., Tatzelt, J., Haass, C. and Winklhofer, K. F. (2009) 'Loss of parkin or PINK1 function increases Drp1-dependent mitochondrial fragmentation', *J Biol Chem*, 284(34), pp. 22938-51.
- Ma, L., Chen, Z., Erdjument-Bromage, H., Tempst, P. and Pandolfi, P. P. (2005) 'Phosphorylation and functional inactivation of TSC2 by Erk implications for tuberous sclerosis and cancer pathogenesis', *Cell*, 121(2), pp. 179-93.
- Ma, X., Jin, M., Cai, Y., Xia, H., Long, K., Liu, J., Yu, Q. and Yuan, J. (2011) 'Mitochondrial electron transport chain complex III is required for antimycin A to inhibit autophagy', *Chem Biol*, 18(11), pp. 1474-81.
- MacVicar, T. D. and Lane, J. D. (2014) 'Impaired OMA1-dependent cleavage of OPA1 and reduced DRP1 fission activity combine to prevent mitophagy in

- cells that are dependent on oxidative phosphorylation', *J Cell Sci*, 127(Pt 10), pp. 2313-25.
- Maejima, Y., Chen, Y., Isobe, M., Gustafsson, Å., Kitsis, R. N. and Sadoshima, J. (2015) 'Recent progress in research on molecular mechanisms of autophagy in the heart', *Am J Physiol Heart Circ Physiol*, 308(4), pp. H259-68.
- Mandal, S., Lindgren, A. G., Srivastava, A. S., Clark, A. T. and Banerjee, U. (2011) 'Mitochondrial function controls proliferation and early differentiation potential of embryonic stem cells', *Stem Cells*, 29(3), pp. 486-95.
- Margulis, L. (1970) *Origin of Eukaryotic Cells. Evidence and Research Implications for a Theory of the Origin and Evolution of Microbial, Plant, and Animal Cells on the Precambrian Earth*. New Haven-London: Yale University Press.
- Margulis, L. (1981) *Symbiosis in Cell Evolution. Life and its Environment on the Early Earth*. San Francisco: W.H. Freeman and Co.
- Martinez, T. N. and Greenamyre, J. T. (2012) 'Toxin models of mitochondrial dysfunction in Parkinson's disease', *Antioxid Redox Signal*, 16(9), pp. 920-34.
- Matsumoto, G., Shimogori, T., Hattori, N. and Nukina, N. (2015) 'TBK1 controls autophagosomal engulfment of polyubiquitinated mitochondria through p62/SQSTM1 phosphorylation', *Hum Mol Genet*, 24(15), pp. 4429-42.
- Matsunaga, K., Morita, E., Saitoh, T., Akira, S., Ktistakis, N. T., Izumi, T., Noda, T. and Yoshimori, T. (2010) 'Autophagy requires endoplasmic reticulum targeting of the PI3-kinase complex via Atg14L', *J Cell Biol*, 190(4), pp. 511-21.
- Matsunaga, K., Saitoh, T., Tabata, K., Omori, H., Satoh, T., Kurotori, N., Maejima, I., Shirahama-Noda, K., Ichimura, T., Isobe, T., Akira, S., Noda, T. and Yoshimori, T. (2009) 'Two Beclin 1-binding proteins, Atg14L and Rubicon, reciprocally regulate autophagy at different stages', *Nat Cell Biol*, 11(4), pp. 385-96.
- McAlpine, F., Williamson, L. E., Tooze, S. A. and Chan, E. Y. (2013) 'Regulation of nutrient-sensitive autophagy by uncoordinated 51-like kinases 1 and 2', *Autophagy*, 9(3), pp. 361-73.
- McCoy, M. K., Kaganovich, A., Rudenko, I. N., Ding, J. and Cookson, M. R. (2014) 'Hexokinase activity is required for recruitment of parkin to depolarized mitochondria', *Hum Mol Genet*, 23(1), pp. 145-56.

- McKnight, N. C., Zhong, Y., Wold, M. S., Gong, S., Phillips, G. R., Dou, Z., Zhao, Y., Heintz, N., Zong, W. X. and Yue, Z. (2014) 'Beclin 1 is required for neuron viability and regulates endosome pathways via the UVRAG-VPS34 complex', *PLoS Genet*, 10(10), pp. e1004626.
- Meissner, C., Lorenz, H., Weihofen, A., Selkoe, D. J. and Lemberg, M. K. (2011) 'The mitochondrial intramembrane protease PARL cleaves human Pink1 to regulate Pink1 trafficking', *J Neurochem*, 117(5), pp. 856-67.
- Melemedjian, O. K., Khoutorsky, A., Sorge, R. E., Yan, J., Asiedu, M. N., Valdez, A., Ghosh, S., Dussor, G., Mogil, J. S., Sonenberg, N. and Price, T. J. (2013) 'mTORC1 inhibition induces pain via IRS-1-dependent feedback activation of ERK', *Pain*, 154(7), pp. 1080-91.
- Menzies, R. A. and Gold, P. H. (1971) 'The turnover of mitochondria in a variety of tissues of young adult and aged rats', *J Biol Chem*, 246(8), pp. 2425-2429.
- Mercer, C. A., Kaliappan, A. and Dennis, P. B. (2009) 'A novel, human Atg13 binding protein, Atg101, interacts with ULK1 and is essential for macroautophagy', *Autophagy*, 5(5), pp. 649-662.
- Michiorri, S., Gelmetti, V., Giarda, E., Lombardi, F., Romano, F., Marongiu, R., Nerini-Molteni, S., Sale, P., Vago, R., Arena, G., Torosantucci, L., Cassina, L., Russo, M. A., Dallapiccola, B., Valente, E. M. and Casari, G. (2010) 'The Parkinson-associated protein PINK1 interacts with Beclin1 and promotes autophagy', *Cell Death Differ*, 17(6), pp. 962-74.
- Miura, K., Kodama, Y., Inokuchi, S., Schnabl, B., Aoyama, T., Ohnishi, H., Olefsky, J. M., Brenner, D. A. and Seki, E. (2010) 'Toll-like receptor 9 promotes steatohepatitis by induction of interleukin-1beta in mice', *Gastroenterology*, 139(1), pp. 323-34 e7.
- Mizushima, N. (1998) 'A New Protein Conjugation System in Human. THE COUNTERPART OF THE YEAST Apg12p CONJUGATION SYSTEM ESSENTIAL FOR AUTOPHAGY', *Journal of Biological Chemistry*, 273(51), pp. 33889-33892.
- Mizushima, N. (2003) 'Mouse Apg16L, a novel WD-repeat protein, targets to the autophagic isolation membrane with the Apg12-Apg5 conjugate', *Journal of Cell Science*, 116(9), pp. 1679-1688.
- Mizushima, N., Yamamoto, A., Hatano, M., Kobayashi, Y., Kabeya, Y., Suzuki, K., Tokuhiya, T., Ohsumi, Y. and Yoshimori, T. (2001) 'Dissection of

- autophagosome formation using Apg5-deficient mouse embryonic stem cells', *The Journal of Cell Biology*, 152, pp. 657-667.
- Mizushima, N., Yoshimori, T. and Ohsumi, Y. (2002) 'Mouse Apg10 as an Apg12-conjugating enzyme: analysis by the conjugation-mediated yeast two-hybrid method', *FEBS Lett*, 532, pp. 450-454.
- Molinoff, P. B. and Axelrod, J. (1971) 'Biochemistry of catecholamines', *Annu Rev Biochem*, (40), pp. 465-500.
- Morais, V. A., Haddad, D., Craessaerts, K., De Bock, P. J., Swerts, J., Vilain, S., Aerts, L., Overbergh, L., Grünewald, A., Seibler, P., Klein, C., Gevaert, K., Verstreken, P. and De Strooper, B. (2014) 'PINK1 loss-of-function mutations affect mitochondrial complex I activity via NdufA10 ubiquinone uncoupling', *Science*, 344(6180), pp. 203-7.
- Morais, V. A., Verstreken, P., Roethig, A., Smet, J., Snellinx, A., Vanbrabant, M., Haddad, D., Frezza, C., Mandemakers, W., Vogt-Weisenhorn, D., Van Coster, R., Wurst, W., Scorrano, L. and De Strooper, B. (2009) 'Parkinson's disease mutations in PINK1 result in decreased Complex I activity and deficient synaptic function', *EMBO Mol Med*, 1(2), pp. 99-111.
- Mouton-Liger, F., Jacoupy, M., Corvol, J. C. and Corti, O. (2017) 'PINK1/Parkin-Dependent Mitochondrial Surveillance: From Pleiotropy to Parkinson's Disease', *Front Mol Neurosci*, 10, pp. 120.
- Murakawa, T., Yamaguchi, O., Hashimoto, A., Hikoso, S., Takeda, T., Oka, T., Yasui, H., Ueda, H., Akazawa, Y., Nakayama, H., Taneike, M., Misaka, T., Omiya, S., Shah, A. M., Yamamoto, A., Nishida, K., Ohsumi, Y., Okamoto, K., Sakata, Y. and Otsu, K. (2015) 'Bcl-2-like protein 13 is a mammalian Atg32 homologue that mediates mitophagy and mitochondrial fragmentation', *Nat Commun*, 6, pp. 7527.
- Nakahira, K., Haspel, J. A., Rathinam, V. A., Lee, S. J., Dolinay, T., Lam, H. C., Englert, J. A., Rabinovitch, M., Cernadas, M., Kim, H. P., Fitzgerald, K. A., Ryter, S. W. and Choi, A. M. (2011) 'Autophagy proteins regulate innate immune responses by inhibiting the release of mitochondrial DNA mediated by the NALP3 inflammasome', *Nat Immunol*, 12(3), pp. 222-30.
- Nakamura, K. (2013) ' α -Synuclein and mitochondria: partners in crime?', *Neurotherapeutics*, 10(3), pp. 391-9.

- Nakamura, S., Ito, Y., Shirasaki, R. and Murakami, F. (2000) 'Local directional cues control growth polarity of dopaminergic axons along the rostrocaudal axis', *J Neurosci*, 20(11), pp. 4112-9.
- Nakamura, S. and Yoshimori, T. (2017) 'New insights into autophagosome-lysosome fusion', *J Cell Sci*, 130(7), pp. 1209-1216.
- Narendra, D., Kane, L. A., Hauser, D. N., Fearnley, I. M. and Youle, R. J. (2010a) 'p62/SQSTM1 is required for Parkin-induced mitochondrial clustering but not mitophagy; VDAC1 is dispensable for both', *Autophagy*, 6(8), pp. 1090-1106.
- Narendra, D., Kane, L. A., Hauser, D. N., Fearnley, I. M. and Youle, R. J. (2014) 'p62/SQSTM1 is required for Parkin-induced mitochondrial clustering but not mitophagy; VDAC1 is dispensable for both', *Autophagy*, 6(8), pp. 1090-1106.
- Narendra, D., Tanaka, A., Suen, D. F. and Youle, R. J. (2008) 'Parkin is recruited selectively to impaired mitochondria and promotes their autophagy', *J Cell Biol*, 183(5), pp. 795-803.
- Narendra, D. P., Jin, S. M., Tanaka, A., Suen, D. F., Gautier, C. A., Shen, J., Cookson, M. R. and Youle, R. J. (2010b) 'PINK1 is selectively stabilized on impaired mitochondria to activate Parkin', *PLoS Biol*, 8(1), pp. e1000298.
- Nelson, D. L., Lehninger, A. L. and Cox, M. M. (2008) *Lehninger Principles of Biochemistry*. 5 edn. New York: W. H. Freeman.
- Neupert, W. and Herrmann, J. M. (2007) 'Translocation of proteins into mitochondria', *Annu Rev Biochem*, 76, pp. 723-49.
- Nixon, R. A. (2013) 'The role of autophagy in neurodegenerative disease', *Nat Med*, 19(8), pp. 983-97.
- Noda, N. N., Ohsumi, Y. and Inagaki, F. (2010) 'Atg8-family interacting motif crucial for selective autophagy', *FEBS Lett*, 584(7), pp. 1379-85.
- Novak, I., Kirkin, V., McEwan, D. G., Zhang, J., Wild, P., Rozenknop, A., Rogov, V., Lohr, F., Popovic, D., Occhipinti, A., Reichert, A. S., Terzic, J., Dotsch, V., Ney, P. A. and Dikic, I. (2010) 'Nix is a selective autophagy receptor for mitochondrial clearance', *EMBO Rep*, 11(1), pp. 45-51.
- O'Toole, M., Latham, R., Baqri, R. M. and Miller, K. E. (2008) 'Modeling mitochondrial dynamics during in vivo axonal elongation', *J Theor Biol*, 255(4), pp. 369-77.
- Oka, T., Hikoso, S., Yamaguchi, O., Taneike, M., Takeda, T., Tamai, T., Oyabu, J., Murakawa, T., Nakayama, H., Nishida, K., Akira, S., Yamamoto, A., Komuro,

- I. and Otsu, K. (2012) 'Mitochondrial DNA that escapes from autophagy causes inflammation and heart failure', *Nature*, 485(7397), pp. 251-5.
- Okamoto, K. (2014) 'Organellophagy: eliminating cellular building blocks via selective autophagy', *J Cell Biol*, 205(4), pp. 435-45.
- Okatsu, K., Oka, T., Iguchi, M., Imamura, K., Kosako, H., Tani, N., Kimura, M., Go, E., Koyano, F., Funayama, M., Shiba-Fukushima, K., Sato, S., Shimizu, H., Fukunaga, Y., Taniguchi, H., Komatsu, M., Hattori, N., Mihara, K., Tanaka, K. and Matsuda, N. (2012) 'PINK1 autophosphorylation upon membrane potential dissipation is essential for Parkin recruitment to damaged mitochondria', *Nat Commun*, 3, pp. 1016.
- Okatsu, K., Saisho, K., Shimanuki, M., Nakada, K., Shitara, H., Sou, Y. S., Kimura, M., Sato, S., Hattori, N., Komatsu, M., Tanaka, K. and Matsuda, N. (2010) 'p62/SQSTM1 cooperates with Parkin for perinuclear clustering of depolarized mitochondria', *Genes Cells*, 15(8), pp. 887-900.
- Okatsu, K., Uno, M., Koyano, F., Go, E., Kimura, M., Oka, T., Tanaka, K. and Matsuda, N. (2013) 'A dimeric PINK1-containing complex on depolarized mitochondria stimulates Parkin recruitment', *J Biol Chem*, 288(51), pp. 36372-84.
- Oliveira, L. M., Falomir-Lockhart, L. J., Botelho, M. G., Lin, K. H., Wales, P., Koch, J. C., Gerhardt, E., Taschenberger, H., Outeiro, T. F., Lingor, P., Schüle, B., Arndt-Jovin, D. J. and Jovin, T. M. (2015) 'Elevated α -synuclein caused by SNCA gene triplication impairs neuronal differentiation and maturation in Parkinson's patient-derived induced pluripotent stem cells', *Cell Death Dis*, 6, pp. e1994.
- Ono, Y., Nakatani, T., Minaki, Y. and Kumai, M. (2010) 'The basic helix-loop-helix transcription factor Nato3 controls neurogenic activity in mesencephalic floor plate cells', *Development*, 137(11), pp. 1897-906.
- Ono, Y., Nakatani, T., Sakamoto, Y., Mizuhara, E., Minaki, Y., Kumai, M., Hamaguchi, A., Nishimura, M., Inoue, Y., Hayashi, H., Takahashi, J. and Imai, T. (2007) 'Differences in neurogenic potential in floor plate cells along an anteroposterior location: midbrain dopaminergic neurons originate from mesencephalic floor plate cells', *Development*, 134(17), pp. 3213-25.
- Ordureau, A., Sarraf, S. A., Duda, D. M., Heo, J. M., Jedrychowski, M. P., Sviderskiy, V. O., Olszewski, J. L., Koerber, J. T., Xie, T., Beausoleil, S. A., Wells, J. A.,

- Gygi, S. P., Schulman, B. A. and Harper, J. W. (2014) 'Quantitative proteomics reveal a feedforward mechanism for mitochondrial PARKIN translocation and ubiquitin chain synthesis', *Mol Cell*, 56(3), pp. 360-75.
- Osellame, L. D., Blacker, T. S. and Duchen, M. R. (2012) 'Cellular and molecular mechanisms of mitochondrial function', *Best Pract Res Clin Endocrinol Metab*, 26(6), pp. 711-23.
- Padman, B. S., Bach, M., Lucarelli, G., Prescott, M. and Ramm, G. (2013) 'The protonophore CCCP interferes with lysosomal degradation of autophagic cargo in yeast and mammalian cells', *Autophagy*, 9(11), pp. 1862-75.
- Palay, S. L. (1956) 'Synapses in the central nervous system', *J Biophysic and Biochem Cytol*, 2(4), pp. 193-202.
- Pankiv, S., Clausen, T. H., Lamark, T., Brech, A., Bruun, J. A., Outzen, H., Overvatn, A., Bjorkoy, G. and Johansen, T. (2007) 'p62/SQSTM1 binds directly to Atg8/LC3 to facilitate degradation of ubiquitinated protein aggregates by autophagy', *J Biol Chem*, 282(33), pp. 24131-45.
- Park, J., Lee, S. B., Lee, S., Kim, Y., Song, S., Kim, S., Bae, E., Kim, J., Shong, M., Kim, J. M. and Chung, J. (2006) 'Mitochondrial dysfunction in Drosophila PINK1 mutants is complemented by parkin', *Nature*, 441(7097), pp. 1157-61.
- Park, S., Lee, K. S., Lee, Y. J., Shin, H. A., Cho, H. Y., Wang, K. C., Kim, Y. S., Lee, H. T., Chung, K. S., Kim, E. Y. and Lim, J. (2004) 'Generation of dopaminergic neurons in vitro from human embryonic stem cells treated with neurotrophic factors', *Neurosci Lett*, 359(1-2), pp. 99-103.
- Parr, B. A., Shea, M. J., Vassileva, G. and McMahon, A. P. (1993) 'Mouse Wnt genes exhibit discrete domains of expression in the early embryonic CNS and limb buds', *Development*, 119(1), pp. 247-61.
- Pattingre, S., Tassa, A., Qu, X., Garuti, R., Liang, X. H., Mizushima, N., Packer, M., Schneider, M. D. and Levine, B. (2005) 'Bcl-2 antiapoptotic proteins inhibit Beclin 1-dependent autophagy', *Cell*, 122(6), pp. 927-39.
- Peng, J., Schwartz, D., Elias, J. E., Thoreen, C. C., Cheng, D., Marsischky, G., Roelofs, J., Finley, D. and Gygi, S. P. (2003) 'A proteomics approach to understanding protein ubiquitination', *Nat Biotechnol*, 21(8), pp. 921-926.
- Peter, C., Wesselborg, S., Herrmann, M. and Lauber, K. (2010) 'Dangerous attraction: phagocyte recruitment and danger signals of apoptotic and necrotic cells', *Apoptosis*, 15(9), pp. 1007-28.

- Petiot, A., Ogier-Denis, E., Blommaert, E. F., Meijer, A. J. and Codogno, P. (2000) 'Distinct classes of phosphatidylinositol 3'-kinases are involved in signaling pathways that control macroautophagy in HT-29 cells', *J Biol Chem*, 275(2), pp. 992-8.
- Phadwal, K., Watson, A. S. and Simon, A. K. (2013) 'Tightrope act: autophagy in stem cell renewal, differentiation, proliferation, and aging', *Cell Mol Life Sci*, 70(1), pp. 89-103.
- Pickart, C. M. and Eddins, M. J. (2004) 'Ubiquitin: structures, functions, mechanisms', *Biochim Biophys Acta*, 1695(1-3), pp. 55-72.
- Pryde, K. R., Smith, H. L., Chau, K. Y. and Schapira, A. H. (2016) 'PINK1 disables the anti-fission machinery to segregate damaged mitochondria for mitophagy', *J Cell Biol*, 213(2), pp. 163-71.
- Puelles, L. and Verney, C. (1998) 'Early neuromeric distribution of tyrosine-hydroxylase-immunoreactive neurons in human embryos', *J Comp Neurol*, 394(3), pp. 283-308.
- Qian, X., Li, X., Cai, Q., Zhang, C., Yu, Q., Jiang, Y., Lee, J. H., Hawke, D., Wang, Y., Xia, Y., Zheng, Y., Jiang, B. H., Liu, D. X., Jiang, T. and Lu, Z. (2017) 'Phosphoglycerate Kinase 1 Phosphorylates Beclin1 to Induce Autophagy', *Mol Cell*, 65(5), pp. 917-931.e6.
- Rakovic, A., Shurkewitsch, K., Seibler, P., Grünewald, A., Zanon, A., Hagenah, J., Krainc, D. and Klein, C. (2013) 'Phosphatase and tensin homolog (PTEN)-induced putative kinase 1 (PINK1)-dependent ubiquitination of endogenous Parkin attenuates mitophagy: study in human primary fibroblasts and induced pluripotent stem cell-derived neurons', *J Biol Chem*, 288(4), pp. 2223-37.
- Ravikumar, B., Imarisio, S., Sarkar, S., O'Kane, C. J. and Rubinsztein, D. C. (2008) 'Rab5 modulates aggregation and toxicity of mutant huntingtin through macroautophagy in cell and fly models of Huntington disease', *J Cell Sci*, 121(Pt 10), pp. 1649-60.
- Rawal, N., Castelo-Branco, G., Sousa, K. M., Kele, J., Kobayashi, K., Okano, H. and Arenas, E. (2006) 'Dynamic temporal and cell type-specific expression of Wnt signaling components in the developing midbrain', *Exp Cell Res*, 312(9), pp. 1626-36.
- Reeve, A., Simcox, E. and Turnbull, D. (2014) 'Ageing and Parkinson's disease: why is advancing age the biggest risk factor?', *Ageing Res Rev*, 14, pp. 19-30.

- Ren, Y., Jiang, H., Hu, Z., Fan, K., Wang, J., Janoschka, S., Wang, X., Ge, S. and Feng, J. (2015) 'Parkin mutations reduce the complexity of neuronal processes in iPSC-derived human neurons', *Stem Cells*, 33(1), pp. 68-78.
- Rhinn, M. and Brand, M. (2001) 'The midbrain--hindbrain boundary organizer', *Curr Opin Neurobiol*, 11(1), pp. 34-42.
- Ronan, B., Flamand, O., Vescovi, L., Dureuil, C., Durand, L., Fassy, F., Bachelot, M., Lamberton, A., Mathieu, M., Bertrand, T., Marquette, J., El-Ahmad, Y., Filoche-Romme, B., Schio, L., Garcia-Echeverria, C., Goulaouic, H. and Pasquier, B. (2014) 'A highly potent and selective Vps34 inhibitor alters vesicle trafficking and autophagy', *Nature Chemical Biology*, 10, pp. 1013-1019.
- Rubinsztein, D. C., Shpilka, T. and Elazar, Z. (2012) 'Mechanisms of autophagosome biogenesis', *Curr Biol*, 22(1), pp. R29-34.
- Russell, R. C., Tian, Y., Yuan, H., Park, H. W., Chang, Y. Y., Kim, J., Kim, H., Neufeld, T. P., Dillin, A. and Guan, K. L. (2013) 'ULK1 induces autophagy by phosphorylating Beclin-1 and activating VPS34 lipid kinase', *Nat Cell Biol*, 15(7), pp. 741-50.
- Russell, R. C., Yuan, H. X. and Guan, K. L. (2014) 'Autophagy regulation by nutrient signaling', *Cell Res*, 24(1), pp. 42-57.
- Saarimäki-Vire, J., Peltopuro, P., Lahti, L., Naserke, T., Blak, A. A., Vogt Weisenhorn, D. M., Yu, K., Ornitz, D. M., Wurst, W. and Partanen, J. (2007) 'Fibroblast growth factor receptors cooperate to regulate neural progenitor properties in the developing midbrain and hindbrain', *J Neurosci*, 27(32), pp. 8581-92.
- Saita, S., Shirane, M. and Nakayama, K. I. (2013) 'Selective escape of proteins from the mitochondria during mitophagy', *Nat Commun*, 4, pp. 1410.
- Sandoval, H., Thiagarajan, P., Dasgupta, S. K., Schumacher, A., Prchal, J. T., Chen, M. and Wang, J. (2008) 'Essential role for Nix in autophagic maturation of erythroid cells', *Nature*, 454(7201), pp. 232-5.
- Sarraf, S. A., Raman, M., Guarani-Pereira, V., Sowa, M. E., Huttlin, E. L., Gygi, S. P. and Harper, J. W. (2013) 'Landscape of the PARKIN-dependent ubiquitylome in response to mitochondrial depolarization', *Nature*, 496(7445), pp. 372-6.
- Scheffler, I. E. (2007) *Mitochondria*. 2 edn.: Wiley-Liss.

- Schmidt, O., Pfanner, N. and Meisinger, C. (2010) 'Mitochondrial protein import: from proteomics to functional mechanisms', *Nat Rev Mol Cell Biol*, 11(9), pp. 655-67.
- Scott, I. and Logan, D. C. (2011) *Plant Mitochondria. Chapter 2: Mitochondrial Dynamics*: Springer Verlag New York, p. 31-63.
- Seibler, P., Graziotto, J., Jeong, H., Simunovic, F., Klein, C. and Krainc, D. (2011) 'Mitochondrial Parkin recruitment is impaired in neurons derived from mutant PINK1 induced pluripotent stem cells', *J Neurosci*, 31(16), pp. 5970-6.
- Shaltouki, A., Sivapatham, R., Pei, Y., Gerencser, A. A., Momčilović, O., Rao, M. S. and Zeng, X. (2015) 'Mitochondrial alterations by PARKIN in dopaminergic neurons using PARK2 patient-specific and PARK2 knockout isogenic iPSC lines', *Stem Cell Reports*, 4(5), pp. 847-59.
- Sheng, Z. H. and Cai, Q. (2012) 'Mitochondrial transport in neurons: impact on synaptic homeostasis and neurodegeneration', *Nat Rev Neurosci*, 13(2), pp. 77-93.
- Shi, G., Lee, J. R., Grimes, D. A., Racacho, L., Ye, D., Yang, H., Ross, O. A., Farrer, M., McQuibban, G. A. and Bulman, D. E. (2011) 'Functional alteration of PARL contributes to mitochondrial dysregulation in Parkinson's disease', *Hum Mol Genet*, 20(10), pp. 1966-74.
- Shiba, K., Arai, T., Sato, S., Kubo, S., Ohba, Y., Mizuno, Y. and Hattori, N. (2009) 'Parkin stabilizes PINK1 through direct interaction', *Biochem Biophys Res Commun*, 383(3), pp. 331-5.
- Shiba-Fukushima, K., Imai, Y., Yoshida, S., Ishihama, Y., Kanao, T., Sato, S. and Hattori, N. (2012) 'PINK1-mediated phosphorylation of the Parkin ubiquitin-like domain primes mitochondrial translocation of Parkin and regulates mitophagy', *Sci Rep*, 2, pp. 1002.
- Shirane, M. and Nakayama, K. I. (2003) 'Inherent calcineurin inhibitor FKBP38 targets Bcl-2 to mitochondria and inhibits apoptosis', *Nat Cell Biol*, 5(1), pp. 28-37.
- Singleton, A. B., Farrer, M., Johnson, J., Singleton, A., Hague, S., Kachergus, J., Hulihan, M., Peuralinna, T., Dutra, A., Nussbaum, R., Lincoln, S., Crawley, A., Hanson, M., Maraganore, D., Adler, C., Cookson, M. R., Muentner, M., Baptista, M., Miller, D., Blancato, J., Hardy, J. and Gwinn-Hardy, K. (2003)

- 'alpha-Synuclein locus triplication causes Parkinson's disease', *Science*, 302(5646), pp. 841.
- Smidt, M. P., Asbreuk, C. H., Cox, J. J., Chen, H., Johnson, R. L. and Burbach, J. P. (2000) 'A second independent pathway for development of mesencephalic dopaminergic neurons requires Lmx1b', *Nat Neurosci*, 3(4), pp. 337-41.
- Smidt, M. P., Smits, S. M., Bouwmeester, H., Hamers, F. P., van der Linden, A. J., Hellemons, A. J., Graw, J. and Burbach, J. P. (2004) 'Early developmental failure of substantia nigra dopamine neurons in mice lacking the homeodomain gene Pitx3', *Development*, 131(5), pp. 1145-55.
- Song, L., McMackin, M., Nguyen, A. and Cortopassi, G. (2017) 'Parkin deficiency accelerates consequences of mitochondrial DNA deletions and Parkinsonism', *Neurobiol Dis*, 100, pp. 30-38.
- Song, P., Li, S., Wu, H., Gao, R., Rao, G., Wang, D., Chen, Z., Ma, B., Wang, H., Sui, N., Deng, H., Zhang, Z., Tang, T., Tan, Z., Han, Z., Lu, T., Zhu, Y. and Chen, Q. (2016) 'Parkin promotes proteasomal degradation of p62: implication of selective vulnerability of neuronal cells in the pathogenesis of Parkinson's disease', *Protein Cell*, 7(2), pp. 114-29.
- Soubannier, V., McLelland, G. L., Zunino, R., Braschi, E., Rippstein, P., Fon, E. A. and McBride, H. M. (2012a) 'A vesicular transport pathway shuttles cargo from mitochondria to lysosomes', *Curr Biol*, 22(2), pp. 135-41.
- Soubannier, V., Rippstein, P., Kaufman, B. A., Shoubridge, E. A. and McBride, H. M. (2012b) 'Reconstitution of mitochondria derived vesicle formation demonstrates selective enrichment of oxidized cargo', *PLoS One*, 7(12), pp. e52830.
- Specht, L. A., Pickel, V. M., Joh, T. H. and Reis, D. J. (1981a) 'Light-microscopic immunocytochemical localization of tyrosine hydroxylase in prenatal rat brain. I. Early ontogeny', *J Comp Neurol*, 199(2), pp. 233-53.
- Specht, L. A., Pickel, V. M., Joh, T. H. and Reis, D. J. (1981b) 'Light-microscopic immunocytochemical localization of tyrosine hydroxylase in prenatal rat brain. II. Late ontogeny', *J Comp Neurol*, 199(2), pp. 255-76.
- Stauch, K. L., Villeneuve, L. M., Purnell, P. R., Ottemann, B. M., Emanuel, K. and Fox, H. S. (2016) 'Loss of Pink1 modulates synaptic mitochondrial bioenergetics in the rat striatum prior to motor symptoms: concomitant

- complex I respiratory defects and increased complex II-mediated respiration', *Proteomics Clin Appl*, 10(12), pp. 1205-1217.
- Sterky, F. H., Lee, S., Wibom, R., Olson, L. and Larsson, N. G. (2011) 'Impaired mitochondrial transport and Parkin-independent degeneration of respiratory chain-deficient dopamine neurons in vivo', *Proc Natl Acad Sci U S A*, 108(31), pp. 12937-42.
- Stolz, A., Putyrski, M., Kutle, I., Huber, J., Wang, C., Major, V., Sidhu, S. S., Youle, R. J., Rogov, V. V., Dötsch, V., Ernst, A. and Dikic, I. (2017) 'Fluorescence-based ATG8 sensors monitor localization and function of LC3/GABARAP proteins', *EMBO J*, 36(4), pp. 549-564.
- Strappazzon, F., Nazio, F., Corrado, M., Cianfanelli, V., Romagnoli, A., Fimia, G. M., Campello, S., Nardacci, R., Piacentini, M., Campanella, M. and Cecconi, F. (2014) 'AMBRA1 is able to induce mitophagy via LC3 binding, regardless of PARKIN and p62/SQSTM1', *Cell Death Differ*, 22(3), pp. 419-32.
- Sun, Y., Vashisht, A. A., Tchieu, J., Wohlschlegel, J. A. and Dreier, L. (2012) 'Voltage-dependent anion channels (VDACs) recruit Parkin to defective mitochondria to promote mitochondrial autophagy', *J Biol Chem*, 287(48), pp. 40652-60.
- Suzuki, S., Akamatsu, W., Kisa, F., Sone, T., Ishikawa, K. I., Kuzumaki, N., Katayama, H., Miyawaki, A., Hattori, N. and Okano, H. (2017) 'Efficient induction of dopaminergic neuron differentiation from induced pluripotent stem cells reveals impaired mitophagy in PARK2 neurons', *Biochem Biophys Res Commun*, 483(1), pp. 88-93.
- Takahashi, K. and Yamanaka, S. (2006) 'Induction of pluripotent stem cells from mouse embryonic and adult fibroblast cultures by defined factors', *Cell*, 126(4), pp. 663-76.
- Takahashi, Y., Coppola, D., Matsushita, N., Cuaing, H. D., Sun, M., Sato, Y., Liang, C., Jung, J. U., Cheng, J. Q., Mulé, J. J., Pledger, W. J. and Wang, H. G. (2007) 'Bif-1 interacts with Beclin 1 through UVRAG and regulates autophagy and tumorigenesis', *Nat Cell Biol*, 9(10), pp. 1142-51.
- Tanaka, A., Cleland, M. M., Xu, S., Narendra, D. P., Suen, D. F., Karbowski, M. and Youle, R. J. (2010) 'Proteasome and p97 mediate mitophagy and degradation of mitofusins induced by Parkin', *J Cell Biol*, 191(7), pp. 1367-80.

- Tanida, I., Sou, Y. S., Minematsu-Ikeguchi, N., Ueno, T. and Kominami, E. (2006) 'Atg8L/Apg8L is the fourth mammalian modifier of mammalian Atg8 conjugation mediated by human Atg4B, Atg7 and Atg3', *FEBS J*, 273(11), pp. 2553-62.
- Tanida, I., Tanida-Miyake, E., Komatsu, M., Ueno, T. and Kominami, E. (2002) 'Human Apg3p/Aut1p homologue is an authentic E2 enzyme for multiple substrates, GATE-16, GABARAP, and MAP-LC3, and facilitates the conjugation of hApg12p to hApg5p', *J Biol Chem*, 277(16), pp. 13739-44.
- Tanida, I., Tanida-Miyake, E., Ueno, T. and Kominami, E. (2001) 'The human homolog of *Saccharomyces cerevisiae* Apg7p is a Protein-activating enzyme for multiple substrates including human Apg12p, GATE-16, GABARAP, and MAP-LC3', *J Biol Chem*, 276(3), pp. 1701-6.
- Tasaki, T., Kim, S. T., Zakrzewska, A., Lee, B. E., Kang, M. J., Yoo, Y. D., Chamolstad, H. J., Hwang, J., Soung, N. K., Sung, K. S., Kim, S., Nguyen, M. D., Sun, M., Yi, E. C., Kim, B. Y. and Kwon, Y. T. (2013) 'UBR box N-recognin-4 (UBR4), an N-recognin of the N-end rule pathway, and its role in yolk sac vascular development and autophagy', *Proc Natl Acad Sci U S A*, 110(10), pp. 3800-3805.
- Todd, L. R., Damin, M. N., Gomathinayagam, R., Horn, S. R., Means, A. R. and Sankar, U. (2010) 'Growth factor *erv1*-like modulates Drp1 to preserve mitochondrial dynamics and function in mouse embryonic stem cells', *Mol Biol Cell*, 21(7), pp. 1225-36.
- Tooze, S. A. and Yoshimori, T. (2010) 'The origin of the autophagosomal membrane', *Nat Cell Biol*, 12(9), pp. 831-5.
- Tra, T., Gong, L., Kao, L. P., Li, X. L., Grandela, C., Devenish, R. J., Wolvetang, E. and Prescott, M. (2011) 'Autophagy in human embryonic stem cells', *PLoS One*, 6(11), pp. e27485.
- Tsiper, M. V., Sturgis, J., Avramova, L. V., Parakh, S., Fatig, R., Juan-García, A., Li, N., Rajwa, B., Narayanan, P., Qualls, C. W., Robinson, J. P. and Davisson, V. J. (2012) 'Differential mitochondrial toxicity screening and multi-parametric data analysis', *PLoS One*, 7(10), pp. e45226.
- Turrens, J. F. (2003) 'Mitochondrial formation of reactive oxygen species', *J Physiol*, 552(Pt 2), pp. 335-44.

- Twig, G., Elorza, A., Molina, A. J. A., Mohamed, H., Wikstrom, J. D., Walzer, G., Stiles, L., Haigh, S. E., Katz, S., Las, G., Alroy, J., Wu, M., Py, B. F., Yuan, J., Deeney, J. T., Corkey, B. E. and Shirihai, O. S. (2008) 'Fission and selective fusion govern mitochondrial segregation and elimination by autophagy', *EMBO J*, 27, pp. 433-443.
- Ugun-Klusek, A., Tatham, M. H., Elkharaz, J., Constantin-Teodosiu, D., Lawler, K., Mohamed, H., Paine, S. M., Anderson, G., John Mayer, R., Lowe, J., Ellen Billett, E. and Bedford, L. (2017) 'Continued 26S proteasome dysfunction in mouse brain cortical neurons impairs autophagy and the Keap1-Nrf2 oxidative defence pathway', *Cell Death Dis*, 8(1), pp. e2531.
- Urbánek, P., Fetka, I., Meisler, M. H. and Busslinger, M. (1997) 'Cooperation of Pax2 and Pax5 in midbrain and cerebellum development', *Proc Natl Acad Sci U S A*, 94(11), pp. 5703-8.
- Vadlamudi, R. K., Joung, I., Strominger, J. L. and Shin, J. (1996) 'p62, a phosphotyrosine-independent ligand of the SH2 domain of p56lck, belongs to a new class of ubiquitin-binding proteins', *J Biol Chem*, 271(34), pp. 20235-20237.
- Valente, E. M., Abou-Sleiman, P. M., Caputo, V., Muqit, M. M., Harvey, K., Gispert, S., Ali, Z., Del Turco, D., Bentivoglio, A. R., Healy, D. G., Albanese, A., Nussbaum, R., González-Maldonado, R., Deller, T., Salvi, S., Cortelli, P., Gilks, W. P., Latchman, D. S., Harvey, R. J., Dallapiccola, B., Auburger, G. and Wood, N. W. (2004) 'Hereditary early-onset Parkinson's disease caused by mutations in PINK1', *Science*, 304(5674), pp. 1158-60.
- Van den Heuvel, D. M. and Pasterkamp, R. J. (2008) 'Getting connected in the dopamine system', *Prog Neurobiol*, 85(1), pp. 75-93.
- Van Humbeeck, C., Cornelissen, T., Hofkens, H., Mandemakers, W., Gevaert, K., De Strooper, B. and Vandenberghe, W. (2011) 'Parkin interacts with Ambra1 to induce mitophagy', *J Neurosci*, 31(28), pp. 10249-61.
- Van Laar, V. S., Arnold, B., Cassady, S. J., Chu, C. T., Burton, E. A. and Berman, S. B. (2011) 'Bioenergetics of neurons inhibit the translocation response of Parkin following rapid mitochondrial depolarization', *Hum Mol Genet*, 20(5), pp. 927-40.

- Van Laar, V. S., Mishizen, A. J., Cascio, M. and Hastings, T. G. (2009) 'Proteomic identification of dopamine-conjugated proteins from isolated rat brain mitochondria and SH-SY5Y cells', *Neurobiol Dis*, 34(3), pp. 487-500.
- Varum, S., Momcilovic, O., Castro, C., Ben-Yehudah, A., Ramalho-Santos, J. and Navara, C. S. (2009) 'Enhancement of human embryonic stem cell pluripotency through inhibition of the mitochondrial respiratory chain', *Stem Cell Res*, 3(2-3), pp. 142-56.
- Verstreken, P., Ly, C. V., Venken, K. J., Koh, T. W., Zhou, Y. and Bellen, H. J. (2005) 'Synaptic mitochondria are critical for mobilization of reserve pool vesicles at *Drosophila* neuromuscular junctions', *Neuron*, 47(3), pp. 365-78.
- Villeneuve, L. M., Purnell, P. R., Stauch, K. L. and Fox, H. S. (2016) 'Neonatal mitochondrial abnormalities due to PINK1 deficiency: Proteomics reveals early changes relevant to Parkinson's disease', *Data Brief*, 6, pp. 428-32.
- Vincow, E. S., Merrihew, G., Thomas, R. E., Shulman, N. J., Beyer, R. P., MacCoss, M. J. and Pallanck, L. J. (2013) 'The PINK1-Parkin pathway promotes both mitophagy and selective respiratory chain turnover in vivo', *Proc Natl Acad Sci U S A*, 110(16), pp. 6400-6405.
- Vives-Bauza, C., Zhou, C., Huang, Y., Cui, M., de Vries, R. L., Kim, J., May, J., Tocilescu, M. A., Liu, W., Ko, H. S., Magrane, J., Moore, D. J., Dawson, V. L., Grailhe, R., Dawson, T. M., Li, C., Tieu, K. and Przedborski, S. (2010) 'PINK1-dependent recruitment of Parkin to mitochondria in mitophagy', *Proc Natl Acad Sci U S A*, 107(1), pp. 378-83.
- Von Stockum, S., Nardin, A., Schrepfer, E. and Ziviani, E. (2015) 'Mitochondrial dynamics and mitophagy in Parkinson's disease: A fly point of view', *Neurobiol Dis*.
- Walls, K. C., Ghosh, A. P., Franklin, A. V., Klocke, B. J., Ballestas, M., Shacka, J. J., Zhang, J. and Roth, K. A. (2010) 'Lysosome dysfunction triggers Atg7-dependent neural apoptosis', *J Biol Chem*, 285(14), pp. 10497-507.
- Wang, H. L., Chou, A. H., Wu, A. S., Chen, S. Y., Weng, Y. H., Kao, Y. C., Yeh, T. H., Chu, P. J. and Lu, C. S. (2011a) 'PARK6 PINK1 mutants are defective in maintaining mitochondrial membrane potential and inhibiting ROS formation of substantia nigra dopaminergic neurons', *Biochim Biophys Acta*, 1812(6), pp. 674-84.

- Wang, X., Su, B., Liu, W., He, X., Gao, Y., Castellani, R. J., Perry, G., Smith, M. A. and Zhu, X. (2011b) 'DLP1-dependent mitochondrial fragmentation mediates 1-methyl-4-phenylpyridinium toxicity in neurons: implications for Parkinson's disease', *Aging Cell*, 10(5), pp. 807-23.
- Wei, Y., Chiang, W. C., Sumpter, R., Mishra, P. and Levine, B. (2017) 'Prohibitin 2 Is an Inner Mitochondrial Membrane Mitophagy Receptor', *Cell*, 168(1-2), pp. 224-238.e10.
- Wei, Y., Pattingre, S., Sinha, S., Bassik, M. and Levine, B. (2008) 'JNK1-mediated phosphorylation of Bcl-2 regulates starvation-induced autophagy', *Mol Cell*, 30(6), pp. 678-88.
- Weidberg, H., Shvets, E., Shpilka, T., Shimron, F., Shinder, V. and Elazar, Z. (2010) 'LC3 and GATE-16/GABARAP subfamilies are both essential yet act differently in autophagosome biogenesis', *The EMBO Journal*, 29(11), pp. 1792-1802.
- Whitworth, A. J. and Pallanck, L. J. (2017) 'PINK1/Parkin mitophagy and neurodegeneration-what do we really know in vivo?', *Curr Opin Genet Dev*, 44, pp. 47-53.
- Whitworth, A. J., Theodore, D. A., Greene, J. C., Benes, H., Wes, P. D. and Pallanck, L. J. (2005) 'Increased glutathione S-transferase activity rescues dopaminergic neuron loss in a Drosophila model of Parkinson's disease', *Proc Natl Acad Sci U S A*, 102(22), pp. 8024-9.
- Wilkinson, D. G., Bailes, J. A. and McMahon, A. P. (1987) 'Expression of the proto-oncogene int-1 is restricted to specific neural cells in the developing mouse embryo', *Cell*, 50(1), pp. 79-88.
- Wirth, M., Joachim, J. and Tooze, S. A. (2013) 'Autophagosome formation--the role of ULK1 and Beclin1-PI3KC3 complexes in setting the stage', *Semin Cancer Biol*, 23(5), pp. 301-9.
- Wong, E. S., Tan, J. M., Wang, C., Zhang, Z., Tay, S. P., Zaiden, N., Ko, H. S., Dawson, V. L., Dawson, T. M. and Lim, K. L. (2007) 'Relative sensitivity of parkin and other cysteine-containing enzymes to stress-induced solubility alterations', *J Biol Chem*, 282(16), pp. 12310-8.
- Wong, Y. C. and Holzbaur, E. L. (2014) 'Optineurin is an autophagy receptor for damaged mitochondria in parkin-mediated mitophagy that is disrupted by an ALS-linked mutation', *Proc Natl Acad Sci U S A*, 111(42), pp. E4439-48.

- Wong, Y. C. and Holzbaur, E. L. (2015) 'Temporal dynamics of PARK2/parkin and OPTN/optineurin recruitment during the mitophagy of damaged mitochondria', *Autophagy*, 11(2), pp. 422-4.
- Wu, W., Tian, W., Hu, Z., Chen, G., Huang, L., Li, W., Zhang, X., Xue, P., Zhou, C., Liu, L., Zhu, Y., Zhang, X., Li, L., Zhang, L., Sui, S., Zhao, B. and Feng, D. (2014) 'ULK1 translocates to mitochondria and phosphorylates FUNDC1 to regulate mitophagy', *EMBO Rep*, 15(5), pp. 566-75.
- Xiao, B., Deng, X., Lim, G. G. Y., Zhou, W., Saw, W. T., Zhou, Z. D., Lim, K. L. and Tan, E. K. (2017) 'p62-Mediated mitochondrial clustering attenuates apoptosis induced by mitochondrial depolarization', *Biochim Biophys Acta*, 1864(7), pp. 1308-1317.
- Xie, H., Hu, L. and Li, G. (2010) 'SH-SY5Y human neuroblastoma cell line: in vitro cell model of dopaminergic neurons in Parkinson's disease', *Chin Med J*, 123(8), pp. 1086-1092.
- Xun, Z., Lee, D. Y., Lim, J., Canaria, C. A., Barnebey, A., Yanonne, S. M. and McMurray, C. T. (2012) 'Retinoic acid-induced differentiation increases the rate of oxygen consumption and enhances the spare respiratory capacity of mitochondria in SH-SY5Y cells', *Mech Ageing Dev*, 133(4), pp. 176-85.
- Yamamoto, A., Tagawa, Y., Yoshimori, T., Moriyama, Y., Masaki, R. and Tashiro, Y. (1998) 'Bafilomycin A1 prevents maturation of autophagic vacuoles by inhibiting fusion between autophagosomes and lysosomes in rat hepatoma cell line, H-4-II-E cells', *Cell Structure and Function*, 23, pp. 33-42.
- Yamano, K., Fogel, A. I., Wang, C., van der Bliek, A. M. and Youle, R. J. (2014) 'Mitochondrial Rab GAPs govern autophagosome biogenesis during mitophagy', *eLife*, 3(01612), pp. 1-24.
- Yamano, K. and Youle, R. J. (2013) 'PINK1 is degraded through the N-end rule pathway', *Autophagy*, 9(11), pp. 1758-69.
- Yan, C. H., Levesque, M., Claxton, S., Johnson, R. L. and Ang, S. L. (2011) 'Lmx1a and lmx1b function cooperatively to regulate proliferation, specification, and differentiation of midbrain dopaminergic progenitors', *J Neurosci*, 31(35), pp. 12413-25.
- Yoshii, S. R., Kishi, C., Ishihara, N. and Mizushima, N. (2011) 'Parkin mediates proteasome-dependent protein degradation and rupture of the outer mitochondrial membrane', *J Biol Chem*, 286(22), pp. 19630-40.

- Youle, R. J. and van der Bliek, A. M. (2012) 'Mitochondrial fission, fusion, and stress', *Science*, 337, pp. 1062-1065.
- Yu, W., Sun, Y., Guo, S. and Lu, B. (2011) 'The PINK1/Parkin pathway regulates mitochondrial dynamics and function in mammalian hippocampal and dopaminergic neurons', *Hum Mol Genet*, 20(16), pp. 3227-40.
- Yue, X. S., Fujishiro, M., Nishioka, C., Arai, T., Takahashi, E., Gong, J. S., Akaike, T. and Ito, Y. (2012) 'Feeder cells support the culture of induced pluripotent stem cells even after chemical fixation', *PLoS One*, 7(3), pp. e32707.
- Zalckvar, E., Berissi, H., Mizrachy, L., Idelchuk, Y., Koren, I., Eisenstein, M., Sabanay, H., Pinkas-Kramarski, R. and Kimchi, A. (2009) 'DAP-kinase-mediated phosphorylation on the BH3 domain of beclin 1 promotes dissociation of beclin 1 from Bcl-XL and induction of autophagy', *EMBO Rep*, 10(3), pp. 285-92.
- Zeigerer, A., Gilleron, J., Bogorad, R. L., Marsico, G., Nonaka, H., Seifert, S., Epstein-Barash, H., Kuchimanchi, S., Peng, C. G., Ruda, V. M., Del Conte-Zerial, P., Hengstler, J. G., Kalaidzidis, Y., Koteliansky, V. and Zerial, M. (2012) 'Rab5 is necessary for the biogenesis of the endolysosomal system in vivo', *Nature*, 485(7399), pp. 465-70.
- Zetterström, R. H., Williams, R., Perlmann, T. and Olson, L. (1996) 'Cellular expression of the immediate early transcription factors Nurr1 and NGFI-B suggests a gene regulatory role in several brain regions including the nigrostriatal dopamine system', *Brain Res Mol Brain Res*, 41(1-2), pp. 111-20.
- Zhang, Q., Raoof, M., Chen, Y., Sumi, Y., Sursal, T., Junger, W., Brohi, K., Itagaki, K. and Hauser, C. J. (2010) 'Circulating mitochondrial DAMPs cause inflammatory responses to injury', *Nature*, 464(7285), pp. 104-7.
- Zhao, P., Luo, Z., Tian, W., Yang, J., Ibáñez, D. P., Huang, Z., Tortorella, M. D., Esteban, M. A. and Fan, W. (2014) 'Solving the puzzle of Parkinson's disease using induced pluripotent stem cells', *Exp Biol Med (Maywood)*, 239(11), pp. 1421-32.
- Zheng, X. and Hunter, T. (2013) 'Parkin mitochondrial translocation is achieved through a novel catalytic activity coupled mechanism', *Cell Res*, 23(7), pp. 886-97.
- Zhong, Y., Wang, Q. J., Li, X., Yan, Y., Backer, J. M., Chait, B. T., Heintz, N. and Yue, Z. (2009) 'Distinct regulation of autophagic activity by Atg14L and

- Rubicon associated with Beclin 1-phosphatidylinositol-3-kinase complex', *Nat Cell Biol*, 11(4), pp. 468-76.
- Zhou, C., Huang, Y., Shao, Y., May, J., Prou, D., Perier, C., Dauer, W., Schon, E. A. and Przedborski, S. (2008) 'The kinase domain of mitochondrial PINK1 faces the cytoplasm', *Proc Natl Acad Sci U S A*, 105(33), pp. 12022-7.
- Zhou, Z. D., Refai, F. S., Xie, S. P., Ng, S. H., Chan, C. H., Ho, P. G., Zhang, X. D., Lim, T. M. and Tan, E. K. (2014) 'Mutant PINK1 upregulates tyrosine hydroxylase and dopamine levels, leading to vulnerability of dopaminergic neurons', *Free Radic Biol Med*, 68, pp. 220-33.
- Zhu, J. H., Horbinski, C., Guo, F., Watkins, S., Uchiyama, Y. and Chu, C. T. (2007) 'Regulation of autophagy by extracellular signal-regulated protein kinases during 1-methyl-4-phenylpyridinium-induced cell death', *Am J Pathol*, 170(1), pp. 75-86.
- Zhuang, N., Li, L., Chen, S. and Wang, T. (2016) 'PINK1-dependent phosphorylation of PINK1 and Parkin is essential for mitochondrial quality control', *Cell Death Dis*, 7(12), pp. e2501.
- Zweifel, L. S., Parker, J. G., Lobb, C. J., Rainwater, A., Wall, V. Z., Fadok, J. P., Darvas, M., Kim, M. J., Mizumori, S. J., Paladini, C. A., Phillips, P. E. and Palmiter, R. D. (2009) 'Disruption of NMDAR-dependent burst firing by dopamine neurons provides selective assessment of phasic dopamine-dependent behavior', *Proc Natl Acad Sci U S A*, 106(18), pp. 7281-8.